Synthesis and reactivity of cyclopentadienyl based organometallic compounds and their electrochemical and biological properties

Sasmita Mishra

Department of Chemistry
National Institute of Technology Rourkela

Synthesis and reactivity of cyclopentadienyl based organometallic compounds and their electrochemical and biological properties

Dissertation submitted to the

National Institute of Technology Rourkela

In partial fulfillment of the requirements of the degree of

Doctor of Philosophy

in

Chemistry

by

Sasmita Mishra

(Roll Number: 511CY604)

Under the supervision of

Prof. Saurav Chatterjee

February, 2017

Department of Chemistry

National Institute of Technology Rourkela

Department of Chemistry
National Institute of Technology Rourkela

Certificate of Examination

Roll Number: 511CY604

Name: Sasmita Mishra

Title of Dissertation: "Synthesis and reactivity of cyclopentadienyl based organometallic compounds and their electrochemical and biological properties

We the below signed, after checking the dissertation mentioned above and the official record book(s) of the student, hereby state our approval of the dissertation submitted in partial fulfillment of the requirements of the degree of Doctor of Philosophy in Chemistry at National Institute of Technology Rourkela. We are satisfied with the volume, quality, correctness, and originality of the work.

Prof. Saurav Chatterjee
Principal Supervisor

Prof. A. Sahoo.
Member (DSC)

Prof. G. Hota
Member (DSC)

Prof. R. Dinda
Member (DSC)

Examiner

Prof. N. Panda
Chairman (DSC)

Department Of Chemistry
National Institute of Technology Rourkela

Prof. Saurav Chatterjee
Associate Professor,
Department of Chemistry
NIT, Rourkela

February 16, 2017

Supervisor's Certificate

This is to certify that the work presented in this dissertation entitled "Synthesis and reactivity of cyclopentadienyl based organometallic compounds and their electrochemical and biological properties" by "*Sasmita Mishra*", Roll Number 511CY604, is a record of original research carried out by her under my supervision and guidance in partial fulfillment of the requirements of the degree of *Doctor of Philosophy* in *Chemistry*. Neither this dissertation nor any part of it has been submitted for any degree or diploma to any institute or university in India or abroad.

Prof. Saurav Chatterjee

Dedicated

to

my loving parents

Declaration of Originality

I, Sasmita Mishra, Roll Number 511CY604 hereby declare that this dissertation entitled "Synthesis and reactivity of cyclopentadienyl based organometallic compounds and their electrochemical and biological properties" represents my original work carried out as a doctoral student of NIT Rourkela and, to the best of my knowledge, it contains no material previously published or written by another person, nor any material presented for the award of any other degree or diploma of NIT Rourkela or any other institution. Any contribution made to this research by others, with whom I have worked at NIT Rourkela or elsewhere, is explicitly acknowledged in the dissertation. Works of other authors cited in this dissertation have been duly acknowledged under the section "Bibliography". I have also submitted my original research records to the scrutiny committee for evaluation of my dissertation.

I am fully aware that incase of any non-compliance detected in future, the Senate of NIT Rourkela may withdraw the degree awarded to me on the basis of the present dissertation.

February 16, 2017

NIT Rourkela *Sasmita Mishra*

Abstract

The current focus of organometallic chemistry is based upon their synthesis, eloectrochemical properties, diverse biological behavior and their facet towards a new field of bioorganometallics concerning both organometallic and coordination chemistry. Organometallic complexes involving metal - cyclopentadienyl linkages have been an important fragment due to their unique structural variety, stability and their potential applications in organic synthesis, catalysis, bioorganometallic, advance materials, molecular recognition etc. Ferrocene and its derivatives are the most versatile aspect in organometallic chemistry because of their unique structural integrity, reversible redox behavior and have been responsible for the development of material science, molecular wires, catalysis, molecular recognition, sensing, electronic communication, bio-conjugates and medicinal chemistry. The use of ferrocenyl compounds as bioactive molecule has been established recently and several reports show that a large number of ferrocene containing compounds display interesting cytotoxic and DNA cleaving activities. Ferrocene substituted tamoxifen and chloroquine derivatives are among the many examples where systematic functionalization of ferrocene has improved the cytotoxic activity of the standard drug itself. In parallel, the half sandwich based organometallic compounds are also drawing interest because their various biological properties ranging from antimalarial, antimicrobial, anticancer, enzyme inhibitors and phototoxicity. Half sandwich compounds containing metal carbonyls are the most significant ligands in medicinal chemistry and can play a vital role as tracers in immunological analysis based on several analytical methods like FTIR, electrochemical, atomic absorption techniques etc. Moreover, ferrocenyl Schiff base compounds have been reported for their interesting coordination features and exciting biological properties. In view of the enormous potential applications of ferrocenyl and half sandwich based organometallic compounds, we focused our study to synthesize some sandwich and half sandwich based Schiff base compounds and to study their biological properties. We have been able to synthesize a range of novel ferrocene and cymantrene based Schiff base compounds and characterize by spectroscopic and crystallographic technique. We have also described the synthesis of hetero-bimetallic chalcones containing both ferrocenyl and cymantrenyl fragments and studied their reactivity towards mono- and diphosphine substitution. In addition, compounds

containing multiple redox centers have also been highly focused due to their various application related to electronic communication, sensors and molecular wires. In this regard, we focused on the synthesis of diferrocenyl bifunctional molecular systems containing both hydrazone and enone units using simple and systematic synthetic route. Efforts have been made to study the unique structural feature and to understand the biological and sensing properties of some of the compounds. We have carried out cyclic-voltammetric studies with different analogs of the diferrocenyl compounds to understand the electronic communication behavior inside the molecule. DFT calculation was also performed to establish some of the interesting features related to structural stability, metal ion interaction and molecular orbital energies.

Keywords: Ferrocenyl, Cymantrenyl, Chalcone, Hydrazone, Bioorganometallic, Electronic communication

Contents

	Page
Certificate of Examination	**ii**
Supervisor's Certificate	**iii**
Dedication	**iv**
Declaration of Originality	**v**
Abstract	**vi**
Contents	**vii**
Acknowledgements	**xi**
Bio-data	**xii**
Chapter 1: Introduction	**1**
1.1. Metal-cyclopentadienylcomplex	**2**
1.1.1. Cyclopentadienyl ligand	**3**
1.1.2. Bonding modes of cyclopentadienyl ligand	**4**
1.1.3. Classification of cyclopentadienyl complexes	**12**
1.2. Structural variety of metal cyclopentadienyl complex	**15**
1.2.1. Half sandwich and Piano stool complexes	**16**
1.2.2. Sandwich complexes	**22**
1.2.3. Other variety of metallocenes	**24**
1.2.4. Bent metallocenes	**26**
1.2.5. Bimetallic cyclopentadienyl complexes	**27**
1.2.6. Multimetallic cyclopentadienyl complexes	**30**
1.2.7. Multidecker sandwich compounds	**31**
1.3. Cymantrene based organometallic compounds	**33**
1.3.1. Chelated Cymantrenyl complex	**36**
1.3.2. Biological properties	**39**
1.3.3. Electrochemical properties	**42**
1.4. Ferrocene based organometallic compound	**44**

1.4.1. C-H bond functionalization of ferrocene **47**

1.4.2. Ferrocenyl derivatives having biological properties **49**

1.4.3. Ferrocenyl compounds as biosensor **55**

1.4.4. Ferrocenyl compounds as chemosensor **57**

1.4.5. Electronic communication in ferrocene based molecules **61**

1.4.6. Diferrocenyl organometallic compounds **64**

1.5. Half-sandwich and ferrocenyl conjugate system **69**

1.6. References **73**

Chapter 2: Synthesis, characterization and structural evaluation of cymantrenyl hydrazone derivatives **82**

2.1. Introduction **83**

2.2. Experimental Sections **89**

2.2.1. General Procedures **89**

2.2.2. Synthesis of $[(CO)_3Mn\{(\eta^5\text{-}C_5H_4)C(CH_3)=NN(H)C(O)R\}]$ **89**

2.2.3. Crystal structure determination for **1** and **2** **90**

2.2.4. Antibacterial activity **91**

2.3. Results and Discussion **92**

2.3.1. Molecular structure of **1 - 3** **93**

2.3.2. Antibacterial activity of **1 - 3** **98**

2.4. References **100**

Chapter 3: Synthesis, characterization and redox properties of unsymmetrically substituted 1,1' ferrocenyl dihydrazone compound **103**

3.1. Introduction **104**

3.2. Experimental Sections **108**

3.2.1. General Procedures **108**

3.2.2. Synthesis of 1,1'-$[\{CH_3C(O)(\eta^5\text{-}C_5H_4)\}Fe\{(\eta^5\text{-}C_5H_4)C(CH_3)=NN(H)C(O)R\}]$ (**5-8**) **108**

3.2.3. Reaction of **7** with hydrazide **110**

3.2.4. Crystal structure determination for **7** **110**

3.3. Results and Discussion **112**

3.4. References **119**

Chapter 4: Ferrocenyl-cymantrenyl hetero-bimetallic chalcones: Synthesis, reactivity and biological properties **121**

4.1. Introduction **122**

4.2. Experimental Sections **126**

4.2.1. General Procedures **126**

4.2.2. Synthesis of $[(CO)_3Mn(\eta^5\text{-}C_5H_4)COCH{=}CH(\eta^5\text{-}C_5H_4)Fe(\eta^5\text{-}C_5H_5)]$ (**11**) **127**

4.2.3. Synthesis of 1,1'-$[\{(CO)_3Mn(\eta^5\text{-}C_5H_4)COCH{=}CH(\eta^5\text{-}C_5H_4)\}_2Fe]$(**12**) **127**

4.2.4. Synthesis of $[(CO)_2(PPh_3)Mn(\eta^5\text{-}C_5H_4)COCH{=}CH(\eta^5\text{-}C_5H_4)Fe(\eta^5\text{-}C_5H_5)]$(**13**) **128**

4.2.5. Reaction of **11** with Bis-diphenylphosphino ferrocene (dppf) **129**

4.2.6. Synthesis of $[\{(CO)_2(PPh_3)Mn(\eta^5\text{-}C_5H_4)COCH{=}CH(\eta^5\text{-}C_5H_4)\}_2Fe]$ (**16**) **130**

4.2.7. Crystal structure determination for **11** and **13** **131**

4.2.8. Computational details **133**

4.2.9. Antibacterial activity **133**

4.2.10. Antimalarial activity **134**

4.3. Results and Discussion **134**

4.3.1. Molecular structure of **11** **137**

4.3.2. Molecular structure of **1**3 **139**

4.3.3. Redox properties of **11 – 14** **143**

4.3.4. Anti-malarial activity **146**

4.3.5. Anti-bacterial activity **147**

4.3.6. DFT calculation of **11** **148**

4.3.7. TD-DFT calculation and Correlation with electronic transitions **149**

4.4. References **154**

Chapter 5: Synthesis of diferrocenyl hydrazone-enone receptor molecule: Biological evaluation, electronic communication and metal binding study **158**

5.1. Introduction **159**

5.2. Experimental Sections **165**

5.2.1. General Procedures **165**

5.2.2. Synthesis of $[(\eta^5\text{-}C_5H_5)Fe(\eta^5\text{-}C_5H_4)CH{=}CHC(O)(\eta^5\text{-}C_5H_4)Fe\{(\eta^5\text{-}C_5H_4)C(CH_3){=}N\text{-}N\text{-}(H)C(O)\text{-}R\}]$ (**16 -19**) **166**

5.2.3. Crystal structure determination for **18** and **19** **167**

5.2.4. Antibacterial activity **169**

5.2.5. BSA binding experiment **170**

5.2.6. Computational details **170**

5.3. Results and Discussion **170**

5.3.1. Molecular structure of **18** and **19** **172**

5.3.2. Redox properties of **17**-**20** **175**

5.3.3. Antibacterial activity of **17**-**2**0 **178**

5.3.4. BSA Protein binding studies **179**

5.3.5. Metal ion interaction study by UV–Visible spectroscopy **182**

5.3.6. DFT Studies **184**

5.4. References **189**

Summary **193**

CHAPTER 1

INTRODUCTION

1.1. Metal -cyclopentadienyl complex

Organometallic complex containing metal - cyclopentadienyl linkage has been an important fragment in the chemistry of organometallic molecules since the discovery of ferrocene. Electrophilic aromatic-type substitution reaction on ferrocene by Woodward and coworkers in 1952 played a key role and led to the development of metal cyclopentadienyl chemistry.[1, 2] Similar substitution reaction was subsequently extended to other cyclopentadienyl – metal complexes like ruthenocene, osmocene, (η^5-cyclopentadienyl)tricarbonylmanganese, rhenium and technetium, (η^5-cyclopentadienyi)tetra -carbonylvanadium, (η^5-cyclopentadienyl)dicarbonylcobalt etc.[3-16] For the last 60 years, research on metal cyclopentadienyl chemistry has continued to develop at a rapid pace giving rise to structurally unique molecules and novel compounds containing sandwich and open sandwich entities. The non ending interest on these organometallic moieties is because of their immense potential to various applications related to organic synthesis, catalysis, bioorganometallic, advance materials, molecular recognition etc.[17] However, the synthesis of substituted ferrocene and derivatization of cyclopentadienyl ring in various different metallocenes and half sandwich complexes pose numerous challenges in regard to reaction condition, reagents and methodologies. Therefore, it is highly required to optimize the strategies based upon facile synthetic methods and suitability of the precursors for the functionalization of different Cp based organometallic compounds. Different types of substituent on the Cp ring often result in significant changes in reactivity and properties of the complex due to the electronic and steric factor that influences the molecular entity. Cyclopentadienyl ligand has the ability to stabilize high as well as low oxidation states of metals and a range of different derivatives with varying hapticity are well known. Remarkably, these variations result in extensive complex chemistry with flexible electronic, structural and steric behavior. Therefore, it has been very important to deeply understand such organometallic complexes containing cyclopentadienyl - metal linkages and their derivatives and explore the opportunities for related application.

1.1.1. Cyclopentadienyl ligand

Cyclopentadienyl group (C_5H_5 or Cp), the deprotonated form of cyclopentadiene, has been one of the versatile and widely used ligand in organometallic chemistry. It is a monoanionic, aromatic, electron rich species containing six-electrons and forms a variety of complexes with main group and transition metals. The cyclopentadienyl group is a significant ligand because of its aromaticity and high stability and plays an active role in stabilizing organometallic complexes. Reaction of cyclopentadiene with sodium hydride and bases like amines, hydroxides, alkyllithium compounds and Grignard reagents furnishes the reactive cyclopentadienyl anion by losing a proton. Cyclopentadiene can be obtained by distilling ("cracking") it from commercially available dimer solution and stored at lower temperature for further use. Free neutral cyclopentadiene, which is used to deprotonate with a strong base to generate the Cp^- is unstable and reacts with itself via Diels-Alder reaction to generate the dimerised product, dicyclopentadiene (Scheme 1.1).

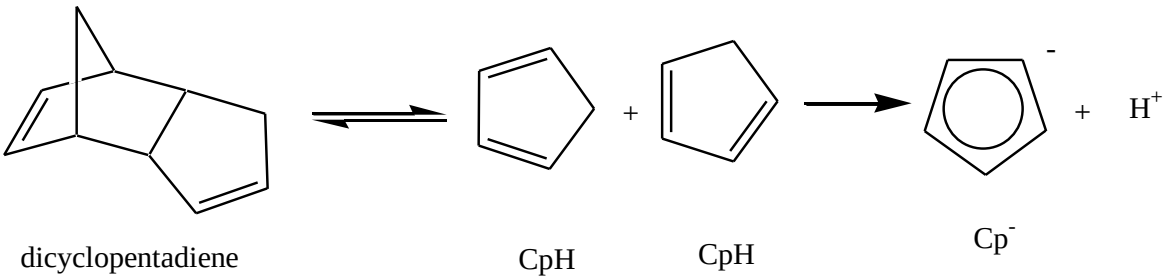

Scheme 1.1. Cracking of dicyclopentadiene

Cyclopentadienyl anion creates a stable and strong metal-ligand bond with five almost equal metal-carbon bond distances. The wide range of reactions that can be performed on cyclopentadienyl complexes reveals the unique stability of the metal-Cp bond including functionalization of the Cp ring and modification of other ligands without disturbing the M – Cp structural framework.[18]

1.1.2. Bonding modes of Cyclopentadienyl ligand

Cyclopentadienyl ligand can adopt η^5 (pentahapto), η^3 (trihapto) and η^1 (monohapto) coordination modes with metals. Among the three coordinations, η^5 is the most common mode of bonding forming a six electrons donating ligand (Figure 1.1). The change in heptacity modifies the electronic and steric factor of the metal resulting in alteration in properties of the whole complex system. When attached to main group metals, the ligand generally behaves as good leaving group, while they are found to be firmly coordinated to transition metals in high and low oxidation states.

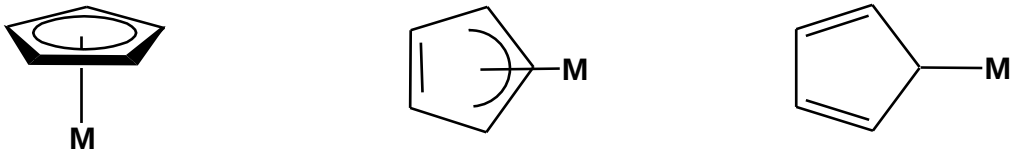

η^5 η^3 η^1

Figure 1.1. Binding modes of cyclopentadienyl group

The frontier molecular orbital of the cyclopentadienyl ligand contains five orbitals (Ψ_1–Ψ_5) residing in three different energy levels as shown in Figure 1.2. The lowest energy orbital Ψ_1 is represented by an a_1 state which does not contain any node, followed by a doubly degenerate e_1 states that comprise of the Ψ_2 and Ψ_3 orbitals having a single node, and another doubly degenerate e_2 states consisting of Ψ_4 and Ψ_5 orbitals having two nodes. The energy of the states increases as the number of nodes increases from 0 to 2.

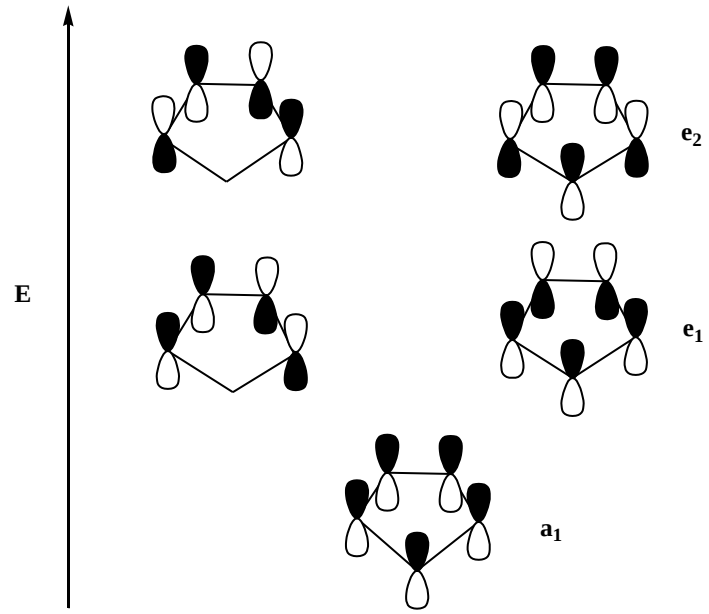

Figure 1.2. Molecular orbital diagram of cyclopentadienyl ligand.

The atomic orbitals of metal which are involved in the interaction with the orbitals of cyclopentadienyl ligand to form Metal-Cp molecular orbitals are shown in the Figure 1.3.

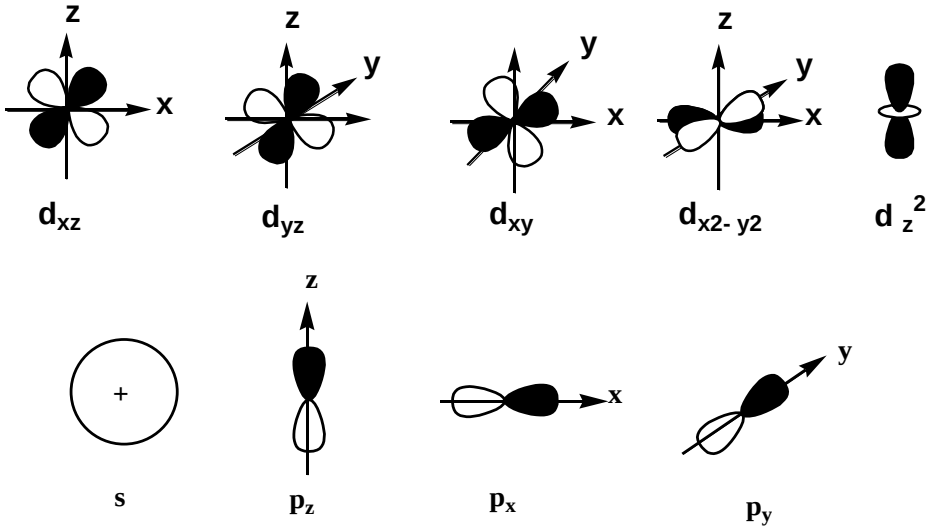

Figure 1.3. Atomic orbitals of metal

The metal d- orbitals which are mainly found to overlap with the Cp MOs having the matching symmetry are shown in Figure 1.4. The orbital d_z^2 interact with the a_1 type

orbital of cyclopentadienyl ligand, while d_{yz} and d_{xz} overlaps compatibly with the e_1 - symmetry orbitals. The metal orbitals $d_{x^2-y^2}$ and d_{xy} overlaps with e_2 type orbitals having similar symmetry.

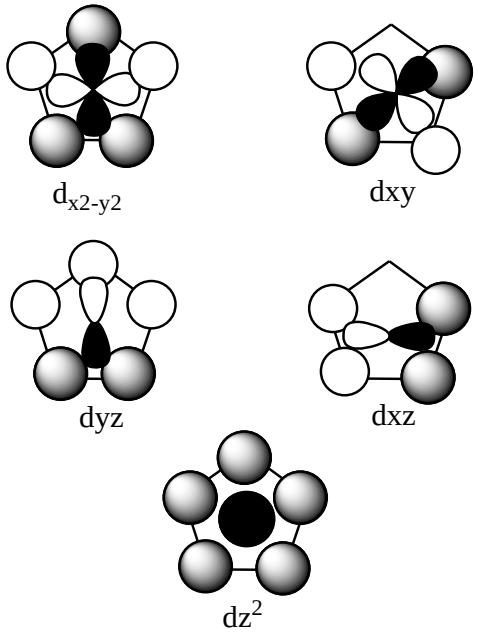

Figure 1.4. Metal-cyclopentadienyl bonding interactions.

In the Cp_2M system, (*e. g.* ferrocene) each of these five molecular orbitals of the two cyclopentadienyl ligands combines to give ten ligand molecular orbitals in three energy levels. During combination, all these ligand groups undergo addition and subtraction of wave functions which can be labeled as g (gerade) having centre of symmetry or u (ungerade) without centre of symmetry. All these ligand group orbitals on combination gives rise to a_{1g}, a_{1u}, e_{1g}, e_{1u}, e_{2g}, e_{2u} ligand group orbitals.

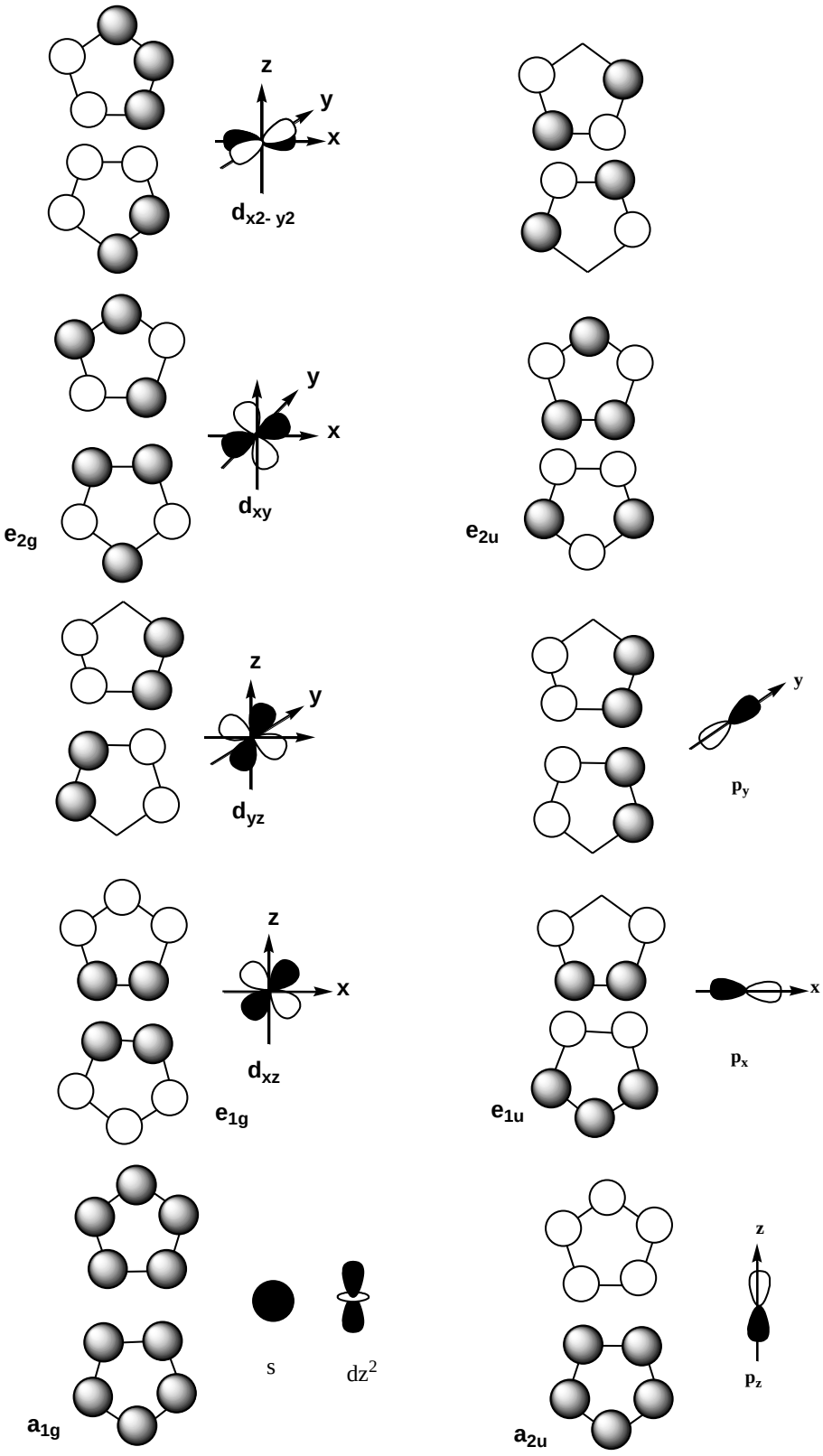

Figure 1.5. Symmetrical interaction in Cp_2M type molecules

The ligand group of both the cyclopentadienyl ligand and atomic orbital of metal atom with matching symmetry overlaps during combination to form molecular orbital of metallocene molecule (Figure 1.5). Overlap of a_{1g} and a_{2u} of Cp ring with the s and d_z^2 metal orbitals form σ bond with lowest energy as shown in the molecular orbital energy diagram. The 4p orbital of metal lies above the energy diagram due to their higher energy and contribute a little to the bonding. The well matched e_{1g} and e_{2u} of Cp ring and d_{xz}, d_{yz}, $4p_x$ and $4p_y$ forms π-bonds by means of their overlap while interaction of e_{2g} of Cp ring with d_{xy}, $d_{x^2-y^2}$ or bitals of metal gives rise to δ-bond. The e_{1u} orbital remains non bonding as there are no metal orbital of suitable symmetry and energy. The electron distribution in the molecular orbitals of ferrocene, shown in Figure 1.6, reveals the presence of paired electronic arrangement giving rise to diamagnetic character of the molecule. Both the highest occupied molecular orbital containing the pair of electrons and the lowest unoccupied molecular orbital lying above the filled orbitals are largely metal-based with the minor contribution from the molecular orbital of ligands.

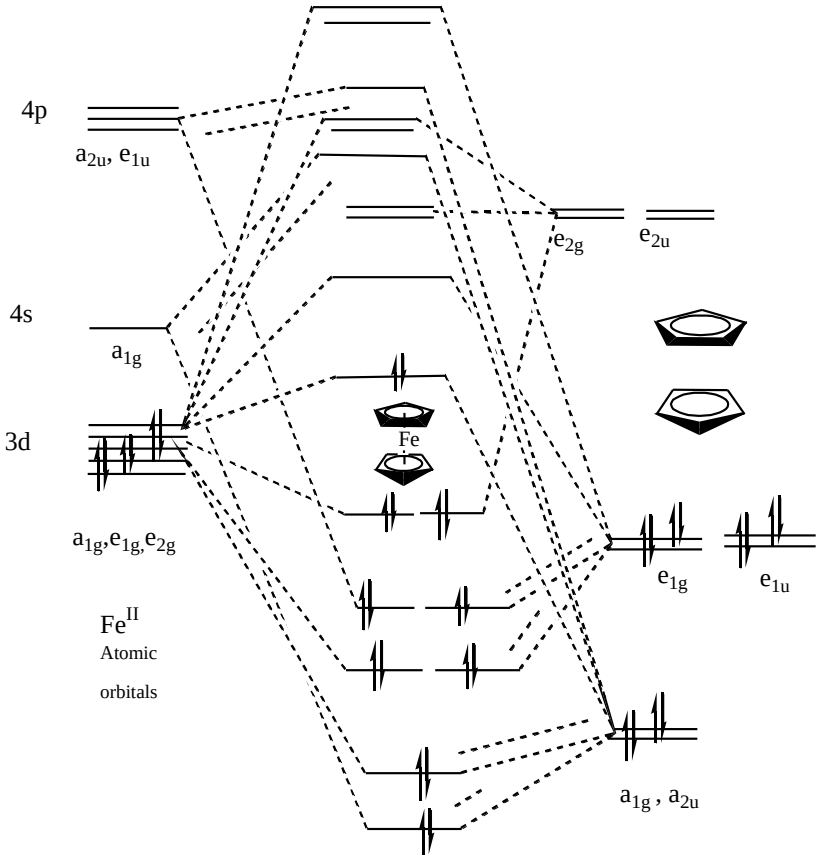

Figure 1.6. Molecular orbital of ferrocene

Cyclopentadienyl ring are well known to undergo ring slippage in which the bonding shift from one coordination mode to other modes by variation of the number of electrons of the metal attached to the Cp ring. For instance, Cp ring can move from a η^5 (pentahapto) to η^3 (trihapto) coordination mode which reduces the electron of the metal attached to the Cp ring by two, resulting in creation of an empty space for an incoming ligand to coordinate and acquire 18 electron configuration. Ring slippages are common in transition metal based Cp complexes and give rise to different types of organic transformation. Casey and coworkers have explained the monohapto nature of [(η^1-C_5H_5)$Re(CO)_3(PMe_3)_2$] complex obtained from the ring slippage reaction in which the η^3 coordination mode transforms to a stable η^1 coordinated rhenium complex.[19] The ring slippage is also accompanied by an extra phosphine coordination to obtain stable 18 electron complex (Scheme 1.2). Ring slippage transformation from η^3 coordination mode to η^5 mode may also result in decarbonylation of the complex to give [(η^5-C_5H_5)$Re(CO)_2(PMe_3)$].

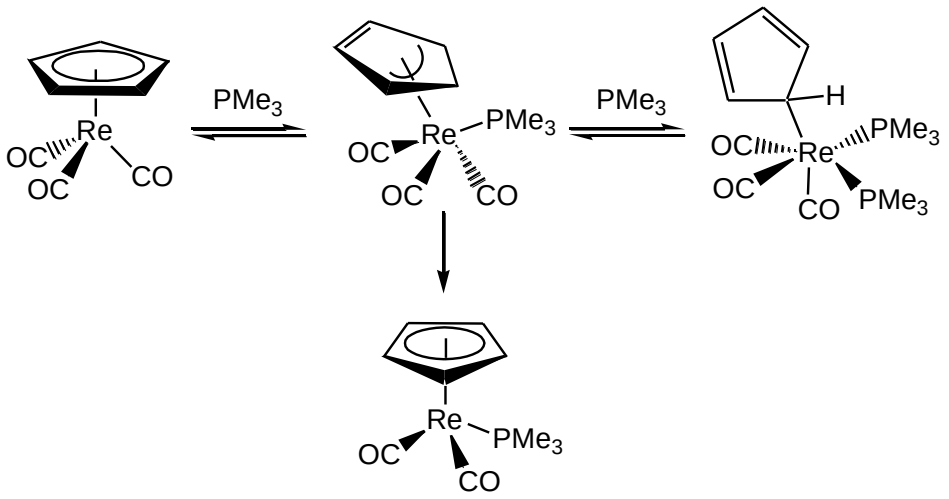

Scheme 1.2. Ring slippage in Rhenium based half sandwich compound

Early studies on fluxional behavior reveals that the monohapto cyclopentadienyl ring in the compounds [(η^1-C_5H_5)(η^5-C_5H_5)$Fe(CO)_2$] and [(η^1-C_5H_5)HgX], **(X** = Cl, Br, I, η^1-C_5H_5) have been shown to undergo reorientation of the organic moieties by solid state nuclear magnetic resonance studies (Figure 1.7).[20] The room-temperature proton NMR

spectrum of $[(\eta^1\text{-}C_5H_5)(\eta^5\text{-}C_5H_5)Fe(CO)_2]$ showed only two proton resonances which revealed that the sigma bond of the monohapto ring with the metal was in a dynamic equilibrium giving rise to fluxional property in the molecule. The proton resonance of all these Cp based compounds is found to be temperature dependent.

Figure 1.7. Ring slippage in $[(\eta^1\text{-}C_5H_5)(\eta^5\text{-}C_5H_5)Fe(CO)_2]$ and $[(\eta^1\text{-}C_5H_5)HgX]$

Recently, Elizabeth and coworkers have synthesized a series of nickel complexes $[(\eta^5\text{-}C_5H_5)(\eta^1\text{-}C_5H_4)\{(CH_3)_2C\}Ni]$ and $[(\eta^5\text{-}C_5H_5)(\eta^1\text{-}C_7H_9)\{(CH_3)_2C\}Ni]$ by the reaction of 1,3-bis(2,6-diisopropylphenyl)-1,3-dihydro-2H-imidazol-2-ylidene and the mixture of 1,3-bis(2,6-diisopropylphenyl)-1,3-dihydro-2H-imidazol-2-ylidene and lithium indenyl with nickelocene respectively. Similarly, palladium complexes $[(\eta^5\text{-}C_5H_5)(\eta^1\text{-}C_7H_9)\{(CH_3)_2C\}Pd]$ and $[(\eta^5\text{-}C_5H_5)(\eta^1\text{-}C_5H_4)\{(CH_3)_2C\}Pd]$ have been prepared by the reaction of sodium cylopentadienyl with $[(\eta^3\text{-}C_7H_9)\{(CH_3)_2C\}PdCl]$ and $[(\eta^5\text{-}C_5H_5)\{(CH_3)_2C\}PdCl]$ respectively.[21] Nickel and palladium complexes contains both η^1 and η^5 binding modes in the molecule and obey 18 electron rule as confirmed by the NMR and structural studies. X-ray crystallographic investigation showed the existence of five similar C-C bonds between 1.381(4) Å and 1.426(3) Å for η^5 bound Cp ring and three long C−C bonds between 1.426(4) Å and 1.448(4) Å and two short C−C bonds between 1.335(2) and 1.363(4) Å for the η^1 bound Cp ring in case of $[(\eta^5\text{-}C_5H_5)(\eta^1\text{-}C_5H_4)\{(CH_3)_2C\}M]$, (M = Ni. Pd) complexes.

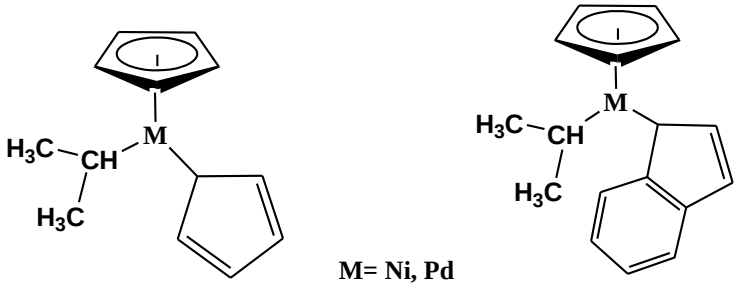

M= Ni, Pd

Figure 1.8. η^1 and η^5 binding modes of Cp

1,4- diphenylcyclopentadiene on treatment with thalium ethoxide ($TlOC_2H_5$) or $NaNH_2$ in tetrahydrofuran has given the half-sandwich compounds $Tl(C_5H_3Ph_2)$ and $Na(C_5H_3Ph_2)$ respectively which further reacted with $FeCl_2$ to give $Fe(C_5H_3Ph)_2$.[22] The molecular structure of the half-sandwich $Tl(C_5H_3Ph_2)$ showed the presence of two phenyl rings on the 1,4 position of Cp ring, each of the thallium attached to the oxygen atom of the tetrahydrofuran solvent molecule and another thallium atom of the adjacent molecule forming a square planar structure containing two thallium atoms and two adjacent atoms and also a honeycomb layered like structure with the adjacent six thallium atoms. In case of $Fe(C_5H_3Ph)_2$, iron atom was found sandwiched in between two Cp rings with an angle of 178.3^0C and each Cp containing two phenyl rings.

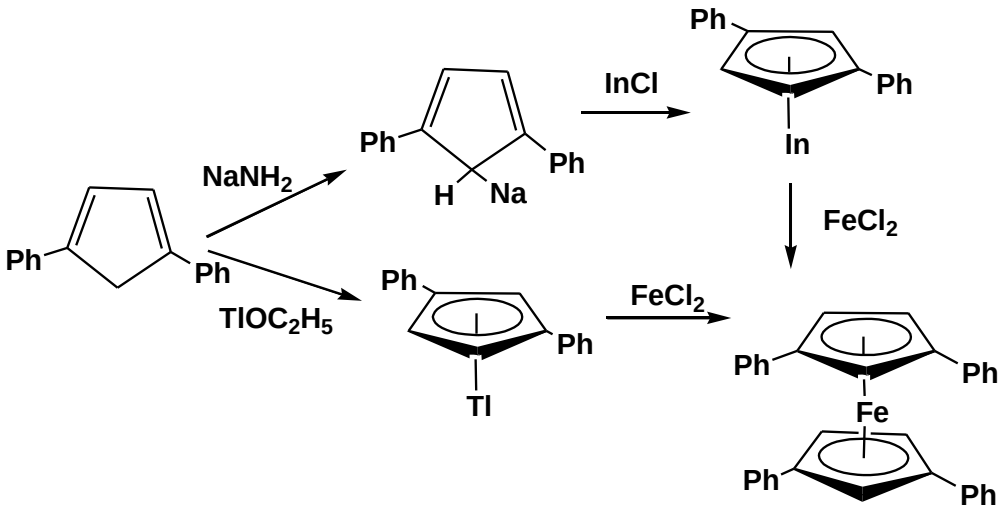

Scheme 1.3

Ring slippage of osmocene, $[(\eta^5-C_5H_5)_2Os]$ and ruthenium indenyl $[Ru(\eta^5-ind)_2]$ complexes has been reported by Cheung and coworkers.[23] However, ring slippage type of transformation for Group 8 metallocenes has been thought to be unusual as they are expected to be stable due to 18 electron rule. They found that both osmocene and $[Ru(\eta^5-ind)_2]$ did not react with nitrogen based ligands such as aniline, pyridine, acetonitrile but the compounds underwent ring slippage by reacting with ruthenium (VI) nitride ligand (Scheme 1.3). DFT calculation explained the complexes involving $Ru^{IV}-Os^{VI}-Ru^{IV}$ and $Ru^{IV}-Ru^{VI}-Ru^{IV}$ metal interaction via metal-N multiple

bond indicating that the ruthenium (VI) nitride ligand is crucial for ring slippage due to its electrophilic character. The $\eta^5 - \eta^1$ ring slippage has been found energetically more favorable than the $\eta^5 - \eta^3$ ring slippage. The linearity of Ru-N-Os and Ru-N-Ru has been confirmed by single crystal X-ray diffraction study in both the cyclopentadienyl based ruthenium and osmium complexes

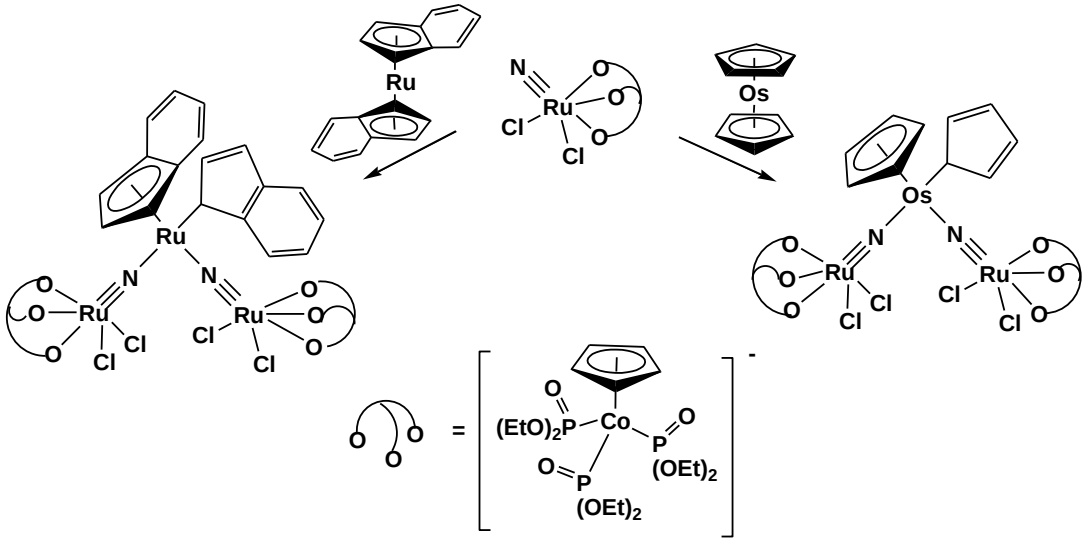

Scheme 1.4. $\eta^5 - \eta^3$ ring slippage in osmocene and ruthenium indenyl complexes

1.1.3. Classification of cyclopentadienyl complexes

A range of different metal-cyclopentadienyl complexes are known with unlike metal – carbon bonds or having diverse ligands attached to the metal center. However, in view of the extensive variety of these compounds, cyclopentadienyl complexes can be classified into the following three categories based on the type of bonding between the metals and the cyclopentadienyl moieties: a) π-complexes, b) σ-complexes and c) ionic complexes.

(a) π-complexes

In π–complexes, metals and cyclopentadienyl anions are connected through π-bonds, especially in the η^5-type coordination mode. This is the most common mode of bonding found mostly with the transition metals. η^3-type π-complexes are also known, depending on the electronic configuration of the metal centre. In this mode, three atoms are bonded to the metal as an allyl-anion ligand, and the remaining two atoms of the Cp resemble a simple alkene.

Tetraphenyl-1,5- diketones on treatment with zinc in acetic acid has formed tetraphenylcyclopentadiene (η^5-$C_5Ph_4H_2$)Fe [24] which further reacted with iron pentacarbonyl to yield (η^4-$C_5Ph_4H_2$)$Fe(CO)_3$, (η^5-C_5Ph_4H)$_2$Fe and [(η^5-C_5Ph_4H)$Fe(CO)_2$]$_2$.pi-complexes as depicted in Scheme1.5.[25] The molecular structure of the pi-complex (η^4-$C_5Ph_4H_2$)$Fe(CO)_3$ has been shown the bonding of Fe to cyclopentadiene group in a η^4 fashion and bonds between Fe and and two carbon atoms on the Cp was found to be shorter (2.03 Å -2.08 Å) than the other three carbons of the cyclopentadiene group (2.15 Å -2.25 Å).

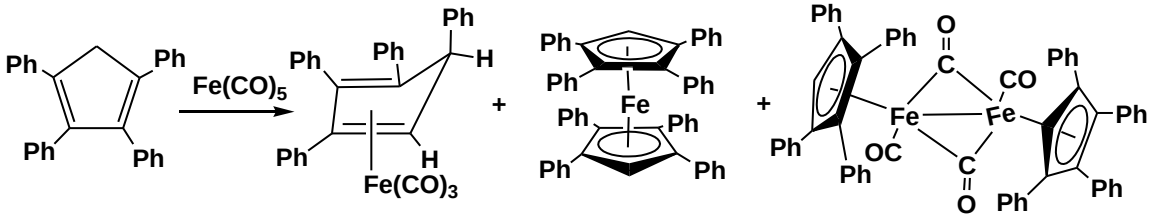

Scheme 1.5. Metal carbonyl mediated cyclization

(b) σ-complexes

σ-Complexes have a direct σ-bond between the metal and one of the carbon atoms of the cyclopentadienyl moiety. The piano-stool-type iron complex [Fe{(η^5 -C_5H_4)(η^1-C_5H_4)P(=S)Ph}{$P(OMe)_2Ph$}$_2$] where the iron atom was attached to η^5 - C_5H_5, η^1 - C_5H_4 and two $P(OMe)_2Ph$ ligands as legs has been formed by photolysis of [Fe{(η^5-C_5H_4)$_2$P(=S)Ph}] in presence of $P(OMe)_2Ph$ (Figure 1.9).[26] The ^{1}H NMR analysis

carried out for compound [Fe{(η^5 -C_5H_4)(η^1-C_5H_4)P(=S)Ph}{$P(OMe)_2Ph$}$_2$] showed peaks for the presence of CH_2 and two olefin protons of η^1-C_5H_4 ring at δ 3.09 and δ 3.22 and at δ 6.46 and δ 6.53 respectively. The piano stool structure of the complex bearing a sigma bond in between η^1-C_5H_4 group and iron atom has been further confirmed by single X-ray crystallography where the bond distance between the Fe-C (1.979 Å) was found to be shorter than that in η^5 - C_5H_5 (2.088 Å). Some of these sigma complexes having η^1-C_5H_4 moiety can lead to η^5-C_5H_4 coordination with another metal atom and considered as promising precursors for bridged heterodinuclear complexes.

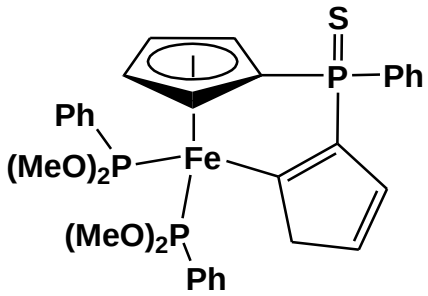

Figure 1.9. Fe(η^1 - C_5H_4) sigma complex

(c) Ionic complexes

Cp based ionic complexes mostly involves metal cations of the alkali metal and alkali earth metal. These complexes are generally synthesized by reaction of cyclopentadiene and the metal in a non- aromatic solvent like benzene and are used as precursors for a range of π-type cyclopentadienyl complexes.[27] The binding affinity of cyclopentadienyl anion with K^+ and Na^+ ions in aqueous phase has been studied by Desai et al. to separate these cations from their mixture using the cyclopentadienyl as receptor by optimizing the geometry by density functional method in half sandwich, sandwich, inversed sandwich and multidecker chain.[26] The study showed strong ionic interaction between the metal cation and cyclopentadienyl anion (Figure 1.10).

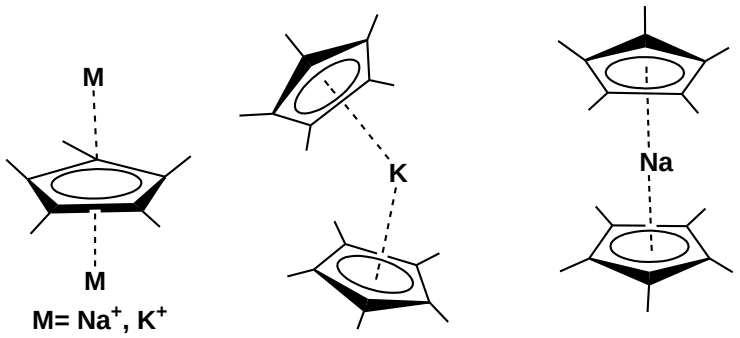

Figure 1.10. Ionic metal-Cp interation

1.2. Structural variety of metal cyclopentadienyl complex

Different types of structural framework for metal – cyclopentadienyl units are known in the literature and shows diverse properties depending upon the structural integrity. Some of the general types of metal complexes containing the Cp ligand are shown in the Figure 1.11. Metallocenes or "sandwich" compounds (Cp_2M) in which the metal remains in between the two cyclopentadienyl moieties are among the widely recognized complexes. The two cyclopentadienyl rings are known to form staggered or eclipsed conformation with a range of different torsional angle. A second category contains a bent metallocene compounds (Cp_2ML_x), which have two Cp ring in non-parallel position and are slightly bent with an angle. Bent metallocenes may contain ligands attached to the metal centers along with two η^5 cyclopentadienyl group. Another category consists of a half metallocenes or half sandwich complexes (CpMLy), sometimes also referred to as "piano stool" complexes. These complexes have one η^5 - cyclopentadienyl moiety bonded to the metal unit, while the other half contains different other ligands linked to the metal atom. Depending upon the number of ligands, L, bound to the metal center, the complex can be named as two leg, three leg etc piano stool (or half sandwich) complexes. In addition, bimetallic, multimetallic half sandwich compounds and multi-decker compounds containing (Cp_xM_y) are also well known. Bimetallic and multimetallic half sandwich compounds have more than one metal-Cp

fragment bound together by one or more than one metal –metal bonds. Such system has been categorized as a different area of metal complexes, usually referred to as metal cluster complexes. Multi-decker type of compounds are relatively less known than other metal cp complexes but requires prime attention because of their unique structural identity and complicated synthetic processes.

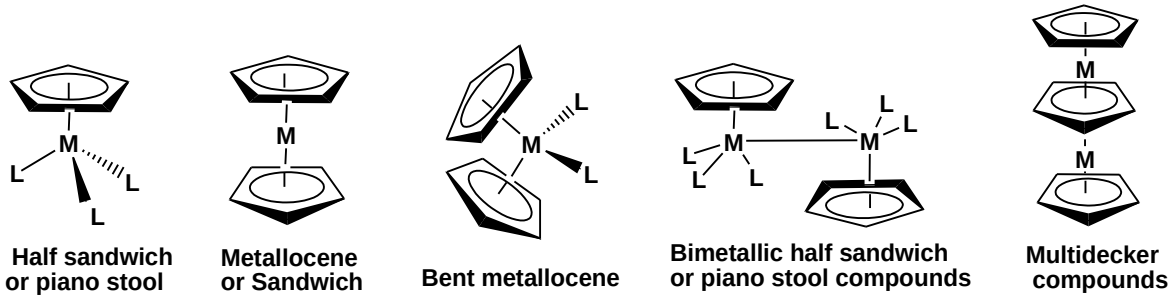

Figure 1.11. Structural varieties of Cp based metal complexes

1.2.1. Half sandwich and Piano stool complexes

Half sandwich or piano stool compounds are organometallic complexes containing cyclic polyhapto ligand attached to a ML_n centre, with the general formula $((\eta^x\text{-}C_5H_5)ML_n)$ in which the number (n) of unidentate ligands L may vary from one to four and the heptacity may be 5 or 3. Half sandwich compounds containing cyclopentadienyl group are also called 2-, 3- or 4- legged piano stools depending upon the number of ancillary ligands, with the Cp being regarded as the seat and the other ligands as the legs. Ligand, L is usually a 2-electron anionic or neutral ligand like CO, PR_3, Cl etc. In the last two decades, a range of half sandwich compounds with C5 and C6 carbocyclic rings with a variety of ligands have been synthesized which showed remarkable properties, structural variety and reactivity. However, our discussion will only be concentrated on half sandwiches containing cyclopentadienyl (C5) carbocyclic rings to suit the title of the report.

Simple half sandwich complexes, like $[(\eta^5\text{-}C_5H_5)M(CO)_3Cl]$, (M= Mo, W) have been prepared by a mutistep reaction process using CpNa and $M(CO)_6$ under thermolytic conditions. Cyclopentadienyl metalcarbonyl halide complexes of the type $[CpM(CO)_nX]$ are used as precursor molecule for a variety of representative reaction to incorporate groups like alkyl, olefine, alkynyl etc. Some of these complexes of iron and ruthenium are also prepared by the cleavage of their dimers, $[(\eta^5\text{-}C_5H_5)M(CO)_2]_2$ with halogen or using photochemical reaction condition in presence of halogenated hydrocarbons.[28-33]

A variety of half sandwich derivatives having interesting coordination features have been synthesized from cyclopentadienyl metalcarbonyl halide complexes. Ruthenium based piano stool compound, $[(\eta^5\text{-}C_5H_5)Ru(PPh_3)_2Cl]$ has been prepared by the addition of cyclopentadiene to the mixture of triphenylphosphine, ruthenium trichloride in ethanol.[34] Further reaction of $[(\eta^5\text{-}C_5H_5)Ru(PPh_3)_2Cl]$ and phosphine ligands (1,2-bis(diphenylphosphino)ethane, 1,1-bis(diphenylphosphino)methane) with ethanolic solution of 2-mercaptopyrimidine or 4-mercaptopyrimidine and sodium metal and gave a phosphine chelated thiolato ruthenium complex $[(\eta^5\text{-}C_5H_4)Ru(Ph_2P\text{-}(CH_2)_n\text{-}P\ Ph_2)\text{-}4\text{-}S\text{-}(C_6H_4N)]$ and $[(\eta^5\text{-}C_5H_4)Ru(Ph_2P\text{-}(CH_2)_n\text{-}P\ Ph_2)_2\text{-}4\text{-}S\text{-}(C_6H_3N_2)]$ in which the half sandwich CpRu framework was retained, while a heterocycle based thiolato moiety gets attached to the ruthenium centre as confirmed by single X-ray crystallography (Scheme1.6). [35] Presence of a bidentate diphosphine group attached to the ruthenium atom has variable spacers, which regulates the P-Ru-P bond angle. Metal complex $[(\eta^5\text{-}C_5H_4)Ru(Ph_2P\text{-}CH_2\text{-}P\ Ph_2)\text{-}4\text{-}S\text{-}(C_6H_4N)]$ with n = 1, having a four membered Ru-P-C-P ring reveals a strained system with P-Ru-P bond angle of 71º in comparison to that of five membered ring complex.

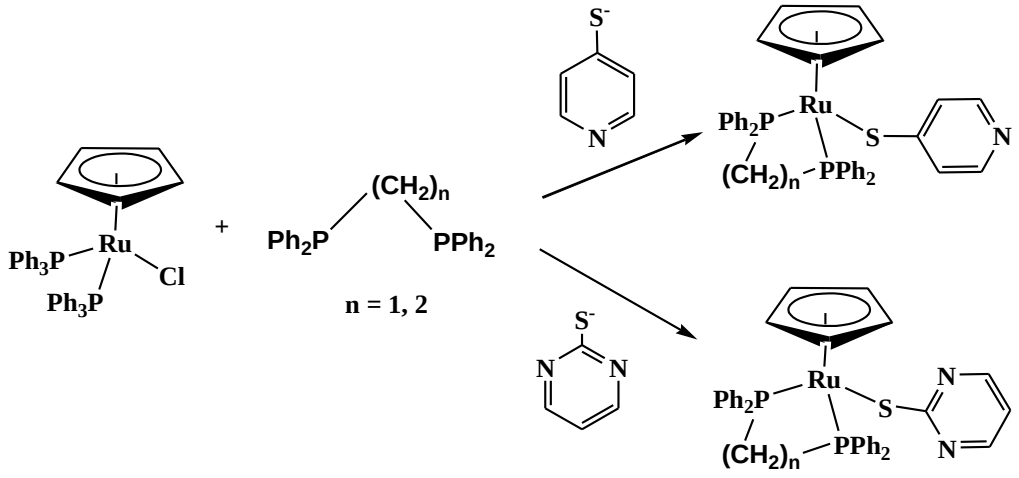

Scheme 1.6. Diphosphine substituted ruthenium half sandwich complexes

Substitution on the cyclopentadienyl ring and formation of a chelated ring system attached to the metal has the potential to impart remarkable effect on chemical and biological activities of the organometallic complexes.[36-40] Therefore, a large of the research has been concentrated on substitution of the cyclopentadienyl ring and on the variation of the ligand attached to the metal center. Systematic derivatization leads to useful molecules with unique structural behavior and photophysical properties.

Recently, photolytic properties of a bifunctionalized monosubstituted cymantrenyl complex, $[(CO)_3Mn\{\eta^5\text{-}(C_5H_4)CH(O\text{-allyl})(CH_2\text{-}C_5H_4N)\}]$, containing an allyl fragment and N- donating pyridine group has been explored.[41] Compound $[(CO)_3Mn\{\eta^5\text{-}(C_5H_4)CH(O\text{-allyl})(CH_2\text{-}C_5H_4N)\}]$ was prepared by reaction of α-picoline with n-butyllithium and subsequent reaction with cymantrenecarbaldehyde, followed by alkylation reaction with allyl bromide. Irradiation of the bifunctionalized cymantrenyl derivative led to the formation of two structurally different molecules obtained by decarbonylation and subsequent binding of pyridine or allylic group to the manganese metal center. A six membered chelate ring involving either manganese – nitrogen bond or manganese – olefin pi- bond was formed and has been observed to undergo photoinduced linkage isomerization (Scheme 1.7).

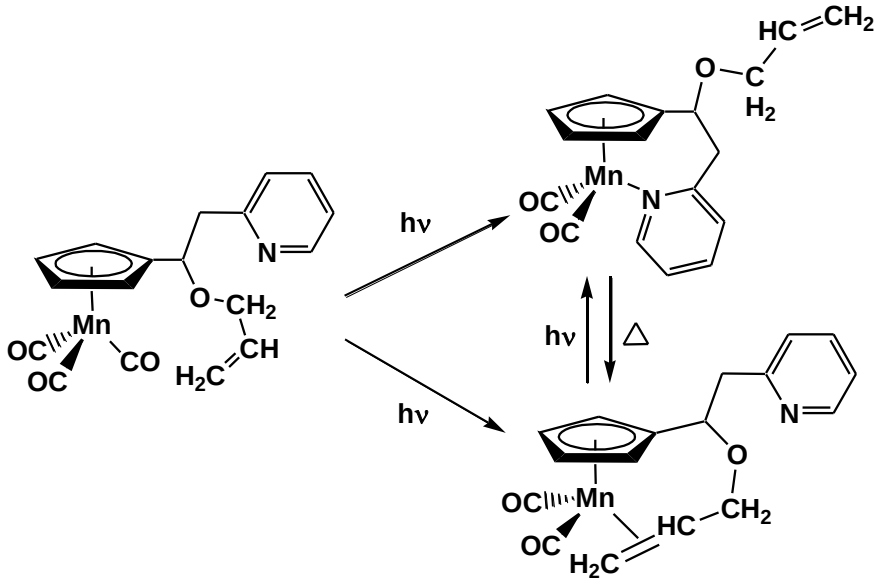

Scheme 1.7. Photolytic behavior of bifunctionalized cymantrenyl derivative

Reaction of $[(CO)_2Co\{\eta^5\text{-}(C_5Me_4)CH_2CH_2N(CH_3)_2\}]$ with iodine in ethereal solution gave a cobalt (III) chelated complex, $[(I)_2Co\{\eta^5\text{-}(C_5Me_4)CH_2CH_2N(CH_3)_2\}]$, via the non-chelated intermediate, $[\{I_2(CO)Co\{\eta^5\text{-}(C_5Me_4)CH_2CH_2N(CH_3)_2\}]$.[42] The formation of the metal-chelate ring between the Cp* and $N(CH_3)_2$ result in downfield shift of the ethyl proton in ^1H NMR compared to that of the reactant due to the different environment caused by the chelate formation. The structural analysis showed the presence of four methyl groups and a side chain, $(CH_2)_2N(CH_3)_2$, attached to the cyclopentadienyl ring. The central cobalt atom is bonded to the cyclopentadienyl ring in η^5 mode and coordinated to the amine group of the side chain with a Co-N bond distance of 2.115 Å and two iodides with Co-I bond distances of 2.630 Å and 2.613 Å.

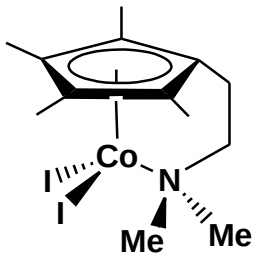

Figure 1.12. Cobalt N-chelated half sandwich complex

A O-chelated five membered ring complex, $[Cl_3Ti\{\eta^5\text{-}(C_5H_4)CH_2CH_2O(Me)\}]$ has been synthesized from$[Cl_2Ti\{\eta^5\text{-}(C_5H_4)CH_2CH_2O(Me)\}]$, thionyl chloride and sulfuryl chloride.[43] The ethereal oxygen atom attached to the side chain of Cp coordinates with titanium metal centre forming a five membered O-chelate ring having a Ti-O bond length of 2.214 Å (Figure 1.13). Two independent molecules in the asymmetric unit cell with the sterically free titanium metal (II) were able to form chelate with the substituted cyclopentadienyl moiety itself.

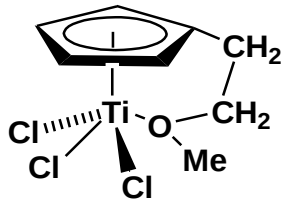

Figure 1.13. Titanium O-chelated half sandwich complex

Piano stool complexes are also regarded as a type of half sandwich complexes having a general formula ($CpML_n$), where Cp is regarded as the seat and the ligands, L, as the legs of the stool where n can be two to four. A large variety of such complexes has been known and shows interesting reactivity and electrochemical properties. $[CpFe(CO)_2(I)]$ reacted with MeS (MeS= 1,3-bis(2,4,6-trimethylphenyl)imidazol-2-ylidene) followed by the addition of dichloromethane to give the [CpFe(CO)(MeS)I] through the ionic intermediate $[CpFe(CO)_2MeS]^+I^-$.[44] Molecular structure of the pianostool compound [CpFe(CO)(MeS)I] has been revealed the presence of a Fe atom attached with a Cp ring, carbonyl carbon, Iodine atom and to a heterocyclic imidazole carbene atom. The bond length 1.641 Å of Fe-C(O) has found to be shorter than that of Fe-C bond distances (1.71 - 1.76 Å) of piano-stool compounds which indicated the increase of Fe-CO pi- back bonding due to the presence of electron rich heterocyclic carbene ligand. Further investigation using cyclic voltammetry also showed the lower oxidation potential of [CpFe(CO)(MeS)I] at 0.416 V compared to that of similar type substituted phenyl derivative $[CpFe(CO)(PPh_3)I]$ (0.69 V). [42]

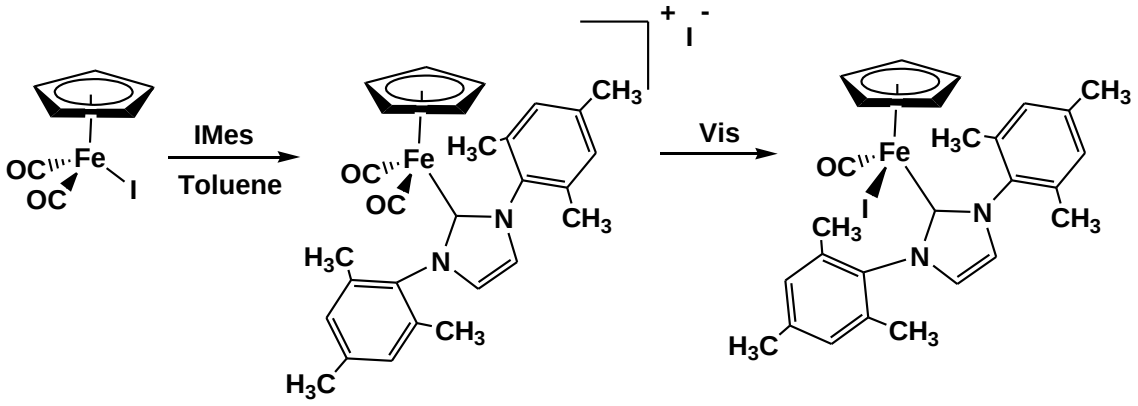

Scheme 1.8. Synthesis of [CpFe(CO)(MeS)I], L= 1,3-bis(2,4,6-Me_3Ph)-$N_2C_3H_4$

A half sandwich based heteronuclear cluster compound [(η^5-C_5H_5)M(η^1–CCPh) (CO)$Fe_2(CO)_6(\mu_3$-E)$_2$], (M= Mo, W; E= Se, Te) has been synthesized by the reaction of iron chalcogenide, [$Fe_3(CO)_9(\mu_3$-E)$_2$] with a metal acetylide [(η^5-C_5H_5)M$(CO)_3$(CCPh)] in presence of trimethylamine-oxide.[45] The structural analysis revealed a unique cluster-acetylide type of compound with distorted square pyramidal core, Fe_2MoSe_2, and the presence of a cyclopentadienyl ring and an acetylide group attached to the molybdenum metal centre. The metals obey 18 electron rule when the bridged chalcogens were considered as 4-electron donor species. The molecule has shown its potential to react with unsaturated metallic fragments to ligate with the pi electrons of the alkyne moiety resulting in the growth of the cluster framework.

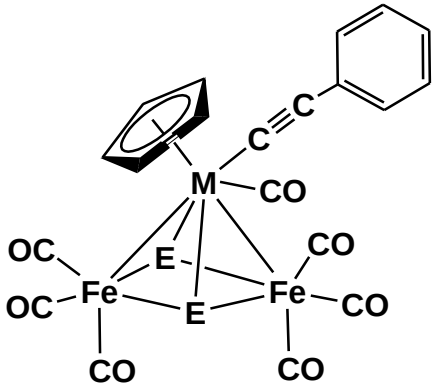

Figure 1.14. Half sandwich heterometallic cluster

Some half sandwich moieties are known to support the formation of unique fragments, which are otherwise difficult to stabilize. Species containing group 15 and 16 elements are one of rare combination which requires special metallic framework to stabilize different types of Group 15 -16 fragments. Mathur and group observed the formation of a half sandwich based trichalcogenophosphonato compounds, [{$Fe_2(CO)_6$}(μ_3-Y_3P){$CpCr(CO)_2$}], (Y.= S or Se) by the reaction of [$Fe_3(CO)_9(\mu_3$-$Y)_2$] (Y =.S or Se) and [$CpCr(CO)_2(\eta^3$-$P_3)$] in presence of trimethylamineoxide.[46] The trichalcogenophosphonato compound contains a rarely known -PY_3 fragment (with two P-Y and one P═Y) stabilized in between the cluster and half sandwich framework. The ^{31}P NMR for the compound showed a phosphorus peak at 230-261 region, while proton NMR showed a very distinct splitting of Cp protons into doublet due to the coupling of Cp protons with the Phosphorus atom. Single crystal X-ray diffraction study revealed the unique Group 15 -16 fragment, PY_3, attached to Fe_2CO_6 unit at one end and $CpCr(CO)_2$ half sandwich moiety at the other end. The structural analysis also showed the presence of two long (2.11 – 2.29 Å) and one short (1.978 – 2.133Å) P-Y bonds of the stable PY_3 fragment.

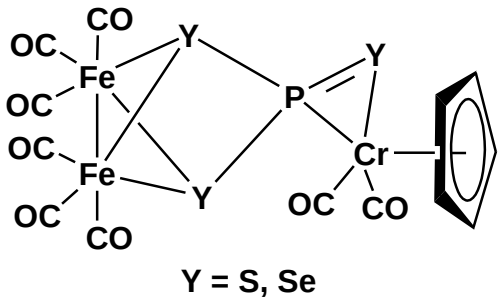

Figure 1.15. [{$Fe_2(CO)_6$}(μ_3-Y_3P){$CpCr(CO)_2$}]

1.2.2. Sandwich complexes

When the two cyclopentadienyl rings are parallel to each other with the metal atom in between, then the complex is known as sandwich compound. Metallocenes are

the unique class of sandwich compounds with the general formula $(C_5H_5)_2M$ or Cp_2M, where two cyclopentadienyl anions (Cp, which is $C_5H_5^-$) are bound to a metal center (M) in +2 oxidation state. The first sandwich structure was obtained for ferrocene in 1952 by Wilkinson and Woodward in which two Cp rings are perfectly parallel to each other and bound to iron atom through pi bonds having aromatic character and found to be highly stable due to 18 electron rule.[2] Synthetic study of sandwich complexes with other transition metals opens up a route to organometallic chemistry of different pi complexes. The ability of sandwich or metallocene complexes to exist in different oxidation states having variable number of valence electrons makes them an exceptional molecule from the other families of inorganic and organometallic complexes. The different oxidation states are characterized by cyclic voltammetry techniques where each of the oxidation state indicates different wave or peak. Metallocenes with their magnetic behavior, charge transfer property and redox behavoiur makes them unique from the other organometallic complexes.[47 - 49] Metallocenes with various metal atoms like chromium, iron, cobalt and nickel have been well studied for their diverse reactivity and could well be suited for variety of applications. Importantly, the steric and electronic properties of these metallocenes can be suitably tuned by the variation of the substituents on the cyclopentadienyl ring. The influences of alkyl or silyl substituents on the steric and electronic properties of the metallocenes can by itself lead to significant information for several future applications. However, synthetic strategies to prepare substituited metallocenes are still not very well known except for ferrocene compound. A recent synthetic strategy shows that the reaction of sodium 2, 3-diisopropyl-1,4-dimethyl-cyclopentadienide with $[MBr_2(dimethoxyethane)]$ (M = Fe, Co, Ni) at room temperature gave the corresponding ferrocene, cobaltocene and nickelocene compounds (Scheme 1.9).[50]

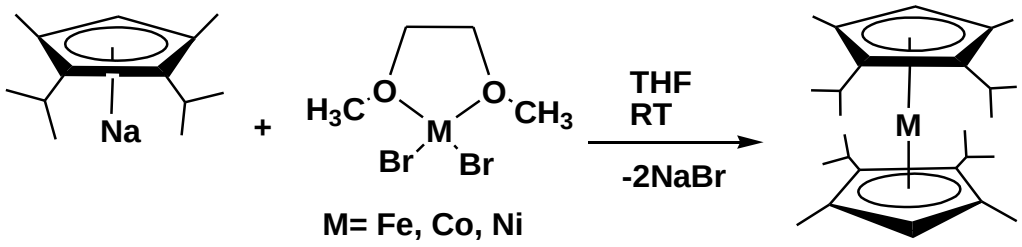

Scheme 1.9. Synthesis of substituted metallocenes

Ruthenium chloride with acetylacetonate and potassium bicarbonate has afforded ruthenium(III) acetylacetonate which on further treatment with cyclopentadienyl magnesium bromide has yielded ruthenocene.[51] Reaction of ruthenocene with substituted arenes has given mixed sandwich type compounds (Scheme 1.10).[52]

R = H, CH_3, Ph, Cl

Scheme 1.10

1.2.3. Other variety of metallocenes

Metallametallocenes are the compounds in which one or both the Cp rings are replaced by metallacyclopentadienyl group. The first metallametallocene was reported in 1972 which was a cobalt derivative synthesised by the photolysis of photo-l-pyrone and cyclopentadienyl cobalt dicarbonyl through the intermediate product cyclobutadiene (cyclopentadienyl) cobalt (Scheme 1.11).[53]

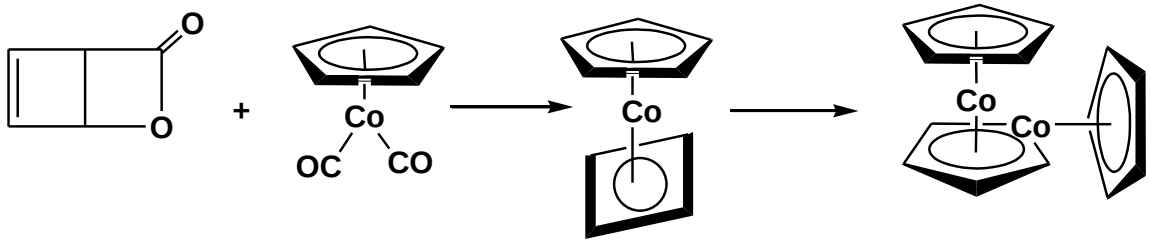

Scheme 1.11

Buchalski and co-workers have synthesized some dinickel metallocene complexes of iron, cobalt and nickel.[54] The X-ray single crystal structure revealed the presence of

two nickel based metallacyclopentadienyl groups bonded to metal ion in sandwich type framework. Zeng et al. have reported the theoretical study of these nickel metallocenes and found that the spin states of these metallametallocenes are similar to that of the metallocenes. Similar, metallametallocenes with fused benzene rings has also been syntheized and showed sandwich type structure as shown in Figure 1.16.

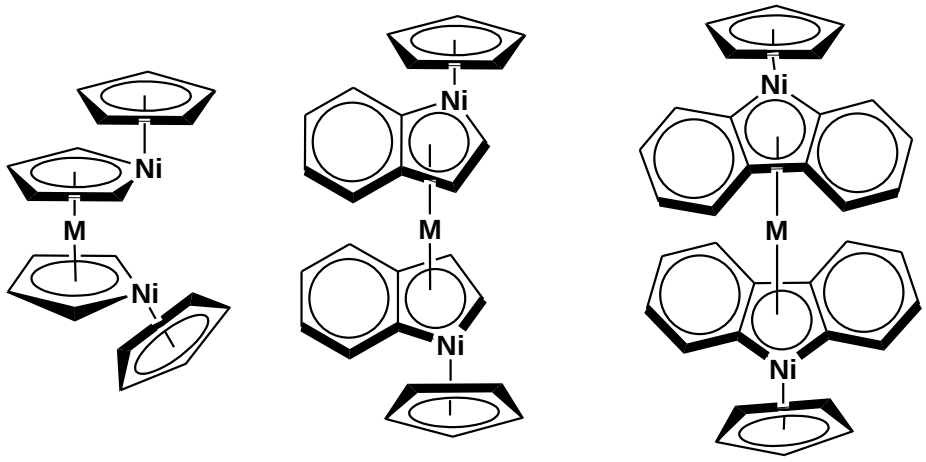

Figure 1.16. Metallametallocenes

Room temperature reaction of iron(II) acetylacetonate and $Li_2C_8Me_6$ has been carried out to afford the homoleptic bis(permethylpentalene)diiron, $[\{(CH_3)_6)C_8\}_2Fe_2]$ (Figure 1.17).[55] Presence of two fused cyclopentadienyl rings, almost parallel with each other were found from the molecular structure of $[\{(CH_3)_6)C_8\}_2Fe_2]$ with a Fe-Fe bond distance of 2.3175 Å.

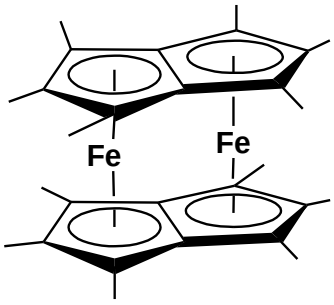

Figure 1.17. Bis(permethylpentalene)diiron metallocene

1.2.4. Bent metallocenes

In bent metallocenes (Cp_2ML_x), the ring systems coordinated to the metal are not parallel, but are tilted at an angle where the L-M-L angle depends on the electron count of the complex and the substituents on the cyclopentadienyl ring avoiding the steric interference between the groups. In a d^2-complex, molybdocene dichloride (Cp_2MoCl_2), the Cl-Mo-Cl angle is 82° whereas, in d^1 complex, niobocene dichloride, this angle is more open at 85.6°. The d^0-complex zirconocene dichloride has an angle which is even more open at 92.1°.[56] In these compounds, the number of ligands (x) may vary from one to three. A common example of a bent metallocene complex is titanocene dichloride **(**Cp_2TiCl_2) which has showed remarkable biological properties and is the first metallocene to undergo clinical trial. A large number of titanium based bent metallocenes are known in the literature and shows a variety of properties related to catalysis, biological and material. Recently, Semproni and coworkers have showed the reduction of the 1,3-disubstituted titanocene complexes to their corresponding titanocene dinitrogen compounds $[(\eta^5\text{-}C_5H_3\text{-}1\text{-}iPr\text{-}3\text{-}R)_2Ti]_2(\mu_2,\eta^2,\eta^2\text{-}N_2)]$ where R = Me or isopropyl (Scheme 1.12).[57] Single crystal study of the titanocene dinitrogen compounds showed the presence of an inversion centre at the center of the dinitrogen fragment and also the existence of meso isomer in $[(\eta^5\text{-}C_5H_3\text{-}1\text{-}iPr\text{-}3\text{-}Me)_2Ti]_2(\mu_2,\eta^2,\eta^2\text{-}N_2)]$ compound.

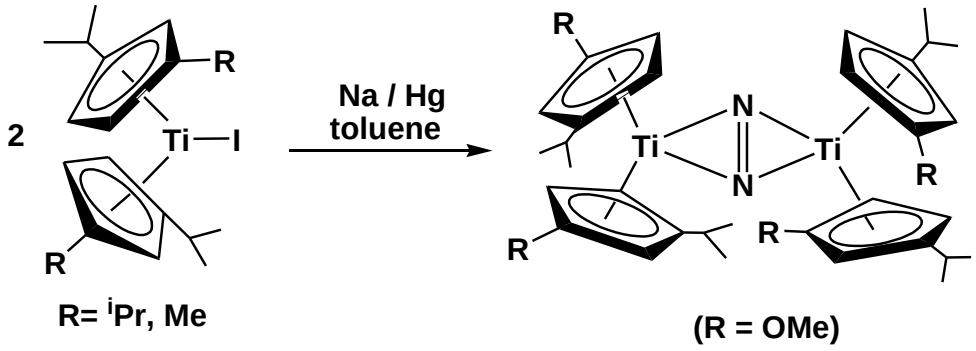

Scheme 1.12. Synthesis of titanocene based dinitrogen compounds

1.2.5. Bimetallic cyclopentadienyl complexes

Cyclopentadienyl based bimetallic organometallic compounds having the general formula ($Cp_2MM'L_x$) are compounds with two metals attached to each other by metal-metal bonds and also linked to Cp and other ligands. When the metals are identical then it is known as homobimetallic compounds and heterometallic when the metals are different. In complexes with metal-metal bonds, each of the two metals has dz^2, dxy, dxz, dyz and dx^2-y^2 orbitals involved in the interaction with its neighbor. A coaxial (σ) interaction and eventually two lateral (π and δ) interactions result depending upon on the number of valence electrons available in these d-orbitals. The d_z^2 orbital of each metal coaxially overlap to make the σ bond whereas d_{xz} and d_{yz} orbitals of each metal can laterally overlap to give rise to π bonds. The d_{xy} and $d_{x^2-y^2}$ orbitals can overlap according to lateral mode to form the δ bond (Figure 1.18).

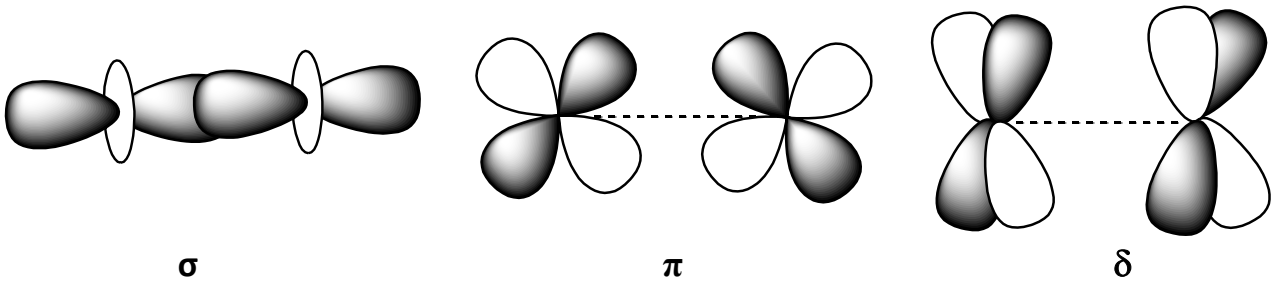

Figure 1.18. Metal- Metal bond interaction

Reaction of nickelocene with pentacarbonyliron in benzene yielded tricarbonylcyclopenta- dienylnickel-cyclopentadienyliron. Photolysis of [(η^5-C_5H_5)$Co(CO)_2$] resulted in [(η^5- C_5H_5)Co(CO)] which reacted with the excess [(η^5-C_5H_5)$Co(CO)_2$] to give [(η^5- C_5H_5)$_2Co_2(CO)_3$] or dimerised to give [(η^5-C_5H_5)$_2Co_2(CO)_2$]. Infrared spectroscopy of [$Cp_2Co_2(CO)_2(\mu$-CO)] has shown absorption at 1965 cm^{-1} and 1814 cm^{-1} for the presence of terminal and bridging metal carbonyls. The density functional theory of heterometallic binuclear cyclopentadienyl iron nickel

carbonyl compound $[Cp_2Fe(CO)Ni(\mu\text{-}CO)_2]$ has shown a coaxial structure with two bridging carbonyl compounds and one terminal carbonyl. However, the isoelectronic $[Cp_2Co_2(CO)_3]$ compound has two different structures, namely $[Cp_2Co_2(CO)_2(\mu\text{-}CO)]$ with a single bridging carbonyl and $[Cp_2Co_2(\mu\text{-}CO)_3]$ with all three carbonyl groups in bridging positions.[58-60]

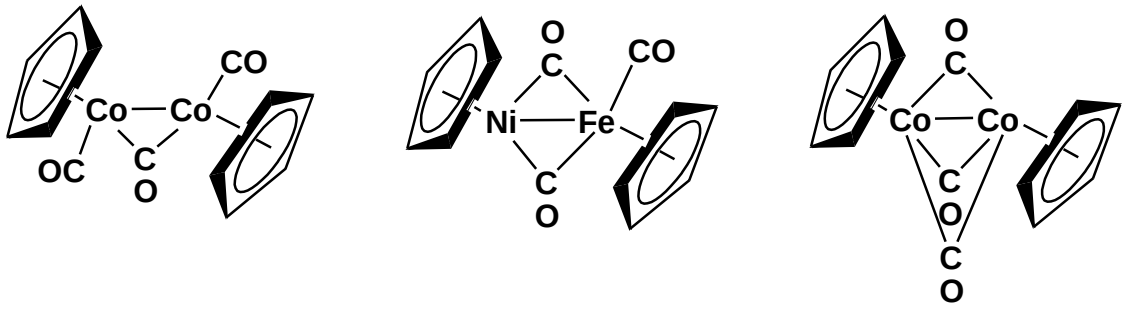

Figure 1.19. $[Cp_2Co_2(CO)_2(\mu\text{-}CO)]$, $[Cp_2Fe(CO)Ni(\mu\text{-}CO)_2]$ and $[Cp_2Co_2(\mu\text{-}CO)_3]$

Ito et al. have used density functional theory to optimize geometries of $Zn_2(\eta5\text{-}Cp^*)_2$ ($Cp^* = C_5Me_5$). The calculated dissociation energies for the metal–metal and metal–ligand bonds predict that $Zn_2(\eta5\text{-}Cp^*)_2$ is a stable complex at room temperature. Ionic bond dominates the interaction between metal atom and ligand. The Zn–Zn bond is a single bond, which is further strengthened by a weak d–d interaction.[61]

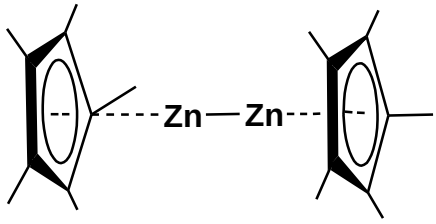

Figure 1.20. Cyclopentadienyl complex with Zn-Zn bond

Bulk electrolysis of $[Re(\eta^5\text{-}C_5R_5)(CO)_3]$ (R = H; Me) in $[NBu_4][TFAB]$ at E_{appl} = 1.4 V has formed the $[Re_2(\eta^5\text{-}C_5R_5)_2(CO)_6][TFAB]_2$ as precipitate which was washed out with dichloromethane and was filtered out. Absorption peaks in the range 1906-2062

cm^{-1} showed the presence of metal carbonyl peaks.[62] Cyclic voltammetry of [Re(η^5-C_5R_5)$(CO)_3$] (R = H; Me) in the anodic direction has given rise to a reversible one electron redox couple with $E_{1/2}$ at 1.16 V and 0.91 V for the oxidation of [Re(η^5-C_5H_5)$(CO)_3$] / [Re(η^5- C_5H_5)$(CO)_3$]$^+$ and [Re(η^5- C_5Me_5)$(CO)_3$] / [Re(η^5- C_5Me_5)$(CO)_3$]$^+$ respectively vs ferrocene / ferrocenium redox couple. Oxidation of the [Re(η^5-C_5R_5)$(CO)_3$] complex at a lower scan rate or with a higher concentration of the complex has caused the formation of an irreversible of the peak at 1.16 V or 0.91 V for Re/Re^+ with a new peak at 0.55V and 0.15V [Re(η^5- C_5H_5)$(CO)_3$] / [Re(η^5- C_5H_5)$(CO)_3$]$^+$ and [Re(η^5- C_5Me_5)$(CO)_3$] / [Re(η^5- C_5Me_5)$(CO)_3$]$^+$ respectively. The further analysis has been revealed that the extremely positive E° value at 1.16V or 0.91V corresponding to Re to Re^+ in both the complexes made the system to behave as stronger oxidizing agent and forming the dimeric dication $[Re_2(C_5R_5)_2(CO)_6]^{2+}$ which was further produced the irreversible cathodic peaks at 0.55V or at 0.15V for the reduction of the $[Re_2(C_5R_5)_2(CO)_6]^{2+}$ / [Re(□^{5}- C_5R_5)$(CO)_3$]. The weakly metal-metal (Re-Re) bonded dication $[Re_2Cp_2(CO)_6]^{2+}$ can be tuned to store and release the powerful one-electron oxidant $[ReCp(CO)_3]^+$.

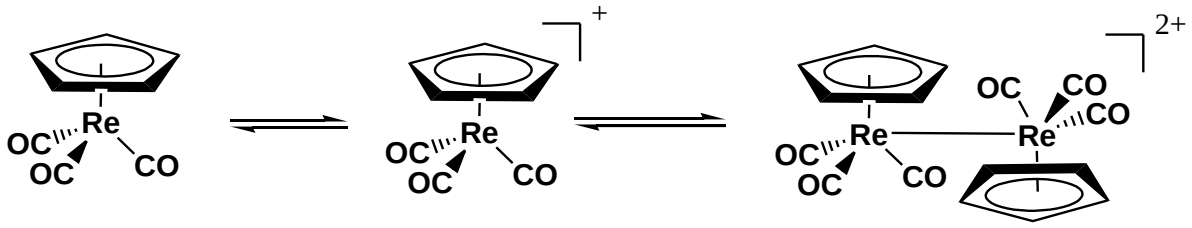

Scheme 1.13. Synthesis of $[Re_2(C_5R_5)_2(CO)_6]^{2+}$

The infrared and raman spectroscopy for the bimetallic $[Cp_2Ni_2(CO)_2]$, $[Cp_2Fe_2(CO)_4]$ (cis and trans forms), and $[Cp_2M_2(CO)_6]$ (M = Mo, W) complexes have been studied and compared to metallocene.[63] Comparison of the spectra shows a common vibrational pattern of the infrared modes, with minor variations in frequency and intensity, which permits the establishment of a vibrational fingerprint of general validity. The spectral patterns are apparently more complicated than the fingerprint scheme. However, the basic features are easily interpreted on this basis.

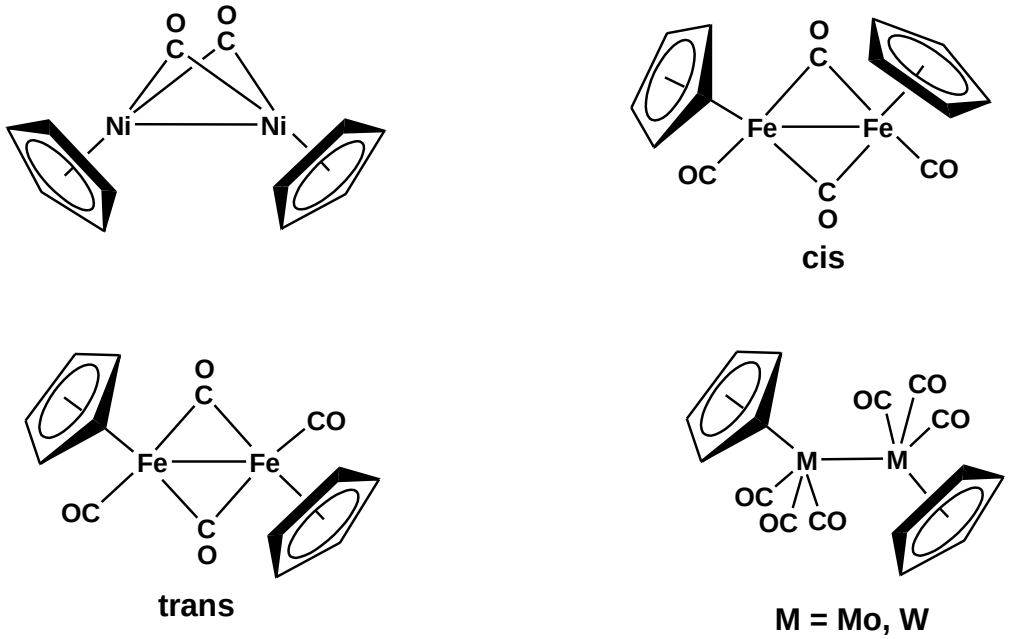

Figure 1.21. $[Cp_2Ni_2(\mu\text{-}CO)_2]$, cis- ,trans-$[Cp_2Fe_2(\mu\text{-}CO)_2(CO)_2]$ and $[Cp_2M_2(CO)_6]$ (M = Mo, W)

1.2.6. Multimetallic cyclopentadienyl complexes

In multimetallic organometallic compounds more than two metals are present with metal-metal bonds. The metal present can be similar or different. Triangular shaped heterotrimetallic polyhydrido complexes containing group 6 and group 8 metals $[(Cp'Ru)_2(Cp'M)(\mu\text{-}H)_5]$ (M= Mo, W) have been synthesized by the reaction of dimeric ruthenium methoxo complex $(Cp'RuOMe)_2$ with dinuclear metal polyhydrido complexes $[Cp'Ru(\mu\text{-}H)_3MH_3Cp']$ as shown in Scheme 1.14 .[64] Molecular structure of these complexes have shown similar triangular metal cores having two short M-M bonds in the range 2.5-2.6 Å bridged by the two hydrido ligands and one long M-M bond of 3.0-3.1 Å bridged by a single hydride ligand. The planes of the $[C_5(CH_3)_5]$ or $[C_5(C_2H_5)(CH_3)_4]$ have been found almost perpendicular to the triangular Ru-Ru-M plane.

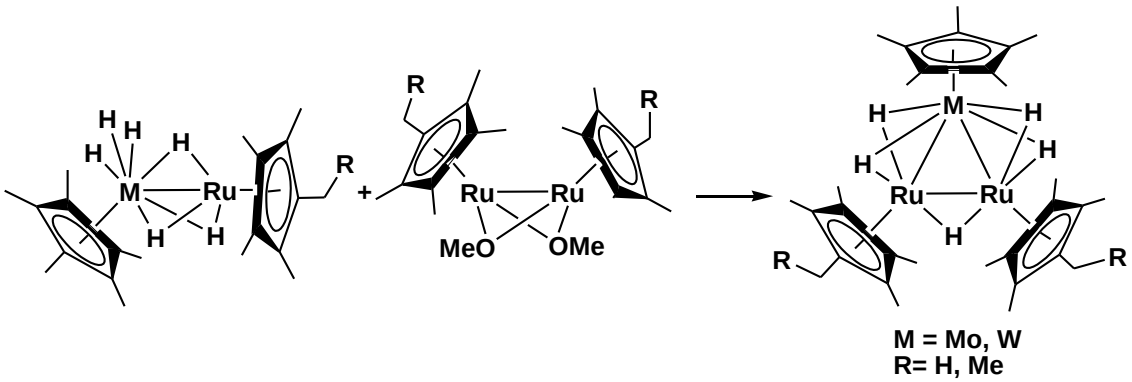

Scheme 1.14. Synthesis of $[(Cp'Ru)_2(Cp'M)(\mu\text{-}H)_5]$ (M= Mo, W)

1.2.7. Multidecker sandwich compounds

Two or more than two metals are stacked through three or more than three Cp rings in multidecker sandwich compounds (Cp_xM_y). The metal linkers can be same or different in these compounds. In these multidecker complexes, the Cp rings may be parallel to each other or may be tilted. $[Ni_2Cp_3]^+$ was the first triple-decker sandwich having 34 valence electrons discovered by Werner and Salzer in 1972 (Figure 1.22).[65] A variety of triple decker and multi decker sandwich compounds were synthesized after that.

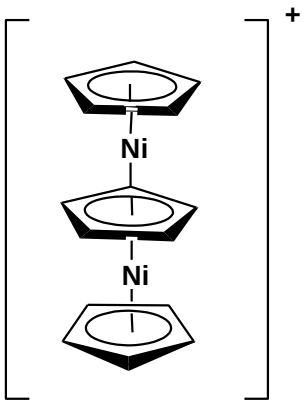

Figure 1.22. $[Ni_2Cp_3]^+$

Equimolar amount of ferrocene and $GaCl_3$ in benzene has been yielded in the blue-green solution of $[(C_5H_5)_2Fe][GaCl_4]$ which was further evaporated to give red coloured multidecker sandwich compound containing Ga(I) and Fe(II) ions in alternating array and stacked between cyclopentadienyl moieties, confirmed by XRD study. The molecular structure also revealed the coordination of Ga(I) to two $[GaCl_4]^-$ and two cyclopentadienyl group and presence of η5-coordination in between each Ga(I) and the cyclopentadienyl moiety of two different ferrocene molecule.[66]

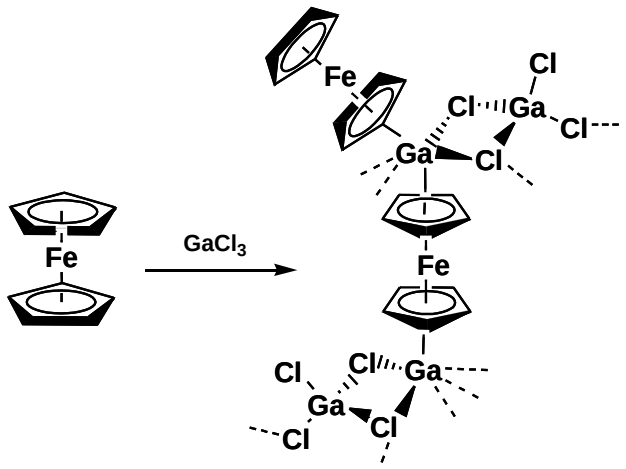

Scheme 1.15. Heterometallic multidecker compound

$[(\eta^5\text{-}C_5H_5)Tl(\mu^5\text{-}C_5H_5)Tl(\eta^5\text{-}C_5H_5)]$- $[Li(12\text{-crown-}4)_2]^+$. thf has been synthesized from $[(\eta^5\text{-}C_5H_5)Tl]$, $[(C_5H_5)Li]$ and 12-crown-4 in 2:1:2 equivalent to obtain a triple decker sandwich compound in its anionic form (Figure 1.23).[67] The molecular structure has been revealed the presence of two Tl atoms stacked in between three cyclopentadienyl rings and were placed symmetrically by a bridged $(\mu^5\text{-}C_5H_5)$ group and each of the Tl atom has made a bond angle 133-135A^0 with the adjacent two Cp rings.

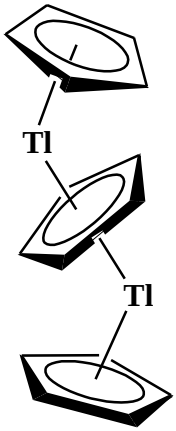

Figure 1.23. $[(\eta^5\text{-}C_5H_5)Tl(\mu^5\text{-}C_5H_5)Tl(\eta^5\text{-}C_5H_5)]$

1.3. Cymantrene based organometallic compounds

Half sandwich cyclopentadienyl tricarbonylmanganese $[(\eta^5\text{-}C_5H_5)Mn(CO)_3]$ commonly known as cymantrene is a significant metal carbonyl compound in organometallic synthetic chemistry. Cymantrene is an important precursor for the synthesis of various organometallic complexes by substitution of the protons at the Cp ring or by replacement of the carbonyl ligand attached to manganese. The metal carbonyls of the cymantrenyl fragement are known to show very sharp and distinguish peaks in the mid infrared region between 1850 cm^{-1} to 2200 cm^{-1}, a region where proteins and most organic molecules do not show any distinguishing peaks. Therefore, it is likely that some of these compounds can be used as sensitive probes or labels by infrared spectroscopy for the detection of carbonyl ligands in biological environment. Cymantrene is a stable molecule with 18 electron system and can undergo one electron redox process at relatively higher potential (0.92 V) with respect to ferrocene. Acylation and alkylation on the cyclopentadienyl ring of cymantrene via Friedel Craft method has been one of the versatile synthetic techniques to obtain large number cymantrenyl derivatives.[68]

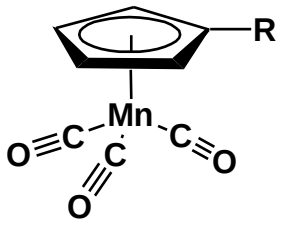

Figure 1.24. Structure of cymantrenyl derivative (R = H, organic group)

The chemistry of cymantrene and its derivatives have most recently been reported across a variety of chemical application. Methylcyclopentadienyl manganese tricarbonyl [{η^5-(C_5H_4)CH_3}$Mn(CO)_3$] has been known as antiknock agent and used in gasoline to increase the efficiency of operation of engine by reducing the engine knocking and enhancing the octane number.[69] Recently, Hamadi studied the octane enhancing properties with some of the organometallic reagents and solvents and concluded that selective blending agents can improve the octane number of the methyl substituted cymantrenyl derivative in various degrees. [70]

Photochemistry of cymantrenyl derivatives have been known from earlier days in which irradiation of light in the wavelength range 300-500 nm resulted in loss of a carbonyl ligand with the dissociation of metal –carbon bond and formation of solvated system which can be further ligated to manganese with desired group. Detail investigation revealed that irradiation of [(η^5 -C_5H_5)$Mn(CO)_3$] results in the formation of excited molecule [(η^5-C_5H_5)$Mn(CO)_3$]* which further forms an unstable 17 electron species [(η^5-C_5H_5)$Mn(CO)_2$] by the removal of one molecule of CO from the excited molecule. The electron deficient molecule [(η^5-C_5H_5)$Mn(CO)_2$] behaves as an electron acceptor and can make stable complexes by the addition of electron donating species as shown in Scheme 1.16.[71]

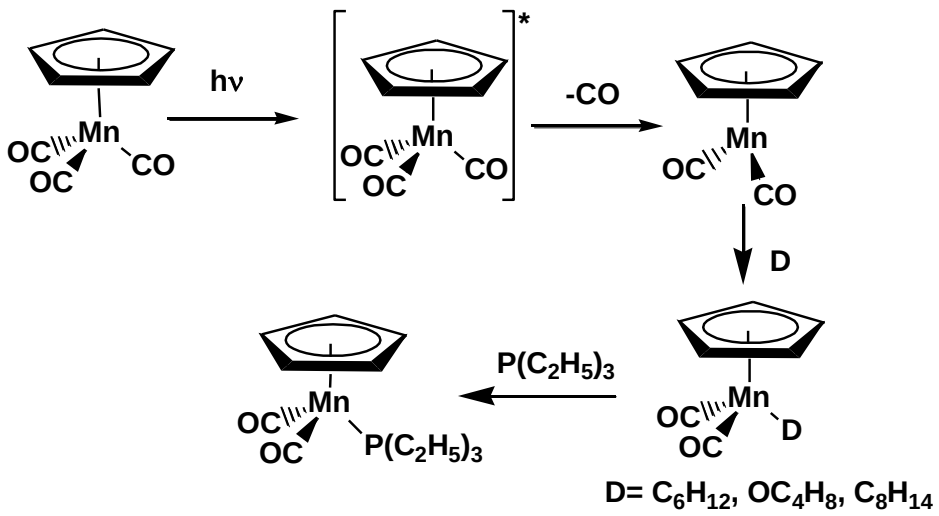

Scheme 1.16. Proposed mechanism of photolysis in $[(\eta^5\text{-}C_5H_5)Mn(CO)_3]$

In general, photolysis of $[(\eta^5\text{-}C_5H_5)Mn(CO)_3]$ carried out in solvents such as hexane (C_6H_{12}), tetrahydrofuran (OC_4H_8), cyclo-octene (C_8H_{14}) etc lead to the formation of a solvated intermediate $[(\eta^5\text{-}C_5H_5)Mn(CO)_2D]$ where D= C_6H_{12}, OC_4H_8, C_8H_{14} which further reacts with donating ligands like triethyl phosphine to give $[(\eta^5\text{-}C_5H_5)Mn(CO)_2\{P(C_2H_5)_3\}]$ (Scheme 1.17).[72] The solvent intermediates and the ligated product can be identified by the help of infrared spectroscopy. The infrared peaks for the tricarbonyl compound, $[(\eta^5\text{-}C_5H_5)Mn(CO)_3]$ comes at 2030 cm^{-1} and 1930 cm^{-1} region which on photolysis in tetrahydrofuran (OC_4H_8) and cyclo-octene (C_8H_{14}) solvents gave new peaks at 1928 cm^{-1}, 1852 cm^{-1} and 1963 cm^{-1}, 1902 cm^{-1} region due to the formation of the solvated compounds $[(\eta^5\text{-}C_5H_5)Mn(CO)_2(OC_4H_8)]$ and $[(\eta^5\text{-}C_5H_5)Mn(CO)_2(C_8H_{14})]$ respectively. Phosphine substitution also showed similar peaks at 1937 cm^{-1} and 1873 cm^{-1} for the compound $[(\eta^5\text{-}C_5H_5)Mn(CO)_2\{P(C_2H_5)_3$

The technique has been recently used in photolysis of $[(\eta^5\text{-}C_5H_5)Mn(CO)_3]$ in a biphasic system to generate hydrogen from water.[73] The method works the process of decarbonylation upon irradiation of UV light followed by coordination of a water molecule as shown in Scheme 1.25. The shorter lived and unstable $[CpMn(CO)_2(H_2O)]$ intermediate was detected by time-resolved IR spectroscopy which showed CO stretching absorption at 1862 and 1934 cm^{-1} region. The lower stability of this intermediate can be

attributed to the weaker donor ability of the oxygen atom in water which further undergoes dissociation to give hydrogen and hydrogen peroxide in the two phase systems.

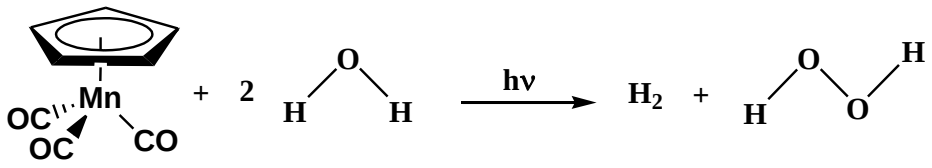

Scheme 1.17

1.3.1. Chelated Cymantrenyl complex

Cymantrene based piano stool compound are interesting molecule to form a variety of derivatives where chelation plays a vital role in providing unique structural and photophysical properties. This particular molecular system has the ability to form chelates involving the cp ring and the group ligated with the manganese centre by photochemical activation technique.

In a typical example to prepare different chelated cymantrenyl molecules, photo-irradiation of cyclopentadienyl manganese tricarbonyl [(η^5-C_5H_5)$Mn(CO)_3$] derivatives with functional groups attached to the cyclopentadienyl ring led to intramolecular chelate formation followed by the dissociation of labile metal-CO bond.

Photochemical properties of cymantrene carbamates have been explored recently to understand their chelation properties and to investigate their potential in the use of photochromic system. UV irradiation of cymantrenyl carbamates, [$(CO)_2Mn\{\eta^5$-$(C_5H_4)CH(R)N(R')(CO)(OCMe_3)\}$] synthesized by the reaction of 1-aminoethylcymantrene with di-tert-butyl- dicarbonate [74], produces a chelated compound in which the oxygen atom of the carbamate ligand is coordinated to the manganese atom. The O-chelated manganese complex reversibly transformed to the parent cymantrenyl compound in dark at room temperature condition. The O-chelated cymantrenyl compound was characterized by infrared spectroscopy with peaks in the region 1955 cm^{-1} -1855 cm^{-1} for the presence of metal carbonyls and in the range 1658 cm^{-1} -1640 cm^{-1} for the carbamate carbonyl.

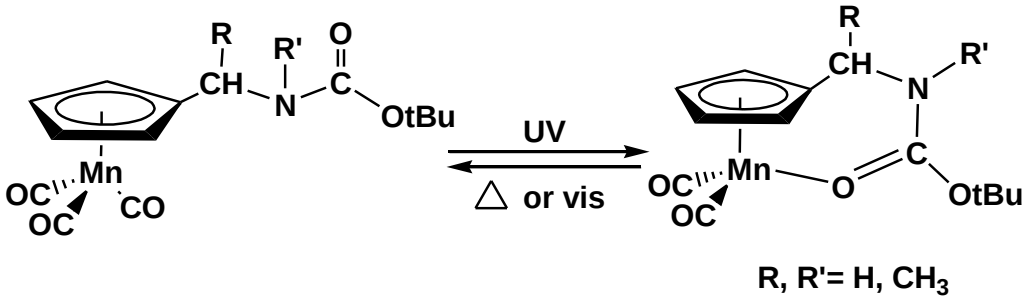

Scheme 1.18

UV irradiation of a bifunctionalized cymantrenyl compounds containing both pyridine and ketone side chains led to the formation of two different types of chelates, O- and N chelate, involving simultaneous decarbonylation.[75] However, interconversion has also been shown between the two chelated compounds using optimized reaction condition. The molecular structure of the N- chelated cymantrenyl derivative confirmed by X-ray crystallography showed the formation of six membered chelate ring involving the Cp carbon and pyridine nitrogen atom. However, irradiation of the N-chelated compound with visible light gave the O chelated cymantrenyl derivative, as shown in Scheme, which being thermally unstable isomerizes back to N- chelate isomer. DFT calculations revealed that compound with tethered, coordinated functional group is labile enough to isomerize by a low-energy pathway involving several transient intermediates.

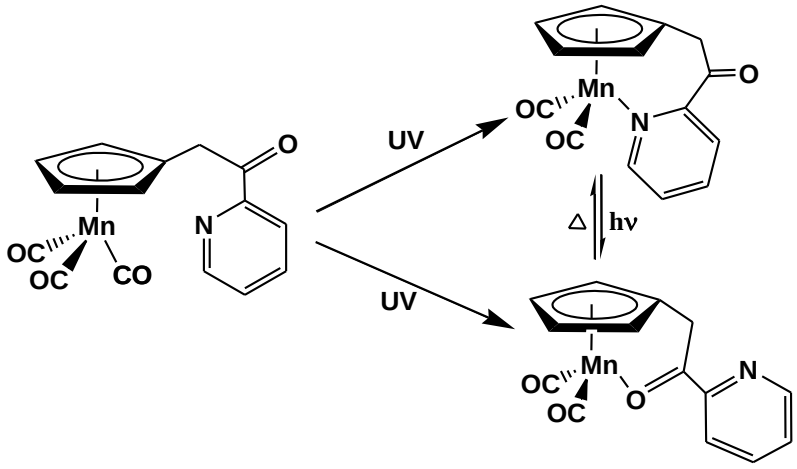

Scheme 1.19

Similar photolytic study of cymantrene based fragment with thioamide and pyridine side chain led to the formation of only S- chelated product. Presence of pyridine group attached to the side chain does not lead to any isomerization of the S- chelated as observed in the earlier case. [75]

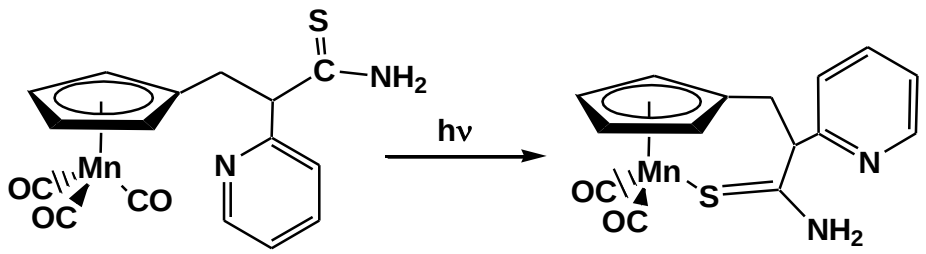

Scheme 1.20

Heilweil et. al. has been described the photo-dissociation of [{η^5-$C_5H_4(CH_2COPh)$}$Mn(CO)_3$] with a side chain having a keto group to form a O-chelated species formed by UV irradiation of the cymantrenyl derivative followed by CO dissociation from the metal centre (Scheme 1.21).[76] The unique half sandwich molecule was identified by various spectroscopic and computational techniques. Irradiation of this compound in non polar solvent changes the pale yellowish solution to a blue colored solution with the formation of a new UV-Vis. absorption peak at 635 nm. Infrared analysis showed that the peaks observed for [{η^5-$C_5H_4(CH_2COPh)$}$Mn(CO)_3$] at 2024 cm^{-1}, 1946 cm^{-1} and 1938 cm^{-1} has changed to 1948 cm^{-1} and 1887 cm^{-1} due to the formation of O-chelated compound, [{η^5-$C_5H_4(CH_2COPh)$}$Mn(CO)_2$].

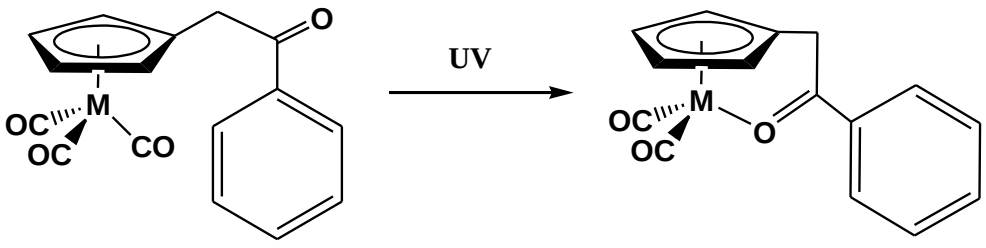

Scheme 1.21

1.3.2. Biological properties

Combination of organometallic groups and peptides together can form a number of conjugates with fascinating and altered biological properties. Particularly, when the organometallic moieties are tagged with cell-penetrating peptides that act as efficient cell delivery vehicles can serve as a new path in biological chemistry. However, conjugations of biomolecules with metal moieties are not only synthetically difficult but pose hard challenges with the standard conjugate synthesis procedures. Recently, Splith et al. have reported the preparation of some cymantrenyl-peptide bioconjugates by solid phase peptide synthetic technique and studied the influence of the linker group of the conjugates on cellular uptake and cell viability with MCF-7 breast cancer cells.[77] The promising biological activity of the cymantrenyl bioconjugates on MCF-7 breast cancer cells was assigned to the combination of functionalized cymantrenyl group with the cell penetrating peptide. In comparison, the independent cymantrenyl derivative as well as the peptide concerned has been found to be inactive towards the anticancerous activity.

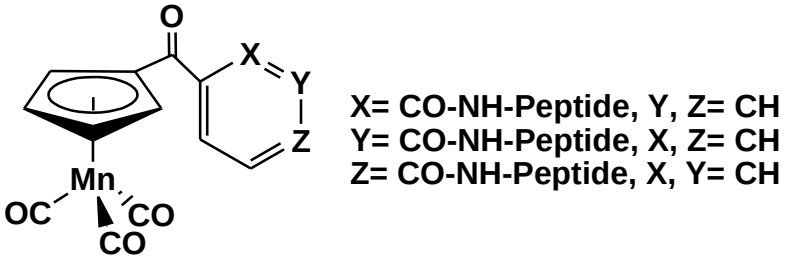

Figure 1.25

Generally, in the immunological methods biomolecules labelled by markers are used which can be detectable by some physical methods. Several such probes based on transition metal fragments have been investigated where electrochemical processes are used for detection. Recently, methyl imidate derivative of cymantrene bound to a protein bovine serum albumin (BSA) in aqueous solution has been reported by the research group of Jaouen which can able to detect the protein concentration by electrochemical reduction method.[78] Cymantrenyl imidate compound has been synthesized from formylcymantrene through two step reaction process in which the first step consist of

formation cymantrenylnitrile derivative which was transformed to the mthyl imidate compound using a base catalyzed addition of methanol. Incubation of the mixture containing methanolic cymantrenyl imidate and BSA protein in phosphate buffer for 24 hours and separation of the unbound cymantrenyl imidate from the mixture by size exclusion chromatography resulted in the formation of cymantrenyl imidate protein conjugate. Electrochemical investigation of the conjugate showed reversible one electron redox process of the cymantrenyl fragment covalently bound to the protein. The redox couple can be used to detect much lower concentration of BSA protein as compared to other traditional methods.

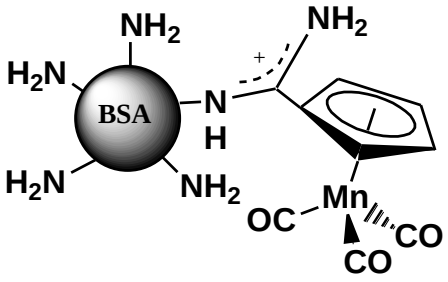

Figure 1.26

The metal carbonyls attached to manganese in the cymantrenyl derivative can be used as IR probe in biological system by strategically labeling the molecule. Fourier transform IR spectroscopy was used as a detection method, because metal carbonyl complexes display very intense and specific absorption bands in the spectral range 1800-2200 cm^{-1} due to the stretching vibration modes of the carbonyl ligands bonded to metal. To understand the feasibility for the use of transition metal carbonyl complexes as labels to perform the immunoassay of biomolecules, functionalization of peptides has been carried out by cymantrene keto carboxylic acid by microwave-assisted solid phase peptide synthesis technique.[79] The infrared bands of the cymantrenyl peptide bioconjugate showed stretching vibrational peaks at 1934 cm^{-1} and 2026 cm^{-1} region indicating the presence of metal carbonyl groups. The negative influence of the cymantrenyl peptide bioconjugate on the cell viability of MCF-7 human breast cancer cell lines was then studied which showed its potency to use as infrared probe in bioimaging of peptides.

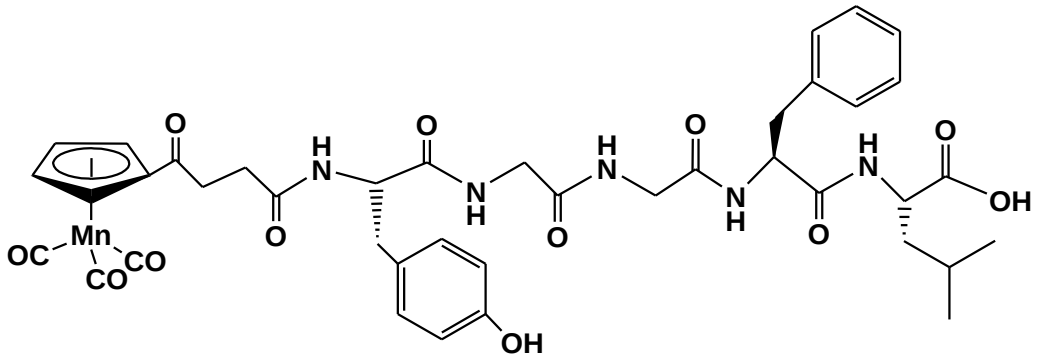

Figure 1.27. Cymantrene peptide conjugate

Recent investigation on organometallic analogues of chloroquine showed significant antimalarial activity overcoming resistance to the parent drug chloroquine. Synthesis and characterization of some cymantrenyl and cyrhetrenyl 4-aminoquinoline conjugates with amine or amide linker such as (2-(7-Chloroquinolin-4-ylamino)ethyl)-4-cymantrenylbutane amide, N-(2-(7-Chloroquinolin-4-ylamino)ethyl)-4-cyrhetrenylbutaneamide and N-(7-Chloroquinolin-4-yl)-N′-(cymantrenylmethyl)ethane-1,2- diamine have been carried out which showed promising antimalarial activity when evaluated against both chloroquine-sensitive and resistant strain of the malaria parasite *Plasmodium falciparum*.[80] The cymantrenyl complex with an amine linker showed high activity against the chloroquine-sensitive strain and was inactive against the chloroquine-resistant strain, but showed promising result against Trypanosoma brucei at a much lower concentration. Both cymantrenyl and cyrhetrenyl conjugates with amide linkage showed activity against both the chloroquine-sensitive and chloroquine resistant strain.

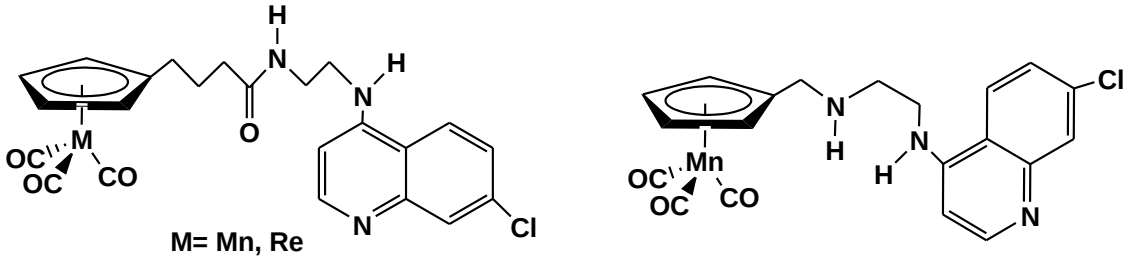

Figure 1.28. Cymantrenyl / Cyrhetrenyl-quinoline complex

1.3.3. Electrochemical properties

Cyclopentadienylmanganese tricarbonyl came into focus for its unique and rich electrochemical properties which can be tuned by various substitution and coordination techniques. However, very little has been explored on the electrochemistry of this half sandwich complex and its derivatives. The study on the anodic one-electron oxidation property of $[(\eta^5\text{-}C_5H_4R)Mn(CO)_3]$, (R=H, NH_2, CH_3) revealed the formation of 17 electron radical cation from the oxidation of the cymantrene, $[MnCp(CO)_3]$ at $E_{1/2}$= 0.92 V are persistent in solution and has been characterized spectroscopically.[81] The cation mostly absorbs in the visible wavelength at 530 nm, near-IR region at 2066 cm^{-1} and at 2118 cm^{-1} and 1934 cm^{-1} in IR regions. Similarly, $E_{1/2}$ of the radical cations for the Cp-functionalized analogues, $[Mn(\eta^5\text{-}C_5H_4NH_2)(CO)_3]$ and $[Mn(\eta^5\text{-}C_5Me_5)(CO)_3]$ were found to be 0.62 V and 0.64 V respectively by cyclic voltammetric analysis. The formation of radical cations $[Mn(\eta^5\text{-}C_5H_4NH_2)(CO)_3]^+$ and $[Mn(\eta^5\text{-}C_5Me_5)(CO)_3]^+$, was confirmed by IR spectroelectrochemistry which showed higher wavelength shift of 98 cm^{-1} and 107 cm^{-1} than that of the parent compound with colour change to green and turquoise for the formation of the respective radical cations. Single crystal X-ray studies of $[Mn(\eta^5\text{-}C_5H_4NH_2)(CO)_3]^+$ and $[Mn(\eta^5\text{-}C_5Me_5)(CO)_3]^+$ showed elongated Mn-C(O) and shortened C-O bonds displaying the effect of weaker metal-to-CO backbonding compared to that of neutral compounds.

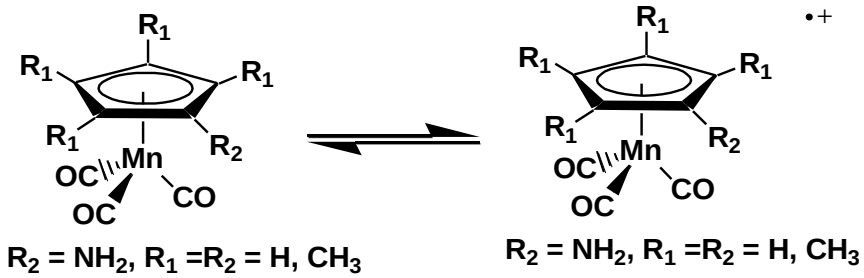

Scheme 1.22

Electrochemical property of cymantrenyl fragment was also studied with a cymantrenyl analog of tamoxifen, a well known anticancer drug, and recently known to

act via electron transfer mechanism. The finely tuned redox potentials of the cymantrenyl-tamoxifen derivative, $[Mn(CO)_3(\eta^5\text{-}C_5H_4(C_2H_5)C{=}C(C_6H_4R)_2]$ impart significantly modified electronic and redox properties to the tamoxifen backbone which may play a effective role in cancer cell inhibition study.[82] The derivative showed successive highly reversible redox processes at 0.78 V and 1.20 V due to the oxidation of the cymantrenyl fragment by cyclic voltammetry. The half-sandwich tamoxifen derivative, gives a radical cation in which the charge is delocalized between the cymantrenyl and diphenylethene moieties and undergoes facile metal-carbonyl substitution reactions. Most importantly, it is observed that the redox potentials of these systems can be readily controlled over a wide potential range by mere substitution of the metal carbonyls by donor groups.

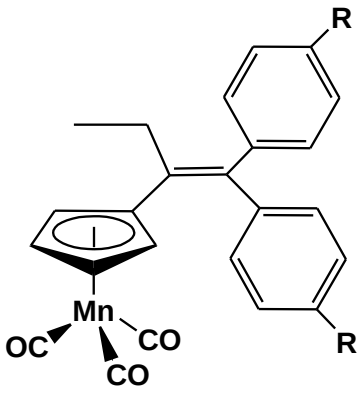

Figure 1.29

Three type of triazole linked cymantrenyl complexes, $[1\text{-}\{(\eta^5\text{–}C_5H_4)Mn(CO)_3\}\text{-}4\text{-}X\text{-}(N\text{-}N{=}N\text{-}CCH)]$, $\{R = C_6H_5, (2\text{-}NH_2\text{-}C_6H_4), (3\text{-}NH_2\text{-}C_6H_4)\}$, have been reported via "click" reaction from cupper catalyzed cycloaddition reaction of cymantrenyl azide with phenylacetelyne and ethynylanilines.[83] The structural analysis of the cymantyrenyl compounds revealed the presence of a phenyl, m-aminophenyl or p-aminophenyl moiety at the 4-position of the triazole ring. Electrochemical study by cyclic voltammetry showed two oxidation peaks in the positive potential due to Mn/Mn^+ redox couple (1.2 V – 1.4 V) and triazole / triazolium redox couple (1.55 V – 1.775 V) for all the cymantrenyl triazole based compounds

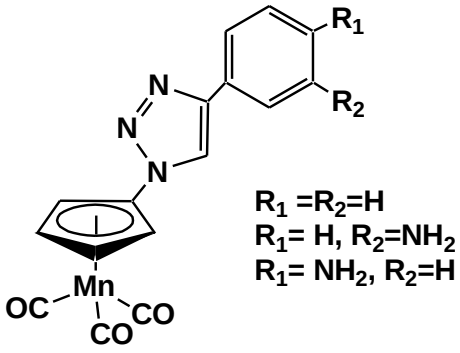

Figure 1.30. Triazole based cymantrene

1.4. Ferrocene based organometallic compounds

Ferrocene and its derivatives are the most versatile organometallic compounds because of their unique structures, chemical and thermal stabilities, reversible redox properties etc. The exclusive nature of their chemistry make them an excellent building block in several processes and their use in the field of material science, molecular wires, catalysis, molecular recognition, sensing, electronic communication, bio-conjugates and medicinal chemistry. The recent focus of ferrocenyl derivatives in application related to biological properties has generated a new field of bioorganometallic chemistry.[84-92]

The synthetic chemistry of ferrocene began in 1951 with the reaction of ferric chloride with a Grignard reagent of cyclopentadienyl magnesium bromide obtained from the synthesis of cyclopentadiene, magnesium and bromoethane in benzene.[93] However, several other methods for the preparation of ferrocene evolved in later years, the most efficient process being the use of freshly cracked cyclopentadiene reagent, deprotonated with potassium hydroxide and subsequent addition of ferric chloride solution. Recent research has been focused on the synthesis of a variety of ferrocenyl derivatives for their potential use in different field. Ferrocene and its derivatives are usually functionalized by electrophilic substitution, lithiation or via transition-metal-catalyzed C−H activation of the Cp ring to give 1,1'-ferrocenyl derivatives.[86, 94-104] The most familiar methods used for the derivatization of ferrocene are Friedel−Crafts acylation, lithiation, borylation, mercuration etc.[105-107]

Tamm and coworkers have reported the synthesis of 1,1′-ferrocenedicarboxylic acid [$Fc(COOH)_2$] in a large scale by a simple and convenient process from the reaction of sodium salts of cyclopentadienecarboxylic methyl and ethyl esters, $Na(C_5H_4COOR)$ (R = Me, Et). 1,1′-ferrocenedicarboxylic acid has been further involved to get a series of 1,1′-disubstituted ferrocenyl compounds of the type FcX_2 (X = CH_2OH, COCl, CON_3, NCO, NHCOOMe, NHBoc, NH_2) (Scheme 1.23).[108] Some of the synthesized 1,1′-disubstituted ferrocenyl compounds have been characterized by single crystal-XRD showing the presence of two functional groups separately attached at the two cyclopentadienyl rings in different orientation.

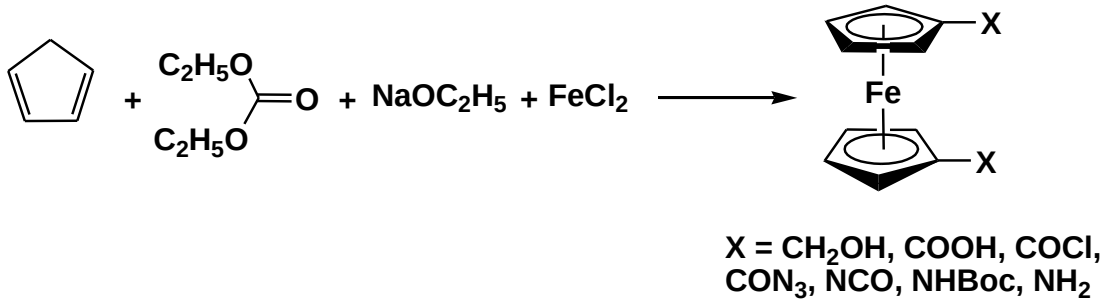

Scheme 1.23. 1,1′-disubstituted ferrocenyl compounds

The ortho substitution containing a hetero atom or electron withdrawing group on ferrocene restrict the synthesis of 1,2- disubstitution of ferrocene having two hetero atoms or two electro withdrawing group. Recently Lang et al. reported the synthesis of planar 1,2-disubstituted ferrocene derivatives anticipating their use in catalysis.[109-110] Lithiation of a series of alcohol derivatives and subsequent addition of $POCl_3$ gave chlorophosphates which was converted to their ferrocenyl phosphates by the addition of lithiated ferrocenol. The ferrocenyl phosphate was subjected to anionic phospho Fries-rearrangement in presence of diisopropylamine, butyllithium, tetramethylethylenediamine and dimethylsulfate to give the 1,2-disubstituted ferrocenyl derivatives as shown in Scheme 1.24.[109]

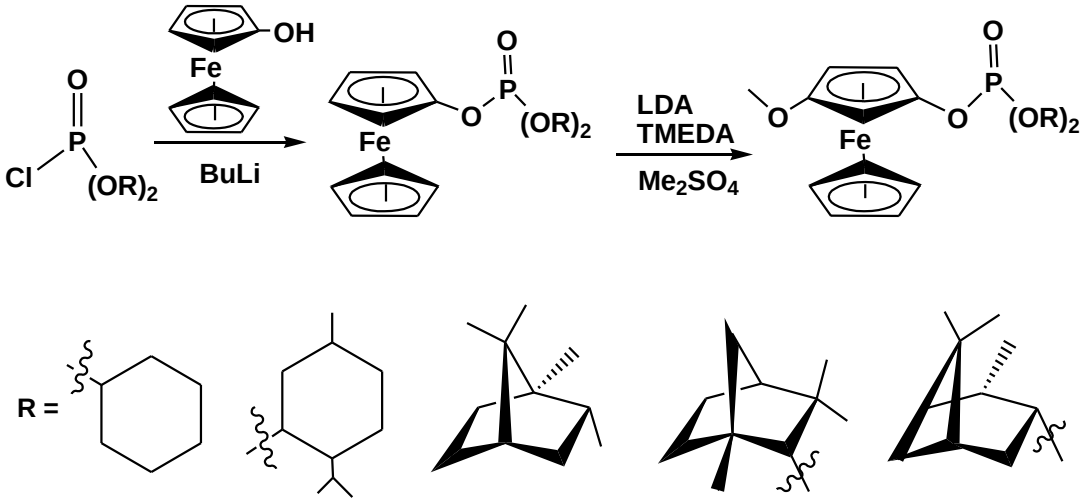

Scheme 1.24

Electrochemical and spectroscopic techniques have been frequently adopted to know the cation complexation properties of a variety of unsymmetrically disubstituted ferrocene compounds. Recently, ferrocene-triazole based compounds are of interest due to their unique coordination ability, sensing properties and ectrochemical behaviour.[111] A unsymmetrical triazole based ferrocenyl system has been obtained by sequential functionalzsation of a bisazidoferrocene through click reaction with ethynylpyrene and Staudinger reaction with trimethylphosphine followed by hydrolysis and treatment with quinoline aldehyde (Figure 1.31).[112] Molecular structure of the unsymmetrical ferrocenyl triazole derivative has shown that the quinoline and pyrene rings attached to the ferrocene fragment are exclusively coplanar and forms an eclipsed conformation across the ferrocenyl Cp rings. The molecule showed hyperchromic shift in UV-Visible absorption spectroscopy by gradual addition of $HP_2O_7^{3-}$, Pb^{2+} and Hg^{2+} confirming their potential in sensor application. The effect on fluroscence emission study also showed the capability of the ferrocenyl triazole derivative to behave as fluorescent probe for $HP_2O_7^{3-}$, Hg^{2+} and cobound Pb^{2+} cations in the presence of $HP_2O_7^{3-}$ anion.

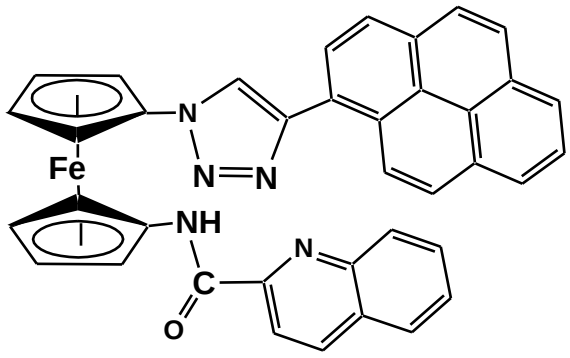

Figure 1.31. Ferrocenyl triazole derivative

1.4.1. C-H bond functionalization of ferrocene

Among several methods to introduce substituents on the cyclopentadienyl rings of ferrocene, metal-catalyzed cross-coupling reactions have become a powerful tool to achieve highly efficient and selective transformations to create C-C and C-Heteroatom bonds directly on one or both the Cp rings of ferrocenyl unit. [113, 114] A method for the direct functionalization of ferrocene compounds to prepare ferrocenyl vinyl derivative catalytically generated from vinyldiazo compounds and gold complexes has been reported recently by Lopez et. al (Scheme 1.25). [115] The presence of different type of esters has been found to be inactive towards the regioselectivity forming E stereoisomer as the single product whereas the substitution at the vinyl group by alkyl and acetyl groups afforded both the isomers predominating E-stereoisomer over Z-stereoisomer.

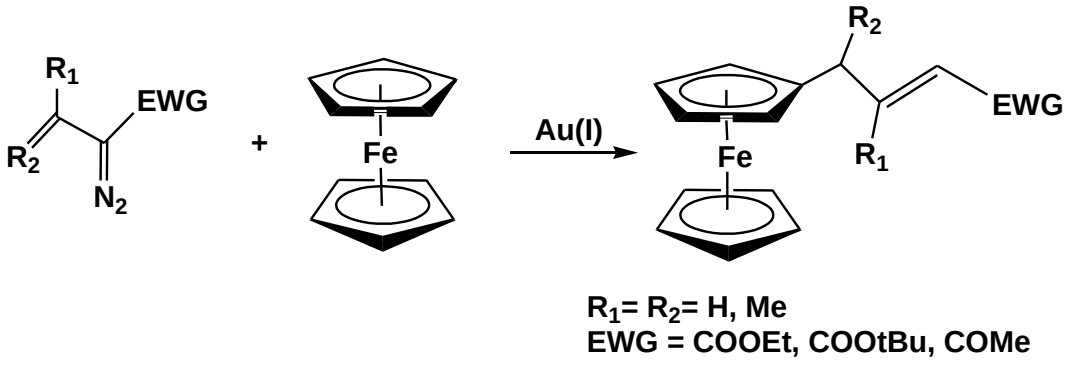

Scheme 1.25

Palladium-catalyzed intramolecular C−H cyclization strategy has been adopted for the synthesis of planar chiral metallocenes with high enantioselectivities by the reaction of acyl ferrocenyl derivatives with $Pd(OAc)_2$ in presence of 2,2'-bis(diphenylphosphino)-1,1'-binaphthyl ligand (Scheme 1.26). This synthetic method provided an efficient way to obtain structurally unique enantioselective ferrocenyl framework with a wide range of functional group such as aldehyde, ketones, carboxyl ester, and amides substituted at the other Cp ring of the ferrocene moiety. The asymmetric 1,2- substitution formed on the same Cp ring by intramolecular cyclization has been offered the planar chirality to all the ferrocenyl derivatives making the reaction unique and distinct.[116]

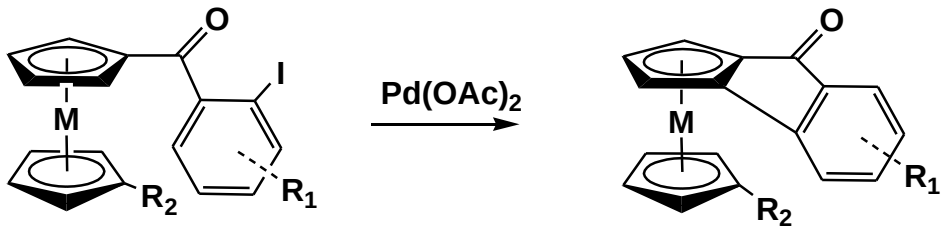

R_1 = H, 5-Me, 4,5-$(OMe)_2$; R_2 = H
R_1 = H; R_2 = -CHO,-$COCH_3$, -COOEt, -C=C

Scheme 1.26

A Rh (III)-catalyzed C-H bond functionalization of ferrocenecarboxamides derivative with alkynes has been reported for the facile synthetic route for planar chiral ferrocenylpyridones for their potential use as organocatalyst. The reaction conditions have been optimized by the preliminary reaction of N-methoxy ferrocenecarboxamide and 1-phenyl-1-propyne in presence of different bases and with different temperature and optimizing the conditions at 60^0C with sodium acetate and triethyl amine as bases and trifluro ethanol as solvent (Scheme 1.27). The optimized reaction conditions have been applied for C-H bond functionalization of different type of substituted ferrocene carboxamide and alkynes to obtain various ferrocenyl pyridone derivatives from good to excellent yield.[117]

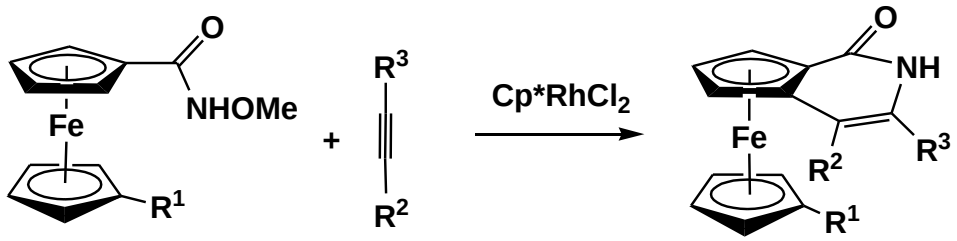

R^1= Br, CH_2OH, CH_2OMe, CHO; R^2= CH_3; R^3=Ph
R^1= H; R^2= C_2H_5, CH_2OH, CH_2OMe; R^3 =Ph
R^1= H; R^2 = CH_3; R^3= 3-BrPh, C_4H_3S, C_5H_4N

Scheme 1.27

1.4.2. Ferrocenyl derivatives having biological properties

The structural diversity and special properties like high stability, redox property and low toxicity of ferrocenyl compounds make them unique from the other metallocenes and are widely employed in drug designing with their improved biological activities and can be used as labelling tags in several biomolecules**.** Conjugation of organometallic compounds with biomolecules such as DNA, amino acids and peptides can serve as a molecular scaffold with a redox active site and a biological marker. The interest on bioconjugates has led to the design of several ferrocene –peptide architecture with unique properties like redox switching and sensor abilities. The ability of ferrocenyl derivatives to act as molecular scaffold through hydrogen bonding interaction has been demonstrated recently by several research groups using peptide chains incorporation. Synthesis of 1,1'-disubstituted ferrocene –peptide bioconjugates and their structural evaluation reveals the formation of two identical intramolecular interchain hydrogen bonds between the carbonyl and NH units of the amino acid fragments to give a ten membered hydrogen bonded ring. The structure resembles the hydrogen bonding pattern observed in an anti-parallel β-sheet. In some cases, the molecules arrange in a helical fashion linked together via intramolecular hydrogen bonding where introduction of peptide chains into ferrocene

moiety induces some kind of conformational enantiomerization by the torsional twist generated by interchain hydrogen bonding interaction (Figure 1.32).[118-121]

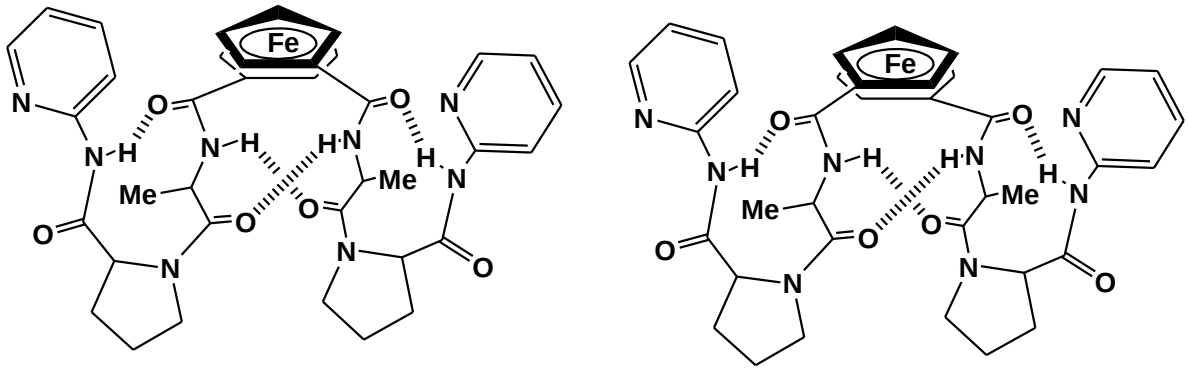

Figure 1.32. Fc(-L-Ala-D-Pro-NHPy)$_2$ and Fc(-D-Ala-D-Pro-NHPy)$_2$

Ferrocene substituted tamoxifen, also known as ferrocifen, and chloroquine derivatives are among the many examples where systematic functionalization of ferrocene has improved the cytotoxic activity of the standard drug itself. Ferrocifen has been prepared from propionylferrocene by McMurry cross coupling reaction with dihydroxybenzophenone giving a halogenated compound which further reacts with dimethylamine chlorhydrate to yield ferrocifen (Figure 1.33).[122] A mechanism have been proposed for the improved cytoxicity found in case of ferrocifen and its derivatives against both hormone dependent and hormone independent cancer cells through the radical formation of OH group attached to the phenyl ring present in the trans position of the ferrocenyl moiety forming quinone methide intermediate. [123, 124] The ferrocenyl group has been predicted to give extra stabilty to the intermediate radical. Inspired by the development of bioorganometallics, several researchers focused their investigation on ferrocenyl derivatives adopting different synthetic methods and studying facts related to biological chemistry, medicinal poperties, cytotoxicity behavior etc. This unexpected boom in the field of bioorganometallic chemistry led to the synthesis of a ferroecnyl analog of chloroquine, a well known antimalarial drug. However, there are several cases

found in medical investigation that the malaria parasite has developed resistant to the chloroquine drug, which posed a major global problem in treating the infection. The ferrocenyl derivative of chloroquine, commonly known as Ferroquine, showed marked activity against both chloroquine susceptible and chloroquine resistant *P. falciparum* strains.[125] Extensive study on the mechanistic aspects predicted that the higher activity of ferroquine is due to the presence of the ferrocene moiety in the lateral side chain of the aminoquinoline ring (Figure 1.33).

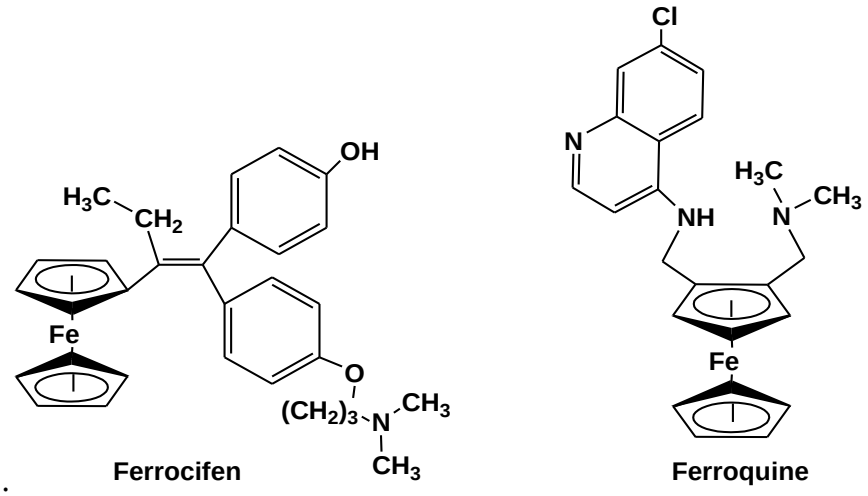

Figure 1.33. Structure of ferrocifen and ferroquine

Multistep reaction of acetyl ferrocene with ethyl trifluoroacetate, hydrazine hydrate and ethyl bromoacetate afforded 5-ferrocenyl-3-(trifluoromethyl)-1H-pyrazole which further reacted with piperidine and sodium ascorbate in different reaction condition to give structurally different ferrocenyl pyrazole compounds (Figure 1.34).[126] Crystal structure analysis revealed the different substitution of the trifluoro and ferrocenyl groups in the pyrazolyl moiety. All the derivatives have been reported to exhibit moderate to potent antitumor activities in vitro against A549 cell line compared to the standard drug 5-fluorouracil.

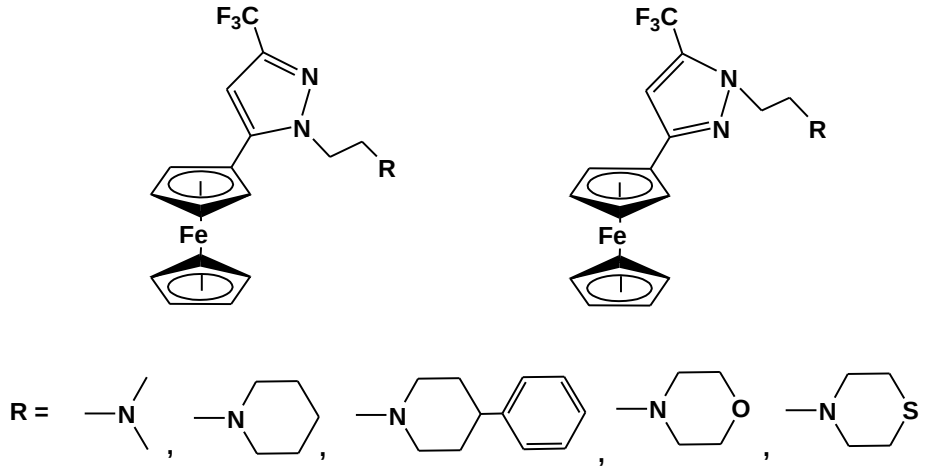

Figure 1.34

Some ferrocenyl compounds containing azines (-C=N-N=C-) have been synthesized by the reaction of 1,2-(dimethylamino) methyl ferrocenyl aldehyde with salicylaldehyde hydrazone derivatives which was further subjected to deprotonation by NaH followed by metallation using $[RhCl(COD)]_2$ as depicted in Figure 1.35.[127] A preliminary antiplasmodial investigation conducted against the chloroquine sensitive NF54 and chloroquine resistant K1 strains of *P. falciparum* showed that ferrocenyl azines exhibited weak to moderate activity across both parasitic strains. However, upon complexation the activity gets enhanced compared to the ferrocenyl azines.[128] The mechanism of the increased activity could not correleated with their β-haematin inhibition. Among all the synthesized ferrocenyl azine derivatives and its complex, the unsubstituted ferrocenyl azine compound and its complex have been found to exhibit the best activity against the chloroquine sensitive NF54 strain whereas the opposite behavior has been found against the chloroquine resistant K1 strains of *P. falciparum*.

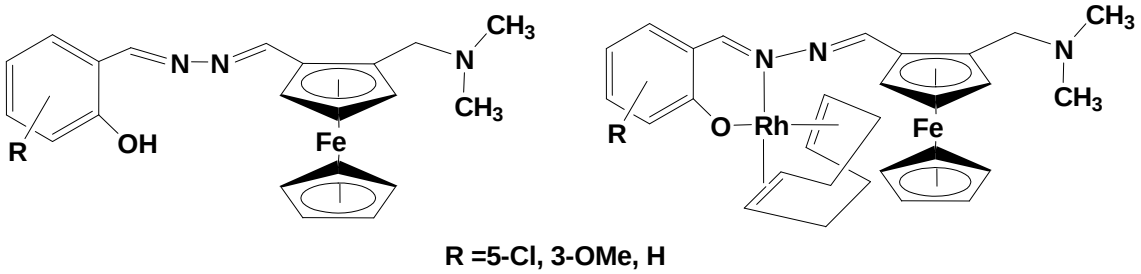

Figure 1.35

The significant role of heterocyclic moieties in a variety of biological processes has prompted a large amount of studies in recent years to link different heterocycles to ferrocene based molecular system. This interest led to the development of synthetic strategies for the design of a variety of ferrocene conjugated heterocyclic compounds and study their biological activity.

Reaction of the precursor ferrocenylazide with 2-(prop-2-ynyloxy)-benzaldehyde through click reaction gave a ferrocenyl triazole aldehyde derivative which further reacted with rhodamine B hydrazide or rhodamine 6G hydrazide under reflux condition to furnish a triazole-rhodamine-ferrocene conjugates (Figure 1.36).[129] Their electrochemical, optical, and metal cation sensing properties have been explored in aqueous medium. The newly synthesized ferrocenyl receptors exhibited high turn-on fluorescence response for Hg^{2+} as well as I^- in an aqueous environment. DFT calculations of the ferrocenyl derivative with Hg^{2+} showed the bonding of the ferrocenyl receptor through one nitrogen atom of the triazole ring, one nitrogen of the imine group, and two oxygen atoms of the carbonyl and ether groups to Hg^{2+}, resulting in a nearly planar geometry around Hg^{2+}. Furthermore, both the ferrocenyl based receptors are less toxic toward MCF-7 cells and could able to detect intracellular Hg^{2+} by fluorescent imaging studies.

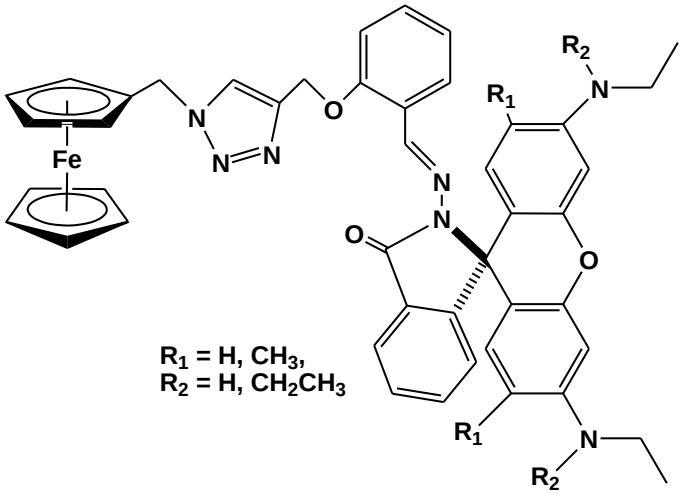

Figure 1.36. Ferrocenyl-triazole-rhodamine hybrid chemosensor

In order to improve the biological response of purely organic drugs, a few novel ferrocene derivatives within the isatin−ferrocene−triazole conjugate family have been synthesized by copper-mediated azide-alkyne cycloaddition method.[130] In the first step, alkyl azido isatin was prepared by alkylation of substituted isatin with dibromoalkane and further substitution with sodium azide. Copper mediated click reaction was then carried out with acetylenic ferrocene or ferrocenyl chalcones to afford the respective isatin-triazole-ferrocene conjugates (Figure 1.37). The compounds with the ferrocenyl fragment showed enhanced antitubercular activity against *M. tuberculosis* in comparison to the isatin precursors.

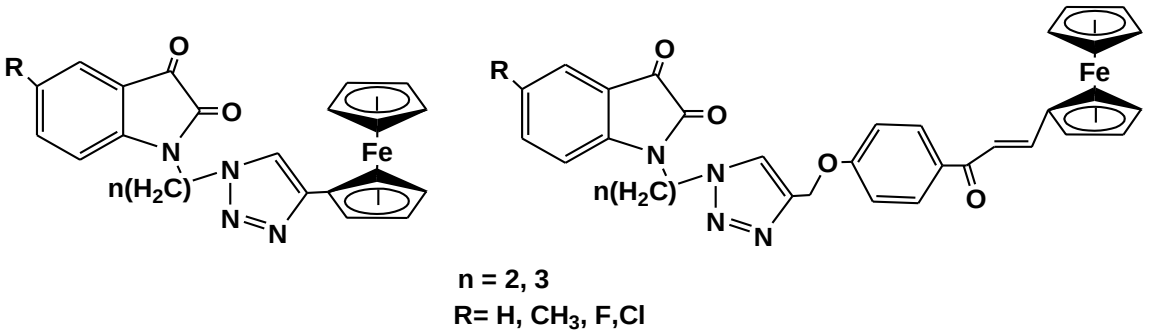

Figure 1.37. Ferrocenyl isatin-triazole hybrid compounds

The use of ferrocenyl derivatives as bioactive molecule has been established in current time and several reports show that a large number of ferrocene containing compounds display interesting cytotoxic and DNA cleaving activities. [131-141] Ferrocenyl aldehyde on reaction with 2,3- butanedione in presence of piperidine followed by reaction with salicylaldehyde under reflux condition afforded a ferrocenene based vinyl imidazole phenol derivatives which on further refluxation with $[Ru(bpy)_2Cl_2]\cdot 2H_2O$ gave the ruthenium complex of ferrocenyl imidazole derivatives as shown in Figure 1.38.[142] The differential pulse voltammetry of the complex $[Ru(bpy)_2$-2-{4,5-bis[(E)-2-ferrocenylvinyl]-1H-imidazol-2-yl}phenol$](PF_6)$ showed two redox peaks at +353 mV and +485 mV for Ru(II)/Ru(III) and Fe(II)/Fe(III) redox couples respectively whereas complex $[Ru(bpy)_2$-2-{4,5-bis[(E)-2-ferrocenylvinyl]-1H-imidazol-2-yl)-4,6-dichlorophenol$](PF_6)$] showed only one peak shifted to more positive value due to the

presence of two electron-withdrawing chloride groups at +505 mV for both Ru(II)/Ru(III) and Fe(II)/Fe(III) redox couples. All the complexes showed DNA cleavage activity which might be due to the presence of three redox active metal centers. The lower redox potential of the metal complex can be responsible for the generation of hydroxyl and peroxide radicals through fenton reaction under the experimental conditions for the DNA cleavage.

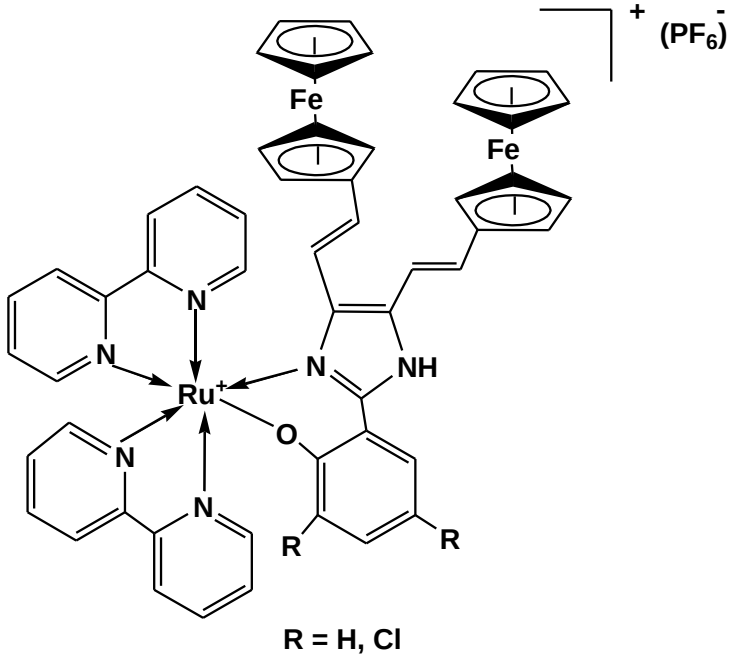

Figure 1.38

1.4.3. Ferrocenyl compound as biosensor

A biosensor is an analytical device which combines a biological component with a physicochemical detector and is used for the detection of an analyte. Biosensors have potential environmental application and can be used in food industry, drug discovery, detecting gases like carbon dioxide and ammonia in blood samples.

Ayranci et al have reported a novel ferrocenyldithiophosphonate functional conducting polymer and its use as an immobilization matrix in amperometric biosensor applications.[143] Reaction of 1,4-bis-2-thienylbutane-1,4-dione with *p*-phenylenediamine gave 4-(2,5-di(thiophen-2-yl)-1*H*-pyrrol-1-yl)aniline which was further reacted with ferrocenyldithiophosphonate to afford 4-(2,5-di(thiophen-2-yl)-1*H*-

pyrrol-1-yl)amidoferrocenyldithiophosphonate. Both the 4-(2,5-di(thiophen-2-yl)-1*H*-pyrrol-1-yl)aniline and 4-(2,5-di(thiophen-2-yl)-1*H*-pyrrol-1-yl)amidoferrocenyldithio phosphonate was then electrochemically polymerized using the potential between -0.5 V to +1.5 V on graphite electrode forming a redox mediated ferrocenyl copolymer surface (Figure 1.39). The ferrocenyl copolymer was immobilized with glucose oxidase by means of glutaraldehyde for their application as a redox mediated ferrocenyl biosensor. The ferrocenyl biosensor can be used for glucose analysis in real samples with better detection limit for glucose by means of the current signal observed at+0.45 V. The changes in current signals at +0.45 V has been observed to be proportional to glucose concentration in the range 0.5 to 5.0 mM. Moreover, the method overcomes the problems such as the oxygen deficiency during the enzymatic reaction and interference of other substances during electrochemical measurements which are of critical points for the biosensor fabrication.

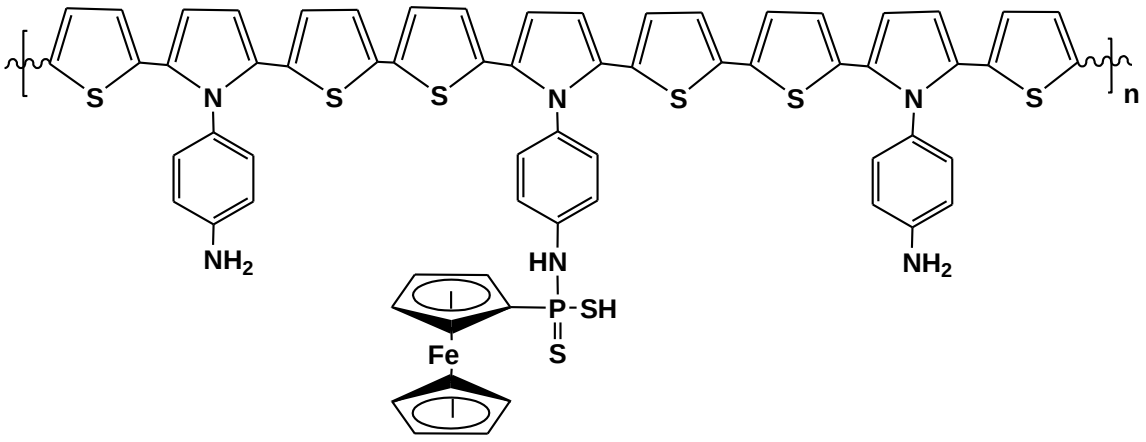

Figure 1.39. A ferrocenyl- polymer conjugate biosensor

Yang et al. has reported the synthetic procedure for a ferrocenyl based derivative used as an intercalator to double stranded DNA (dsDNA) obtained from the reaction of ferrocenecarboxylic acid with oxalyl chloride followed by addition of 2,2'-(ethylenedioxy)bis(ethylamine) and naphthalenetetracarboxylic dianhydride (Figure 1.40).[144] The binding of the ferrocenyl intercalator to dsDNA was measured by

differential pulse voltammetry and was optimized for the recognition of single base pair mismatched sequences. The results reveal the feasibility of detecting human DNA biomarkers in wastewater using the synthesized ferrocenyl based biosensor, which may allow further development of DNA population biomarkers for evaluation of public health.

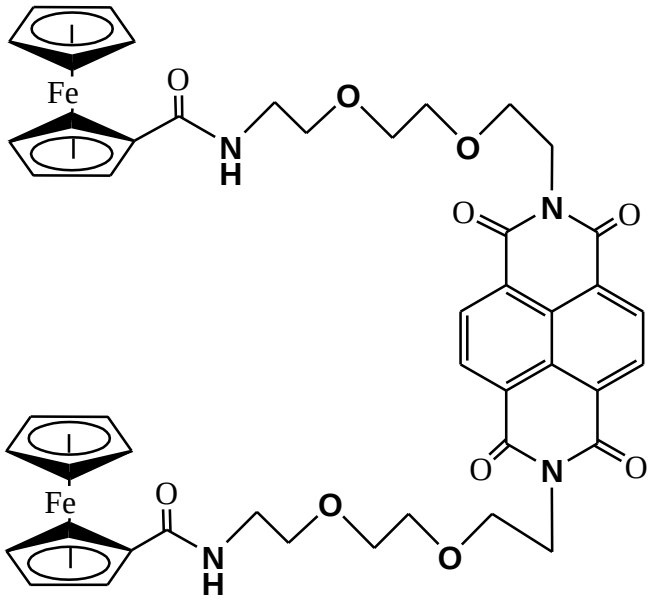

Figure 1.40. Ferrocenyl based intercalator to dsDNA/ ferrocenyl dsDNA intercalator

1.4.4. Ferrocenyl compounds as chemosensor

The design of molecular receptors having the ability of selective binding and recognition of neutral molecules, cations or anions by means of various different physical tools is an interesting area of research. In this context, ferrocene has largely proved to be a simple and remarkably robust building block for the preparation of such ferrocenyl receptors displaying electrochemical sensing properties exploiting the redox activity of ferrocene moiety.[145, 146] Additionally, binding of targets at specific binding site of ferrocenyl unit can affect the UV-visible and fluorescence spectra of the ferrocenyl

derivative and can be applied for the designing of dual sensing and multisensing ferrocenyl based chemosensor.[129, 147]

Karagollua et al. have reported the selective sensing properties of ferrocene-functionalized triazole compounds, [{Ar$(CH_2)_2(C_2HN_3)(\eta^5$-$C_5H_4)$}Fe$(\eta^5$-$C_5H_5)$], (Ar = C_4H_3S or styrene) for phosphate, $H_2PO_4^-$and $HP_2O_7^{3-}$ using electrochemical process (Figure 1.41).[148] The ferrocene-appended thiophene compound was prepared by a three-step process starting from 3-(2-hydroxyethyl)thiophene and subsquent reaction with phosphorus tribromide, azidification and azide-alkyne cycloaddition reaction to give thiophene based ferrocenyl-triazole compound. Ferrocenyl styrenic polymer was prepared using the cycloaddition reaction of azide-functional styrene polymer with ethynylferrocene. The presence of extra populated ferrocenyl groups around the styrenic backbone in ferrocene-styrene copolymer has resulted in more effective interaction improving the chemical recognition ability toward $H_2PO_4^-$ and $HP_2O_7^{3-}$ anions. However, the study showed that both the thiophene and styrene functionalized ferrocenyl compounds have shown better recognition ability for $H_2PO_4^-$ than $HP_2O_7^{3-}$ anion.

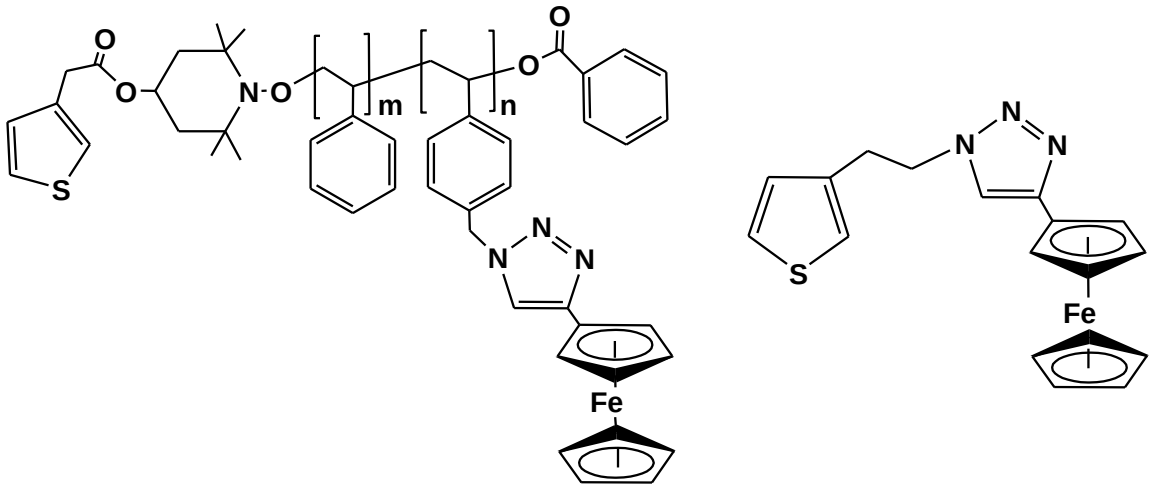

Figure 1.41. Ferrocene functionalized thiophene and styrene copolymer

Kumar and coworker have proposed multichannel ferrocenylpyrazolines, [{(1-(2-C_5NH_4)3-(Ar)-C_3N_2H)(η^5-C_5H_4)}Fe(η^5-C_5H_5)], (Ar = 1-naphthyl, 9-anthryl, 1-pyrenyl) containing ferrocene as a redox unit, an aromatic ring fluorophore and a binding system containing two nitrogen atoms on the pyridylpyrazoline moiety. Aldol condensation of acetyl ferrocene with different aldehyde in basic condition gave the corresponding ketoenones which was further reacted with 2-hydrazinopyridine to afford the ferrocenyl pyrazoline compounds (Scheme 1.28).[149] The binding assay and recognition ability of these compounds was studied towards the metal ions by using electrochemical and optical method. Systematic study showed the ability of the ferrocene compounds to behave as selective multichannel chemosensors in the presence of Co^{2+}, Cu^{2+}, and Zn^{2+} ions. The cathodic shift in the redox potential (ΔE=71-156mv) of the ferrocenyl pyrazoline receptors observed in cyclic voltammetry as well as the decrease of the high energy band at 330 nm- 335 nm with the red shift in UV visible spectra ($\Delta\lambda$= 7-13nm) confirms complexation of the ferrocenyl derivatives with the cations. Furthermore, the downfield shift in proton NMR spectra and the increase in emission accompanied by a red shift at 430 nm in fluorescence spectroscopy during the gradual addition of various cations to the ferrocenyl pyrazoline compound containing naphthyl moiety showed it to be the most significant receptor compared to the other ferrocenyl pyrazolines.

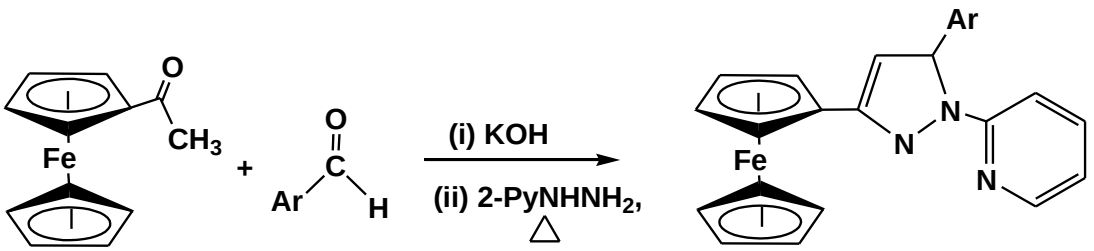

Ar = 1- naphthyl, 9-anthryl, 1-pyrenyl

Scheme 1.28. Synthesis of ferrocenyl pyrazolin derivatives

A ferrocenyl imidazoquinoxaline ion pair receptor has been synthesized from the reaction of 1,2-diamino-4-nitrobenzene, furyl and ferrocenecarboxaldehyde by Molina et al. and has been studied for the sensing ability for HSO_4^- anions in the presence of a

cobound divalent Pb^{2+} or Zn^{2+} cation as guest species (Figure 1.42).[150] The cathodic shift observed during the electrochemical analysis on addition of Pb^{+2} and Zn^{+2} to ferrocenyl imidazoquinoxaline receptor and HSO_4^- has been found to increase by 120mv and 220mv than the complexation of the mixture of Pb^{+2} and Zn^{+2} with the ferrocenyl imidazoquinoxaline receptor alone. Addition of Pb^{+2} and Zn^{+2} to the solution mixture of ferrocenyl imidazoquinoxaline receptor and HSO_4^- has also dramatically enhanced the fluorescence emission by 237-fold and 85-fold respectively than that of the ferrocenyl imidazoquinoxaline receptor and HSO_4^- mixture itself.

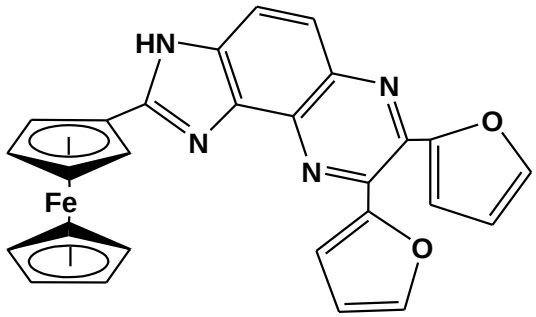

Figure 1.42. Ferrocenyl imidazoquinoxaline

Two step reaction process of pentakis(phenylthio)benzaldehyde with diethyl aminomethylphosphonate followed by the treatment of n-BuLi and formylferrocene gave [4-(η^5-C_5H_5)Fe(η^5-C_5H_4)-1-{$(C_6H_6S)_5C_6H_6$}-1-(C=N-CH=CH)] while the treatment of pentakis(phenylthio)benzaldehyde with diethyl [(ferrocenylmethylidene)aminomethyl] phosphonate afforded the compound [1-(η^5-C_5H_5)Fe(η^5-C_5H_4)-4-{$(C_6H_6S)_5C_6H_6$}-1-(C=N-CH=CH)] (Figure 1.43).[151] Electrochemical and spectroscopic techniques have been carried out to understand the complexation behavior of these compounds with different cations showing their complex formation with Pb^{+2}, Hg^{+2} and Cu^{+2}. Anodic shift ($\Delta E_{1/2}$ = 125 mV) in square wave voltammetry and red shift of the low-energy band in the absorption spectrum ($\Delta\lambda$ = 119 nm) revealed selective dual molecular recognition of the receptor [4-(η^5-C_5H_5)Fe(η^5-C_5H_4){$(C_6H_6S)_5C_6H_6$}(C=N-CH=CH)] with Pb^{+2} cation.

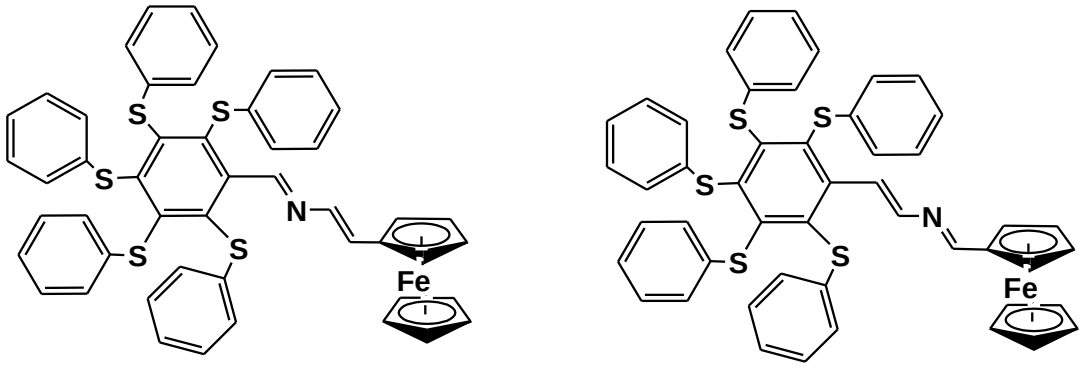

Figure 1.43

1.4.5. Electronic communication in ferrocene based molecules

A large part of the organometallic chemistry has been focused on the studies of electron transfer processes in ferrocenyl conjugated compounds based upon the tunable redox activity of the ferrocene moiety. Stepnicka et al. have reported a series of heterobimetallic cyclopentadienyl complexes connected through different linker groups. Reaction of (2-phenylethyl)ferrocene, (E)-(2-phenylethenyl)ferrocene or (phenylethynyl)ferrocene with $[Ru(\eta^5\text{-}C_5R_5)(MeCN)_3][PF_6]$ (R= H, Me) showed the formation of the heterobimetallic complexes $[(\eta^5\text{-}C_5H_5)Fe(\eta^5\text{-}C_5H_4)\text{-}X\text{-}(\eta^6\text{-}C_6H_5)Ru(\eta^5\text{-}C_5R_5)][PF_6]$, (X = CH_2CH_2, CH=CH, C≡C; R = H, Me) as shown in Figure 1.44.[152] Investigation of the redox chemistry of the bimetallic compounds showed their push−pull behavior involving electron-rich ferrocenyl moiety and the cationic $Ru(\eta^6$-arene) fragment as the electron donor and acceptor components. Cyclic voltammetric and spectroelectrochemical studies revealed electronic communication between the metal centers in compounds possessing the conjugated linking groups. An anodic shift (100−150 mV) of the ferrocene/ ferrocenium couple was observed in the Fe-Ru heterobimetallic complexes as compared to that of the ferrocenyl-benzene analog due to the presence of cationic ruthenium metal center in conjugation with the ferrocene unit resulting in the decrease in electron density at the ferrocenyl centre making the electron removal more difficult.

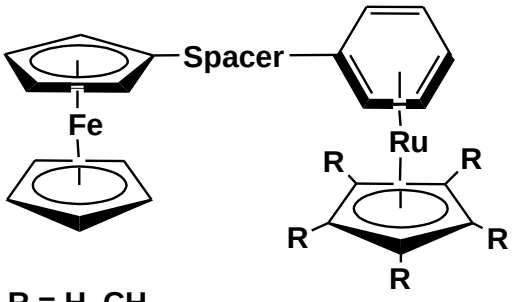

Figure 1.44

A ferrocene based boryl-functionalized bithiophene compound has been obtained from [2,2'-bis(BBr_2)$_2$-5,5'-(C_4H_2S)$_2$] by a systematic synthetic procedure involving addition of boron tribromide and trimethylstannylferrocene and subsequent reaction with pentafluorophenyl copper to give a diferroceneyl compound, [2,2'- bis{B(C_6F_5)(η^5-C_5H_4) Fe (η^5-C_5H_5)}-5,5'-(C_4H_2S)$_2$] (Figure 1.45).[153] The molecule revealed electronic communication in between the ferrocenyl moieties. The cyclic voltammetric study showed one reversible one electron oxidation at -11 mV and a quasi-reversible second oxidation wave at +207 mV relative to the Fe(II) / Fe(III) couple with the peak separation of ΔE = 218 mV due to the moderate degree of metal-metal interaction through the diborylated bithiophene linker. Addition of pyridine to the compound resulted in lowering of the redox potentials with the peak separation of 108 mV indicating decrease in electronic communication between the ferrocene moieties because of the interaction or complexation of the boron center with pyridine.

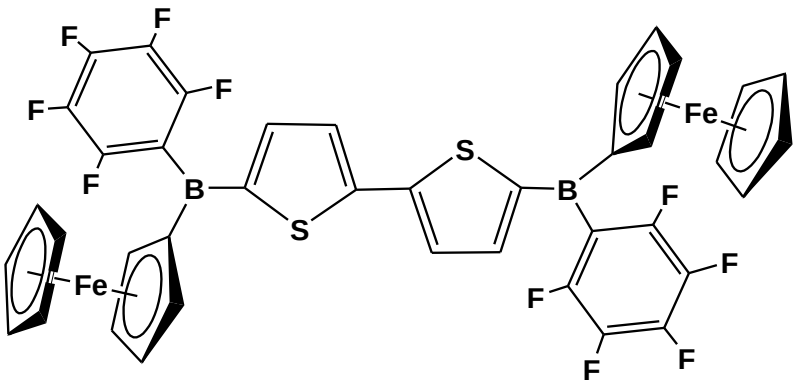

Figure 1.45

Nemykin and group recently reported the synthesis of diferrocenyl azadipyrromethene compound and its borylated derivatives to understand the role of heterocyclic chromophore on electronic coupling behavior through the bridging group. Ferrocene based azadipyrromethene compounds have been prepared by a stepwise reaction process involving aldol condensation of ferrocenecarbaldehyde with acetophenone to give the corresponding ferrocenyl chalcone followed by Michael addition and reaction with ammonium acetate under refluxing condition to obtain diferrocenylazadipyrromethene compound. Further treatment with $BF_3 \cdot Et_2O$ in presence of a base afforded the fluoroboryl analog of diferrocenylazadipyrromethene (Scheme 1.29).[154] The X-ray crystal structure of both the diferrocenyl derivatives has confirmed the presence of the syn-conformation of the ferrocene groups in the molecules. Cyclic voltammetry study showed two reversible redox couple for the two ferrocenyl units while the potential difference between the first and the second oxidation peaks are 340 mV and 640 mV for the diferrocenylazadipyrromethene and its fluoroboryl derivative respectively. Spectroelectrochemical experiment for the diferrocenyl derivative containing fluoroboryl moiety has shown the disappearance of the bands in visible region with the appearance of a new band in NIR region during the first oxidation and disappearance of the NIR band with a new peak in visible region during the second oxidation. The spectroelectrochemical data along with DFT study confirmed marked electronic coupling between the two ferrocenyl units in these types of molecules.

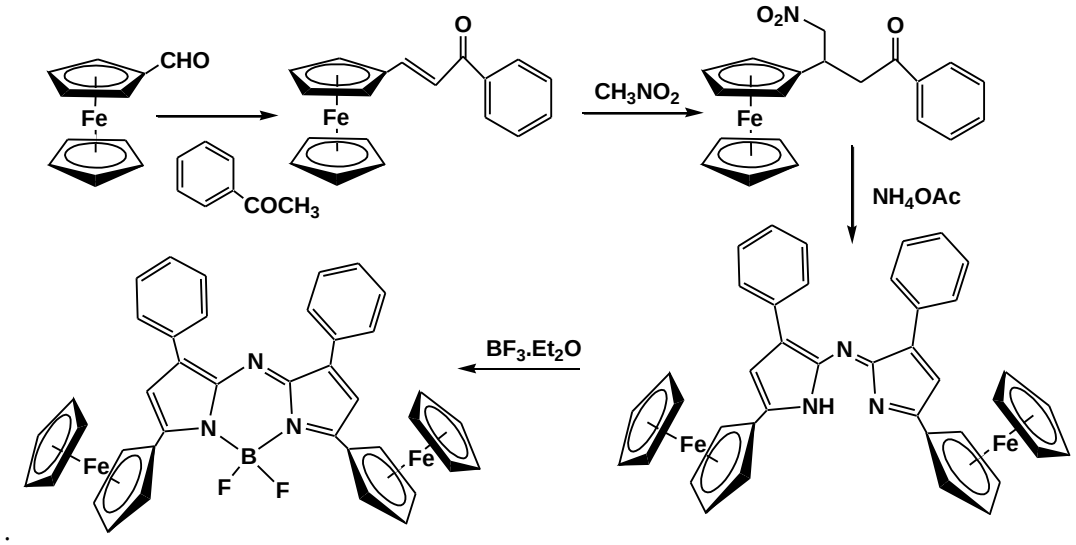

Scheme 1.29

1.4.6. Diferrocenyl organometallic compounds

Compounds containing diferrocenyl system with various bridging units and multiple redox processes have been widely studied because of their potential application in molecular photonics, optoelectronics, redox-driven fluorescence markers and sensors. Such systems have been intensely studied in recent decades for some interesting features related to multiredox and electronic communication properties. A range of different multiferrocenyl compounds with a series of conjugated or non-conjugated bridging moieties have been synthesized and studied their electrochemical properties.

In recent times, molecules having two metal centers linked with bridging ligand are of interest due to their electronic interaction across the ligand which may enhance biological processes, catalytic reactions and show their potency for molecular wires and switches.[155] The bridging ligand should provide electronic coupling pathway in between the metal centres to promote electronic communication by means of their properties like flexibility, degree of delocalization and length of bridging unit. A recent report described the formation of ferrocene conjugated ethynylethenes, [(η^5-C_5H_5)Fe{(η^5-C_5H_4)CC(COOMe)C=C(COOMe)CC(η^5-C_5H_4)}Fe(η^5-C_5H_5)], by a sonogashira coupling reaction of ferrocenylacetylene with a dibromoester derivative (Scheme 1.30).[156] Upon irradiation of light, the E-isomer of the ferrocene-conjugated ethynylethene showed decrease in spectral bands at 355-365 nm and 520-530 nm due to its transformation to the Z-isomer accompanied by reduction of electronic communication between the ferrocenes.

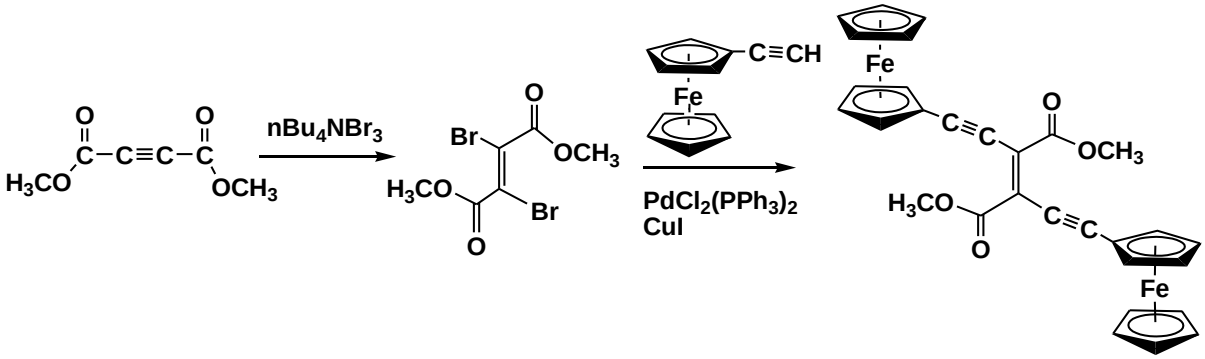

Scheme 1.30

Nonclassical hydrogen bonds such as XH···M and XH···HM with the electron rich metal centres play a significant role in some ferrocenyl chemistry developing the area of organometallic crystal engineering.[157] A strong and thermally stable nonclassical NH···Fe intramolecular hydrogen bond has been observed by Heinz et al recently during the synthesis of a diferrocenyl tosyl hydrazone compound obtained by the reaction of diferrocenyl ketone, p-toluenesulfonyl hydrazide, and p-toluenesulfonic acid (Figure 1.46).[158] Similar type of NH···Ru intramolecular hydrogen bond in diruthenocenyl tosyl hydrazone has also been explored by them. The intramolecular hydrogen bonding interaction, NH···Fe and NH···Ru, in both Z and E isomers have been confirmed by single crystal X-ray Diffraction study.[159] The NH···Ru intramolecular hydrogen bond was found to be stronger than that of NH···Fe. Two redox couple have been found for the diferrocenyl tosyl hydrazones with the lower oxidation potential for the metal without intramolecular hydrogen bonding and the higher oxidation potential for the metal with intramolecular hydrogen bonding.

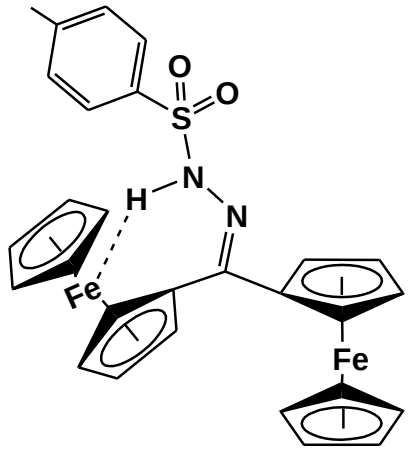

Figure 1.46

A diferrocenyl derivative bis(methylidenamino)[2.2]ferrocenophane containing CH=N linkage has been synthesized from the Staudinger reaction of bis(azido)-ferrocene with triphenylphosphine followed by aza-Wittig type reaction with ferrocenyl dialdehyde in good yield (Figure 1.47) [160]. The structure shows two ferrocenyl fragments attached together by two diaza bridging chains forming a cyclic framework. The two different

cyclopentadienyl rings of the ferrocene groups and the imine protons were identified by the ^{1}H NMR spectroscopy at δ 4.07-5.44 ppm and δ 9.39 ppm respectively. The electrochemical behavior of the diazaferrocenophane derivative has been carried out by the cyclic voltammetry showing two reversible one electron redox processes with $E_{1/2}$ value at -0.06 V and 0.45 V corresponding to two different ferrocenyl units.

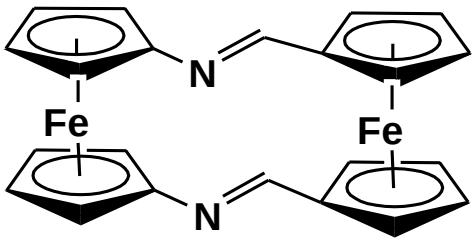

Figure 1.47. Bis(methylidenamino)[2.2]ferrocenophane

A diferrocenyl carbohydrazide Schiff base type derivative, [(η^5-C_5H_5)}Fe{(η^5-C_5H_4)CH=NNHC(S)NHN=CH(η^5-C_5H_4)}Fe{(η^5-C_5H_5)] bearing a methylene thiocarbohydrazide linkage, synthesized from the reaction of formyl ferrocene and thiocarbohydrazide, has been reported as precursor for different heterocyclic diferrocenyl derivatives for their use in pharmaceutical application. Cyclization of the diferrocenyl carbohydrazide with dimethyl-but-2-ynedioate or with methyl iodide and sodium methoxide afforded two diferrocenyl species with different bridging spacers (Scheme 1.31).[161] The compounds contain triazole and thiazolone heterocyclic moiety as bridge across the two ferrocenyl fragments.

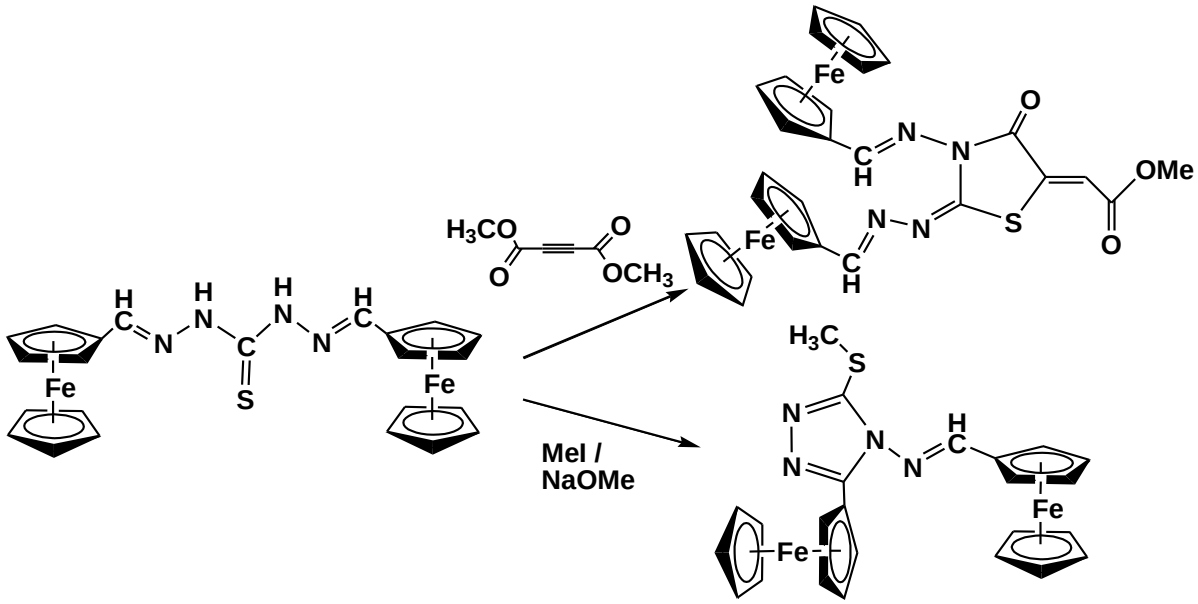

Scheme 1.31. Cyclization of diferrocenyl methylene carbohydrazide

Photochemical reaction of ferrocenylacetylene with sulfur in presence of metal carbonyl ($M(CO)_6$; M = Cr, Mo, W) afforded two deferrocenyl compounds, 2,4-diferrocenylthiophene and 2,6-diferrocenyldithiine involving thiophene and dithiine heterocyclic bridging units respectively as depicted in Scheme 1.32. The molecular structure of 2,6-diferrocenyldithiine revealed the existence of unique puckered 1,4-dithiine ring with ferrocenyl groups attached at 2 and 6 positions forming a syn conformation of the diferrocenyl compound. [162]

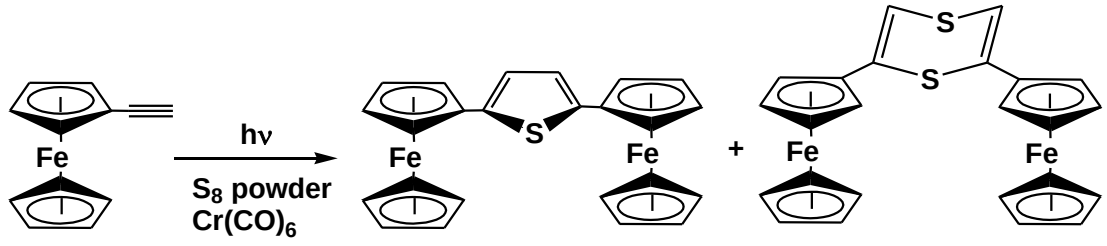

Scheme 1.32

Sohar and coworkers have reported the synthesis of diferrocenyl derivatives with pyrimidine type linkers obtained by the reaction of formyl ferrocene, urea and acetyl

ferrocene in presence of ferric chloride or from the reaction of formyl ferrocene, urea and benzyl-3-oxobutanoate in presence of boric acid as catalyst (Figure 1.48).[163]

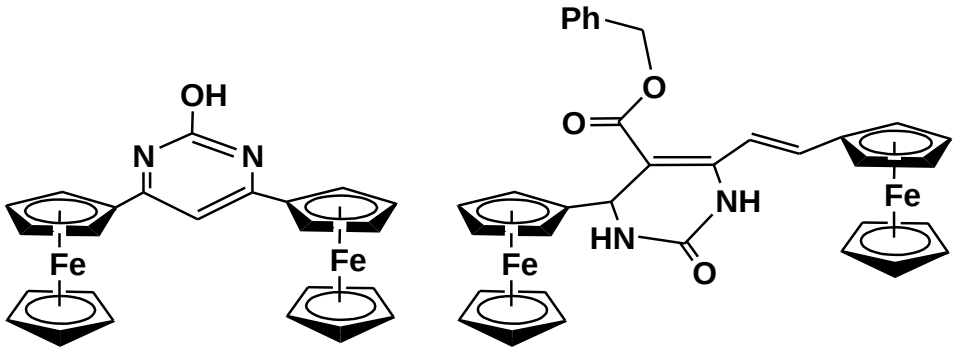

Figure 1.48

Similar type of diferrocenyl systems having a heteroaromatic pyridine group as bridge, namely 2,5- diferrocenyl pyridine and the 2,6- diferrocenyl pyridine have been reported by Lang and coworkers by Negishi C,C cross-coupling reactions of 2,5- dibromo pyridine or 2,6-dibromo pyridine with ferrocenyl zinc chloride in presence of palladium catalyst (Figure 1.49).[164] The presence of the ferrocenyl units and the heterocyclic groups were identified by spectroscopic techniques. Cyclic voltammetry of both the compounds has shown two reversible one electron redox couples for the presence of two ferrocenyl units. Inter valence charge transfer transitions have been observed for both the pyridine bridged diferrocenyl compounds using spectroelectrochemistry. The IVCT analysis revealed improved electronic interaction between the para-substituted metallocenyl redox groups than that of in 2,6- pyridine bridged diferrocenyl compound.

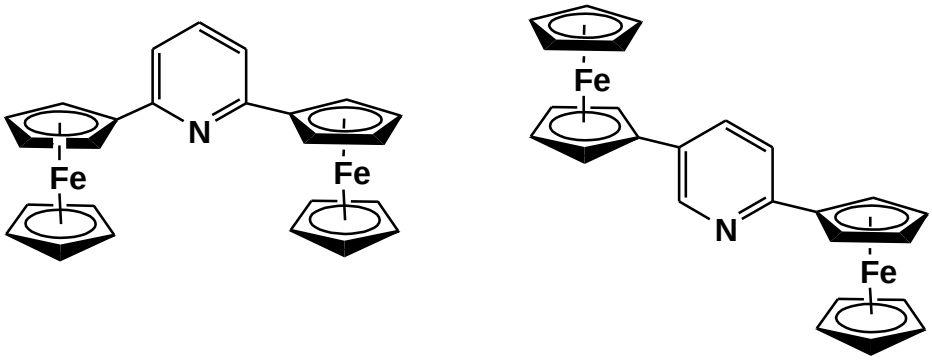

Figure 1.49

Yin et al. have reported the synthesis of a thermally stable differocenyl system linked through a photochromic ligand dithienylethenes by a witting reaction of 1,2-Bis(5'-formyl-2'-methylthien-3'-yl)perflurocyclopentene using ferrocenyl phosphonium bromide as shown in Scheme 1.33.[165] The molecular structure of the diferrocenyl complex revealed the presence of ring opening isomer of the dithienylethene unit in conjufgation with two ferrocenyl groups across the two ends. Irradiation of suitable wavelength of light afforded reversible ring closing and ring opening process observed by the shifting of the absorption peaks in UV-Visible spectroscopy.

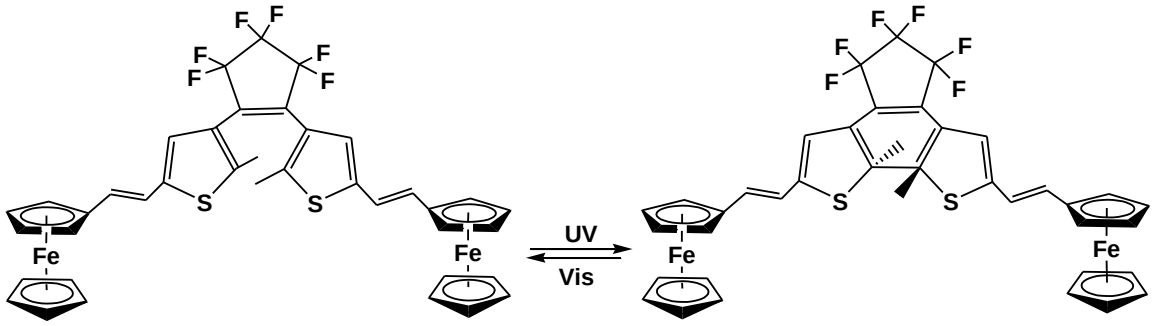

Scheme 1.33

1.5. Half sandwich and Ferrocenyl conjugate system

Heterobimetallic complexes containing both ferrocenyl and iridium or rhodium based half sandwich fragments have been synthesized by a Schiff base condensation reaction of ferrocenyl salicylaldimine derivative with $[M(C_5Me_5)Cl_2]_2$ (M= Ir, Rh) in presence of triethylamine as base (Scheme 1.34).[127] The structural analysis showed the presence of a metal coordinated interaction involving the half sandwich metal bonded to imine nitrogen and phenyl oxo group of the ferrocene based ligand.

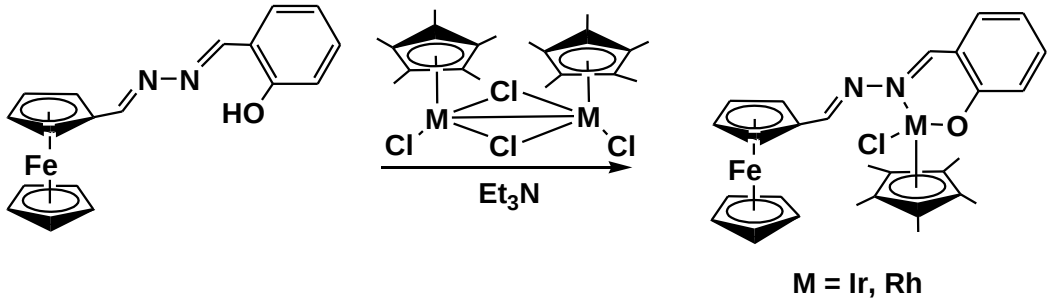

Scheme 1.34

A heterotrimetallic compound containing both ferrocenyl and half sandwich fragments, 1-cymantrenyl-3,5-diferrocenylbenzene, has been formed by the cyclocondensation of acetylferrocene and acetylcymantrene catalyzed by $SiCl_4$ (Figure 1.50).[166] The X-ray crystal structure of the compound revealed the presence of a cymantrenyl and two ferrocenyl fragments linked to each other by a benzene ring.

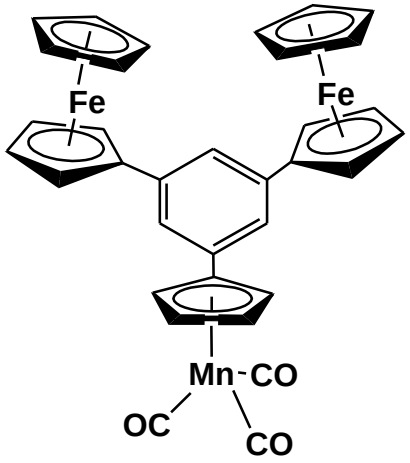

Figure 1.50. 1-cymantrenyl-3,5-diferrocenylbenzene

Lohan et al. have reported a palladium-copper-catalyzed Sonogashira cross-coupling reaction of 2-methyl-3-butyn-2-ol with diiodobiferrocene in refluxing diisopropylamine followed by addition of ML_nX (M=Ru, Os; L=PPh_3; dppf; X=Cl, Br) to form a series of heterometallic complexes of the type $[L_nM\{(\eta^5\text{-}C_5H_4)(CC)(\eta^5\text{-}C_5H_4)\}Fe\{(\eta^5\text{-}C_5H_4)(\eta^5\text{-}C_5H_4)\}Fe\{(\eta^5\text{-}C_5H_4)(CC)R\}]$ (R=H, $(\eta^5\text{-}C_5H_4)L_nM$).[167] In

both the compounds, the biferrocene fragment is linked either by one or two piano stool units via C≡C group (Scheme 1.35).

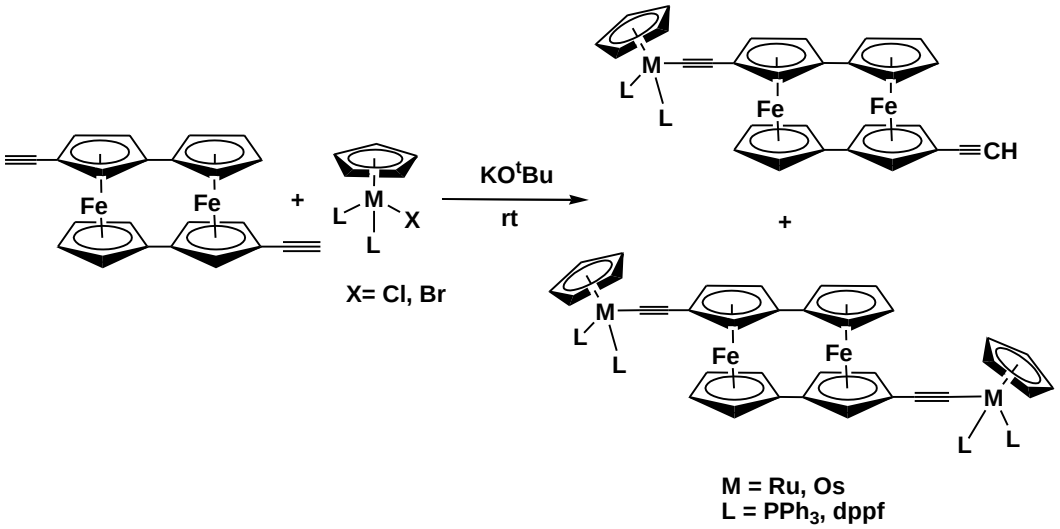

Scheme 1.35

The monolithiation of bromo ferrocene with subsequent addition of 2,3,4,5-tetramethylcyclopent-2-enone in presence of para-toluenesulfonic acid followed by addition of n-BuLi and $TiCl_4$ afforded a fulvalenediyl-bridged heterobimetallic compound $[(\eta^5\text{-}C_5H_5)Fe\{(\eta^5\text{-}C_5H_4)(C_5Me_4)TiCl_3\}]$ (Scheme 1.36).[168] Single crystal X-ray diffraction study has shown the presence of sandwich ferrocene and three legged piano stool $[(C_5Me_4)TiCl_3]$ fragments involving an exo arrangement of iron and titanium atoms with respect to the fulvalenediyl-bridge. UV-Visible spectral analysis for the heterometallic compound showed a low energy band at 660 nm due to the energy transfer from the electron rich ferrocenyl moiety to the electron deficient half sandwich, $[(C_5Me_4)TiCl_3]$. The lower energy band disappeared either by oxidation of ferrocene or by the reduction of $[(C_5Me_4)TiCl_3]$ during the spectroelctrochemical experiment. Two reversible redox couple have been observed at 0.14 V corresponding to Fe (II)/Fe (III) and at -1.11 V due to Ti (IV) / Ti (III) during electrochemical analysis of the heterobimetallic derivative.

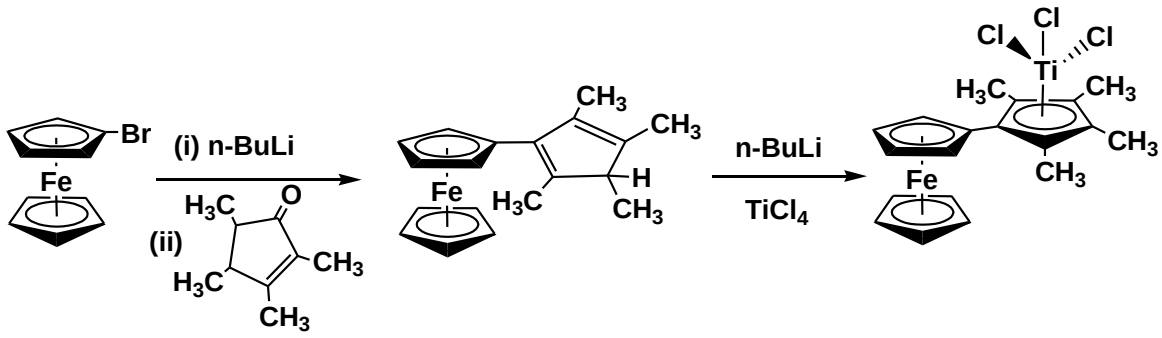

Scheme 1.36

In summary, chapter 1 describes the immense potential of cylopentadienyl based metal complexes and their recent application based upon electrochemistry, bioactivity, catalysis and sensor. In view of their significant contribution, we became interested to design and synthesize different ferrocene and cymantrene based molecular compounds involving functional moieties like hydrazones, enones etc and explore their electrochemical and biological properties. Efforts have also been made to establish the structural characterization of sandwich and half sandwich organometallic compounds by single crystal X-ray diffraction technique and understand their potential as metal sensing and biological agents.

1.6. References

[1] R. B. Woodward, M. Rosenblum, M. C. Whiting. J. Am. Chem. Soc. 74 (1952) 3458.

[2] M. Rosenblum, R. B. Woodward, J. Am. Chem. Soc. 80 (1958) 5443.

[3] M. D. Rausch, E. O. Fisher, H. Grubert, Chem. Ind. (1958) 756.

[4] M. D. Rausch, E. O. Fischer, H. Grubert, J. Am. Chem. Soc. 82 (1960) 76.

[5] F. A. Cotton, J. Leto, Chem. Ind. (1958) 1368.

[6] E. O. Fischer, K. Plesske, Chem. Ber. 91 (1958) 2719.

[7] J. Kozikowski, R. E. Maginn, M. S. Klove, J. Am. Chem. Soc. 81 (1959) 2995.

[8] E. O. Fischer, W. Fellman, J. Organomet. Chem. 1 (1963)191.

[9] A. N. Nesmeyanov, K. N. Anisimov, N. E. Kolobova, L. I. Batyshnikova, Dokl. Akad. Nauk SSSR. 154 (1964) 646.

[10] A. N. Nesmeyanov, K. N., Anisimov, N. E, Kolobova, L. I. Baryslnikova, Izv. Akad. Nauk. SSSR. Ser. Khim. (1964) 1135.

[11] E.O. Fischer, K. Plesske, Chem. Ber. 94 (1961) 93.

[12] S. T. Mabrouk, W. P. Hart, M. D. Rausch, J. Organomet. Chem. 527 (1997) 43.

[13] E.O. Fischer, K. Plesske, Chem. Ber. 93 (1960) 1006.

[14] R. Riemschneider, O. Goehring, K. Kruger, Monatsh. Chem. 91 (1960) 305.

[15] R. Ercoli, F. Calderazzo, Chim. Ind. (Milan) 42 (1960) 52.

[16] W. P. Hart, M. D. Rausch, J. Organomet. Chem. 355 (1988) 455.

[17] P. J. Chirik, Organometallics 29 (2010) 1500.

[18] R. H. Crabtree, The Organometallic Chemistry of the Transition Metals, 2nd ed., John Wiley & Sons, NY, 1994, pp. 121-122.

[19] C. P. Casey, J. M. O'Connor, W. D. Jones, K. J. Haller, Organometallics 2 (1983) 535.

[20] J. Campbell, C. A. Fyfe, R. G. Goel, E. Maslowsky, Jr., C. V. Senoff, J. Am.Chem. Soc., 29 (1972) 8387.

[21] E. A. Bielinski, W. Dai, L. M. Guard, N. Hazari, M. K. Takase, Organometallics 32 (2013) 4025.

[22] H. Schumann, A. Lentz, R. Weimann, J. Organomet. Chem. 487 (1995) 245.

[23] W. M. Cheung, E. K. Huang, J. Zhu, X. Y Yi, H. H. Y. Sung, I. D. Williams, W. H. Leung, Inorg. Chem. 52 (2013) 10449.

[24] L. Mehr, E. I. Becker, P. E. Spoerri, J. Am. Chem. Soc. 77 (1955) 984.

[25] S. Xu, F. Yuan, Y. Zhuang, B. Wang , Y. Li, X. Zhou, Inorg. Chem. Commun. 5 (2002) 102.

[26] Y. Imamura, K. Kubo, T. Mizuta, K. Miyoshi, Organometallics 25 *(*2006) 2301.

[27] M. L. Desai, M. K. Si, R. Lo, B. Ganguly, J. Mol. Model 21 (2015) 218.

[28] A. Eisenstadt, R. Tannenbaum , A. Efraty, J. Organomet. Chem. 221(1981) 317.

[29] R. J. Haines, A. L. duPreez, J. Chem. Soc. Dalton. (1972) 944.

[30] D. H. Gibson. W. L. Hsu, A. L. Steinmetz, J. Organomet. Chem. 208 (1981) 89.

[31] R. J. Haines, A. L. duPreez. J. Am. Chem. Soc. 91 (1969) 769; J. Chem. Soc. (A), (1970) 2341.

[32] H. B. Abrahamson. M. C. Palazzotto. C. L. Reichel , M. S. Wrighton. J. Am. Chem. Soc. 101 (1979) 4123.

[33] J. V. Spar, T. J. Meyers, J. Am. Chem. Soc. 102 (1980) 7794.

[34] M. Bruce, C. Ilameister, A. Swincer, R. Wallis, Inorg. Synth. 21 (1982) 21.

[35] M. E. Khateeb, K. Shawakfeh, M. A. Btoosh, H. Görls, W. Weigand, Polyhedron 89 (2015) 70.

[36] A. J. Millett, A. Habtemariam, I. R. Canelón, G. J. Clarkson, P. J. Sadler, Organometallics 34 (2015) 2683.

[37] J. Ruiz, V. Rodríguez, N. Cutillas, K. G. Samper, M. Capdevila, Ò. Palaciosb, A. Espinosac, Dalton Trans. 41 (2012) 12847.

[38] Z. Liu, A. Habtemariam, A. M. Pizarro, S. A. Fletcher, A. Kisova, O. Vrana, L. Salassa, P. C. A. Bruijnincx, G. J. Clarkson, V. Brabec, P. J. Sadler, J. Med. Chem. 54 (2011) 3011.

[39] Z. Liu, L. Salassa, A. Habtemariam, A. M. Pizarro, G. J. Clarkson, P. J. Sadler, Inorg. Chem. 50 (2011) 5777.

[40] J. Foerstner, A. Kakoschke, D. Stellfeldt, H. Butenschon, Organometallics 17 (1998) 893.

[41] E. S. Kelbysheva, M. G. Ezernitskaya, T. V. Strelkova, Y. A. Borisov, A. F. Smol'yakov, Z. A. Starikova, F. M. Dolgushin, A. N. Rodionov, B. V. Lokshin, N. M. Loim, Organometallics 30 (2011) 4342.

[42] P. Jutzi, M. O. Kristen, J. Dahlhaus, B. Neumann, H. G. Stammler, Organometallics 12 (1993) 2980.

[43] Q. Huang, Y. Qian, G. Li, Y. Tang; Transition Met. Chem. 15 (1990) 483.

[44] P. Buchgraber, L. Toupet, V. Guerchais, Organometallics. 22 (2003) 5144.

[45] P. Mathur, A. K. Bhunia, A. Kumar, S. Chatterjee, S. M. Mobin, Organometallics, 21 (2002) 2215.

[46] M. Scheer, S. B. Umbarkar, S. Chatterjee, R. Trivedi, P. Mathur, Angew. Chem. Int. Ed. 40 (2001) 376.

[47] K. D. Warren, Inorganic Chemistry 13 (1974) 1317.

[48] S. P. Gubin, S. K Smirnova, L. I. Denisovich, A. A. Lubovich, J. Organomet. Chem. 30 (1971) 243.

[49] A. J. Augystyniak, J. Wojtczak, Monatshefte fur chemie 110 (1979) 1113.

[50] H. Bauer, J. Weismann, D. Saurenz , C. Farber , M. Schär, W. Gidt, I. Schädlich, G. Wolmershäuser, Y. Sun, S. Harder, H. Sitzmann, J. Organomet.chem. 809 (2016) 63.

[51] G. Wilkinson, J. Am. Chem. Soc. 74 (1952) 6146.

[52] A. N. Nesmeyanov, N. A. Volxenau', I. N. Bolesova, L. S. Shul'pina, J. Organomet. Chem. 182 (1979) C36.

[53] M. Rosenblum, B. North, D. Wells, W. P. Giering, J. Am. Chem. Soc. 94 (1972) 1239.

[54] Y. Zeng, H. Feng, R. B. King, H. F. Schaefer, Organometallics 33 (2014) 4410.

[55] S. C. Binding, J. C. Green, W. K. Myers, D. O'Hare, Inorg. Chem. 54 (2015) 11935.

[56] J. C. Green, Chem. Soc. Rev. 27 (1998) 263.

[57] S. P. Semproni, C. Milsmann, P. J. Chirik, Organometallics 31 (2012) 3672.

[58] W. S. Lee, J. Organomet. Chem. 127 (1977) 87.

[59] J. D. Zhang, Z. Chen, R. B. King, H. F. Schaefer, Eur. J. Inorg. Chem. 2008, 1219.

[60] H. Wang, Y. Xie, R. B. King, H. F. Schaefer, J. Am. Chem. Soc. 127 (2005) 11646.

[61] Z. Z. Xie, W. H. Fang, Chemical Physics Lett. 404 (2005) 212.

[62] D. Chong, A. Nafady, P. J. Costa, M. J. Calhorda, W. E. Geiger, J. Am. Chem. Soc. 127 (2005) 15676.

[63] E. Diana, R. Rossetti, P. L. Stanghellini, S. F. A. Kettle, Inorg. Chem. 36 (1997) 382.

[64] J. I. Ito, T. Shima, H. Suzuki, Organometallics 25 (2006) 1333.

[65] A. Salzer, H. Werner, Angew. Chem. 84 (1972) 949; Angew. Chem. Int. Ed. Engl. 11 (1972) 930.

[66] S. Scholz, J. C. Green, H. W. Lerner, M. Boltec, M. Wagner, Chem. Commun. (2002) 36.

[67] D. R. Armstrong, A. J. Edwards, D. Moncrieff, M. A. Paver, P. R. Raithby, M. A. Rennie, C. A. Russella, D. S. Wright, J . Chem. Soc., Chem. Commun. (1995) 927.

[68] J. Kozikowski, R. E. Maginn, M. S. Klove, Contribution from the Detroit research laboratories of ethyl corporation 1959, 2995.

[69] Federal Register 60 (1995) 36414.

[70] A. S. Hamadi, Tikrit J. Eng. Sciences 17 (2010) 22.

[71] W. Strohmeier, Angew. Chem. Internat. Edit. 3 (1964) 730.

[72] M. Herberhold, W. Kremnitz, H. Trampisch, R. B. Hitam, A. J. Rest, D. J. Taylor, J. Chem. Soc. Dalton Trans. (1982) 1261.

[73] J. W. Kee, Y. Y. Tan, B. H. G. Swennenhuis, A. A. Bengali, W. Y. Fan, Organometallics 30 (2011) 2154.

[74] L. N. Telegina, M. G. Ezernitskaya, I. A. Godovikov, K. K. Babievskii, B. V. Lokshin, T. V. Strelkova, Y. A. Borisov, N. M. Loim, Eur. J. Inorg. Chem. (2009) 3636.

[75] T. T. To, C. B. Duke, C. S. Junker, C. M. O'Brien, C. R. Ross, C. E. Barnes, C. E. Webster, T. J. Burkey, Organometallics 27 (2008) 289.

[76] E. J. Heilweil, J. O. Johnson, K. L. Mosley, P. P. Lubet, C. E. Webster, T. J. Burkey, Organometallics 30 (2011) 5611.

[77] K. Splith, I. Neundorf, W. Hu, H. W. P. N'Dongo, V. Vasylyeva, K. Merz, U. Schatzschneider, Dalton Trans. 39 (2010) 2536.

[78] M. Hromadova´, M. Salmain, R. Sokolova´, L. Pospı´sˇil, G. Jaouen, J Organomet. Chem. 668 (2003) 17.

[79] H. W. Peindy, N. Dongo, I. Neundorf, K. Merz, U. Schatzschneider, J. Inorg. Biochem. 102 (2008) 2114.

[80] L. Glans, W. Hu, C. Jöst, C. Kock, P. J. Smith, M. Haukka, H. Bruhn, U. Schatzschneider, E. Nordlander, Dalton Trans.41 (2012) 6443.

[81] D. R. Laws, D. Chong, K. Nash, A. L. Rheingold, W. E. Geiger, J. Am. Chem. Soc. 130 (2008) 9859.

[82] K. Wu, S. Top, E. A. Hillard, G. Jaouen, W. E. Geiger, Chem. Commun. 47 (2011) 10109.

[83] D. P. Day, T. Dann, D. L. Hughes, V. S. Oganesyan, D. Steverding, G. G. Wildgoose, Organometallics 33 (2014) 4687.

[84] K. Heinze, H. Lang, Organometallics 32 (2013) 5623.

[85] S. Takebayashi, T. Shibata, Organometallics 31 (2012) 4114.

[86] S. R. Bayly, P. D. Beer, G. Z. Chen, Ferrocene sensors. In Ferrocenes: Ligands, Materials and Biomolecules; Stepnicka, P., Ed.; Wiley: Hoboken, NJ, 2008; pp 281.

[87] W. Skibar, H. Kopacka, K. Wurst, C. Salzmann, K. H. Ongania, F. F. Biani, P. Zanello, B. Bildstein, Organometallics. 23 (2004) 1024.

[88] L. X. Dai, T. Tu, S. L You, W. P. Deng, X. L. Hou, Acc. Chem. Res. 36 (2003) 659.

[89] R. Sun, L. Wang, H. Yu, Z. Abdin, Y. Chen, J. Huang, R. Tong, Organometallics 33 (2014) 4560.

[90] R. H. Fish, G. Jaouen, Organometallics 22 (2003) 2166.

[91] T. Y. Dong, L. S. Chang, I. M. Tseng, S. J. Huang, Langmuir 20 (2004) 4471.

[92] S. S. Braga, A. M. S. Silva, Organometallics 32 (2013) 5626.

[93] T. J. Kealy, P. L. Pauson, Nature, 168 (1951) 1039.

[94] Ferrocenes: Homogeneous Catalysis/Organic Synthesis/Materials Science; Togni, A.; Hayashi, T., Eds.; Wiley-VCH: Weinheim 1995.

[95] M. F. R. Fouda, M. M. Abd-Elzaher, R. A. Abdelsamaia, A. A. Labib, Appl. Organomet. Chem. 21 (2007) 613.

[96] W. A. Amer, L. Wang, A. M. Amin, L. Ma, H. Yu, J. Inorg. Organomet. Polym. Mater. 20 (2010) 605.

[97] T. L. Choi, K. H. Lee, W. J. Joo, S. Lee, T. W. Lee, M. Y. Chae, J. Am. Chem. Soc. 129 (2007) 9842.

[98] T. Daeneke, T. H. Kwon, A. B. Holmes, N. W. Duffy, U. Bach, L. Spiccia, Nat. Chem. 3 (2011) 211.

[99] M. Tropiano, N. L. Kilah, M. Morten, H. Rahman, J. J. Davis, P. D. Beer, S. J. Faulkner, Am. Chem. Soc. 133 (2011) 11847.

[100] R. G. Arrayás, J. Adrio, J. C. Carretero, Angew. Chem. Int. Ed. 45 (2006) 7674.

[101] Chiral Ferrocenes in Asymmetric Catalysis; Dai, L.- X.; Hou, X.-L., Eds.; Wiley-VCH: Weinheim, 2009.

[102] S. Siegel, H. G. Schmalz, Angew. Chem. Int. Ed. Engl. 36 (1997) 2456.

[103] A. Datta, A. Köllhofer, H. Plenio, Chem. Commun. (2004) 1508.

[104] J. B. Xia, S. L You, Organometallics 26 (2007) 4869.

[105](a) A. Togni, T. Hayashi, Eds. Ferrocenes: Homogeneous Catalysis, Organic Synthesis, Materials Science; VCH: Weinheim, 1995; (b) Chapter 5.2.

[106] M. Rosenblum, R. B. Woodward, J. Am. Chem. Soc. 80 (1958) 5443.

[107] M. D. Rausch, Can. J. Chem. 41 (1963) 1289.

[108] A. R. Petrov, K. Jess, M. Freytag, P. G. Jones, M. Tamm, Organometallics 32 (2013) 5946.

[109] M. Korb, H. Lang, Organometallics 33 (2014) 6643.

[110] M. Korb, Heinrich Lang, Organometallics 33 (2014) 2099.

[111] V. Ganesh; V. S Sudhir; T. Kundu; S. Chandrasekaran; Chem. Asian J. 6 (2011) 2670.

[112] F. Otón, M. C. González, A. Espinosa, C. R. Arellano, A. Tárraga, P. Molina, J. Org. Chem. 77 (2012) 10083.

[113] L. A. López, E. López, Dalton Trans. 44 (2015) 10128.

[114] V. Mamane, Mini-Reviews in Organic Chemistry, 5 (2008) 303.

[115] E. López, G. Lonzi, L. A. López, Organometallics 33 (2014) 5924.

[116] R. Deng, Y. Huang, X. Ma, G. Li, R. Zhu, B. Wang, Y.-B. Kang, Z. Gu, J. Am. Chem. Soc. 136 (2014) 4472.

[117] S. B. Wang, J. Zheng, S. L. You, Organometallics 35 (2016) 1420.

[118] T. Moriuchi, K. Yoshida, T. Hirao, Organometallics 20 *(*2001) 3101.

[119] T. Moriuchi, T. Nagai, T. Hirao, Organic Letters 7 (2005) 5265.

[120] W. Bauer, K. Polborn, W. Beck, J. Organomet. Chem. 579 (1999) 269.

[121] T. Moriuchi, T. Hirao, Top Organomet. Chem. 17 (2006) 143.
[122] S. Top , A. Vessie`res, C. Cabestaing , I. Laios, G. Leclercq, C. Provot, G. Jaouen, J. Organomet. Chem. 637–639 (2001) 500.
[123] E. Hillard, A. Vessières, L. Thouin, G. Jaouen, C. Amatore, Angew. Chem. Int. Ed. 45 (2006) 285.
[124] P. Pigeon, S. Top, O. Zekri, E. A. Hillard, A. Vessières, M.-A. Plamont, O. Buriez, E. Labbé, M. Huché, S. Boutamine, C. Amatore, G. Jaouen, J. Organomet. Chem. 694 (2009) 895.
[125] C. Biot, N. Chavain, F. Dubar, B. Pradines, X. Trivelli, J. Brocard, I. Forfar, D. Dive, J. Organomet. Chem. 694 (2009) 845.
[126] X.-F. Huang, L.-Z. Wang, L. Tang, Y.-X. Lu, F. Wang, G.-Q. Song, B.-F. Ruan, J. Organomet. Chem. 749 (2014) 157.
[127] W. Nkoana, D. Nyoni, P. Chellan, T. Stringer, D. Taylor, P. J. Smith, A. T. Hutton, G. S. Smith, J. Organomet. Chem., 752 (2014) 67.
[128] T. Stringer, H. Guzgay, J. M. Combrinck, M. Hopper, D. T. Hendricks, P. J. Smith, K. M. Land, T. J. Egan, G. S. Smith, J. Organomet. Chem. 788 (2015) 1.
[129] C. Arivazhagan, R. Borthakur, S. Ghosh, Organometallics 34 (2015) 1147.
[130] K. Kumar, S. C. Kremer, L. Kremer, Y. Guérardel, C. Biot, V. Kumar, Organometallics 32 (2013) 5713.
[131] D. R. V. Staveren, N. Metzler-Nolte, Chem. Rev. 104 (2004) 5931.
[132] A. R. Pike, L. C. Ryder, B. R. Horrocks, W. Clegg, M. R. J. Elsegood, B. A. Connolly, A. Houlton, Chem. Eur. J. 8 (2002) 2891.
[133] M. Patra, G. Gasser, M. Wenzel, K. Merz, J. E. Bandow, N. Metzler- Nolte, Organometallics 29 (2010) 4312.
[134] M. Navarro, W. Castro, C. Biot, Organometallics 31 (2012) 5715.
[135] O. Payen, S. Top, A. Vessières, E. Brulé, A. Lauzier, M.-A. Plamont, M. J. McGlinchey, H. Müller-Bunz, G. Jaouen, J. Organomet. Chem. 696 (2011)1049-1056.
[136] J. Quirante, F. Dubar, A. González, C. Lopez, M. Cascante, R. Cortés, I. Forfar, B. Pradines, C. Biot, J. Organomet. Chem. 696 (2011) 1011-1017.
[137] V. Zsoldos-Mády, A. Csámpai, R. Szabó, E. Mészáros-Alapi, J. Pásztor, F. Hudecz, P. Sohár, Chem. Med. Chem. 1 (2006) 1119.

[138] B. Maity, B. V. S. K. Chakravarthi, M. Roy, A. A. Karande, A. R. Chakravarty, Eur. J. Inorg. Chem. (2011) 1379.

[139] J. Zhang, Appl. Organomet. Chem. 22 (2008) 6.

[140] Z. H. Chohan, C. T. Supuran, Appl. Organomet. Chem. 19 (2005) 1207.

[141] Z. H. Chohan, H. Pervez, K. M. Khan, C. T. Supuran, J. Enzym. Inhib. Med. Chem. 20 (2005) 81.

[142] G. Sathyaraj, M. Kiruthika, T. Weyhermüller, B. U. Nair, Organometallics 31 (2012) 6980.

[143] R. Ayranci, D. O. Demirkol, M. Ak , S. Timur, Sensors 15 (2015) 1389.

[144] Z. Yang, M. A. Auriac, S. Goggins, B. K. Hordern, K. V. Thomas, C. G. Frost, P. Estrela, Environ. Sci. Technol. 49 (2015) 5609−5617.

[145] P. Molina, A. Tárraga, A. Caballero, Eur. J. Inorg. Chem. (2008) 3401–3417.

[146] T. Romero, A. Caballero, A. Ta´rraga, P. Molina, Org. Lett. 11 (2009) 3466.

[147] S. Barlow, H. E. Bunting, C. Ringham, J. C. Green, G. U. Bublitz, S. G. Boxer, J. W. Perry, S. R. Marder, J. Am. Chem. Soc. 121 (1999) 3715.

[148] O. Karagollua, M. Gorurb, F. Godea, B. Sennikb, F. Yilmazc, Sensors and Actuators B193 (2014) 788.

[149] C. K. Kumar, R. Trivedi, K. R. Kumar, L. Giribabu, B. Sridhar, Eur. J. Inorg. Chem. (2013) 6019.

[150] M. Alfonso, A. Espinosa, A. Ta´ rraga, P. Molina, Chem. Commun. 48 (2012) 6848.

[151] A. Caballero, A. Espinosa, A. Ta´rraga, P. Molina, J. Org. Chem. 73 (2008) 5489.

[152] J. Schulz, F. Uhlík, J. M. Speck, I. Císarova, H. Lang, P. Stepnicka, Organometallics 33 (2014) 5020.

[153] A. Sundararaman, K. Venkatasubbaiah, M. Victor, L. N. Zakharov, A. L. Rheingold, F. Ja¨ kle, J. Am. Chem. Soc. 128 (2006) 16554.

[154] C. J. Ziegler, K. Chanawanno, A. Hasheminsasab, Y. V. Zatsikha, Eranda Maligaspe, V. N. Nemykin, Inorg. Chem. 53 (2014) 4751.

[155] (a) M. H. Delville, Inorganica Chimica Acta 291 (1999) 1; (b) M. D. Ward, Chem. Soc. Rev. 24 (1995) 121.

[156] R. Sakamoto, M. Murata, H. Nishihara, Angew. Chem. Int. Ed. 45 (2006) 4793 .

[157] D. Braga, Chem. Commun. (2003) 2751.
[158] C. Fo¨rster, P. Veit, V. Ksenofontov, K. Heinze, Chem. Commun. 51 (2015) 1514
[159] P. Veit, E. Prantl, C. Förster, K. Heinze, Organometallics. 35 (2016) 249.
[160] F. Oton, I. Ratera, A. Espinosa, A. Tarraga, J. Veciana, P. Molina, Inorg. Chem. 49 (2010) 3183.
[161] B. Fábián, A. Csámpai, T. Z. Nagy, M. Czugler, P. Sohár, J. Organomet. Chem. 694 (2009) 3732.
[162] P. Mathur, A. K. Singh, S. Chatterjee, V. K. Singh, S. M. Mobin, J Organomet. Chem. 695 (2010) 950–954.
[163] A. Csámpai, A. Z. Györfi, Gy.I. Túrós, P. Sohár, J Organomet. Chem. 694 (2009) 3667.
[164] U. Pfaff, A. Hildebrandt, D. Schaarschmidt, T. Hahn, S. Liebing, J. Kortus, H. Lang, Organometallics 31 (2012) 6761.
[165] J. Yin, G.-A Yu, H. Tu, S. H. Liu, Appl. Organometal. Chem. 20 (2006) 869.
[166] F. O. Oginia, Y. Ortin, A. H. Mahmoudkhani, A. F. Cozzolino, M. J. McGlinchey, I. V. Baca, J Organomet. Chem. 693 (2008) 1957.
[167] M. Lohan, P. Ecorchard, T. Ru¨ffer, F. Justaud, C. Lapinte, H. Lang, Organometallics 28 (2009) 1878.
[168] A. Jakob, P. Ecorchard, T. Ruffer, M. Linseis, R. F. Winter, H. Lang, J. Organomet. Chem. 694 (2009) 3542.

Chapter 2

Synthesis, characterization and structural evaluation of cymantrenyl hydrazone derivatives

2.1. Introduction

Studies of Schiff-base compounds with organometallic tags are increasingly drawing much interest due to their distinctive properties and features concerning both organometallic and coordination chemistry [1-9]. Molecular compounds containing organometallic tags have been found to be potential therapeutics against major diseases and can play a vital role as tracers in immunological analysis based on several analytical methods like FTIR, electrochemical, atomic absorption techniques etc [10-13, 24-26]. The use of ferrocenyl derivatives as bioactive molecule has been established recently and several reports show that a large number of ferrocene containing compounds display interesting cytotoxic and DNA cleaving activities [14-20]. Recently, some Cp based half sandwich organometallic fragments have been studied for their various biological properties ranging from antimalarial, antimicrobial, anticancer, enzyme inhibitors and phototoxicity [21-28].

Cyclopentadienyl based metal complexes with functionalized side-chains are presently being explored by several research groups anticipating some unique properties that may be different from {CpM} systems without the functional side chain. In this regard, a large number of half sandwich metal complex with functionalized side chains have been studied for biological, photophysical and electronic properties. Recently, synthesis of cyrhetrenyl, [$CpRe(CO)_3$], system with Schiff base type funtionalization carried out by the condensation reaction of 5-nitro-2-furanaldehyde with different cyrhetrenyl amines showed higher trypanocidal activity as compared to their organic and ferrocenyl analogs (Figure 2.1).[8] The efficient antichagasic properties has been attributed to the enhanced lipophilic character of the metal fragment and a possible synergy between the cyrhetrenyl and 5-nitrofuran groups.

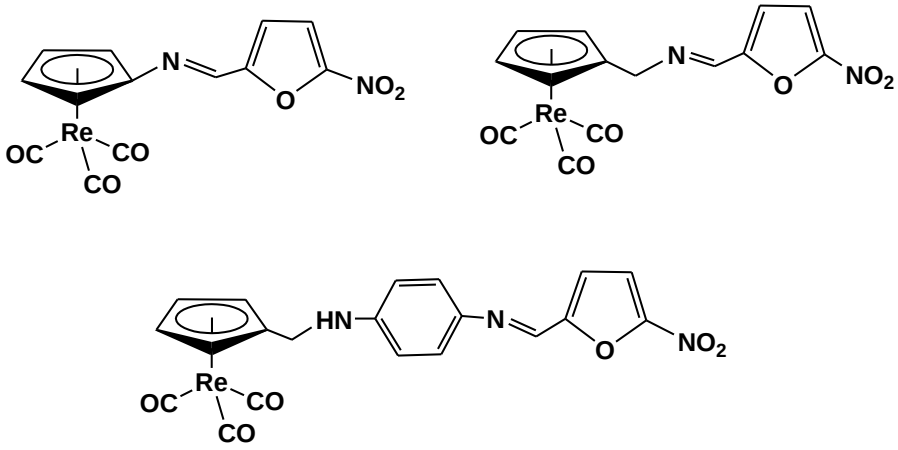

Figure 2.1. Cyrhetrenylimine derivatives

A number of biologically active compounds of technicium, $[(CpR)^{99m}Tc(CO)_3]$ have been synthesized for their probable therapeutic and radionuclide based diagnostic applications [24, 25]. Alberto's group demonstrated the formation of {CpTc} based compounds with different side chains at the cyclopentadienyl moiety by using Diels-Alder dimerized precursor bearing biologically active substituents with $[^{99m}TcO_4]^-$ or $[^{99m}Tc(OH_2)_3(CO)_3]^+$ in aqueous medium (Scheme 2.1). This interesting synthetic strategy provided an access to use labeled biomolcules with ^{99m}Tc in water phase and could able to play a vital role in the development of radiopharmaceuticals.

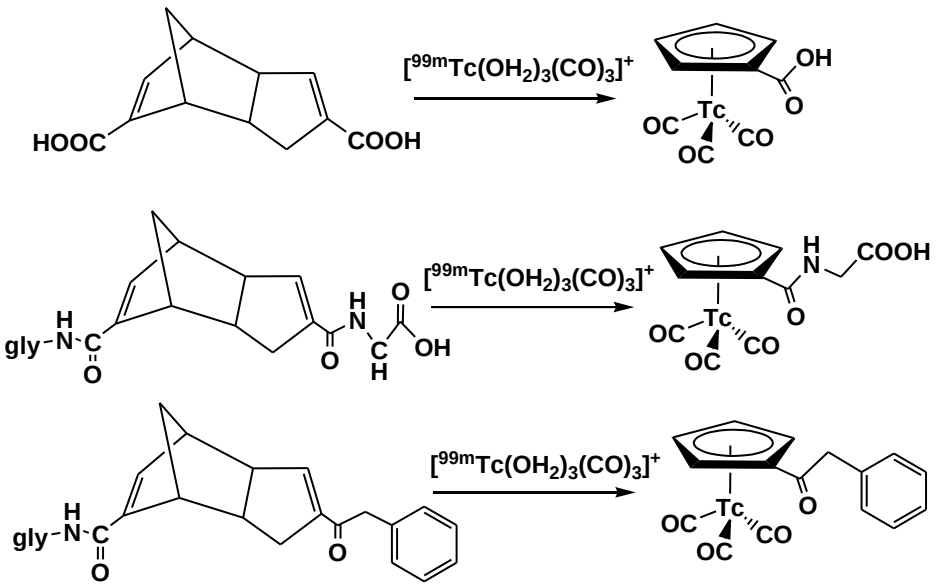

Scheme 2.1

Meggers et al. reported protein inhibitor property of a organoruthenium analogue of staurosporine, which contains a half sandwich, [CpRu(CO)], fragment attached to indolocarbazole heterocycle [27]. The half sandwich based staurosporine derivative was synthesized from aryl hydrazine precursor using multistep reaction processes involving Fischer indole synthesis to prepare a pyridoindole derivative which was subsequently coupled with dibromomaleimide using anaerobic photocyclization to give the indolocarbazole heterocyclic ligand. The heterocycle was then treated with $[CpRu(CO)(CH_3CN)_2]PF_6$ to give the half sandwich ruthenium-staurosporine complex (Figure 2.2).

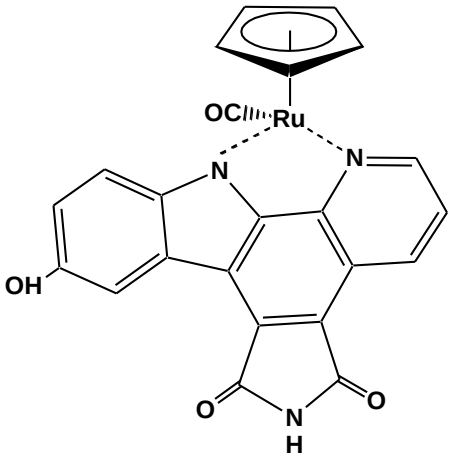

Figure 2.2. Ruthenium staurosporine derivative

Some of these half sandwich complexes have been very interestingly used as labelling agents in the field of metalloimmunoassay. In most cases for the study related to metalloimmunoassay using organometallic system, the metal based tracers are molecules derived from the analyte to be assayed to which an organometallic moiety has been attached. This gives rise to some type of competition between the analyte and the tracer to bind to a limited amount of antibody. In this regard it is highly required that the metal fragments to be used as tracer must be stable in air and biological media and can be structurally fine tuned, if required, for optimum sensitivity of the assay. Different

labelling studies in recent times showed that half sandwich complexes are well suited for metallic agents and can be used with a variety of biomolecular entities. Among them, cymantrenyl derivative based tracers are significant molecule which are stable, can be easily tuned by different substitution at the Cp ring and at the metal carbonyl part and show specific IR signals with intense absorption in the range1900-2200 cm^{-1} for their use as IR probes in various biological samples. Cymantrenyl fragment has been succesfully labelled with biotine molecule by the coupling reaction of cymantrenyl carboxaldehyde with biotine hydrazide. Metallo-biotins have been suitable for a wide range of antigens and provide several possibilities for immunoassays of antibodies. Biotinylated cymantrene complex a biotine fragment attached to the Cp ring of the cymantrene via a Schiff base type C=N bond. The Cp ring remains pi –bonded with the manganese metal atom by a pentahapto mode of bonding. Three metal carbonyls are also attached with the metal center to make the system stable with 18 valence electrons (Scheme2.2).[28]

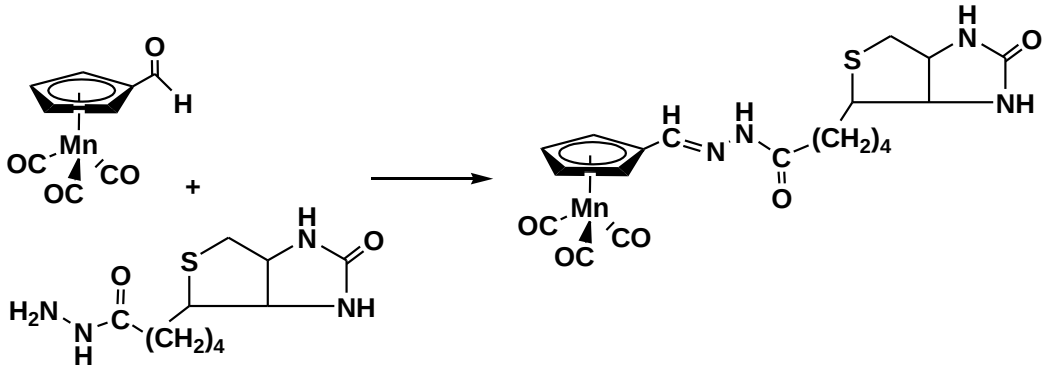

Scheme 2.2

Cymantrene based labeling of phenobarbital was carried out by using simple acylation reaction of p-aminophenobarbital by cymantrenyl acylchloride (Figure 2.3). The labelled phenobarbital was used for a non-radioisotopic immunoassay, also termed as cabonylmetalloimmunoassay (CMIA), using FTIR spectroscopy to detect the CO

stretching modes of the organometallic label. The method was of comparable sensitivity to a [^{14}C] radio-immunoassay for the detection of Phenobarbital at femtomole level.[29] Similarly nortriptyline, a tricyclic antidepressant drug, was labelled by acylation of the secondary amino group with cymantrenyl acylchloride (Figure 2.3).[30]

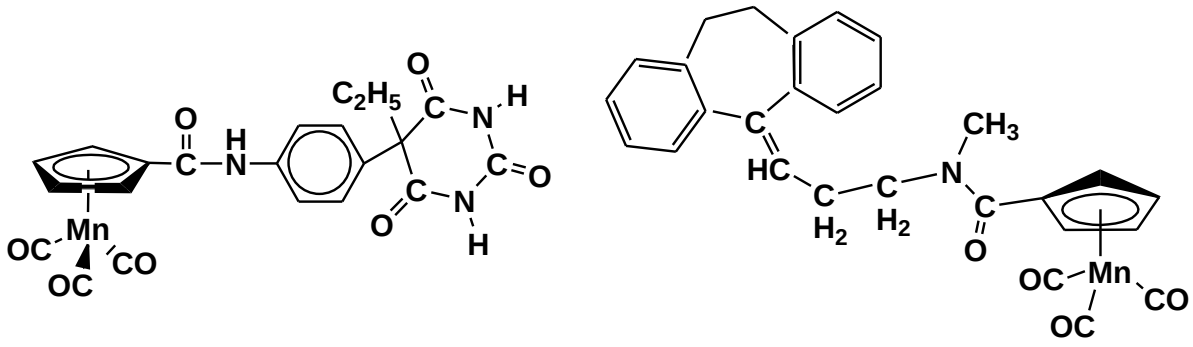

Figure 2.3

Other than the carbonyl immunoassay, cymantrenyl fragments have also been used conjugated with cell-penetrating peptide, hCT(18-32)-k7, which transformed the intracellular distribution of the peptide inducing cytotoxic properties against MCF-7 cancer cells.[31] Recently, some sandwich and half sandwich metal fragments were coupled with a platencimycin to investigate structure- property relationship of their biological properties and the influence of the organometallic fragments on the bioactive part of the molecule. Synthesis of cymantrene based platencimycin derivative was carried out by a multistep reaction process involving derivatization of the cymantrenyl side chain linked to the Cp ring to obtain first a fused cyclohexenone ring system and then a series of reaction step to get the desired platensimycin linked cymantrenyl compounds (Figure 2.4).[32] The antibacterial, antitumor activity and molecular modeling for platencimycine derivatives have been studied and a comparative investigation was carried out to understand the involvement of a specific fragment or group in the biological activity.

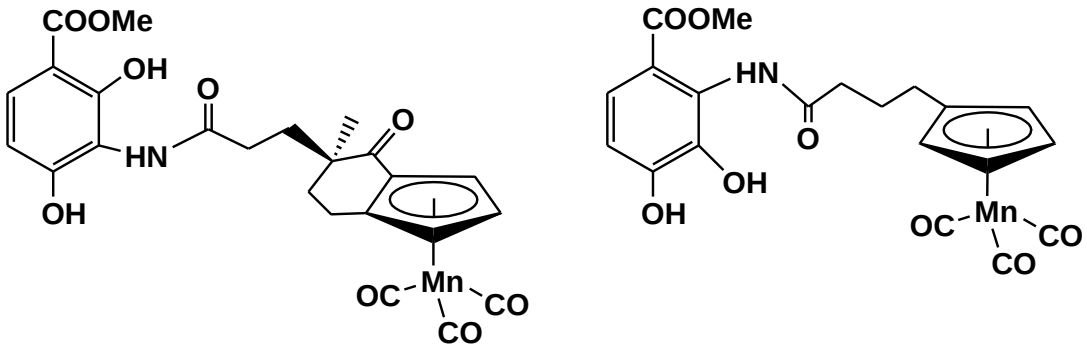

Figure 2.4

In view of their enormous opportunity, we became interested to synthesize some Schiff base compounds containing [(η^5-C_5H_4R)Mn] organometallic tags and investigate their structural and biological properties. We selected cymantrenyl moieties as because these compounds contain metal carbonyls which show specific IR signals with intense absorption in the range1900-2200 cm^{-1} and can be used as IR probes in various biological samples. Moreover, to our knowledge cymantrenyl Schiff base compounds have been rarely studied and one of the reports show the synthesis of cymantrenyl-biotine compounds for their use as tracer molecule [28], whereas cymantrenyl - hydrazone compounds have been largely unexplored and are yet to be investigated for their possible antibacterial activities. In this chapter, we describe the synthesis and characterization of four cymantrenyl hydrazone Schiff base compounds (**1 - 4**). Compound **1 -3** have been characterized structurally by single crystal X-ray diffraction techniques. Antibacterial activity and electrochemical properties have been studied for some of the cymantrenyl compounds.

2.2. Experimental Sections

2.2.1. General Procedures

All reactions and manipulations were carried out under an inert atmosphere of dry, pre-purified argon using standard schlenk line techniques. Solvents were purified, dried and distilled under argon atmosphere prior to use. Infrared spectra were recorded on a Perkin Elmer Spectrum RX-I spectrometer as KBr pellet or CH_2Cl_2 solution and NMR spectra on a 400 MHz Bruker spectrometer in $CDCl_3$ or DMSO-d6 solvent. Elemental analyses were performed on a Vario El Cube analyser. Mass spectra were obtained on a SQ-300 MS instrument operating in ESI mode. TLC plates (20x20 cm, Silica gel 60 F254) were purchased from Merck. $[(CO)_3Mn(\eta^5\text{-}C_5H_4COCH_3)]$, $[H_2NN(H)C(O)R]$, (R = $\text{-}C_6H_4OH\text{-}o$, $C_6H_4N\text{-}p$, C_6H_5, $C_6H_4N\text{-}o$) were prepared following reported procedures [33, 34].

2.2.2. Synthesis of $[(CO)_3Mn\{(\eta^5\text{-}C_5H_4)C(CH_3)=NN(H)C(O)R\}]$ (1-4)

In a typical synthetic procedure, respective hydrazide (0.1 mmol) was taken in a two-neck round bottomed flask and ethanol (10 ml) solvent was added. The solution was stirred under nitrogen atmosphere to obtain a clear solution. To the reaction mixture 0.1 mmol of monoacetyl cymantrene (25 mg, 0.1 mmol) and 2 drops of acetic acid was added at room temperature and under stirring condition and the reaction was continued for 3-4 hrs. After the reaction, the solution was filtered and the pale yellow precipitate was washed with cold ethanol and vacuum dried. The product was purified by preparative TLC in 5% ethanol: n-hexane solvent mixture. (Yield = 35 mg (92 %) (**1**); 32 mg (88 %) (**2**), 29 mg (81 %) (**3**); 31 mg (86 %) (**4**))

1: Anal. calcd. (found): C, 53.68 (53.45); H, 3.42 (3.37); N, 7.36 (7.45). IR(ν, cm^{-1}, CH_2Cl_2): 3278.7 (br), 3057.4 (br), 2010 (s), 1923.7 (vs), 1630.4 (s), 1601.5 (m). ^1H NMR (δ, $CDCl_3$): 2.15 (s, 3H, CH_3), 4.84 (s, 2H, η^5-C_5H_4), 5.38 (s, 2H, η^5-C_5H_4), 6.92 (t, J = 7 Hz, 1H, C_6H_4), 7.05 (d, J = 7 Hz, 1H, C_6H_4), 7.45-7.49 (m, 1H, C_6H_4), 9.01 (br, 1H, N*H*), 11.66 (br, 1H, O*H*). MS (ESI): m/z 381 $(M)^+$.

2: Anal. calcd. (found): C, 52.60 (52.78); H, 3.28 (3.21); N, 11.50 (11.62). IR(ν, cm^{-1}, CH_2Cl_2): 3210 (br), 2019 (vs), 1929.8 (vs, br), 1669 (s), 1603 (w). ^1H NMR (δ, $CDCl_3$): 2.09 (s, 3H, CH_3), 4.79 (s, 2H, η^5-C_5H_4), 5.11-5.40 (m, 2H, η^5-C_5H_4), 7.67 (s, 2H, C_6H_4N), 8.78 (s, 2H, C_6H_4N), 8.95 (br, 1H, N*H*).

3: IR(ν, cm^{-1},CH_2Cl_2): 3213 (br), 2018 (vs), 1926 (vs, br), 1658 (br), 1604 (w). ^1H NMR (δ, $CDCl_3$): 2.09 (s, 3H, CH_3), 4.79 (s, 2H, η^5-C_5H_4), 5.17-5.34 (m, 2H, η^5-C_5H_4), 7.49-7.84 (m, 5H, C_6H_5), 8.83 (br, 1H, N*H*). MS (ESI): m/z 365 $(M+1)^+$.

4: IR(ν, cm^{-1},CH_2Cl_2): 3195 (br), 2017 (vs), 1925.5 (vs, br), 1654 (br), 1590 (w). ^1H NMR (δ, $CDCl_3$): 2.1 (s, 3H, CH_3), 4.78 (s, 2H, η^5-C_5H_4), 5.15-5.36 (m, 2H, η^5-C_5H_4), 7.47 (s, 1H, C_6H_4N), 8.17 (s, 1H, C_6H_4N), 8.89 (br, 2H, C_6H_4N), 9.16 (br, 1H, N*H*). MS (ESI): m/z 366 $(M+1)^+$.

2.2.3. Crystal structure determination for 1 - 3.

Single crystal X-ray structural studies of **1** - **3** were performed on a CCD Oxford Diffraction XCALIBUR-S diffractometer equipped with an Oxford Instruments low-temperature attachment. Data were collected at 150(2) K using graphite-monochromated Mo Kα radiation (λ_α = 0.71073 Å). The strategy for the data collection was evaluated by using the CrysAlisPro CCD software. The data were collected by the standard phi-omega scan techniques, and were scaled and reduced using CrysAlisPro RED software. The structures were solved by direct methods using SHELXS-97 and refined by full matrix least-squares with SHELXL-97, refining on F^2 [35]. The positions of all the atoms were

obtained by direct methods. All non-hydrogen atoms were refined anisotropically. The remaining hydrogen atoms were placed in geometrically constrained positions and refined with isotropic temperature factors, generally $1.2U_{eq}$ of their parent atoms. The crystallographic details are summarized in Table 2.1.

2.2.4. Antibacterial activity

Compounds **1**, **2** and **3** were screened for their antibacterial activity in vitro following the protocol described elsewhere [36]. The antibacterial effect was assayed against both Gram positive bacteria *viz., Staphylococcus aureus, Bacillus subtilis* and Gram negative bacteria *viz., Escherichia coli, Pseudomonas aeruginosa and Klebsiella pneumoniae* by the agar well diffusion method [36]. The compounds were dissolved in DMSO at different concentrations ranging from 500 to 15.625 μg/ml. Mueller Hinton-agar (containing 1% peptone, 0.6% yeast extract, 0.5% beef extract and 0.5% NaCl, at pH 6.9–7.1) plates were prepared and 0.5 – McFarland culture (1.5×10^8 cells/ml) of the test organisms were swabbed onto the agar plate. 9mm wells were made in the LB agar petri dishes. 100μl of each of the compound with decreasing concentrations was added to separate wells. DMSO was used as the negative control and *Ampicillin* was used as positive control. The plates were incubated at 37°C and observed for zones of inhibition around each well after 24 hours. The results were compared with the activity of *Ampicillin* at identical concentrations. The MIC, defined as the lowest concentration of the test compound, which inhibits the visible growth, was determined visually after incubation for 24 h at 37ºC.

2.3. Results and Discussion

Cymantrenyl based hydrazone compounds, $[(CO)_3Mn\{(\eta^5\text{-}C_5H_4)C(CH_3)=N\text{-}N(H)C(O)\text{-}C_6H_4\text{-}OH\}]$ (**1**), $[(CO)_3Mn\{(\eta^5\text{-}C_5H_4)C(CH_3)=N\text{-}N(H)C(O)\text{-}C_6H_4N\text{-}p\}]$ (**2**), $[(CO)_3Mn\{(\eta^5\text{-}C_5H_4)C(CH_3)=N\text{-}N(H)C(O)\text{-}C_6H_5\}]$ (**3**) and $[(CO)_3Mn\{(\eta^5\text{-}C_5H_4)C(CH_3)=N\text{-}N(H)C(O)\text{-}C_6H_4N\text{-}o\}]$ (**4**) were synthesized by the room temperature reaction of $[Mn(CO)_3\{(\eta^5\text{-}C_5H_4)COCH_3\}]$ with the appropriate hydrazide compounds (salicyloyl hydrazide, isonitinyl hydrazide, benzoyl hydrazide and nicotinyl hydrazide) (Scheme 2.3). All the compounds have been isolated and purified by preparative chromatography and characterized by spectroscopic techniques.

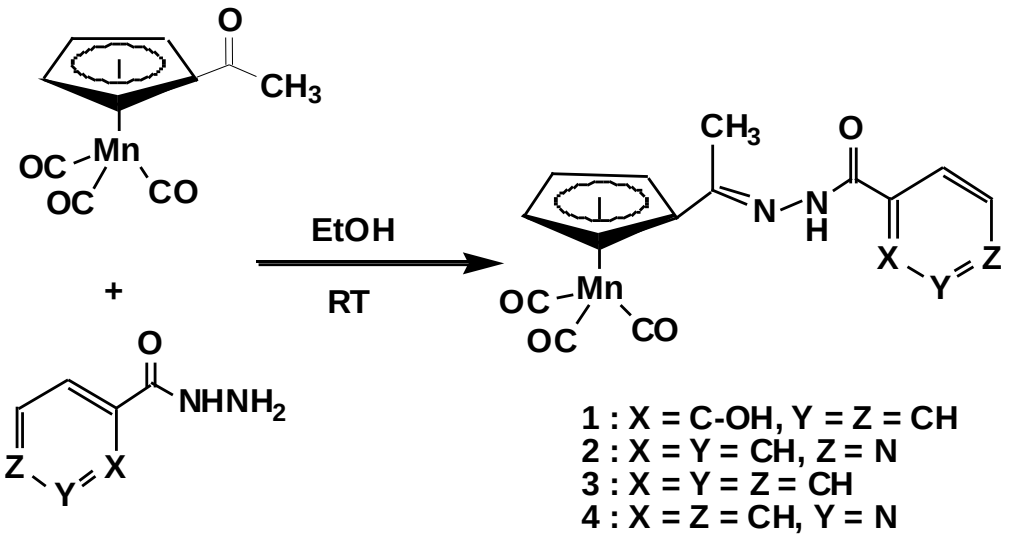

Scheme 2.3

Infrared spectral analysis for compounds **1** - **4** reveals the presence of terminal metal carbonyl groups in the region 1923 – 2019 cm^{-1} and peaks corresponding to C=O and C=N in the range 1601.5 cm^{-1} - 1669 cm^{-1}. ^1H NMR spectra shows the presence of protons corresponding to substituted cyclopentadienyl unit, methyl group, NH and aromatic ring protons for each of the four cymantrenyl hydrazone compounds.

Compound **1** also shows a broad peak at δ 11.66 corresponding to -OH proton. Mass spectral analysis for **1** shows the characteristic molecular ion peak (M^+) at m/z 381 whereas for compounds **3** and **4**, ESI-MS peaks are observed at m/z 365 [$(M+1)^+$] and 366 [$(M+1)^+$] respectively.

2.3.1. Molecular structure of 1 - 3

Single crystal X-ray diffraction studies have been successfully carried out for **1- 3** with the respective single crystals, grown from dichloromethane/n-hexane solvent mixture at -10 ºC. The molecular structure of compound **1**, **2** and **3** confirms the presence of a cymantrenyl unit linked to the hydrazone chain, [C═NN(H)C(O)-R] involving a C═N bond (Figure 2.5, Figure 2.6 and Figure 2.7). In molecules **1** and **3**, the cyclopentadienyl and phenyl rings are almost coplanar, whereas in compound **2** the cyclopentadienyl ring and the pyridyl rings are perpendicular to each other forming a dihedral angle of around 72º between the cyclopentadienyl and pyridyl plane. The C═N bond distances for **1, 2** and **3** are 1.279(2) Å, 1.280(3) Å and 1.285(3) Å respectively, which are comparable to that in ferrocenyl Schiff base compounds, [(η^5-C_5H_5)Fe{(η^5-C_5H_4)C(H) ═NN(H)C(O)C_6H_5}] (1.277(4) Å) [4] and [Fe{(η^5-C_5H_4)C(CH_3) ═NN═C(C_5H_4N)}$_2$] (1.241 (7) – 1.300(7) Å) [37]. The N1-N2 single bond distance in **1** (1.372(2) Å) is shorter than that in **2** (1.391(3) Å), **3** (1.377(2) Å) and in [(η^5-C_5H_5)Fe{(η^5-C_5H_4)C(H)═NN(H)C(O)C_6H_5}] [4]. In the structures of **1** - **3**, the C═O and N-H bonds have been found to be trans to each other. (CCDC Numbers, **1**: 882043, **2**: 882044).

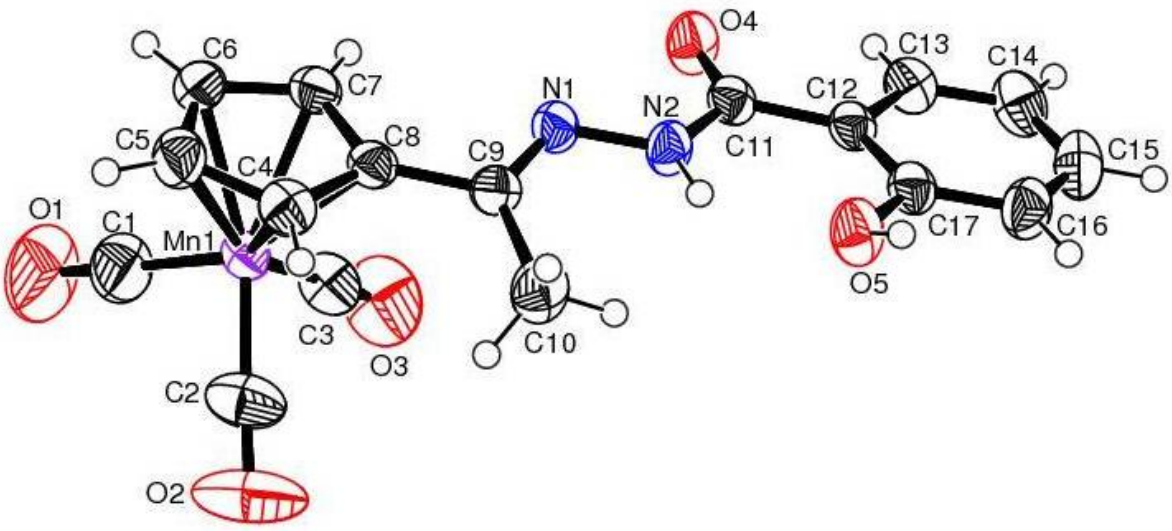

Figure 2.5. ORTEP diagram of **1.** Selected bond lengths (Å) and bond angles (º): N(1)-C(9) = 1.273(3), N(1)-N(2) =1.372(2), N(2)-C(11)=1.338(3), O(4)-C(11) =1.227(2), C(9)-N(1)-N(2) =116.39(16), C(11)-N(2)-N(1) =120.80(16).

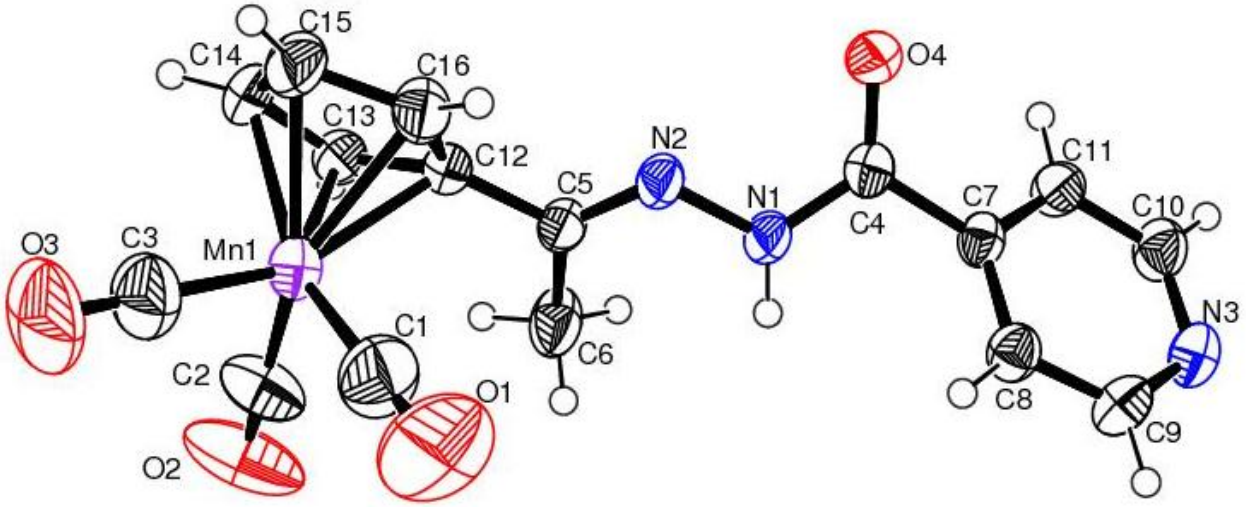

Figure 2.6. ORTEP diagram of **2.** Selected bond lengths (Å) and bond angles (º): N(2)-C(5) =1.280(3), N(1)-N(2) =1.391(3), N(1)-C(4) =1.340(3), O(4)-C(4) =1.221(3), O(1)-C(1) =1.144(4), C(5)-N(2)-N(1) =116.3(2), C(4)-N(1)-N(2) =118.3(2).

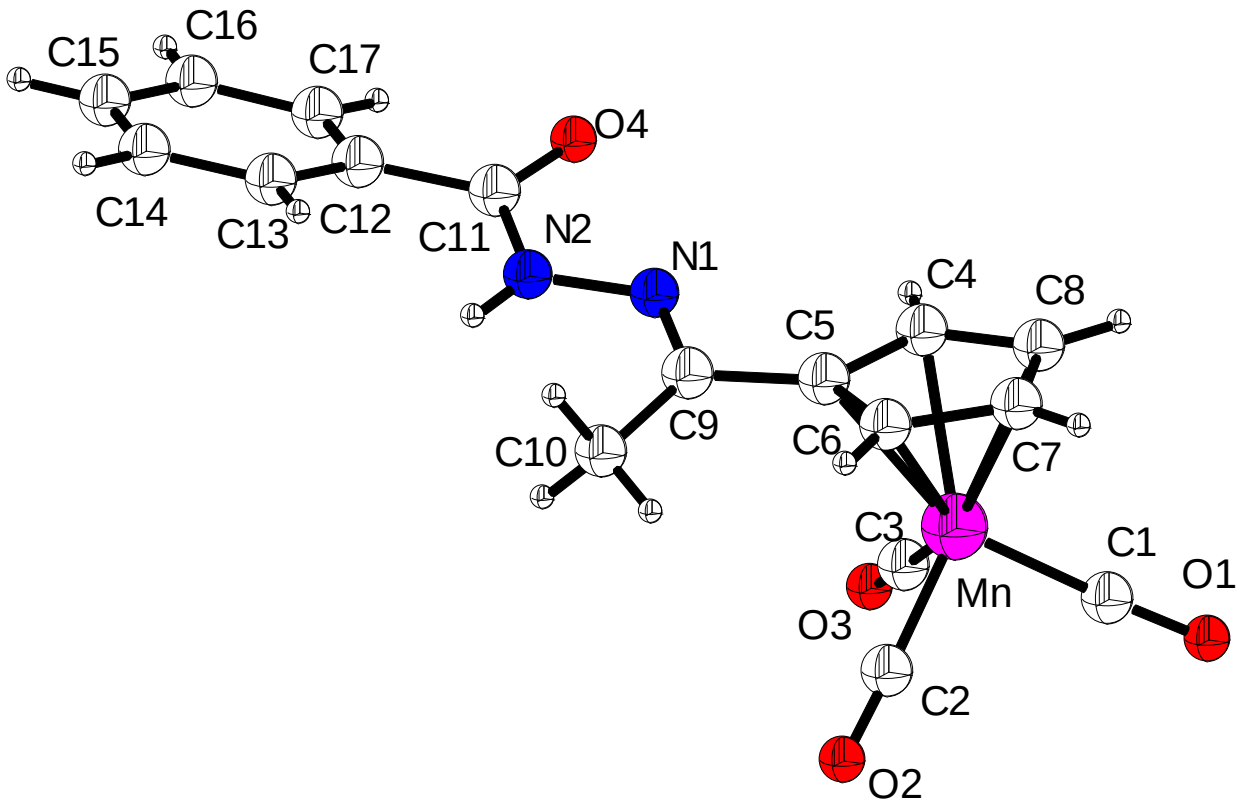

Figure 2.7. ORTEP diagram of **3.** Selected bond lengths (Å) and bond angles (º): N(1)-C(9) = 1.285(3), N(1)-N(2) =1.377(2), N(2)-C(11)= 1.368(3), O(4)-C(11) =1.227(2), C(9)-N(1)-N(2) =117.98(17), C(11)-N(2)-N(1) =117.13(17).

The crystal packing of **1** shows two types of H-bonding interactions involving N2-H…O5 (2.646 Å) and O5-H…O4 (2.680 Å) as shown in Figure 2.8. On the other hand, compound **2** has intermolecular hydrogen bonding involving O4…H1-N1 atoms, thus forming a chain with alternately aligned parallel units (Figure 2.9).

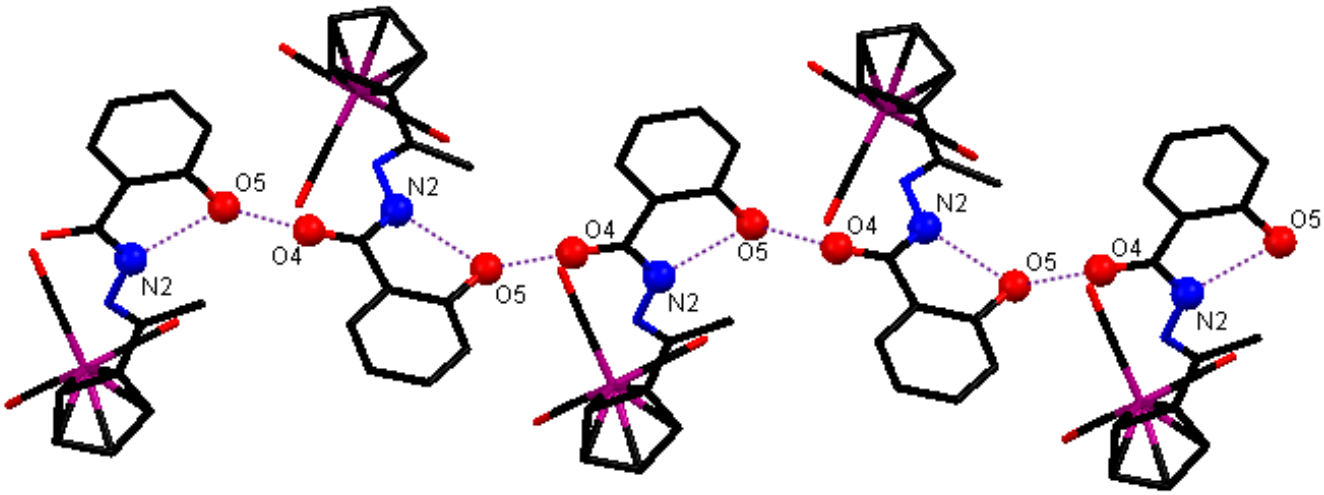

Figure 2.8. Packing diagram for compound **1**

(Hydrogen atoms have been omitted for clarity).

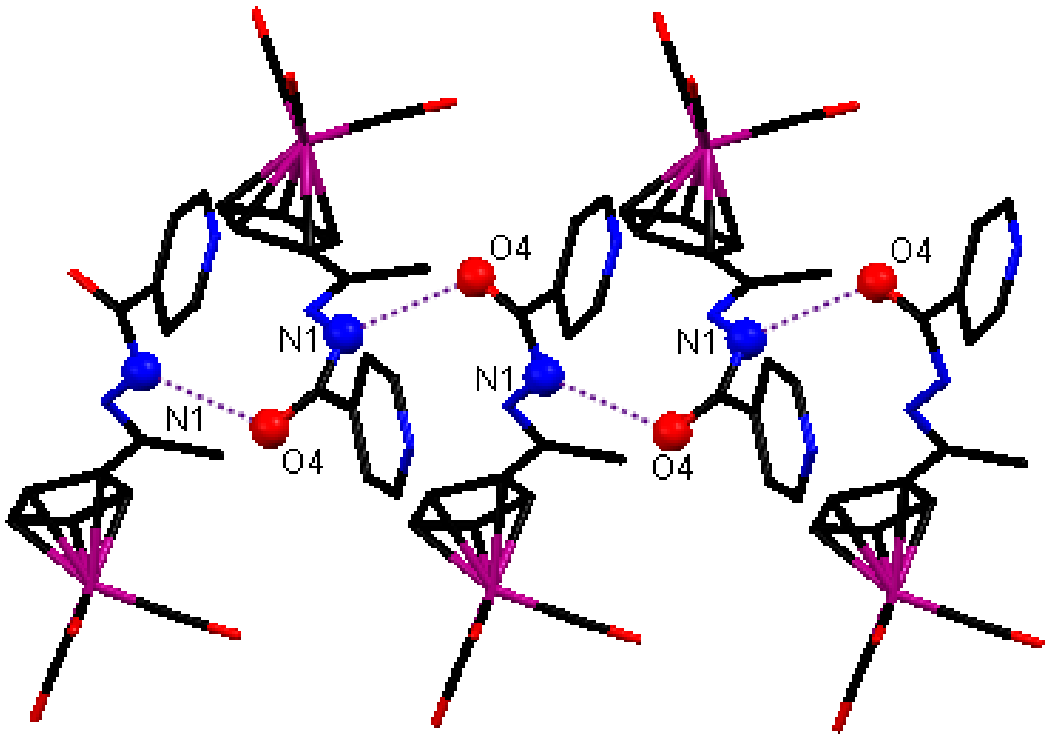

Figure 2.9. Packing diagram for compound **2** along ac plane

(Hydrogen atoms have been omitted for clarity).

Table 2.1. Crystal data and structure refinement parameters for compounds **1 - 3.**

	1	**2**	**3**
Empirical formula	C_{17} H_{13} Mn N_2 O_5	C_{16} H_{12} Mn N_3 O_4	C_{17} H_{13} Mn N_2 O_4
Formula weight	380.23	365.23	364.23
Crystal system	Monoclinic	Orthorhombic	Monoclinic
Space group	*P* $2_1/c$	P b c a	*P* $2_1/c$
a, Å	12.2632(6)	7.9517(3)	18.6221(9)
b, Å	10.5915(6)	18.8279(6)	8.6924(4)
c, Å	12.7224(7)	21.5734(7)	29.4752(13)
α deg	90	90	90
β deg	99.307(5)	90	99.770(2)
γ deg	90	90	90
V, $Å^3$	1630.70(15)	3229.84(19)	4702.0(4)
Z	4	8	12
Dcalcd, Mg m^{-3}	1.549	1.502	
abs coeff, mm^{-1}	0.840	0.842	0.866
F(000)	776	1488	2232
Cryst size, mm	0.33 x 0.28 x 0.23	0.32 x 0.26 x 0.23	0.189 x 0.134 x 0.051
θ range, deg	3.17 to 25.00	2.94 to 24.99	2.22 to 30.26
index ranges	-14≤ h ≤ 14, -12≤ k ≤ 12, -15≤ l ≤ 15	-9≤ h ≤ 9, -20≤ k ≤ 22, -25≤ l ≤ 25	-26≤ h ≤26, -12≤ k ≤ 12, -37 ≤ l ≤ 41
reflections collected/ unique	12573 / 2869 [R(int) = 0.0305]	19145 / 2820 [R(int) = 0.0496]	100674/ 13160 [(Rint = 0.0376)]
data/ restraints / parameters	2869 / 0 / 231	2820 / 0 / 218	13160 / 0 / 664
goodness-of-fit on F^2	1.063	1.051	1.070

Final R indices	R1 = 0.0304,	R1 = 0.0387,	R1 = 0.0451,
[I>2σ(I)]	wR2 = 0.0832	wR2 = 0.0939	wR2 = 0.1081
R indices (all	R1 = 0.0346,	R1 = 0.0478,	R1 = 0.0730,
data)	wR2 = 0.0867	wR2 = 0.1011	wR2 = 0.1218
largest diff peak	0.236	0.319	2.297
and hole, eÅ^{-3}	-0.179	-0.381	-0.640

2.3.2. Antibacterial activity of 1 - 3

Antibacterial study was carried out for three of the synthesized compounds, **1, 2** and **3**. All of them showed potential inhibition activity against the bacterial strains as shown in Table 2.1. Among the cymantrenyl hydrazones, compound **3** has better MIC against *E.coli* and *P. aeruginosa* bacterial strain whereas cymantrenyl isonicotinyl hydrazone (**2**) showed better result when tested with *K. pneumoniae.* Comparison of the inhibition activity for these cymantrenyl compounds with the reported antimicrobial properties of their organic analogue reveals increased inhibitory activity for the compounds containing organometallic fragments [38]. For example, the MIC for the hydroxyphenyl benzoylhydrazone, [(OH)C_6H_4CH=NNHC(O)Ph] has been found in the range 125-500, much higher than that for the cymantrenyl analogs.[22] Isonicotinic hydrazide and their hydrazone derivative, [$C_6H_4N(CH_3)C(O)C{=}NNHC(O)C_5H_4N$] shows MIC greater than 200 μg/ml against *E.coli*, *S.aureus* and *B. subtilis* [39]. Antibacterial study on similar types of ferrocenyl compounds reported recently by other groups against some bacterial strains also showed promising results [20], whereas inhibition activity with cymantrenyl compound has been rarely studied. Significant antibacterial activity for the reported organometallic compounds could possibly be due to the presence of cymantrenyl groups that are playing a vital role to increase the cell permeability and lipophilicity of the compounds. Factors like better π-electron delocalization and blocking of metal binding sites of the enzyme of microorganism may also result in better inhibition activity in metal containing compounds. The MIC data reported in Table 2.2 for cymantrenyl hydrazones will eventually help us in understanding the properties of these types of compounds.

Table 2.2. Minimum inhibitory concentration (MIC) value in μg/ml

Compounds	*B. subtilis*	*E. coli*	*S. aureus*	*K. pneumoniae*	*P. aeruginosa*
1	125	250	125	--	125
2	250	125	--	62.5	250
3	--	62.5	--	125	31.25
Ampicillin	15.62	31.25	15.62	31.25	62.5

In summary, chapter 2 describe the synthesis of four new cymantrenyl hydrazone Schiff base compounds $[(CO)_3Mn\{(\eta^5\text{-}C_5H_4)C(CH_3)=NN(H)C(O)\text{-}C_6H_4\text{-}OH\}]$ (R = C_6H_5, C_6H_4-OH, C_6H_4N-p, C_6H_4N-m) (**1-4**). Three of the cymantrenyl hydrazones have been structurally characterized by single crystal X-ray diffraction study. Some of the compounds have shown moderate antibacterial activities in vitro against different bacterial strains compared to ampicillin as standard drug. We are presently trying to understand the scope of hydrazone type compounds having the cymantrenyl scaffold in biological imaging studies and as tracer molecules.

2.4. References

[1] S. R. Patil, U. N. Kantak, D. N. Sen, Inorg. Chim. Acta 63 (1982) 261.

[2] M. Yongxiang, L. Feng, S. Hongsui, X. Jishan, Inorg. Chim. Acta 149 (1988) 209.

[3] Z. L. Lu, W. Xiao, B. S. Kang, C. Y. Su, J. Liu, J. Mol. Structure 523 (2000) 133.

[4] P. Barbazán, R. Carballo, U. Abram, G. P. Gabián, E. M. Vázquez-López, Polyhedron 25 (2006) 3343.

[5] P. Barbazán, R. Carballo, I. Prieto, M. Turnes, E. M. Vázquez-López, J. Organomet. Chem. 694 (2009) 3102.

[6] Á. Gyömöre, A. Csámpai, J. Organomet. Chem. 696 (2011) 1626.

[7] Z. F. Chen, H. L. Zou, H. Liang, R. X. Yuan, Y. Zhang, Appl. Organomet. Chem. 18 (2004) 438.

[8] R. Arancibia, A. H. Klahn, G. E. Buono-Core, E. Gutierrez-Puebla, A. Monge, M. E. Medina, C. Olea-Azar , J. D. Maya, F. Godoy, J. Organomet. Chem. 696 (2011) 3238.

[9] J. W. Steed, Chem. Soc. Rev. 38 (2009) 506.

[10] G. Jaouen, A. Vessières, I. S. Butler, Acc. Chem. Res. 26 (1993) 361.

[11] (a) C. G. Hartinger, N. Metzler-Nolte, P. J. Dyson, Organometallics 31 (2012) 5677; (b) C. G. Hartinger, P. J. Dyson, Chem. Soc. Rev. 38 (2009) 391.

[12] M. F. R. Fouda, M. M. Abd-Elzaher, R. A. Abdelsamaia, A. A. Labib, Appl. Organomet. Chem. 21 (2007) 613.

[13] R. H. Fish, G. Jaouen, Organometallics 22 (2003) 2166.

[14] (a) D. R. V. Staveren, N. Metzler-Nolte, Chem. Rev. 104 (2004) 5931; (b) A. R. Pike, L. C. Ryder, B. R. Horrocks, W. Clegg, M. R. J. Elsegood, B. A. Connolly, A. Houlton, Chem. Eur. J. 8 (2002) 2891.

[15] (a) M. Patra, G. Gasser, M. Wenzel, K. Merz, J. E. Bandow, N. Metzler-Nolte, Organometallics 29 (2010) 4312; (b) M. Navarro, W. Castro, C. Biot, Organometallics 31 (2012) 571.

[16] O. Payen, S. Top, A. Vessières, E. Brulé, A. Lauzier, M.-A. Plamont, M. J. McGlinchey, H. Müller-Bunz, G. Jaouen, J. Organomet.Chem. 696 (2011) 1049.

[17] J. Quirante, F. Dubar, A. González, C. Lopez, M. Cascante, R. Cortés, I. Forfar, B. Pradines, C. Biot, J. Organomet. Chem. 696 (2011) 1011.

[18] V. Zsoldos-Mády, A. Csámpai, R. Szabó, E. Mészáros-Alapi, J. Pásztor, F. Hudecz, P. Sohár, Chem. Med. Chem. 1 (2006) 1119.

[19] (a) B. Maity, B. V. S. K. Chakravarthi, M. Roy, A. A. Karande, A. R. Chakravarty, Eur. J. Inorg. Chem. (2011) 1379; (b) J. Zhang, Appl. Organomet. Chem. 22 (2008) 6.

[20] (a) Z. H. Chohan, C. T. Supuran, Appl. Organomet. Chem. 19 (2005) 1207; (b) Z. H. Chohan, H. Pervez, K. M. Khan, C. T. Supuran, J. Enzyme Inhib. Med. Chem. 20 (2005) 81.

[21] E. Meggers, G. E. Atilla-Gokcumen, H. Bregman, J. Maksimoska, S. P. Mulcahy, N. Pagano, D. S. Williams, Synlett (2007) 1177.

[22] S. Pasayat, S. P. Dash, Saswati, P. K. Majhi, Y. P. Patil, M. Nethaji, H. R. Dash, S. Das, R. Dinda, Polyhedron 38 (2012) 198.

[23] H. Bregman, D. S. Williams, G. E. Atilla, P. J. Carroll, E. Meggers, J. Am. Chem. Soc. 126 (2004) 13594.

[24] Y. Liu, B. Spingler, P. Schmutz, R. Alberto, J. Am. Chem. Soc. 130 (2008) 1554.

[25] C. Policar, J. B. Waern, M.-A. Plamont, S. Clède, C. Mayet, R. Prazeres, J.-M. Ortega, A. Vessières, A. Dazzi, Angew. Chem. Int. Ed. 50 (2011) 860.

[26] H. W. P. N'Dongo, I. Neundorf, K. Merz, U. Schatzschneider, J. Inorg. Biochem. 102 (2008) 2114.

[27] D. S. Williams, G. E. Atilla, H. Bregman, A. Arzoumanian, P. S. Klein, E. Meggers, Angew. Chem. Int. Ed. 44 (2005) 1984.

[28] I. Rémy, P. Brossier, I. Lavastre, J. Besançon, C. Moise, J. Pharm. Biomed. Anal. 9 (1991) 965.

[29] M. Salmain, A. Vessières, P. Brossier, I. S. Butler, G. Jaouen, J. Immunol. Methods 148 (1992) 65.

[30] I. Lavastre, J. Besançon, P. Brossier, C. Moise, Appl. Organomet. Chem. 4 (1990) 9.

[31] I. Neundorf, J. Hoyer, K. Splith, R. Rennert, H.W.P. N'Dongo, U. Schatzschneider, Chem. Commun. (2008) 5604.

[32] M. patra, G. Gasser, M. Wenzel, K. Merz, J. E. Bandow, N. Metzler-Nolte, Organometallics 31 (2012) 5760.

[33] J. Kozikowski, R. E. Maginn, M. S. Klove, J. Am. Chem. Soc. 81 (1959) 2995.

[34] (a) N. S. Navaneetham, R. Kalyanasundaram, S. Soundararajan, Inorg. Chim. Acta 110 (1985) 169; (b) H. Meyer, J. Mally, Monatshefte fuer Chemie 33 (1912) 393.

[35] G. M. Sheldrick, A short history of *SHELX*, Acta Cryst. A 64 (2008) 112.

[36] A. U. Rahman, M. I. Choudhary, W.J. Thomsen, Bioassay techniques for drug development, Harwood Academic Publishers, The Netherlands, 22 (2001).

[37] C. J. Fang, C. Y. Duan, H. Mo, C. He, Q. J. Meng, Y. J. Liu, Y. H. Mei, Z. M. Wang, Organometallics 20 (2001) 2525.

[38] (a) V. P. Singh, A. Katiyar, S. Singh, Synthesis Biometals 21 (2008) 491; (b) N. Nawar, N. M. Hosny, Trans. Met. Chem. 25 (2000) 1; (c) S. Rollas, Ş. G. Küçükgüzel, Molecules 12 (2007) 1910.

[39] M. C. Rodríguez-Argüelles, S. M.-Vázquez, P. Tourón-Touceda, J. Sanmartín-Matalobos, A. M. García-Deibe, M. Belicchi-Ferrari, G. Pelosi, C. Pelizzi, F. Zani, J. Inorg. Biochem.101 (2007) 138.

Chapter 3

Synthesis, characterization and redox properties of unsymmetrically substituted 1,1’-Ferrocenyl dihydrazone compound

3.1. Introduction

The use of ferrocenyl derivatives as bioactive molecule has been established recently and several reports show that a large number of ferrocene containing compounds display interesting cytotoxic and DNA cleaving activities [1-7]. A large part of the research is also concentrated on the synthesis of conjugates of peptides and peptide nucleic acids with organometallic fragments, in particular having ferrocene moiety. Very recent studies on Schiff base compounds containing organometallic fragments reveal that ferrocenyl Schiff base compounds have exciting biological properties and are potential compounds for antitumor, antibacterial, antimalarial and antifungal activities [6-9]. Carbohydrazones are a special class of azomethine type Schiff base compounds that act as ionic or neutral moieties and their derivatives shows a range of biological activity like anticonvulsant, antidepressant, analgesic, antimicrobial, antitumor, anti-platelet, vasodilator, antiviral etc.[10–17] Reactivity of hydrazones with transition metal salts give rise to some interesting coordination features and has been well investigated for the last two decades. The β-nitrogen and carbonyl oxygen atom present in these compounds coordinates to the metal atom with unique stereochemical features, whereas the α-nitrogen remains uncoordinated. Metal complexes of acyl-hydrazones are known for wide spectrum of biological and pharmaceutical activities, such as inhibition of tumor growth, antioxidative effect, antimicrobial and antiviral properties.[18-23] However, a very few literatures are known on the synthesis of ferrocene based hydrazones and study related to reactivity and biological activity. Some early studies on ferrocenyl hydrazones show the preliminary investigation of ferrocenylidene derivatives of N-aroyl hydrazone and their metal chelate complexes.[24-26] Synthesis of ferrocene containing bis-bidentate Schiff-base ligands, $[Fe\{(\eta^5\text{-}C_5H_4)C(Me)NN(H)C(S)NH_2\}_2]$ have been synthesized by the condensation reaction of diacetylferrocene with thiosemicarbazide which further reacted with $[Zn(MeCO_2)_2{\cdot}2H_2O]$ to generate a double-helical zinc complex via self-assemble process (Figure 3.1).[27]

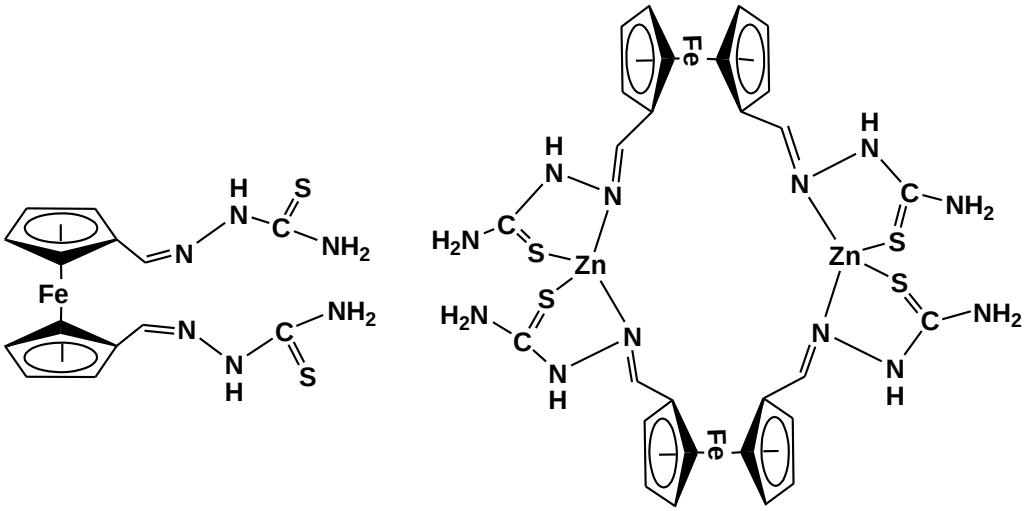

Figure 3.1

Another set of ferrocenyl Schiff base compounds containing disubstituted hydrazone groups have been prepared by the reaction of 1,1'-diacetylferrocene with salicylaldehyde and pyridine carboxyaldehyde in a 1:2 ratio in refluxing ethanol solution. Structural analysis of the disubstituted ferrocenyl hydrazones reveals the presence of two hydrazone chains attached to the Cp rings of the ferrocenyl fragment which are projected in the same direction to obtain an eclipsed geometry as shown in Figure 3.2. The ferrocenyl hydrazone subsequently forms metal complexes by reaction with the respective metal salts by self assembled type of reaction process.[28]

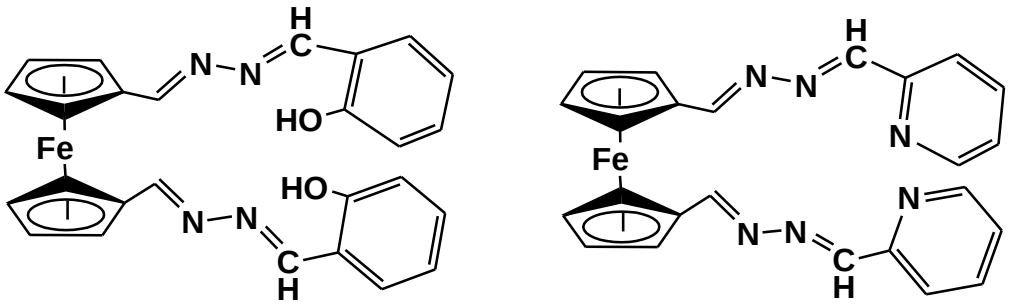

Figure 3.2

Vazquez-Lopez and group reported recently the reaction of 2-hydroxybenzoic hydrazide and ferrocenyl carbaldehyde to give the respective hydrazones which act as tetra or tridentate planar chelating ligand that co-ordinate through the phenolic

hydroxylamide oxygen and one or two imine nitrogen atoms. Complexes of the type $[ReX(CO)_3\{(\eta^5\text{-}C_5H_5)Fe(\eta^5\text{-}C_5H_4)C(H)NN(H)C(O)(C_6H_4OH)\}]$, (X = Cl, Br) have thus been formed by the reaction of rhenium carbonyl with the ferrocenyl hydrazone in reflux condition (Scheme 3.1).[29]

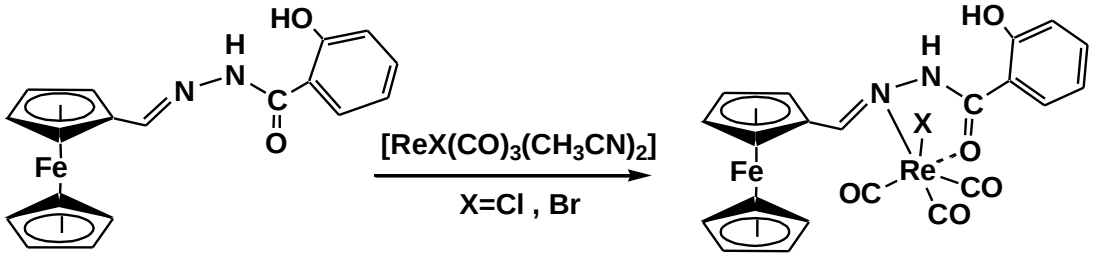

Scheme 3.1

Biologicaly active ferrocenyl amino hydrazones were prepared by the reaction of 7-chloroquinolinylhydrazine and chloro hydrazinyl-2-methoxyacridine with ferrocenyl aminoaldehyde derivatives to give a range of substituted ferrocenyl hydrazone linked to heterocyclic moieties. Ferrocenylamino aldehyde precursors was synthesized from N,N-dimethylaminomethylferrocene by a two step reactions involving substitution of the amino alkyl by the desired amines like pyrroline and morpholine and subsequent ortholithiation followed by dimethylformamide addition to form the aldehyde. The quinoline and acridine based ferrocenyl hydrazones showed high anti-mycobacterial activity for tuberculosis inhibition against *M. tuberculosis* $H_{37}R_v$ strain. [30]

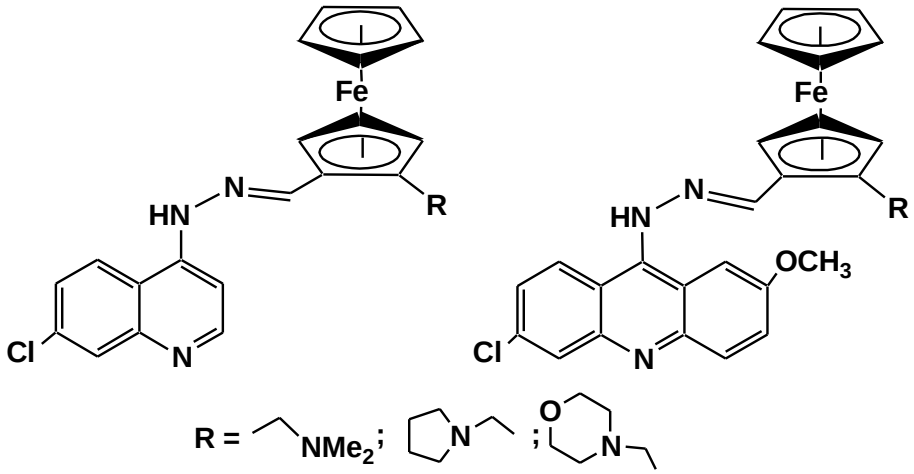

Figure 3.3

Reaction of Schiff bases derived from ferrocenylmethylamine with Li_2PdCl_4 led to the formation of a unique heteroannular palladium complexes obtained from a cyclometalation type of reaction with the unsubstituted cyclopentadienyl ring (Scheme 3.2). Single-crystal X-ray analysis confirmed that the carbon−palladium bond formed by using a carbon atom in the unsubstituted Cp ring. The palladacyclic ferrocenyl hydrazone exhibits high catalytic activity for the Suzuki−Miyaura coupling reaction of aryl bromides with phenylboronic acid giving high yields of the biaryl products.[31]

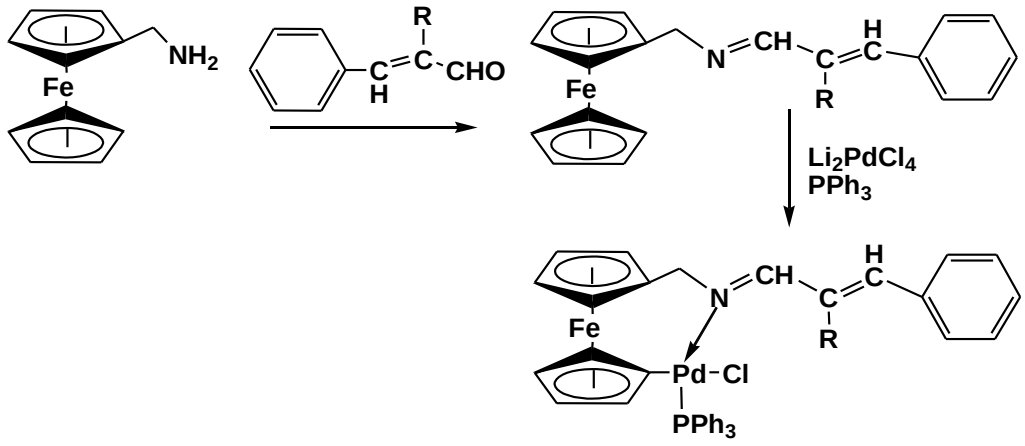

Scheme 3.2

In view of the importance of ferrocenyl hydrazone in coordination and biological chemistry, efforts were made to prepare different types of hydrazone linked to ferrocene fragment. However, literature search revealed that a good number of mono ferrocenyl hydrazone compounds have been reported [7, 24-26], but the synthesis of 1,1'-unsymmetrically substituted ferrocenyl hydrazone compounds have been rarely carried out. In this chapter, we describe the synthesis of hydrazone derivatives containing unsymmetrically 1,1' disubstituted ferrocenyl fragment by using unsymmetrical acetylferrocene precursor. Electrochemical investigations have also been carried out to understand their redox processes for some of the ferrocenyl hydrazone compounds.

3.2. Experimental Sections

3.2.1. General Procedures

All reactions and manipulations were carried out under an inert atmosphere of dry, pre-purified argon using standard Schlenk line techniques. Solvents were purified, dried and distilled under argon atmosphere prior to use. Infrared spectra were recorded on a Perkin Elmer Spectrum RX-I spectrometer as KBr pellet or CH_2Cl_2 solution and NMR spectra on a 400 MHz Bruker spectrometer in $CDCl_3$ or d_6-DMSO solvent. Elemental analyses were performed on a Vario El Cube analyser. Mass spectra were obtained on a SQ-300 MS instrument operating in ESI mode. Cyclic voltammetric and differential pulse voltammetric measurements were carried out using a CH Instruments model 600D electrochemistry system. A platinum working electrode, a platinum wire auxiliary electrode and a silver / silver chloride reference electrode were used in a three–electrode configuration. The supporting electrolyte was 0.1 M $[NEt_4]ClO_4$ and the solute concentration was $\sim 10^{-3}$ M. The scan rate used was 50 mV s^{-1}. All electrochemical experiments were carried out under a nitrogen atmosphere and are uncorrected for junction potentials. TLC plates (20x20 cm, Silica gel 60 F254) were purchased from Merck. $[Fe(\eta^5\text{-}C_5H_4COCH_3)_2]$, $[H_2NN(H)C(O)R]$, (R = $-C_6H_4$-OH, C_6H_4N-p, C_6H_5, C_6H_4N-o) were prepared following reported procedures [32, 33].

3.2.2. Synthesis of 1,1'-$[CH_3C(O)(\eta^5\text{-}C_5H_4)Fe\{(\eta^5\text{-}C_5H_4)C(CH_3)$=$NN(H)C(O)R\}]$ (5 - 8)

In a two-necked round bottomed flask ethanol solution (10 ml) of the respective hydrazide (0.5 mmol) was taken and 1,1'-diacetyl ferrocene (135 mg ;0.5 mmol) was added. The reaction mixture was stirred under inert atmosphere and two drops of acetic acid was added and the stirring was continued for 6-12 hours at room temperature. The reaction was monitored using TLC. After the reaction, the solution was vacuum dried and the mixture was subjected to chromatographic work up using preparative TLC. Elution with 70% Ethyl acetate : n-hexane solvent mixture afforded 1,1'-diacetyl

ferrocene and an orange colored compound 1,1'-[$CH_3C(O)(\eta^5\text{-}C_5H_4)Fe\{(\eta^5\text{-}C_5H_4)C(CH_3)$═N-N(H)C(O)-R}] {R = C_6H_5 (**5**), C_6H_4-OH (**6**), C_6H_4N-p (**7**), C_6H_4N-m (**8**)}, in the order of elution. Trace amount of other orange bands and unreacted hydrazides were also obtained during chromatographic workup. {Yields: **5**, 90 mg (46 %); **6**: 87 mg (43%); **7**: 103 mg (53 %); **8**: 94 mg (44 %)}

5: Anal. calcd. (found): C, 64.97 (65.12); H, 5.19 (5.05); N, 7.22 (7.34). IR(ν, cm^{-1}, CH_2Cl_2): 1666 (vs), 1650 (vs, br), 1603 (m), 1581 (m). ^{1}H NMR (δ, $CDCl_3$): 2.09 (s, 3H, CH_3), 2.29 (s, 3H, CH_3), 4.33 (t, 2H, η^5-C_5H_4), 4.44 (t, 2H, η^5-C_5H_4), 4.75 (t, 2H, η^5-C_5H_4), 4.80 (t, 2H, η^5-C_5H_4), 7.42 – 7.86 (m, 5H, -C_6H_4). MS (ESI): m/z 389 [M+H].

6: Anal. calcd. (found): C, 62.40 (62.58); H, 4.99 (4.86); N, 6.93 (6.84). IR(ν, cm^{-1}, CH_2Cl_2): 3086 (br), 1665 (vs), 1643 (s), 1605 (m), 1552 (s, br). ^{1}H NMR (δ, $CDCl_3$): 2.21 (s, 3H, CH_3), 2.38 (s, 3H, CH_3), 4.45 (t, 2H, η^5-C_5H_4), 4.54 (t, 2H, η^5-C_5H_4), 4.84 (t, 2H, η^5-C_5H_4), 4.87 (t, 2H, η^5-C_5H_4), 6.93 – 7.56 (m, 4H, -C_6H_4), 11.89 (s, 1H, O*H*). MS (ESI): m/z 405 [M+H].

7: Anal. calcd. (found): C, 61.72 (61.90); H, 4.92 (4.83); N, 10.80 (10.68). IR(ν, cm^{-1}, CH_2Cl_2):, 1665 (vs), 1649 (s), 1600 (m), 1552 (s), 1536(s). ^{1}H NMR (δ, d_6-DMSO): 2.20 (s, 3H, CH_3), 2.32 (s, 3H, CH_3), 4.49 (t, 2H, η^5-C_5H_4), 4.61 (t, 2H, η^5-C_5H_4), 4.78 (t, 2H, η^5-C_5H_4), 4.81 (t, 2H, η^5-C_5H_4), 7.8 (s, 2H, C_5H_4N), 8.77 (s, 2H, C_5H_4N), 10.91 (s, 1H, N*H*). MS (ESI): m/z 390 [M+H].

8: IR(ν, cm^{-1},CH_2Cl_2): 1667 (vs), 1652 (s, br), 1592 (m), 1537 (m, br). ^{1}H NMR (δ, d_6-DMSO): 2.12 (s, 3H, CH_3), 2.23 (s, 3H, CH_3), 4.30 (t, 2H, η^5-C_5H_4), 4.39 (t, 2H, η^5-C_5H_4), 4.69 (t, 2H, η^5-C_5H_4), 4.72 (t, 2H, η^5-C_5H_4), 7.46 (t, J = 7.2 Hz, 1H, C_5H_4N), 8.13 (d, J = 7.2 Hz, 1H, C_5H_4N), 8.67 (s, 1H, C_5H_4N), 8.94 (s, 1H, C_5H_4N), 10.75 (s, 1H, N*H*). MS (ESI): m/z 390 [M+H].

3.2.3. Reaction of 7 with hydrazide

Ethanol solution (10 ml) of compound **7** (39 mg, 0.1 mmol) was taken in a two - necked round bottomed flask and an equivalent amount of the respective hydrazide (0.1 mmol) (isonicotinyl hydrazide or salicyloyl hydrazide) and acetic acid (2 drops) was added under stirring and inert atmospheric condition. The solution was stirred at room temperature and under nitrogen atmosphere for 2 hrs. The reaction was continuously monitored using TLC. After the completion of the reaction, the solution was filtered and the volume was reduced to minimum amount. Preparative TLC was carried out with the reaction mixture using n-hexane:ethanol (80:20v/v) solvent mixture to separate an orange colored compound [Fe{(η^5-C_5H_4)C(CH_3)═N-N(H)C(O)(C_5H_4N)}$_2$] (**9**) (Yield = 32 mg, 62 %)) or [{(η^5-C_5H_4)C(CH_3)═N-N(H)C(O)-C_6H_4-OH}Fe{(η^5-C_5H_4)C(CH_3)═N-N(H)C(O)(C_5H_4N)}] (**10**) (Yield= 40 mg, 78 %). Some amounts of unreacted compound and decomposition have also been observed after the reaction.

9: Anal. calcd. (found): C, 61.41 (61.75); H, 4.70 (4.59); N, 16.53 (16.64). IR(ν, cm^{-1}, KBr): 3420 (vs), 1642 (vs), 1617, 1595. ^{1}H NMR (δ, d_6-DMSO): 2.29 (s, 6H, CH_3), 4.61 (s, 4H, η^5-C_5H_4), 4.81 (s, 4H, η^5-C_5H_4), 7.84 (m, 4H, C_5H_4N), 8.81 (m, 4H, C_5H_4N). MS (ESI): m/z 509 [M+H].

10: Anal. calcd. (found): C, 61.95 (62.27); H, 4.78 (4.70); N, 13.38 (13.46). IR(ν, cm^{-1}, CH_2Cl_2): 3418 (m), 3274.5 (m), 1658.7 (s), 1642.4 (s), 1599.5 (s), 1564.7 (s), 1549.6 (vs). ^{1}H NMR (δ, d_6-DMSO): 2.15 (s, 3H, CH_3), 2.28 (s, 3H, CH_3), 4.43 (s, 2H, η^5-C_5H_4), 4.57 (s, 2H, η^5-C_5H_4), 4.74 (s, 2H, η^5-C_5H_4), 4.79 (s, 2H, η^5-C_5H_4), 6.52-7.82 (m, 8H, C_5H_4N, C_6H_4). MS (ESI): m/z 523 [M].

3.2.4. Crystal structure determination for 7

A single crystal X-ray structural study of **7** was performed on a CCD Oxford Diffraction XCALIBUR-S diffractometer equipped with an Oxford Instruments low-temperature attachment. Data were collected at 150(2) K using graphite-monochromated

Mo Kα radiation (λ_α = 0.71073 Å). The strategy for the data collection was evaluated by using the CrysAlisPro CCD software. The data were collected by the standard phi-omega scan techniques, and were scaled and reduced using CrysAlisPro RED software. The structure was solved by direct methods using SHELXS-97 and refined by full matrix least-squares with SHELXL-97, refining on F^2 [34]. The positions of all the atoms were obtained by direct methods. All non-hydrogen atoms were refined anisotropically. The remaining hydrogen atoms were placed in geometrically constrained positions and refined with isotropic temperature factors, generally 1.2U_{eq} of their parent atoms. The crystallographic details are summarized in Table 3.1. (CCDC Number, **7**: 1476351)

Table 3.1. Crystal data and structure refinement parameters for compound **7**

	7
Empirical formula	C_{20} H_{21} Fe N_3 O_4
Formula weight	423.25
Crystal system	Monoclinic
Space group	*P* $2_1/c$
a, Å	24.209(4)
b, Å	9.6025(18)
c, Å	8.4544(17)
α deg	90
β deg	94.706(8)
γ deg	90
V, Å^3	1958.8(6)
Z	4
Dcalcd, Mg m^{-3}	1.435
abs coeff, mm^{-1}	0.801
F(000)	880
Cryst size, mm	0.260x0.190 x 0.160

θ range, deg	2.711 to 24.993
index ranges	$-19 \leq h \leq 28, -10 \leq k \leq 10, -9 \leq l \leq 10$
reflections collected/ unique	5810 / 2893 [R(int) = 0.0650]
data/ restraints / parameters	2893 / 0 / 263
goodness-of-fit on F^2	1.022
Final R indices [$I>2\sigma(I)$]	R1 = 0.0479, wR2 = 0.0798
R indices (all data)	R1 = 0.1135, wR2 = 0.0993
largest diff peak	0.266
and hole, $eÅ^{-3}$	-0.287

3.3. Results and Discussion

Unsymmetrically 1,1'-disubstituted ferrocenyl compounds have been of interest due to their multifunctional properties with unique structural features and tunable electrochemical responses. In the current study, we have been able to synthesize unsymmetrically 1,1'-disubstituted ferrocenyl compounds containing two different hydrazone units by using simple synthetic methodology involving selective transformation of one of the Cp substituent. Reaction of 1,1'-diacetylferrocene (135 mg, 0.5 mmol) with equivalent amount of benzoyl, salicyloyl, isonicotinyl and nicotinyl hydrazide (0.5 mmol) results in the formation of 1,1'-[$CH_3C(O)(\eta^5\text{-}C_5H_4)Fe\{(\eta^5\text{-}C_5H_4)C(CH_3)$═$N\text{-}N(H)C(O)\text{-}R\}$] {R = C_6H_5 (**5**), C_6H_4-OH (**6**), C_6H_4N-p (**7**), C_6H_4N-m (**8**)} respectively. The reaction also gave some amount of side products, one of them has been identified by comparison of the literature spectroscopic data as the disubstituted ferrocenyl hydrazones, 1,1'-[$Fe\{(\eta^5\text{-}C_5H_4)C(CH_3)$═$N\text{-}N(H)C(O)\text{-}R\}_2$], {R = C_6H_5, C_6H_4-OH, C_6H_4N-p, C_6H_4N-m}.[11] Compounds **5** - **8** were isolated and purified by chromatography using 70% ethylacetate-hexane solvent mixture and characterized by IR, NMR, Mass spectral analysis and single crystal X-ray Crystallography.

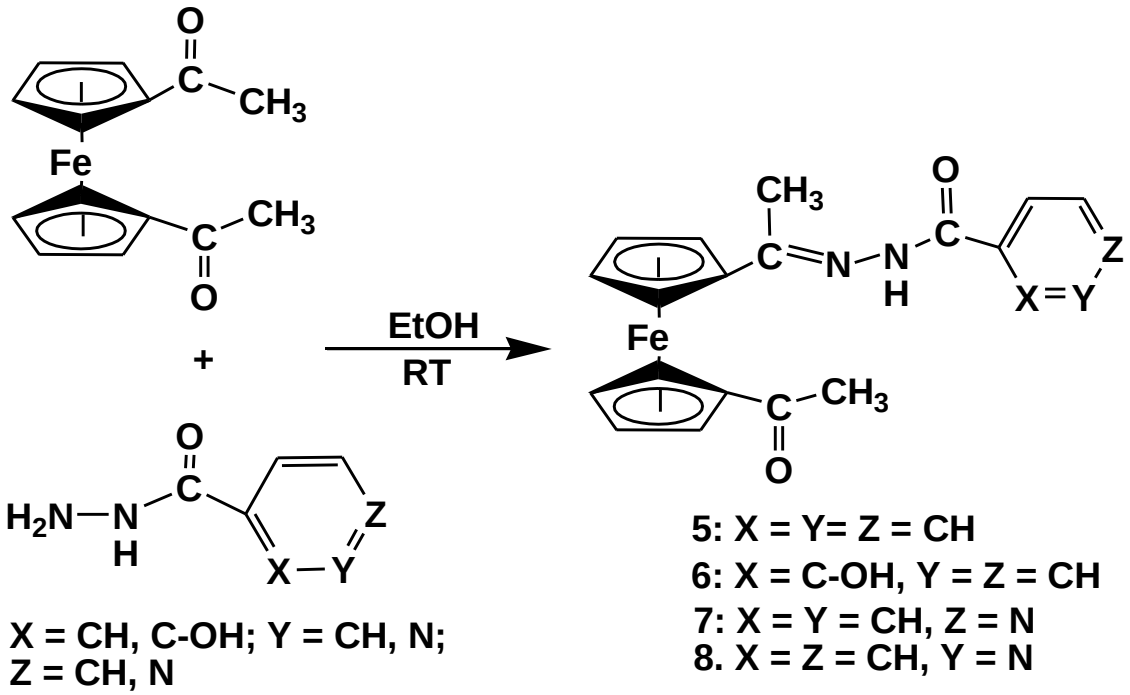

Scheme 3.3

Infrared spectra for compounds **5-8** show peaks corresponding to C=O and C=N stretching frequency in the range 1667–1600 cm^{-1} region. ^{1}H NMR spectra of **5** and **6** reveals the presence of singlet peaks at δ 2.09-2.21 and δ 2.29-2.38 region respectively corresponding to two different methyl protons. Four triplet (broad) peaks at δ 4.33-4.87 region corresponding to eight substituted ferrocenyl Cp protons, while a multiplet at δ 6.93–7.86 region for phenyl protons have been observed for each of the two compounds. A singlet peak at downfield region (δ 11.89) shows the presence of OH proton in compound **6**. ^{1}H NMR spectra of **7** and **8** show two peaks at δ 2.20 - δ 2.32 region corresponding to the methyl protons, δ 4.3-4.81 (four peaks each) for disubstituted ferrocenyl Cp protons and at δ 7.46 - δ 8.94 due to the pyridyl protons. NH protons have also been observed at δ 10.91 and δ 10.75 for compounds **7** and **8** respectively. Mass spectral analysis of compounds **5-8** shows the presence of [M+H] peak at m/z 389, 405 and 390 respectively.

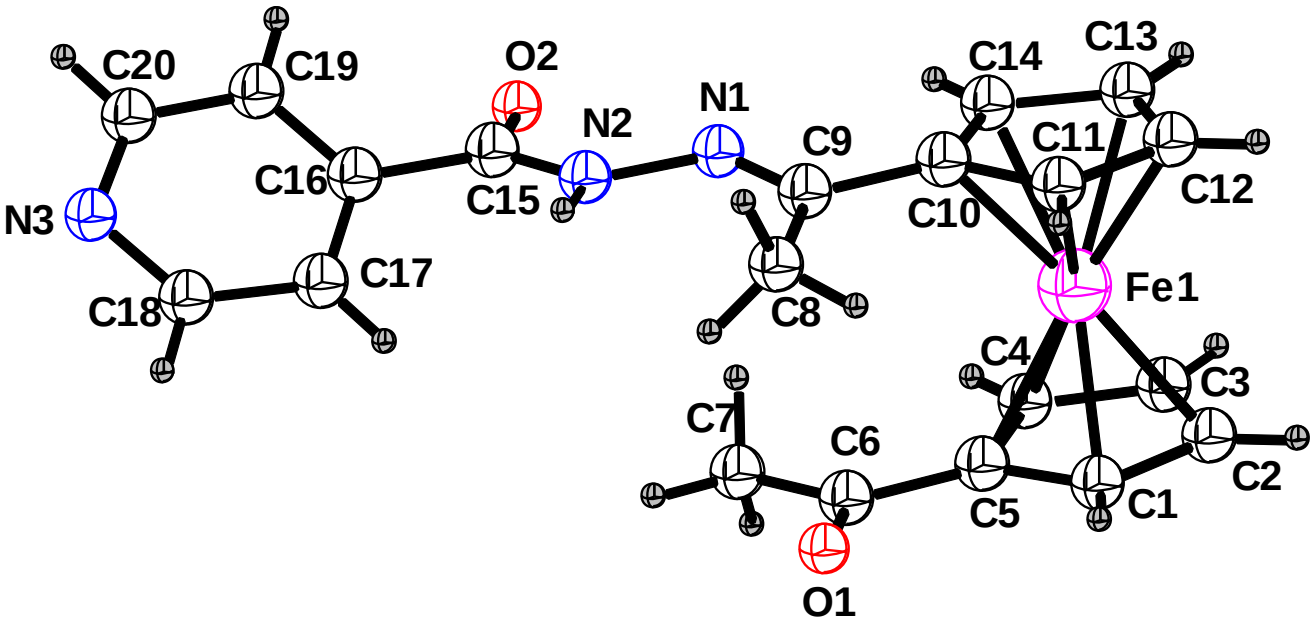

Figure 3.4. Molecular structure of 7. Selected bond lengths (Å) and bond angles (º): N(2)-C(15) = 1.338(11), N(1)-N(2) = 1.381(9), O(2)-C(15) = 1.187 (10), N(1)-C(09) = 1.284(10), C(09)-N(1)-N(2) = 116.0(7), O(2)-C(15)-N(2) = 123.7(8).

Single crystal, grown from dichloromethane/n-hexane solvent mixture at -10 ºC has been used for single crystal X-ray diffraction study. Molecular structure of **7** confirms the presence of a $-COCH_3$ group attached to one of the Cp ring, while the other Cp ring is linked to a hydrazone unit via a C═N bond. The structural analysis confirms a double bond character of C(9)-N(1) bond with a bond length of 1.289 (3) Å, while N(1)-N(2) corresponds to single bond character (1.394(2) Å). The two ferrocenyl Cp rings are at eclipsed position and the plane of the pyridyl ring is almost perpendicular to the Cp ring with a torsional angle of 153º. The C-O bond length corresponding to keto group attached to pyridine ring is slightly shorter (C(15)-O(2)= 1.203(2) Å) than the keto group linked to Cp ring (C(6)-O(1) = 1.220(2) Å). Packing diagram reveals inter-molecular hydrogen bonding interaction between O2…H-N2 (2.124 Å) with the formation of linear polymeric chain with alternate molecular units as shown in Figure 3.5.

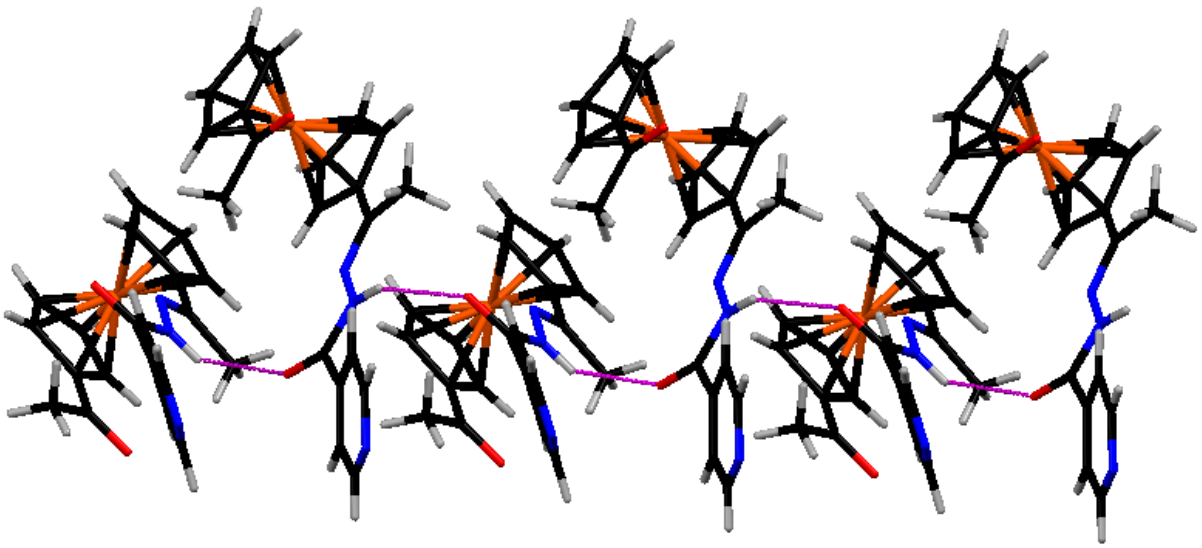

Figure 3.5. Packing diagram showing H-bonding interaction.

To understand its reactivity, we added equivalent amount of isonicotinyl hydrazide to an ethanol solution of **7** under inert atmosphere to isolate the symmetrically disubstituted derivative [Fe{(η^5-C_5H_4)C(CH_3)═N-N(H)C(O)(C_5H_4N)}$_2$] (**9**). This reveals that the pendant acetyl group attached to one of the Cp ring in compound **7** is taking part in the reaction to form Schiff base type hydrazone linkage. Therefore, we carried out similar reaction technique to prepare 1,1' unsymmetrically disubstituted ferrocenyl compounds containing two different hydrazone units. Thus, compound **7** was reacted with equivalent amount of salicyloyl hydrazide to obtain a new ferrocene containing mixed hydrazone compound [Fe{(η^5-C_5H_4)C(CH_3)═N-N(H)C(O)(C_5H_4N)}{(η^5-C_5H_4)C(CH_3)═N-N(H)C(O)-C_6H_4-OH}] (**10**) (Scheme 3.4).

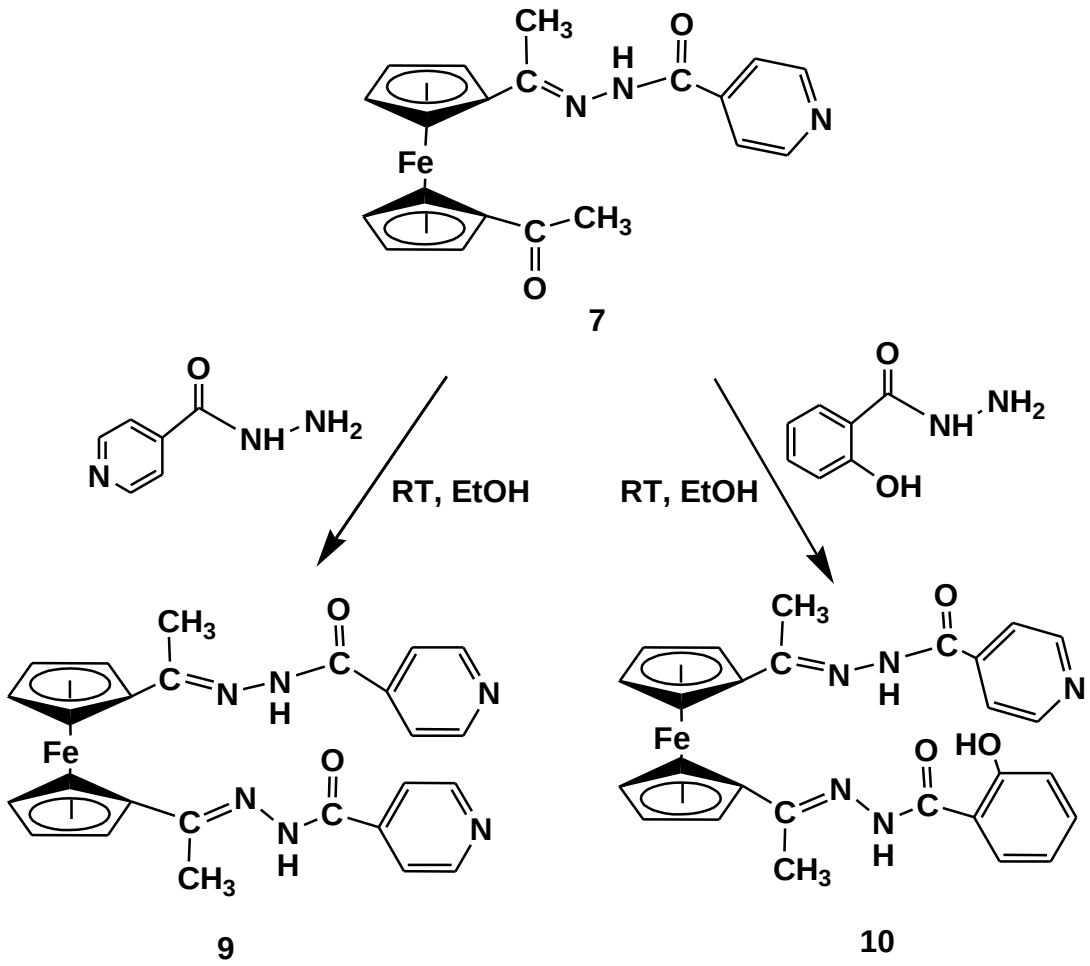

Scheme 3.4

Compounds **9** and **10** have been characterized by IR and ^{1}H NMR spectroscopy. Infrared spectra for compounds **9** and **10** show peaks corresponding to C=O and C=N stretching frequency in the range 1595-1642 cm^{-1} and 1600-1659 cm^{-1} respectively. Presence of CH_3, disubstituted ferrocenyl and pyridyl protons for compound **9** have been confirmed from their corresponding peaks in ^{1}H NMR spectra at δ 2.29, δ 4.61-4.81 and δ 7.84-8.81 respectively. Proton NMR spectra for compound **10** shows two methyl peaks at δ 2.28 and δ 2.15 region, four peaks in the range δ 4.43-4.79 corresponding to eight ferrocenyl protons and phenyl and pyridyl protons are observed in the range δ 6.52-7.82 as

multiplet. ESI mass spectral analysis for **10** reveals the presence of [M] fragment at 523 m/z region. To our knowledge 1,1'-unsymmetrically substituted ferrocenyl mixed hydrazone compounds are novel and the synthetic method described here can be used to prepare a varied range of ferrocenyl hydrazone compounds containing unsymmetrically Cp substituted side chains.

The electrochemical properties of compounds **5-8** have been examined in acetonitrile solution (0.1M TBAP) by cyclic voltammetry and differential pulse voltammetry (Table 3.2). Compounds **5-8**, involving a ferrocenyl moiety linked to an acetyl and a hydrazone group exhibited a reversible redox process in between + 0.66 and +0.69 V due to the Fe(II)/Fe(III) redox couple. Among the four compounds, the redox couple of **6** have been observed in slightly lower potential region due to the presence of o-hydroxy substituent making the oxidation more easier. When redox couple was compared with the oxidation potential of 1,1'-diacetyl ferrocene, it has been observed that the presence of acetyl group exerts a quite strong electron withdrawing effect than that of the hydrazone moiety. For instance, the oxidation of **5-8** is 140 mV – 110 mV less positive than that of diacetylferrocene which reveals that the presence of one hydrazone group in **5-8** makes the oxidation more easier than diacetyl ferrocene.

Table 3.2. Cyclic voltammetric data for **5-8**

Compounds	E_{pa}	E_{pc}	dpv (V)	$E_{1/2}$ (V) (ΔE_p (mV))
5	0.717	0.657	0.66	0.69 (60)
6	0.69	0.633	0.634	0.66 (57)
7	0.708	0.643	0.653	0.676 (65)
8	0.70	0.638	0.645	0.67 (62)

In summary, methodology has been designed to obtain unsymmetrically substituted ferrocenyl dihydrazone compound from 1-acetyl-1'-isonicotinylferrocenylhydrazone precursor. Study of their electrochemical properties by cyclic voltammetric techniques showed responses corresponding to ferrocene-ferrocenium couple. These ferrocenyl Schiff base compounds are further suited for

complexation reaction to obtain multimetallic compounds and various modification for their application in the field of bioorganometallic chemistry. We are currently engaged in the synthesis and reactivity of a variety of Cp based organometallic compounds and exploring their possibility for effective medicinal properties.

3.4. References

[1] (a) D. R. V. Staveren, N. Metzler-Nolte, Chem. Rev. 104 (2004) 5931; (b) A. R. Pike, L. C. Ryder, B. R. Horrocks, W. Clegg, M. R. J. Elsegood, B. A. Connolly, A. Houlton, Chem. Eur. J. 8 (2002) 2891.

[2] (a) M. Patra, G. Gasser, M. Wenzel, K. Merz, J. E. Bandow, N. Metzler-Nolte, Organometallics 29 (2010) 4312; (b) M. Navarro, W. Castro, C. Biot, Organometallics 31 (2012) 5715.

[3] O. Payen, S. Top, A. Vessières, E. Brulé, A. Lauzier, M.-A. Plamont, M. J. McGlinchey, H. Müller-Bunz, G. Jaouen, J. Organomet.Chem. 696 (2011) 1049.

[4] J. Quirante, F. Dubar, A. González, C. Lopez, M. Cascante, R. Cortés, I. Forfar, B. Pradines, C. Biot, J. Organomet. Chem. 696 (2011) 1011.

[5] V. Zsoldos-Mády, A. Csámpai, R. Szabó, E. Mészáros-Alapi, J. Pásztor, F. Hudecz, P. Sohár, Chem. Med. Chem. 1 (2006) 1119.

[6] (a) B. Maity, B. V. S. K. Chakravarthi, M. Roy, A. A. Karande, A. R. Chakravarty, Eur. J. Inorg. Chem. (2011) 1379; (b) J. Zhang, Appl. Organomet. Chem. 22 (2008) 6.

[7] (a) Z. H. Chohan, C. T. Supuran, Appl. Organomet. Chem. 19 (2005) 1207; (b) Z. H. Chohan, H. Pervez, K. M. Khan, C. T. Supuran; J. Enzyme Inhib. Med. Chem. 20 (2005) 81.

[8] G. M. Maguene, J. Jakhlal, M. Ladyman, A. Vallin, D. A. Ralambomanana, T. Bousquet, J. Maugein, J. Lebibi, L. Pélinski, Eur. J. Med. Chem. 46 (2011) 31.

[9] D. A. Ralambomanana, D. Razafimahefa, A. C. Rakotohova, J. Maugein, L. Pelinski, Biorg. Med. Chem.16 (2008) 9546.

[10] S. G. Ku¨ çu¨ kgu¨ zel, E. E. Oruç, S. Rollas, F. Sahin, A. O¨ zbek, Eur. J. Med. Chem. 37(2002) 197.

[11] S.G. Ku¨ çu¨ kgu¨ zel, S. Rollas, I. Ku¨ çu¨ kgu¨ zel, M. Kiraz, Eur. J. Med. Chem. 34 (1999)1093.

[12] I. G. Ribeiro, K. C. M. da Silva, S. C. Parrini, A. L. P. de Miranda, C. A. M. Fraga, E. J. Barreiro, Eur. J. Med. Chem. 33 (1998) 225.

[13] D. R. Richardson, P. V. Bernhardt, J. Biol. Inorg. Chem. 4 (1999) 226.

[14] U¨ .O¨. O¨ zmen, G. Olgun, Spectrochim. Acta Part A 70 (2009) 641.

[15] P. G. Avaji, C. H. V. Kumar, S. A. Patil, K. N. Shivananda, C. Nagaraju, Eur. J. Med. Chem. 44 (2009) 3552.

[16] Y. Zang, L. Zang, L. Liu, J. Guo, D. Wu, G. Xu, X. Wang, D. Jia, Inorg. Chim. Acta 363 (2010) 289.

[17] L. M. Lima, F. S. Frattani, J. L. dos Santos, H. C. Castro, C. A. M. Fraga, R. B. Zingali, E. J. Barreiro, Eur. J. Med. Chem. 43 (2008) 348.

[18] P. V. Bernhardt, J. Mattson, D. R. Richardson, Inorg. Chem. 45 (2006) 752.

[19] M. F. Iskander, L. El-Sayed, N. M. H. Salem, W. Haase, H. J. Linder, S. Foro, Polyhedron 23 (2004) 23.

[20] S. Yu, S. Wang, Q. Luo, L. Wang, Z. Peng, X. Gao, Polyhedron 12 (1993) 1093.

[21] G. F. Qi, Z.-Y. Yang, D.-D. Qin, Chem. Pharm. Bull. 57 (2009) 69.

[22] V. P. Singh, P. Gupta, J. Enz. Inhib. Med. Chem. 23 (2008) 797.

[23] V. Singh, A. Singh, J. Coord. Chem. 61 (2008) 2767.

[24] S. R. Patil, U. N. Kantak, D. N. Sen, Inorg. Chim. Acta, 63 (1982) 261.

[25] M. Yongxiang, Z. Gang, Polyhedron, 7 (1988) 1101.

[26] M. Yongxiang, L. Zhong-Lin, S. Qing-Bao, W. Xiao-Li, J. Coord. Chem., 32 (1994) 353.

[27] F. Chen-jie, D. Chun-ying, H. Cheng, M. Qing-jin, Chem. Commun. (2000) 1187.

[28]. F. Chen-jie, D. Chun-ying, M. Hong, H. Cheng, M. Qing-jin, L. Yong-jiang, M. Yu-hua, W. Zhe-ming, Organometallics 20 (2001) 2525.

[29]. P. Barbazan, R. Carballo, I. Prieto, M. Turnes, E. M. Vazquez-Lopez; J. Organomet. Chem. 694 (2009) 3102.

[30] G. M. Maguene, J. Jakhlal, M. Ladyman, A. Vallin , D. A. Ralambomanana, T. Bousquet, J. Maugein, J. Lebibi, L. Pélinski, Eur. J. Med. Chem. 46 (2011) 31.

[31] H. Qian, Z. Yin, T. Zhang, S. Yan, Q. Wang, C. Zhang, Organometallics 33 (2014) 6241.

[32] M. Vogel, M. Rausch, H. Rosenberg, J. Org. Chem. 22 (1957) 1016.

[33] (a) N. S. Navaneetham, R. Kalyanasundaram, S. Soundararajan, Inorg. Chim. Acta 110 (1985) 169; (b) H. Meyer, J. Mally, Monatshefte fuer Chemie 33 (1912) 393.

[34] G. M. Sheldrick, Acta Cryst. A 64 (2008) 112.

Chapter 4

Ferrocenyl-cymantrenyl hetero-bimetallic chalcones: Synthesis, reactivity and biological properties.

4.1. Introduction

Ferrocenyl chalcone compounds belong to a chalcone family in which one or both the aromatic groups are substituted by ferrocenyl units and are connected by an enone bridge. Recently, a bunch of different ferrocenyl chalcones and their derivatives have been synthesized which show marked electrochemical and biological properties [1]. These systems have been investigated as precursors for a variety of ferrocene containing heterocycles like pyrazoles, pyrimidines etc [2]. It has now been well established that chalcone moieties constitute an important class of naturally occurring flavonoids and exhibit a wide spectrum of biological activities such as anti-cancer, anti-microbial, anti-malarial and anti-inflammatory activities [3]. In recent years, a number of synthetic studies have been carried out on monosubstituted ferrocenyl chalcone of types A and B (Figure 4.1) [2, 4], while the structural types C and D containing 1,1'-disubstituted ferrocenyl chalcone moiety have been studied to a lesser extent [5]. Literature survey also reveals that there are only three reports for the synthesis of hetero-bimetallic chalcones of types E and F [6,20], whereas the disubstituted analogs of hetero-bimetallic chalcone (types G and H) have not been studied so far. In this chapter, we have focused our study on ferrocenyl chalcones of types F and H containing polynuclear bimetallic moieties with multiple redox centers.

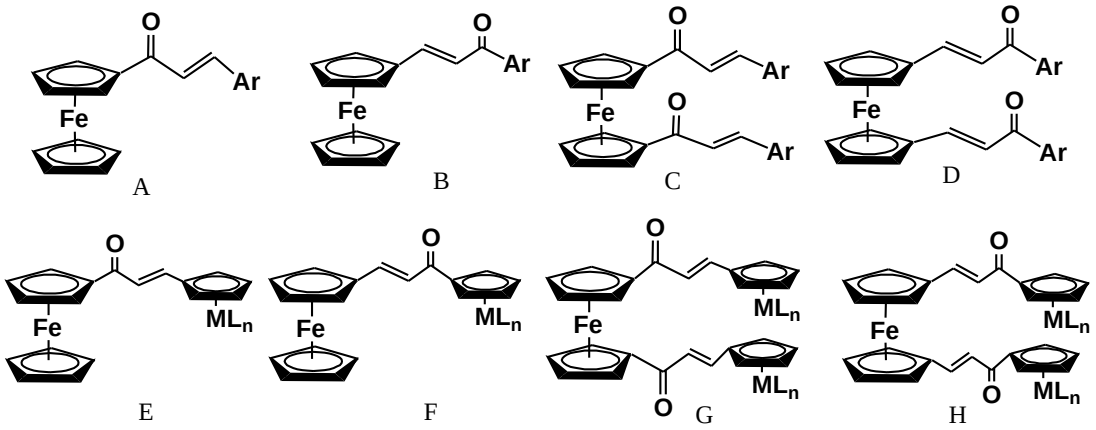

Ar = Aryl or ferrocenyl group

ML_n = Metal-ligand fragment

Figure 4.1. Ferrocenyl chalcones, types A-H.

Recently, multimetallic redox active systems have attracted interest due to their various application related to electronic communication, bioactivity, sensors, molecular electronic devices, optical properties etc [7-11]. To understand the significance of multimetallic compounds, a series of fluorinated bimetallic complexes containing both sandwich and half sandwich moieties have been synthesized by Roemer et al. using [2+2] cycloaddition reaction to give cymantrene and ferrocene based complexes with perfluorinated bridging moieties. Introduction of fluorinated chains into Cp rings of metal organic framework and presence of bimetallic arrangement remarkably altered the reactivity and electrochemical behavior of the complexes (Figure 4.2).[19]

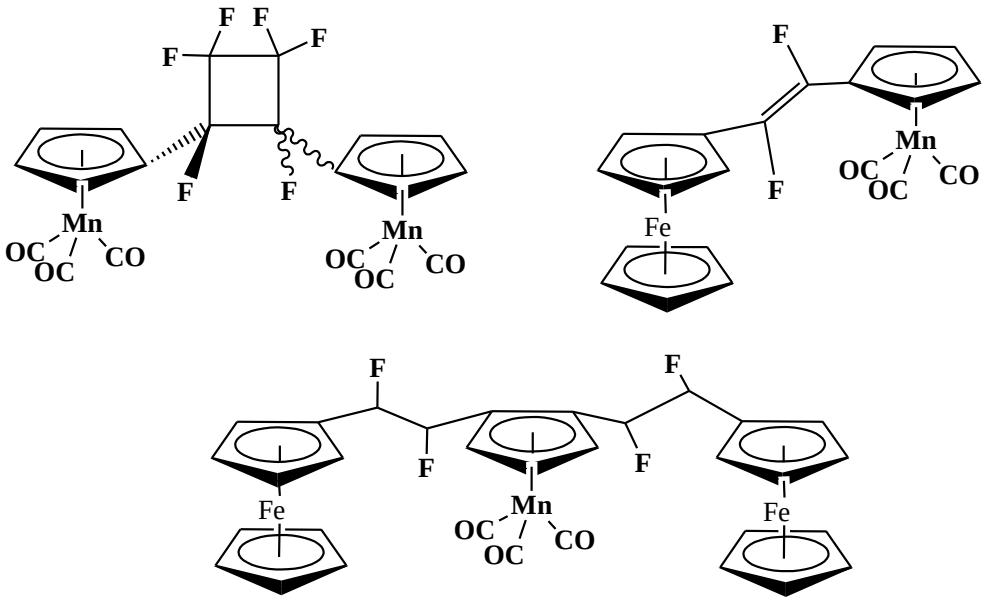

Figure 4.2

In the area of biological chemistry, ferrocene based organometallic compounds constitute an interesting class of molecules with potential application in the field of anticancer, antimalarial and other therapeutical activities [12, 13]. Some of these recent investigations led to the immergence of a relatively new field of bioorganometallic chemistry [14], where a large number of ferrocene and half sandwich based compounds

have been found to display interesting cytotoxic, DNA cleaving and other biological activities [12,13, 15-18]. Ferrocene substituted tamoxifen and ferrocenyl chloroquine derivatives are among the many examples in which ferrocene incorporation have improved the activity of the drug [17]. Recently, we have also reported some biologically active ferrocenyl and cymantrenyl hydrazone compounds and synthesized half-sandwich based dithiocarboxylato-alkyne complexes by sunlight driven reaction which also showed remarkable antibacterial activity [18]. Arancibia and coworkers have synthesized a new series of hybrid organometallic-organic and dinuclear organometallic chalcones containing the cyrhetrenyl fragment as shown in Figure 4.3.[20] ^{1}H and ^{13}C NMR spectral data signify an E-stereochemistry at the C=C bond, as well as predicts a -cis conformation of the enone moiety in solution. In the solid state a similar structural identity was established for 1-ferrocenyl-3-cyrhetrenyl-2-propen-1-one by single crystal X-ray crystallography. The cyrhetrenyl group exerts electron withdrawing effect on the ketonic carbonyl and olefinic carbons and correlate exactly with the shift in ^{13}C NMR of the compound. The antimalarial activity of the compounds against the chloroquine-susceptible strain 3D7 and the chloroquine-resistant strain W2 of *Plasmodium falciparum* were evaluated in vitro which indicates that these cyrhetrene conjugates are more active compared to their ferrocenic analogues.

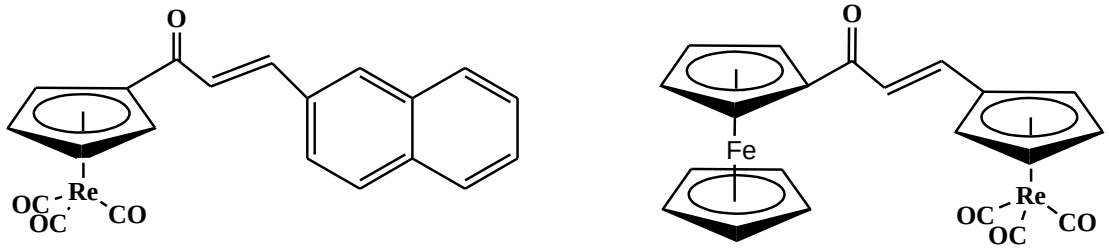

Figure 4.3

Two hetero tri-metallic compounds with potent activity against Gram-positive bacteria including multi-resistant *Staphylococcus aureus* were synthesized. The compound consist of two different functionality, one having a peptide nucleic acid

backbone and an alkyne side chain, substituted with cymantrenyl, (dipicolyl)$Re(CO)_3$ and ferrocenyl moieties (Figure 4.4).[21] The unique nature of trimetallic compound with the presence of a pseudopeptide backbone, a positive charge, and three lipophilic organometallic residues, namely, ferrocene, cymantrene, and a (dipicolyl)$Re(CO)_3$ moiety, are considered to be responsible for the potent antibacterial activity against Gram-positive bacteria.

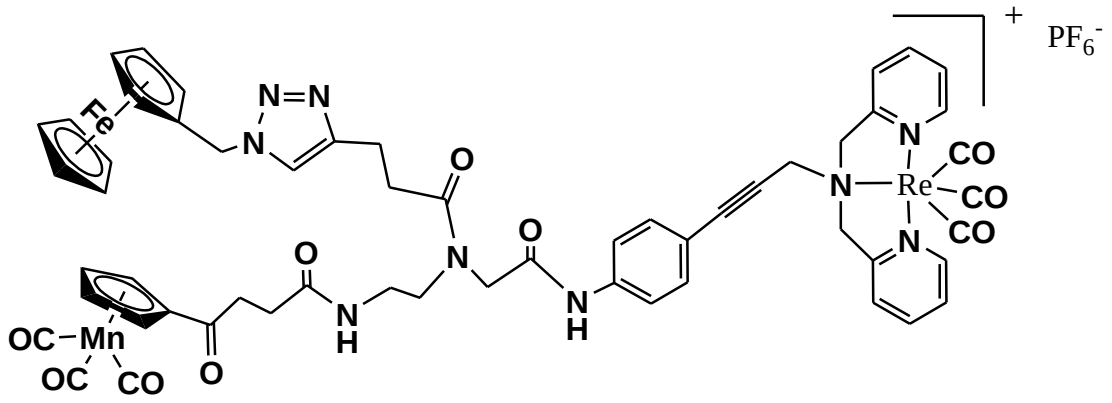

Figure 4.4

In view of the interesting properties of sandwich –half sandwich conjugate molecular system and their emerging potential in biological and electrochemical activities, we focused our studies on the synthesis of ferrocene and half-sandwich based multimetallic compounds, in particular, types F and H (Figure 4.1) and use them for electrochemical studies and biological evaluation. To the best of our knowledge, synthesis and bioactivity of trinuclear ferrocenyl chalcone of type H has so far remain unreported. However, only a few studies on chalcones of type F have been reported but a large part of the synthetic, structural and biological chemistry of type F compounds have remain unexplored. In this chapter, we describe the synthesis of novel hetero-metallic chalcones containing both ferrocenyl and cymantrenyl fragments and studied their reactivity towards mono- and diphosphine substitution. Antimalarial and antibacterial

properties were studied for two bimetallic chalcones and electrochemical analysis was carried out to understand their redox properties. TD-DFT study was also conducted for ferrocenyl-cymantrenyl hetero-metallic chalcone (**10**) to predict the molecular orbitals involved for various electronic transitions. Molecular structural characterizations for two new ferrocenyl-cymantrenyl chalcones have been carried out which revealed the conformational identity of the compounds.

4.2. Experimental Sections

4.2.1. General Procedures

All reactions and manipulations were carried out under an inert atmosphere of dry, pre-purified argon using standard Schlenk line techniques. Solvents were purified, dried and distilled under inert atmosphere prior to use. Infrared spectra were recorded on a Perkin Elmer Spectrum RX-I spectrometer as CH_2Cl_2 solution and NMR spectra on a 400 MHz Bruker spectrometer in $CDCl_3$ solvent. Elemental analyses were performed on a Vario El Cube analyzer. Mass spectra were obtained on a SQ-300 MS instrument operating in ESI mode. Cyclic voltammetric and differential pulse voltammetric measurements were carried out using a CH Instruments model 600D electrochemistry system. A platinum working electrode, a platinum wire auxiliary electrode and a silver / silver chloride reference electrode were used in a three−electrode configuration. The supporting electrolyte was 0.1 M $[NEt_4]ClO_4$ and the solute concentration was ~10^{-3} M. The scan rate used was 50-200 mV s^{-1}. All electrochemical experiments were carried out under nitrogen atmosphere and are uncorrected for junction potentials. TLC plates (20x20 cm, Silica gel 60 F254) were purchased from Merck. $[(CO)_3Mn(\eta^5\text{-}C_5H_4COCH_3)]$ [22], $[(\eta^5\text{-}C_5H_5)Fe(\eta^5\text{-}C_5H_4CHO)]$ and $[Fe(\eta^5\text{-}C_5H_4CHO)_2]$ [23] were prepared following reported procedures.

4.2.2. Synthesis of $[(CO)_3Mn(\eta^5\text{-}C_5H_4)COCH{=}CH(\eta^5\text{-}C_5H_4)Fe(\eta^5\text{-}C_5H_5)]$ (11).

An ethanolic solution (10 ml) of ferrocenyl carboxyaldehyde (21mg, 0.1 mmol) was taken in a round bottom flask and acetyl cymantrene (28 mg, 0.1 mmol) was added under stirring condition. Two equivalents of sodium hydroxide in ethanol solution was then added to the reaction mixture and stirring was continued at room temperature under inert atmosphere for 3 hours. The reaction was continuously monitored by TLC and on completion of the reaction the solution was dried under vacuum and the residue was dissolved in dichloromethane solvent and subjected to chromatographic work-up using column chromatography. Elution with dichloromethane/hexane (30:70 v/v) solvent mixture separated the following compounds in the order of elution: $[(CO)_3Mn(\eta^5\text{-}C_5H_4)COCH_3]$, $[(\eta^5\text{-}C_5H_5)Fe(\eta^5\text{-}C_5H_4CHO)]$ and violet colored compound $[(\eta^5\text{-}C_5H_4)Mn(CO)_3COCH{=}CH(\eta^5\text{-}C_5H_4)Fe(\eta^5\text{-}C_5H_5)]$ (**11**). {Yield: 32 mg (73 %)}

11: Anal. calcd. (found): C, 57.01 (57.23); H, 3.39 (3.34). IR (ν_{CO}, cm^{-1},CH_2Cl_2) 2022.8 (vs), 1937 (vs, br), 1653 (s), 1586 (s). ^{1}H NMR (δ, $CDCl_3$): 4.2 (s, η^5-C_5H_5, 5H), 4.52 (t, J = 2 Hz, η^5-C_5H_4, 2H), 4.6 (t, J = 2 Hz, η^5-C_5H_4, 2H), 4.9 (t, J = 2 Hz, η^5-C_5H_4, 2H), 5.55 (t, J = 2 Hz, η^5-C_5H_4, 2H), 6.58 (d, J = 15 Hz, C*H*=, 1H), 7.78 (d, J = 15 Hz, =C*H*, 1H). ^{13}C NMR (δ, $CDCl_3$): 69.16 (η^5-C_5H_5), 69.95 (η^5-C_5H_4), 71.66 (η^5-C_5H_4), 78.47 (η^5-C_5H_4), 83.61 (η^5-C_5H_4), 86.59 (η^5-C_5H_4), 93.78 (η^5-C_5H_4), 117.41 (=*C*H), 146.38 (=*C*H), 185.29 (-*C*=O). UV –Vis. (λ (nm), CH_2Cl_2) =321, 384, 502. MS (ESI): m/z 443 [M+H].

4.2.3. Synthesis of 1,1'-$[\{(CO)_3Mn(\eta^5\text{-}C_5H_4)COCH{=}CH(\eta^5\text{-}C_5H_4)\}_2Fe]$ (12).

A solution of 1,1'-ferrocenyl dialdehyde (24 mg, 0.1 mmol) in ethanol (10 ml) was taken in a round bottomed flask and acetyl cymantrene (56 mg ,0.2 mmol) was added under stirring condition. Ethanolic solution of sodium hydroxide was then added to the reaction mixture dropwise and stirred for 3-4 hours at room temperature under inert

atmosphere. The reaction was continuously monitored by TLC and on disappearance of the reactants the solution was dried under vacuum and the residue was dissolved in dichloromethane solvent and subjected to chromatographic work-up using column chromatography. Elution with dichloromethane/hexane (40:60 v/v) solvent mixture separated the violet colored compound [{(η^5-C_5H_4)Mn(CO)$_3$COCH=CH (η^5-C_5H_4)}$_2$Fe] (**12**) along with trace amount of the reactants. {Yield: 46 mg (65 %)}

12: Anal. calcd. (found): C, 55.01 (55.18); H, 2.87 (2.81). IR (ν_{CO}, cm^{-1},CH_2Cl_2): 2021 (vs), 1925 (vs, br), 1648 (s), 1591 (s). ^{1}H NMR (δ, $CDCl_3$): 4.44 (t, J = 2 Hz η^5-C_5H_4, 4H), 4.47 (t, J = 1.8 Hz, η^5-C_5H_4, 4*H*), 4.82 (t, J = 2 Hz, η^5-C_5H_4, 4H), 5.45 (t, J = 1.8 Hz η^5-C_5H_4, 4H), 6.43 (d, J= 15Hz, C*H*=, 2H), 7.57 (d, J=15Hz, =C*H*, 2H). ^{13}C NMR (δ, $CDCl_3$): 70.76 (η^5-*C*$_5$H$_4$), 73.42 (η^5-*C*$_5$H$_4$), 79.86 (η^5-*C*$_5$H$_4$), 83.77 (η^5-*C*$_5$H$_4$), 86.67 (η^5-*C*$_5$H$_4$), 93.42 (η^5-*C*$_5$H$_4$), 118.60 (=*C*H), 144.43 (*C*H=), 185.31 (-*C*=O). UV – Visible (λ (nm), CH_2Cl_2) = 304, 334, 374 (sh), 505. MS (ESI): m/z 699 [M+H].

4.2.4. Synthesis of [(CO)$_2$(PPh$_3$)Mn(η^5-C$_5$H$_4$)COCH=CH(η^5-C$_5$H$_4$)Fe(η^5-C$_5$H$_5$)] (13).

In a two necked round bottomed flask, compound **11** (22 mg, 0.05 mmol) was taken in THF/ toluene solvent and was stirred at room temperature under inert atmosphere to get a clear violet solution. To the stirring solution, triphenylphosphine (13 mg, 0.05 mmol) was added and the whole reaction mixture was irradiated with UV light for 10 minutes. After the irradiation the stirring was continued at room temperature under inert atmosphere for 17 hours and the solution was dried under vacuum and the residue was dissolved in minimum amount of dichloromethane solvent and subjected to chromatographic work-up using preparative TLC. Elution with dichloromethane/hexane (60:40 v/v) solvent mixture separated the reactant, **11** and an orange colored compound [(CO)$_2$(PPh$_3$)Mn(η^5-C$_5$H$_4$)COCH=CH(η^5-C$_5$H$_4$)Fe(η^5-C$_5$H$_5$)] (**13**) along with trace amount of decomposition. {Yield: 23 mg (68 %)}

13: IR(ν_{CO}, cm^{-1},CH_2Cl_2): 1936 (s), 1874 (s), 1645 (s). ^{1}H NMR (δ, $CDCl_3$): 4.18 (s, η^5-C_5H_5, 5H), 4.47 (t, η^5-C_5H_4, 2H), 4.59 (t, η^5-C_5H_4, 2H), 5.24 (t, η^5-C_5H_4, 2H), 5.32 (t, η^5-C_5H_4, 2H), 6.63 (d, J= 15Hz, C*H*=, 1H), 7.40 – 7.45 (m, C_6H_5, 15H), 7.7 (d, J= 15Hz,=C*H*, 1H). ^{31}P NMR (δ, $CDCl_3$): 89.77 (Mn*P*Ph_2-). MS (ESI): m/z 677 [M].

4.2.5. Reaction of 11 with Bis-diphenylphosphino ferrocene (dppf)

In a two neck round bottomed flask, toluene solution (5 ml) of compound **11** (22 mg, 0.05 mmol) and bis-diphenylphosphino ferrocene (dppf) (26 mg, 0.05 mmol) was taken and stirred at room temperature under inert atmospheric condition. The whole reaction mixture was irradiated with UV light for 7 minutes and stirred for 16 hours. The reaction was continuously monitored using TLC. After the completion of the reaction the solution was dried under vacuum and the residue was dissolved in minimum amount of dichloromethane solvent and subjected to chromatographic work-up using preparative TLC. Elution with dichloromethane/hexane (80:20 v/v) solvent mixture separated the reactants, [{(η^5-C_5H_4)PPh_2}$_2$Fe] and [{(η^5-C_5H_5)Fe(η^5-C_5H_4)CH=CHCO(η^5-C_5H_4)Mn$(CO)_3$] (**11**) and orange colored compounds, [{(η^5-C_5H_5)Fe(η^5-C_5H_4)CH=CHCO(η^5-C_5H_4)Mn$(CO)_2PPh_2$(η^5-C_5H_4)Fe(η^5-C_5H_4)PPh_2] (**14**) in major amount and [{(η^5-C_5H_5)Fe(η^5-C_5H_4)CH=CHCO(η^5-C_5H_4)Mn$(CO)_2PPh_2$(η^5-C_5H_4)}$_2$Fe] (**15**) in minor amount. Trace amount of decomposition and other indistinguishable products was also obtained during TLC separation. {Yields: **14**, 23 mg (47 %); **15**, 8 mg (12 %)}

14: IR (ν_{CO}, cm^{-1}, CH_2Cl_2): 1934 (vs), 1874 (vs), 1646 (s), 1588 (s). ^{1}H NMR (δ, $CDCl_3$): 3.69 (t, η^5-C_5H_4, 2H), 3.97 (t, η^5-C_5H_4, 2H), 4.05 (t, η^5-C_5H_4, 2H), 4.13 (t, η^5-C_5H_4, 2H), 4.22 (s, η^5-C_5H_5, 5H), 4.37 (t, η^5-C_5H_4, 2H), 4.47 (t, η^5-C_5H_4, 2H), 4.60 (t, η^5-C_5H_4, 2H), 5.20 (t, η^5-C_5H_4, 2H), 6.62 (d, J = 15 Hz, C*H*=, 1H), 7.22-7.37 (m, C_6H_5, 20H), 7.72 (d, J = 15 Hz, =C*H*, 1H). ^{31}P NMR (δ, $CDCl_3$): -17.62 (*P*Ph_2-), 82.66 (Mn*P*Ph_2-). MS (ESI): m/z 969 [M+H], 940 [M-CO].

15: IR (ν_{CO}, cm^{-1}, CH_2Cl_2) 1934 (vs), 1873 (vs), 1648 (s), 1587 (s). ^1H NMR (δ, $CDCl_3$): 3.88 (t, η^5-C_5H_4, 4H), 3.9 (t, η^5-C_5H_4, 4H), 4.06 (t, η^5-C_5H_4, 4H), 4.23 (s, η^5-C_5H_5, 10H), 4.48 (t, J = 2 Hz , η^5-C_5H_4, 4H), 4.61 (t, J = 2 Hz, η^5-C_5H_4, 4H), 5.18 (t, J = 2 Hz, η^5-C_5H_4, 4H), 6.60 (d, J = 15.6 Hz, C*H*=, 2H), 7.30-7.38 (m, C_6H_5, 20H), 7.73 (d, J = 15.6 Hz, =C*H*, 2H). ^{31}P NMR (δ, $CDCl_3$): 82.84 (Mn*P*Ph_2-). MS (ESI): m/z 1326 [M-2CO].

4.2.6. Synthesis of [{(CO)$_2$(PPh$_3$)Mn(η^5-C$_5$H$_4$)COCH=CH(η^5-C$_5$H$_4$)}$_2$Fe] (16).

In a two neck round bottom flask, THF solution of compound **12** (35 mg, 0.05 mmol) was taken and stirred at room temperature under inert atmosphere. Triphenylphosphine (26 mg, 0.1 mmol) was then added to the reaction mixture and irradiated with UV light for 10 minutes in continuous stirring condition. After the UV-irradiation, stirring was continued at room temperature for 20 hours and the solution was dried under vacuum. The residue was dissolved in minimum amount of dichloromethane solvent and subjected to chromatographic work-up using preparative TLC. Elution with dichloromethane/hexane (60:40 v/v) solvent mixture separated the reactant, [{$(CO)_3Mn(\eta^5$-$C_5H_4)COCH=CH(\eta^5$-$C_5H_4)\}_2Fe$] (**12**) and an orange colored compound, [{$(CO)_2(PPh_3)Mn(\eta^5$-$C_5H_4)COCH=CH(\eta^5$-$C_5H_4)\}_2Fe$] (**16**) during the elution. Trace amount of decomposition and some minor products was also observed during the workup. {Yields: 32 mg (54 %)}

16: IR(ν_{CO}, cm^{-1},CH_2Cl_2): 1948 (s), 1880 (s), 1648 (m), 1591 (m). ^1H NMR (δ, $CDCl_3$): 4.12 (t, η^5-C_5H_5, 4H), 4.46 (t, η^5-C_5H_4, 4H), 4.55 (t, η^5-C_5H_4, 4H), 5.22 (t, η^5-C_5H_4, 4H), 6.55 (d, J= 15Hz, C*H*=, 2H), 7.39-7.46 (m, C_6H_5, 30H), 7.62 (d, J= 15Hz,=C*H*, 2H). ^{31}P NMR (δ, $CDCl_3$): 89.76 (Mn*P*Ph_2-). MS (ESI): m/z 1167 [M].

4.2.7. Crystal structure determination for 11 and 13

Single crystal X-ray structural studies of **11** and **13** were performed on a CCD Oxford Diffraction XCALIBUR-S diffractometer equipped with an Oxford Instruments low-temperature attachment. Data were collected at 150(2) K using graphite-monochromated Mo Kα radiation (λ_α = 0.71073 Å). The strategy for the data collection was evaluated by using the CrysAlisPro CCD software. The data were collected by the standard 'phi-omega scan techniques, and were scaled and reduced using CrysAlisPro RED software. The structures were solved by direct methods using SHELXS-97 and refined by full matrix least-squares with SHELXL-97, refining on F^2 [24]. The positions of all the atoms were obtained by direct methods. All non-hydrogen atoms were refined anisotropically. The remaining hydrogen atoms were placed in geometrically constrained positions and refined with isotropic temperature factors, generally $1.2U_{eq}$ of their parent atoms. The crystallographic details are summarized in Table 4.1. (CCDC Numbers, **11**: 1025035, **13**: 1025036).

Table 4.1. Crystal data and structure refinement parameters for compounds **11** and **13.**

	11	**13**
Empirical formula	C_{21} H_{15} Fe Mn O_4	C_{39} H_{30} C_{l3} Fe Mn O_3 P
Formula weight	442.12	794.74
Crystal system	Orthorhombic	Triclinic
Space group	*P n a 21*	P -1
a, Å	6.9502(4)	10.2716(5)
b, Å	24.3206(14)	10.3919(5)
c, Å	10.9894(8)	18.6183(9)
α deg	90	92.670(1)
β deg	90	98.100(1)
γ deg	90	116.641(1)

V, $Å^3$	1857.6(2)	1745.1(2)
Z	4	2
Dcalcd, Mg m^{-3}	1.581	1.513
abs coeff, mm^{-1}	1.484	1.091
F(000)	896	810
Cryst size, mm	0.33 x 0.26 x 0.21	0.33 x 0.26 x 0.21
θ range, deg	3.05 to 24.99	2.21 to 27.40
index ranges	$-8 \leq h \leq 8$, $-28 \leq k \leq 28$, $-11 \leq l \leq 13$	$-13 \leq h \leq 13$, $-13 \leq k \leq 13$, $-24 \leq l \leq 24$
reflections collected/ unique	13965 / 3140 [R(int) = 0.0468]	60130 / 7887 [R(int) = 0.0364]
data/ restraints / parameters	3140 / 1 / 245	7887 / 0 / 484
goodness-of-fit on F^2	1.029	0.996
Final R indices [$I>2\sigma(I)$]	R1 = 0.0360, wR2 = 0.0948	R1 = 0.0373, wR2 = 0.0910
R indices (all data)	R1 = 0.0388, wR2 = 0.0976	R1 = 0.0446, wR2 = 0.0959
largest diff peak and hole, $eÅ^{-3}$	0.485 -0.298	0.661 -0.643

4.2.8. Computational details

The Gaussian 03 program was used for the Density Functional Theory (DFT) calculation of compound **11**. The basis set already implemented in the program was used for the different types of calculations. The geometry of the compound was optimized at the Becke's three parameter hybrid method with LYP correlation (B3LYP) level [25, 26] and using LanL2DZ basis set. In addition to optimization, frequency calculation, Time-Dependent Density functional Theory (TD-DFT) calculations were done at same level of calculation and using the same basis sets. The absence of imaginary vibrational frequencies in calculated vibrational spectrum ensures the presence of a true minimum in the potential energy surface. The spectroscopic and electronic property of this complex has been computed by time dependent DFT (TD-DFT) calculation [27] at the same B3LYP level in gaseous phase. The nature and the role of the electronic excitation contributions are rationalized in terms of frontier molecular orbitals (FMO).

4.2.9. Antibacterial activity

Compounds **11** and **12** were screened for their antibacterial activity in vitro following the protocol described elsewhere [28]. The antibacterial effect was assayed against both gram positive bacteria *Bacillus subtilis* and gram negative bacteria *viz., Escherichia coli, Pseudomonas aeruginosa* and *Klebsiella pneumoniae* by the agar well diffusion method [28]. The compounds were dissolved in DMSO at different concentrations ranging from 500 to 15.625 μg/ml. Mueller Hinton-agar (containing 1% peptone, 0.6% yeast extract, 0.5% beef extract and 0.5% NaCl, at pH 6.9–7.1) plates were prepared and 0.5 – McFarland culture (1.5 X 10^8 cells/ml) of the test organisms were swabbed onto the agar plate. 9mm wells were made in the LB agar petri dishes. 100μl of each of the compound with decreasing concentrations was added to separate wells. DMSO was used as the negative control and *Chloramphenicol* was used as positive control. The plates were incubated at 37°C and observed for zones of inhibition around each well after 24 hours. The MIC, defined as the lowest concentration of the test

compound, which inhibits the visible growth, was determined visually after incubation for 24 h at 37ºC.

4.2.10. Antimalarial activity

Compounds **11** and **12** were studied for antimalarial activity against 3D7 as well as K1 strains of *P. falciparum*. The *in vitro* cultures of both Chloroquine - sensitive (3D7) and - resistant (K1) strains of *Plasmodium falciparum* are routinely maintained in medium RPNI supplemented with 25mM HEPES, 0.2% D-glucose, 0.21% sodium bicarbonate and 0.5% ALBUMAX-II [29]. The stock (10mM) solution of compounds was prepared in DMSO and required dilutions were made in test culture medium (RPMI-1640 with 10% FBS). For evaluation of 50% inhibitory concentration (IC_{50}) of the compounds, Malaria SYBR Green I-based fluorescence (MSF) assay [30] was carried out. Two-fold serial dilutions of test samples were made in 96 well plates and incubated with 1.0% parasitized cell suspension containing 0.8% parasitaemia (Asynchronous culture with more than 80% ring stages). The highest concentration used was 100µM. The plates were incubated at 37^{o}C in CO_2 incubator in an atmosphere of 5% CO_2 and air mixture. 72 hours later 100 µl of lysis buffer containing 2x concentration of SYBR Green-I (Invitrogen) was added to each well and incubated for one hour at 37^{o}C. The plates were examined at 485±20nm of excitation and 530±20nm of emission for relative fluorescence units (RFUs) per well using the fluorescence plate reader (FLX800, BIOTEK). Data was transferred into a graphic programme (EXCEL) and IC_{50} values were obtained by Logit regression analysis of dose-response curves. Chloroquine diphosphate (SIGMA) was used as the reference drug.

4.3. Results and Discussion

Room temperature reaction of 1-ferrocenyl carboxyaldehyde and 1,1'-ferrocenyl dicarboxyaldehyde with acetylcymantrene in presence of ethanolic sodium hydroxide under inert atmospheric condition led to the formation of the corresponding di- and tri-metallic chalcone compounds, $[(CO)_3Mn(\eta^5\text{-}C_5H_4)C(O)CH{=}CH(\eta^5\text{-}C_5H_4)Fe(\eta^5\text{-}C_5H_5)]$

(**11**) and [{$(CO)_3Mn(\eta^5\text{-}C_5H_4)C(O)CH{=}CH(\eta^5\text{-}C_5H_4)\}_2Fe$] (**12**) respectively (Scheme 4.1). The compounds were isolated and purified using column chromatography and subjected to spectroscopic characterization.

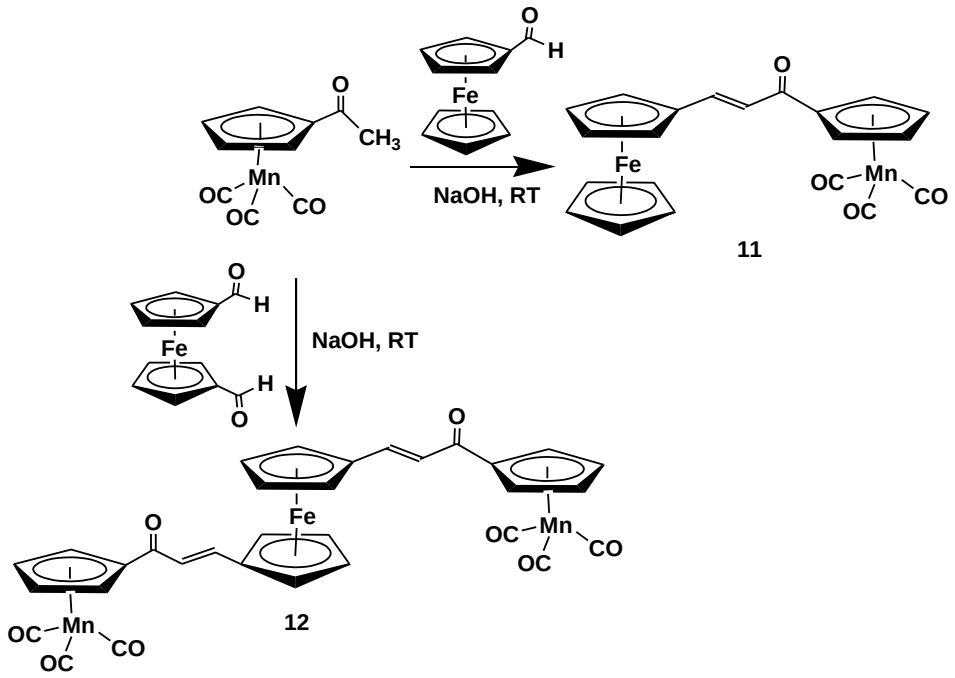

Scheme 4.1

Both the compounds **11** and **12** have been characterized by IR, ^1H, ^{13}C, ^{31}P NMR and mass spectroscopy. Infrared spectra of **11** and **12** show peaks corresponding to ketonic group at 1653 cm^{-1} and 1648 cm^{-1} respectively and terminal metal carbonyls in the region 2023-1925 cm^{-1}. ^1H NMR spectrum for **11** reveals the presence of unsubstituted ferrocenyl Cp protons at δ 4.2 (singlet) and substituted ferrocenyl protons at δ 4.52 (triplet) and δ 4.6 (triplet) region. Peaks corresponding to cymantrenyl Cp protons have been obtained at slightly downfield region at δ 4.9 (triplet) and δ 5.55 (triplet) positions. The two olefinic CH protons have been obtained as a doublet at δ 6.58 and δ 7.78 regions. The more downfield peak represents the α-olefinic proton close to the ketonic group. ^{13}C NMR of **11** also reveals the presence of unsubstituted Cp at

δ 69.16 position and six peaks for susbstituted Cp in the range δ 69.95 - 93.78. Olefinic carbon has been obtained at δ 117.41 and δ 146.38 region and the ketonic group has been identified by a peak at δ 185.29 position. Proton NMR spectrum for **12** is very similar to that of compound **11**, but the unsubstituted Cp peak at δ 4.2 position is absent in the spectrum of compound **12**. ^{1}H NMR spectra shows the presence of peaks at δ 4.44(t) and δ 4.47 (t) for substituted ferrocenyl proton, peaks at δ 4.82 (t) and δ 5.45 (t) corresponds to substituted cymantrenyl protons and at δ 6.43 and δ 7.57 for the four olefinic protons. ^{13}C NMR spectrum of **12** shows the presence of six peaks in the range δ 70.76 - 93.42 corresponding to the susbstituted Cp's attached to iron and manganese centers. Peaks at δ 118.6 and δ 144.43 revealed the presence of olefinic carbon while, peak at δ 185.31 is due to the ketonic groups. UV–visible absorption spectrum for **11** was studied in dichloromethane solvent and shows absorption peaks at 321 nm, a shoulder near 384 nm and a broad band with λ_{max} in the region 502 and UV-Visible spectrum for **12** shows absorption peaks at 304 nm, 334 nm, 374 nm and a broad band at 505 nm region (Figure 4.5).

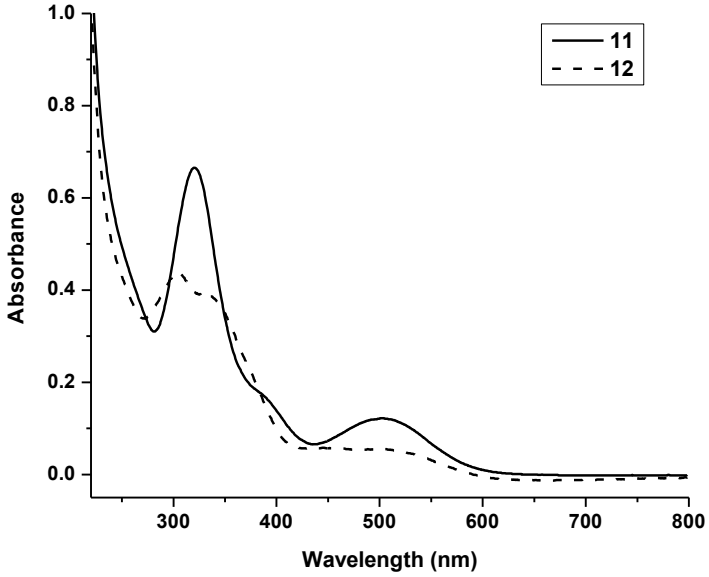

Figure 4.5. UV-Visible spectra of **11** and **12**

4.3.1. Molecular structure of 11

Single crystal X-ray diffraction study has been carried out for [$(CO)_3Mn(\eta^5$-$C_5H_4)C(O)CH=CH(\eta^5$-$C_5H_4)Fe(\eta^5$-$C_5H_5)$] (**11**) with single crystal, grown from dichloromethane/n-hexane solvent mixture at -10 ºC. Compound **11** crystallizes in orthogonal space group *P n a 21* with one formula unit in the unit cell. Molecular structure of **11** shows a ferrocenyl Cp ring bridged to the cymantrenyl Cp ring via three carbon α, β-unsaturated chain unit (Figure 4.6). Three terminal metal carbonyl groups with Mn-C-O bond angles in the range 178.9º -177.5º are attached to the manganese center satisfying the 18 - electron count. The C(6)-C(5) bond distance is 1.331(5) Å revealing a double bond character and the ketonic C═O bond distance was found to be 1.220(5) Å. The torsional angle for H-C5-C4-O4 and H-C6-C5-H are 171.3º and 178º respectively which confirm an E-isomer. The two Cp rings in the ferrocenyl fragment are at a torsional angle of 7º and the average bond distance for the ferrocenyl metal – carbon bond is 2.045 Å. The structural analysis also reveals that the iron and the manganese fragments are oriented trans- to each other with respect to the enone chain representing an anti-conformation. This conformation is unlike to that of recently reported ferrocenyl-cyrhetrenyl chalcone having a syn conformation of the two metal based fragments [6a]. In the solid structure**,** the assembly of the molecule shows an interesting alternate arrangement because of C–O(4)···H(Cp) interactions in the range 2.386 – 2.646 Å as shown in Figure 4.7.

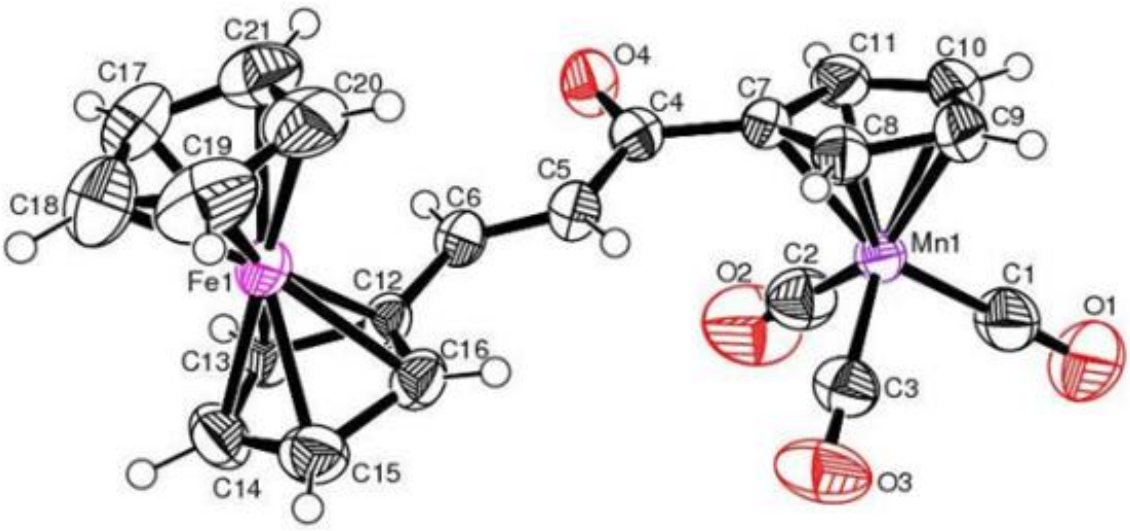

Figure 4.6. Molecular structure of **11.** Selected bond lengths (Å) and bond angles (º): C(5)-C(6) = 1.331(5), O(4)-C(4) = 1.220(5), O(1)-C(1) = 1.143(5), C(4)-C(7) = 1.492(5), C(5)-C(4)-C(7) = 117.2(4), C(6)-C(5)-C(4) = 121.7(4).

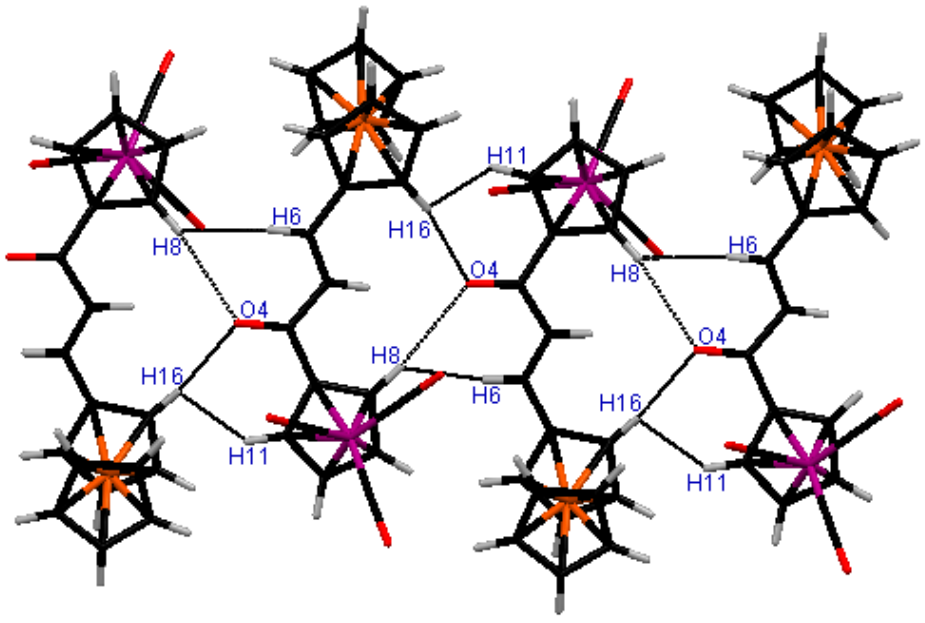

Figure 4.7. Molecular assembly of **11**.

The presence of three terminal carbonyl groups attached to manganese atom prompted us to study the reactivity features of **11** and **12** by phosphine substitution. We anticipated that the presence of enone chain linked to the cp ring may be able to stabilize the THF solvated adduct, $[(thf)(CO)_2Mn(\eta^5\text{-}C_5H_4)R]$ which can then react with phosphine to get the desired product. Therefore, we carried out photochemical reaction, under UV light, of compound **11** with triphenylphosphine in THF solvent. After the UV irradiation the reaction was continued at room temperature to obtain the phosphine substituted compound, $[(CO)_2(PPh_3)Mn(\eta^5\text{-}C_5H_4)COCH{=}CH(\eta^5\text{-}C_5H_4)Fe(\eta^5\text{-}C_5H_5)]$ (**13**) (Scheme 4.2). Compound **13** was characterized by IR, NMR and mass spectroscopy. Infrared spectrum shows bands at 1936 cm^{-1} and 1874 cm^{-1} corresponding to terminal metal carbonyls and the peak pattern exactly matches with that of cymantrenyl compounds with mono carbonyl substitution [31]. A band corresponding to ketonic C=O group for enone moiety has also been detected. Proton NMR of **13** revealed the presence of substituted and unsubstituted cyclopentadienyl ring for ferrocenyl and cymantrenyl fragments. Two doublets due to olefinic protons (δ 6.63 and δ 7.7) and a multiplet equivalent to 15 protons at δ7.40 – δ7.45 region have been obtained for the presence of triphenylphosphine group attached to manganese. ^{31}P NMR showed one peak at δ 89.77 for the only phosphorus present in the molecule. A molecular ion peak at m/z 677 has also been obtained by mass spectral analysis of compound **13**.

4.3.2. Molecular structure of 13

Single crystal X-ray diffraction study has been carried out for $[PPh_3(CO)_2Mn(\eta^5\text{-}C_5H_4)C(O)CH{=}CH(\eta^5\text{-}C_5H_4)Fe(\eta^5\text{-}C_5H_5)]$ (**13**) with the single crystal, grown from chloroform/n-hexane solvent mixture at -10 ºC. Compound **13** crystallizes in triclinic space group P-1 with one formula unit in the unit cell. The asymmetric unit consists of one molecule of **3** and a chloroform solvent molecule. The molecular structure of **13** reveals the presence of a ferrocenyl fragment and a cymantrenyl moiety bridged by an enone unit and the manganese atom is attached to one cp ring by η^5 type of linkage, two terminal carbonyl groups and one triphenylphosphine ligand (Figure 4.8). The bond

distance between manganese and phosphorus atom is 2.24 Å while the two Mn-CO bond distances are 1.78 Å. The Mn-C-O bond angles are in the range of 178.32º -179.83º representing the presence of terminally bonded metal carbonyls. The torsional angle between the two Cp rings of the ferrocenyl fragment is at an angle of 11º, slightly greater than that in **11**. The metal carbonyl bond distance, C(1)-O(1) = 1.153(1) Å has also been found to be longer than that in the parent compound **11** (1.143(5) Å) as expected for a phosphine substituted derivative. The structural analysis of **13** reveals that the two metallic fragments are oriented in syn-conformation with respect to the {CpC(O)CH=CHCp} moiety. The syn-conformation observed in **13** is exactly opposite to that observed for compound **11**.

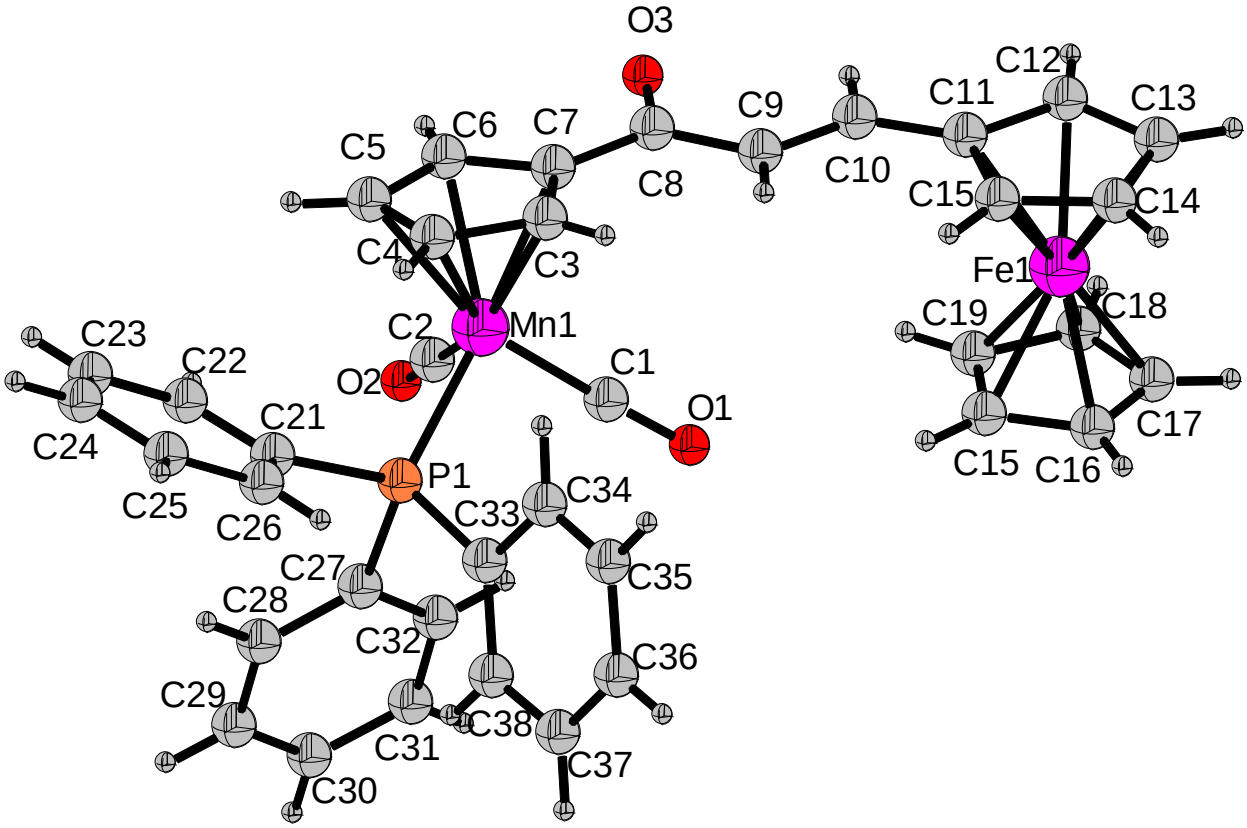

Figure 4.8. Molecular structure of **13 (**Solvent molecules have been deleted for clarity). Selected bond lengths (Å) and bond angles (º): C(9)-C(10) = 1.332(1), O(1)-C(1) = 1.153(1), Mn(1)-P(1) = 2.243(1), O(3)-C(8) = 1.228(0); C(8)-C(9)-C(10) = 122.08(0), O(3)-C(8)-C(9) = 122.28(0), Mn(1)-C(1)-O(1) = 178.32(0).

To understand the reactivity of **11** with diphosphines, we chose bis-(diphenylphosphino ferrocene), due to its better coordinating ability and expecting formation of some new multiferrocenyl derivative. Photochemical reaction under UV light of compound **11** with bis-(diphenylphosphino ferrocene) in toluene/THF solution led to the formation of a major orange compound, [{(η^5-C_5H_5)Fe(η^5-C_5H_4)CH=CHCO(η^5-C_5H_4)Mn(CO)$_2$PPh$_2$(η^5-C_5H_4)Fe(η^5-C_5H_4)PPh$_2$] (**14**) and a minor product, [{(η^5-C_5H_5)Fe(η^5-C_5H_4)CH=CHCO(η^5-C_5H_4)Mn(CO)$_2$PPh$_2$(η^5-C_5H_4)}$_2$Fe] (**15**) (Scheme 4.2). The poor yield of compound **15** could not be improved after several attempts by changing various reaction conditions. Both the compounds have been characterized by IR, ^{1}H NMR, ^{31}P NMR and mass spectroscopy. Infrared spectra of **14** and **15** show peaks corresponding to ketonic group at 1648-1649 cm^{-1} and terminal metal carbonyls at 1934-1935 cm^{-1} and 1872-1876 cm^{-1} region respectively. The pattern of the metal carbonyl peaks in the infrared spectra for both **14** and **15** are similar to that obtained for mono-substituted cymantrenyl derivatives [28] and that of compound **13**. The strong peak at 2024 cm^{-1} observed in **11** is absent in the IR spectra of compounds **14** and **15**, while a new peak at around 1872 cm^{-1} arises due to the substitution of one carbonyl group from the cymantrenyl fragment.

Proton NMR of **14** reveals the presence of unsubstituted ferrocenyl Cp ring at δ 4.22 (singlet) and another eight peaks, each equivalent to two protons, have been obtained corresponding to substituted Cp protons. Olefinic protons are obtained as doublets at δ 6.62 and δ 7.72 region and twenty phenylic protons showed multiplet at δ 7.22-7.37 region. ^{31}P NMR of **14** confirms the presence of two types of phosphorus in the molecule: a metal coordinated phosphine showed a peak at δ 82.66 and uncoordinated phosphorus was obtained at δ -17.62 region. Mass spectral analysis reveals the presence of peak at m/z 969 corresponding to [M+H]$^+$ ion of the compound.

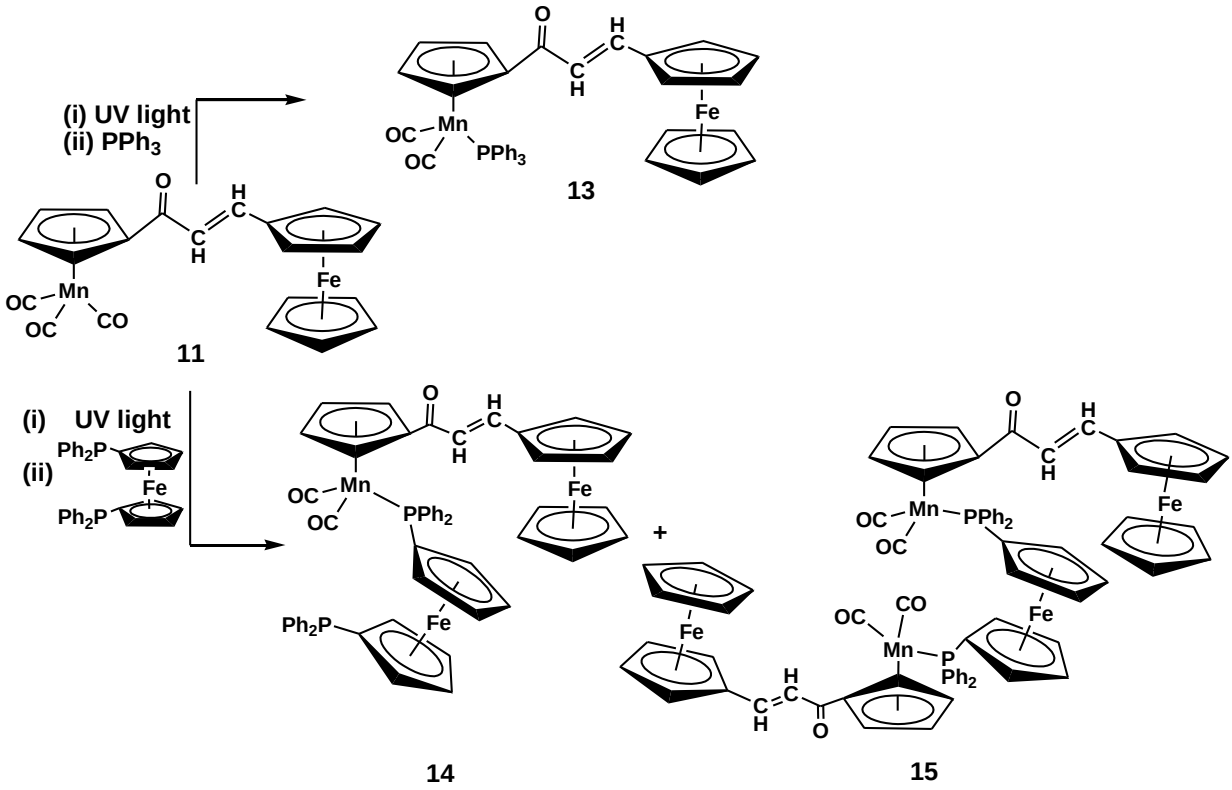

Scheme 4.2

In spite of low yield of compound **15**, we have been able to characterize by IR, NMR and mass spectroscopy. ^{1}H NMR spectra showed unsubstituted ferrocenyl Cp ring at δ 4.23 (singlet) equivalent to ten protons and six peaks was observed for substituted Cp protons, with each peak equivalent to four protons. The spectrum also exhibits two doublets and one multiplet corresponding to four olefinic and twenty phenylic protons respectively. Phosphorus NMR with a peak at δ 82.84 revealed the presence of only one type of metal coordinated phosphorus. Mass spectral analysis of **15** showed the presence of peak at m/z 1326 due to [M-2CO] ion.

Reaction under UV light condition with compound **12** and triphenylphosphine in presence of thf solvent gave an orange product, [{$(CO)_2(PPh_3)Mn(\eta^5$-$C_5H_4)COCH{=}CH(\eta^5$-$C_5H_4)\}_2Fe$] (**16**) (Scheme 4.3). Compound **16** was characterized by IR, NMR and mass spectral analysis. Infrared spectrum of **16** showed peaks corresponding to terminal metal carbonyls at 1948 and 1880 cm^{-1} region and ketonic

C=O at 1648 cm^{-1}. Proton NMR spectrum revealed the presence of substituted ferrocenyl Cp and substituted cymantrenyl cp protons at δ4.12, δ4.46, δ4.55 and δ5.22 region. Two doublets at δ6.55 and δ7.62 with a coupling constant value of 15 Hz revealed the presence of olefinic protons in the molecule, while 30 phenylic protons have been confirmed from a multiplet at δ7.39-7.46 region. One phosphorus peak at δ89.76 has been observed in ^{31}P NMR spectrum. This shows that the two phosphorus groups present in the molecule are equivalent. The ESI mass spectral data shows ion peak at m/z 1167 corresponding to the molecular ion of compound **16**.

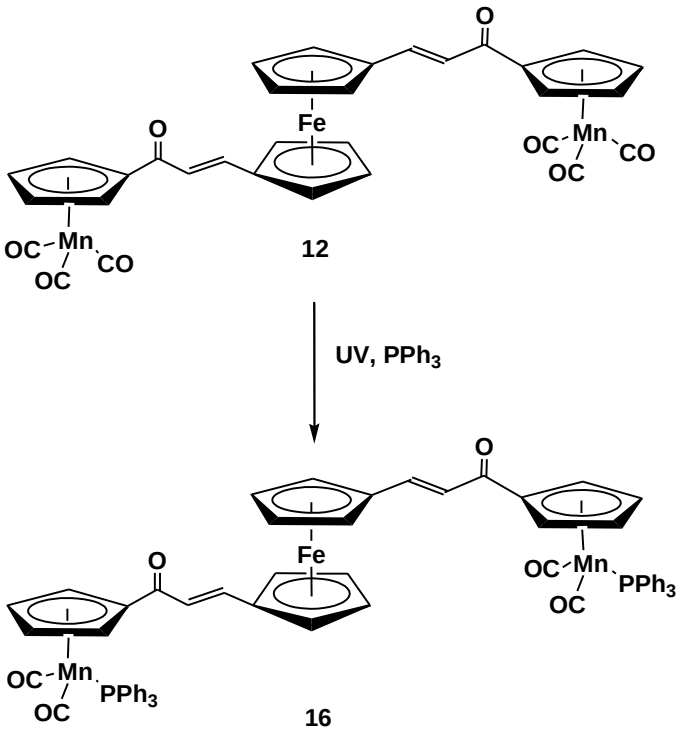

Scheme 4.3

4.3.3. Redox properties of 11 - 14

The electrochemical properties of compounds **11-14** have been examined in acetonitrile solution (0.1M TEAP) by cyclic-voltammetry. Compounds **11** and **12** showed one reversible response in the potential range 0.47-0.50 V involving single

electron Fe(II) / Fe(III) couple of the ferrocenyl fragment and an irreversible response at 1.35 V for **11** and 1.15 V for **12** corresponding to the oxidation of Mn(I) to Mn (II) when scanned in the positive potential side (Figure 4.9). The one-electron nature of Fe(II)/Fe(III) couple have been tentatively established by comparing its current height with that of the standard ferrocene/ferrocenium couple under the same experimental conditions. The much higher potential range at which the oxidative response has been observed for Mn(I)/Mn(II) couple is consistent with the $E_{1/2}$ values in the literature for $[MnCp(CO)_3]^{0/+}$ (0.92 V) [32], $[(Cp\text{-triazolyl})Mn(CO)_3]^{0/+}$ (+1.4 V) [33] and $[Mn(\eta^5\text{-}C_5H_4)CHO(CO)_3]^{0/+}$ (1.10 V) couple [34]. The oxidation at the higher potential range is presumed to decrease the Mn-C(O) bond strength due to the weakening of the metal to CO back bonding which eventually makes the oxidized species unstable and give rise to an irreversible response. The reversibility of the Mn center may be restored by CO-substitution, which will stabilize the oxidized species while lowering the oxidation potential. Compound **13,** triphenylphosphine substituted analogue of **11,** showed accordingly one reversible response at +0.52 V corresponding to ferrocene/ferrocenium couple and one quasi-reversible response at +0.70 V due to Mn(I)/Mn(II) couple (Figure 4.9 & Table 4.2). The oxidative response at higher potential corresponding to Mn(I)/Mn(II) has been shifted to lower potential value on phosphine substitution and showed quasi-reversible behavior as compared to that observed for compounds **11** and **12**. The presence of one phosphine ligand attached to the manganese center in **13** eases the oxidation process and increases the stability of the oxidized species resulting in observation of a quasi-reversible couple under the same experimental condition.

The cyclic voltammogram of **14** showed three responses (one reversible and two irreversible couple) corresponding to two ferrocenyl and one cymantrenyl fragments. The ferrocenyl fragment attached to phosphorus atom showed a reversible couple at +0.28V while the oxidative response of the ferrocenyl attached to enone moiety was observed at +0.57 V having slightly irreversible character. This is unlikely to that observed in compounds **11-13** in which all the three compounds showed reversible response in the range +0.52 - +0.47 V for the ferrocenyl part of the compounds. The Mn(I)/Mn(II) couple has been observed as irreversible response with the presence of only anodic peak at +0.86 V (Table 4.2).

Table 4.2. Cyclic voltammetric data for **11-14**.

Compounds	E_{pa}	E_{pc}	$E_{1/2}$ (ΔE_p (mV))
11	+0.54 V, +1.37 V	+0.46 V, +1.32 V	+0.5 V (80), +1.35 V (50)
12	+0.52 V, +1.25 V	+0.43 V, +1.04 V	+0.475 V (90), +1.145 V (210)
13	+0.55 V, +0.74 V	+0.49 V, +0.66 V	+0.52 V (60), +0.7 V (80)
14	+0.32 V, +0.59 V, +0.86 V	+0.23 V, +0.55 V	+0.28 V (90), +0.57 V (40)

*In acetonitrile at a scan rate of 50-200 mv s. E1/2 (V) = (Epa+Epc)/2, where Epa and Epc are the anodic and cathodic peak potentials Vs. Ag/AgCl respectively. ΔEp (mV) = Epa-Epc

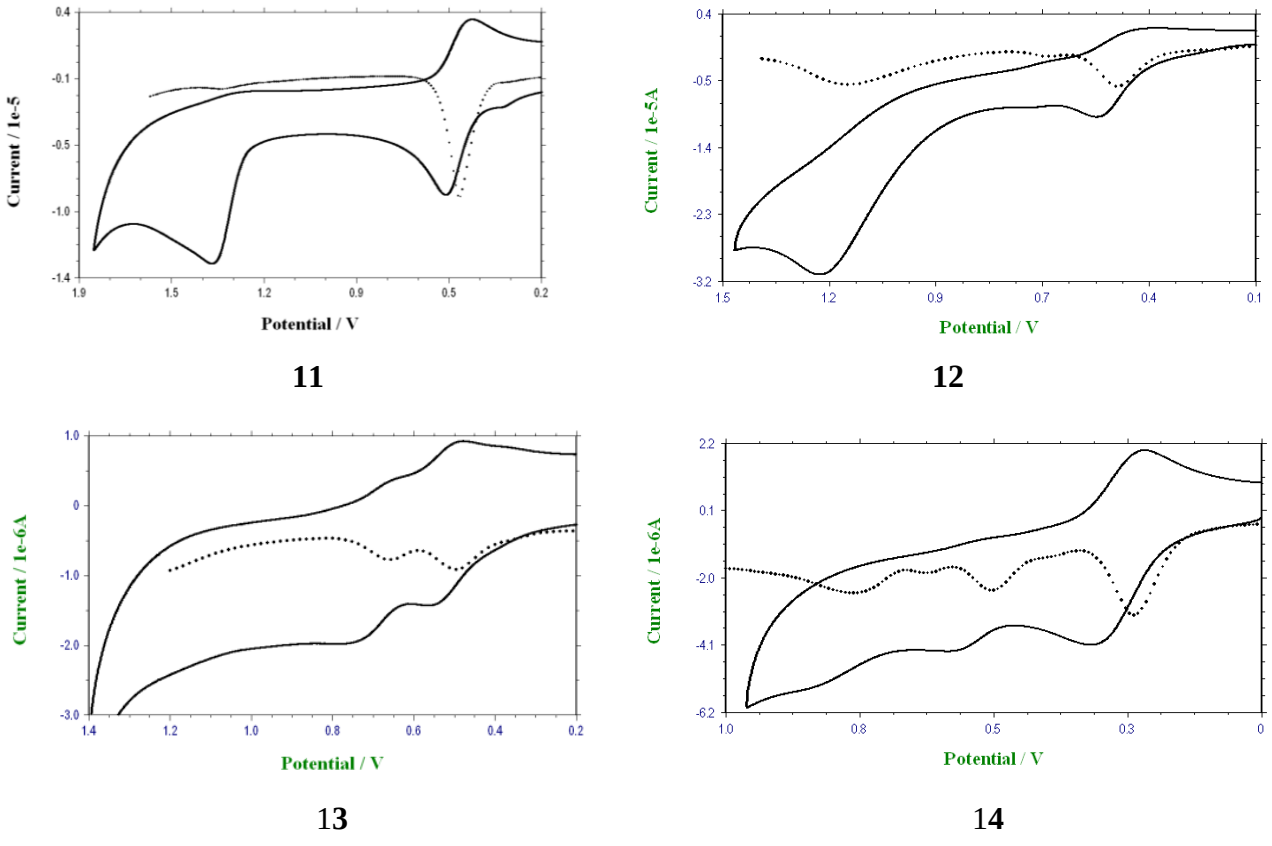

Figure 4.9. Cyclic voltammograms (—) and differential pulse voltammograms (…) of compound **11-14** in Acetonitrile / 0.1 M TEAP at 298 K vs Ferrocene / Ferrocenium couple.

4.3.4. Anti-malarial activity of 11 and 12

In order to understand the biological properties of bimetallic chalcones **11** and **12**, *in vitro* antimalarial activity was studied against chloroquine-susceptible 3D7 as well as chloroquine-resistant K1 strains of *P. falciparum*. IC_{50} values for the compounds are depicted in (Table 4.3). Both the compounds **11** and **12** studied exhibited moderate antimalarial activity against 3D7 as well as K1 strains of *P. falciparum*. The inhibition activities observed for compounds **11** and **12** (IC_{50} = 2.35 & 2.78 (3D7); 9.47 & 8.14 (K1)) are higher than that reported recently for different ferrocenyl chalcones, $[FcC_2H_2C(O)(\eta^5\text{-}C_5H_4)Re(CO)_3]$ (IC_{50} = 18.9 against 3D7), $[FcC(O)C_2H_2(\eta^5\text{-}C_5H_4)Re(CO)_3]$ (IC_{50} = 26.9 (3D7)) [6(a)], $[FcC(O)C_2H_2Ph]$ (IC_{50} = 19 (K1)), $[FcC(O)C_2H_2Ph\text{-}OH]$ (IC_{50} = 20.6 (K1)), $[FcC(O)C_2H_2Ph\text{-}OMe]$ (IC_{50} = 17 (K1)), $[FcC(O)C_2H_2(C_5H_4N)]$ (IC_{50} = 14 (K1)) and $[FcC_2H_2C(O)Ph\text{-}OH]$ (IC_{50} = 36 (K1)) [1(e)], whereas the IC_{50} value for **11** and **12** are comparable to $[FcC(O)C_2H_2Ph\text{-}NO_2]$ (IC_{50} = 5.1 (K1)) and $[FcC_2H_2C(O)\ (3\text{-}C_5H_4N)]$ (IC_{50} = 4.6 (K1)) [1(e)]. The higher activity of **11** and **12** reveals some influence of bimetallic ferrocenyl-cymantrenyl moieties on the antiplasmodial activity of the compounds. The presence of an extra cymantrenyl unit attached to ferrocenyl Cp ring via enone chain in compound **12** may not have much effect on the antiplasmodial activity, although a slight decrease in IC_{50} value was observed when tested against K1 strain. A plausible explanation for the moderate antimalarial activity of **11** and **13** is the presence of ferrocenyl and cymantrenyl moieties which may have influenced the redox properties, lipophilicity and structural orientation of the compounds.

Table 4.3. Antimalarial activity against 3D7 strain and K1 strain of *P. falciparum*

Compounds	IC_{50} (μM)	
	3D7 strain	K1 strain
11	2.35	9.47
12	2.78	8.14
Chloroquine	0.005	0.22

4.3.5. Anti-bacterial activity of 11and 12

Antibacterial study was carried out for compounds **11** and **12** against Gram positive *B. subtilis and Gram negative E. coli, K. pneumoniae, P. aeruginosa* bacterial strains. Both the compounds showed moderate inhibition activity against the bacterial strains as shown in Table 4.4. Compound **12** containing two enone units showed higher activity as compared to compound **11** against *B. subtilis and E. coli,* while compound **11** showed lower MIC value against *K. pneumoniae* strain. Our recent reports also showed high antibacterial activity of ferrocenyl hydrazone compounds and some Cp based half sandwich cymantrenyl hydrazone compounds revealing their potential as medicinal agent [18]. Other half sandwich organometallic compounds showing potential antibacterial properties include $[(\eta^6\text{-}C_6Me_5)Cr(CO)_3]$ incorporated platensimycin derivative and $[(\eta^6$-p-cymene)RuCl(ofloxacin)] [35-37]. Significant antibacterial activity for the reported organometallic compounds could possibly be due to the presence of both ferrocenyl and $[(\eta^5\text{-}C_5H_5)Mn]$ fragments which are supposed to play a vital role in increasing the cell permeability and lipophilicity of the compounds. Different other factors like electron delocalization and blocking of metal binding sites of the enzyme of microorganism may also result in better inhibition activity in metal containing compounds. The MIC data reported in Table 4.4 for multimetallic Cp based compounds will be important to understand the biological potential of these types of compounds.

Table 4.4. Minimum inhibitory concentration (MIC) value in μg/ml

Compounds	*B. subtilis*	*E. coli*	*K. pneumoniae*	*P. aeruginosa*
11	125	N	62.5	250
12	62.5	62.5	N	N
Chloramphenicol	4	4	31.25	31.25

N – Inhibitory activity not observed

4.3.6. DFT calculation of 11

Molecular Geometry Optimization

DFT calculation was carried out for compound **11** using single crystal x-ray diffraction data coordinates for the geometry optimization without any constrain. The DFT optimized molecular structure at B3LYP level and using LanL2DZ basis set has been shown in Figure 4.10. The data reveals that the average bond length for Fe-C(cp) (2.077Å), C=C (1.348 Å) and Mn-C(cp) (2.184 Å) are found to be well correlated with that of experimentally (XRD) obtained data. Calculated C=O and C≡O bond lengths were also found to be matching excellently; 1.225 (exp. 1.219 Å) and 1.148 (exp. 1.147 Å). In general all the optimized bond angles agree well within 1˚ when compared with crystal structure data.

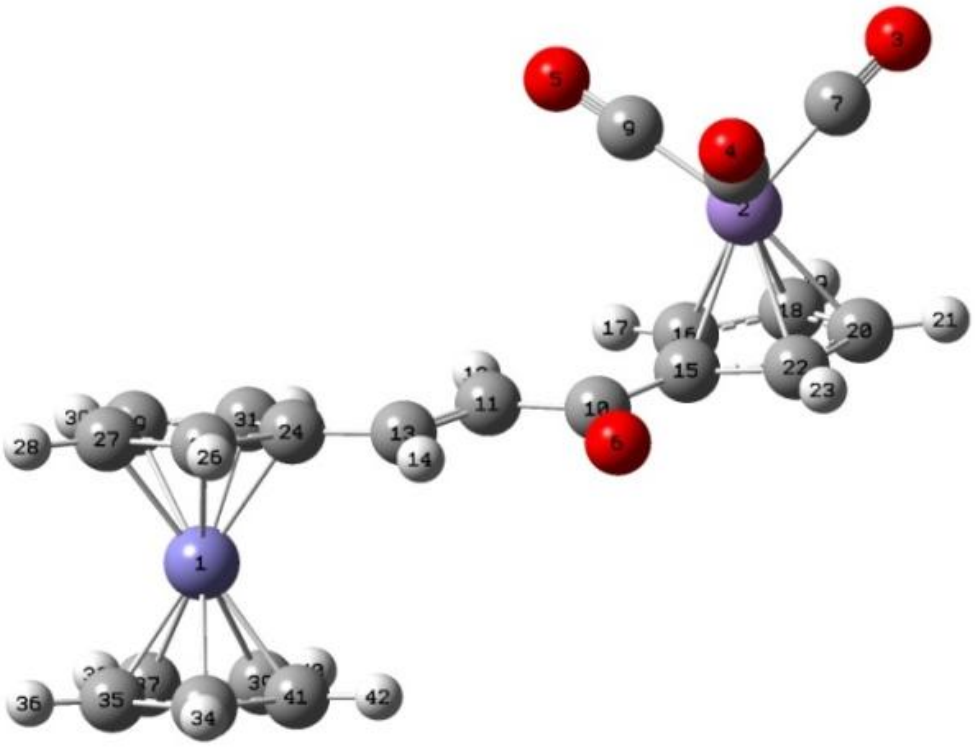

Figure 4.10. DFT optimized molecular structure of **11**

4.3.7. TD-DFT calculation and Correlation with electronic transitions

Absorption spectrum of **11** consists of mainly three bands. The strongest band for the complex in absorption spectrum appears in the region 270-350 nm. A small hump appears at 370-420 nm regions and a broad peak appears at 450-600 nm region. In order to get deeper understandings of transitions occurring in the compound, TD-DFT calculation has been performed. The calculated oscillator strengths, energies and transitions between moleculera orbitals are tabulated in Table 4.4. The assignment of the calculated electronic transitions to the experimental absorption bands was based on an overview of the contour plots and relative energy of highest occupied (HOMO) and lowest unoccupied (LUMO) molecular orbital involved in the electronic transitions (Figure 4.11). Electronic transition at 546 nm corresponds to HOMO-1 to LUMO+ 4 molecular orbital (MO), which may be assigned to a charge transfer transition from iron-

centered orbital to π* (Cp of Fe and $d_{x^2-y^2}$ of Fe atom). Transition at 346 nm corresponds to HOMO to LUMO transition, which may be assigned to charge transfer from π (Cp of Fe and CH-C=O) to π*(Cp of Mn and d_{z^2} of Mn atom). Transition occurring at 332 nm is due to HOMO-2 to LUMO i.e π (Cp of Fe and CH-C=O) to π*(Cp of Mn and C=O). The corresponding calculated oscillator strength represented very well the experimental absorption intensities of various bands. Highest energy band (304nm) corresponds to HOMO to LUMO+2, representing transition from π (Cp of Fe) to π* (Cp of Mn and C≡O) i.e ligand to ligand charge transfer transition (LLCT). The molecular orbitals also show the electronic communication as a result of conjugation between the two metallic fragments linked via an enone moiety. The complete transition phenomenon in UV-Vis region has been represented pictorially with calculated frontier molecular orbital diagram in Figure 4.11.

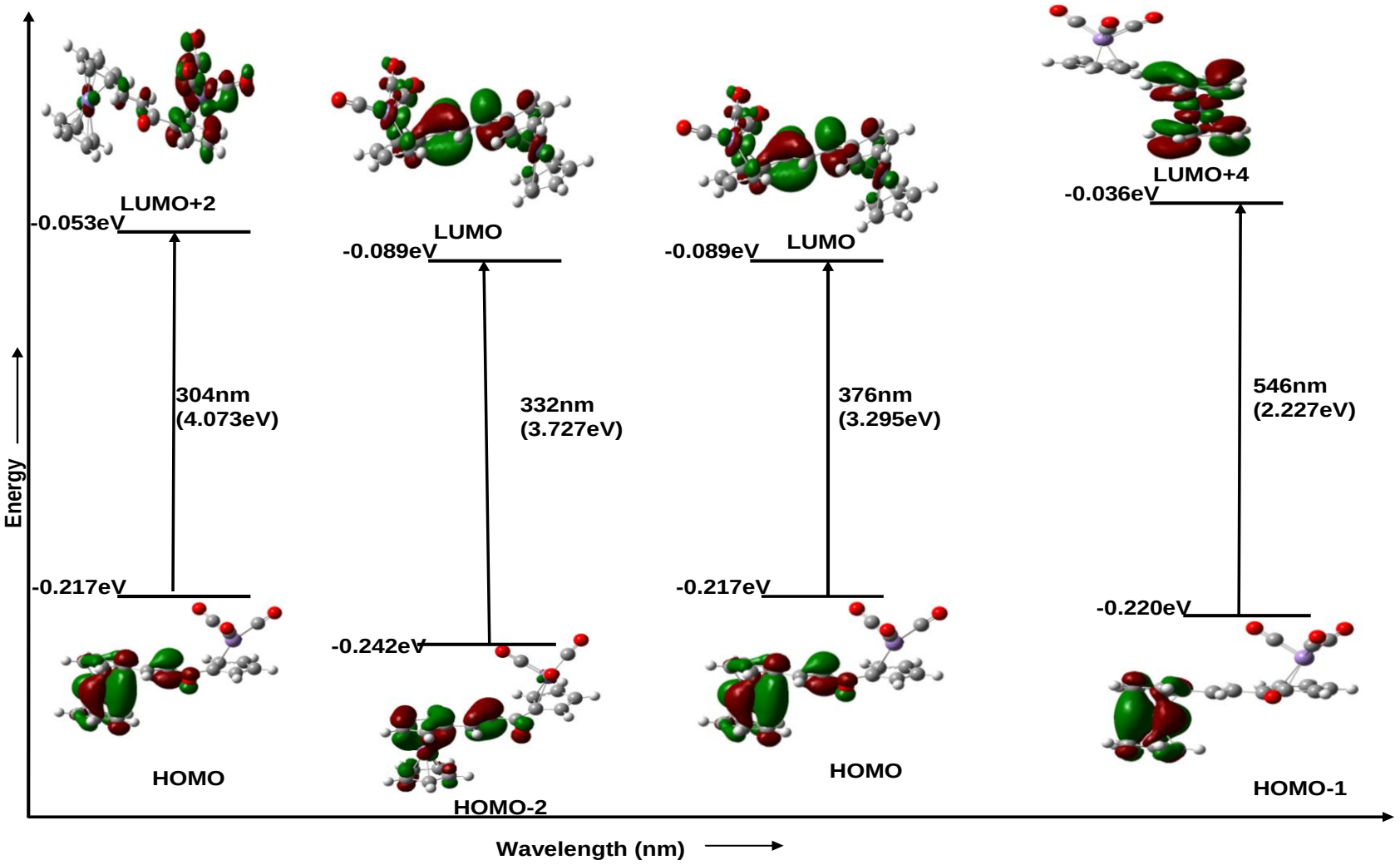

Figure 4.11. Selected molecular orbitals of **11**

Table 4.5. Calculated oscillator strength and their corresponding energies for selected transition of compound **11** using TD-DFT method.

Wavelength (nm)	Oscillator strength	Energy (eV)	Transitions between MOs
546	0.0049	2.2272	HOMO-1 →LUMO+4
423	0.0210	2.9254	HOMO-1 → LUMO
387	0.0279	3.2009	HOMO-1 → LUMO
376	0.0762	3.2946	HOMO → LUMO
332	0.3413	3.7267	HOMO-2 → LUMO
304	0.0790	4.0732	HOMO→ LUMO+2
288	0.0113	4.2914	HOMO-4 → LUMO+3
276	0.0223	4.4762	HOMO-10 → LUMO
267	0.0559	4.6310	HOMO-2 → LUMO+2
264	0.0050	4.6844	HOMO-4 → LUMO+6
256	0.0295	4.8383	HOMO-2 → LUMO+5
253	0.0157	4.8999	HOMO-11 → LUMO
251	0.0051	4.9218	HOMO→ LUMO+6

In summary, synthesis of new ferrocenyl-cymantrenyl bimetallic chalcones have been carried out and their reactivity study with triphenylphosphine and 1,1'-ferrocenyl diphosphine results in the formation of respective phosphine derivatives of the bimetallic chalcones. Structural characterizations of two bimetallic chalcones, **11** and **13** have been carried out. Compound **11** shows anti conformation of the metallic fragments while, the

PPh_3 substituted bimetallic chalcone (**13**) confirms syn conformation, in which the two metallic moieties are on the same side with respect to the enone chain. Antimalarial and antibacterial evaluation on compounds **11** and **12** reveal their moderate inhibition activity. Efforts may be focused to increase the bioactivity by incorporating heterocyclic moieties and understanding the structure –activity relationship on these types of compounds.

4.4. References

[1] (a) G. Nabi, Z. Q. Liu, Med. Chem. Res. 21 (2012) 3015; (b) X. Wu, P. Wilairat, M. L. Go, Bioorg. Med. Chem. Lett. 12 (2002) 2299; (c) K. Kumar, S. Carrère-Kremer, L. Kremer, Y. Guérardel, C. Biot, V. Kumar, Organometallics 32 (2013) 5713; (d) S. Attar, Z. O'Brien, H. Alhadad, M. L. Golden, A. Calderon-Urrea, Bioorg. Med. Chem. 19 (2011) 2055; (e) X. Wu, E. Tiekink, I. Kostetski, N. Kocherginsky, A. L. C. Tan, S. B. Khoo, P. Wilairat, M.-L. Go, Eur. J. Pharm. Sci. 27 (2006) 175; (f) V. Zsoldos-Mády, A. Csampai, R. Szado, E. Meszaros-Alapi, J. Pasztor, F. Hudecz, P. Sohár, Chem. Med. Chem. 1 (2006) 1119.

[2] (a) Z. L. Gong, Y. S. Xie, B. X. Zaho, H. S. Lv, W. Y. Liu, L. W. Zheng, S. Lian, J. Fluoresc. 21 (2011) 355; (b) C. K. Kumar, R. Trivedi, K. R. Kumar, L. Giribabu, B. Sridhar, J. Organomet. Chem. 718 (2012) 64; (c) V. Zsoldos-Mády, O. Ozohanics, A. Csámpai, V. Kudar, D. Frigyes, P. Sohár, J. Organomet. Chem. 694 (2009) 4185; (d) W. Y. Liu, Y.-S. Xie, B.-X. Zhao, B.-S. Wang, H.-S. Lv, Z.-L. Gong, S. Lian, L.-W. Zheng, J. Photochem. Photobio A: Chem. 214 (2010) 135.

[3] (a) N. J. Lawerence, R. P. Patterson, L.-L. Ooi, D. Cook, S. Ducki, Bioorg. Med. Chem. Lett. 16 (2006) 5844; (b) S. J. Won, C. T. Liu, L. T. Tsao, J. R. Weng, H. H. Ko, J. P. Wang, C. N. Lin, Eur. J. Med. Chem. 40 (2005) 103; (c) S. Vogel, S. Ohmayer, G. Brunner, J. Heilmann, Bioorg. Med. Chem. 16 (2008) 4286; (d) C.-T. Hsieh, T.-J. Hsieh, M. El-Shazly, D.-W. Chuang, Y.-H. Tsai, C.-T. Yen. S.-F. Wu, Y.-C. Wu, F.-R. Chang, Bioorg. Med. Chem. Lett. 22 (2012) 3912.

[4] (a) R. Prasath, P. Bhavana, S.W. Ng, E. R. T. Tiekink, J. Organomet. Chem. 726 (2011) 62; (b) Y. J. Jung, K.-I. Son, Y. E. Oh, D.-Y. Noh, Polyhedron, 27 (2008) 861; (c) T. J. Muller, J. Conradie, E. Erasmus, Polyhedron 33 (2012) 257; (d) W. Suh, H. Jeon, J.-Y. Lee, C.-M. Lim, S.-K. Lee, D.-Y. Noh, Bull. Korean Chem. Soc. 33 (2012) 443.

[5] (a) A. Patti, S. Pedotti, Tetrahedron Assymmetry 19 (2008) 1891; (b) A. Tárraga, P. Molina, J. L. López, Tetrahedron letters 41 (2000) 2479; (c) G. Nabi, Z.-Q. Liu, Biorg. Med. Chem. Let. 21 (2011) 944; (d) W. Suh, H. Jeon, J.-Y. Lee, C.-M. Lim, S.-K. Lee, D.-Y. Noh, Bull. Korean Chem. Soc. 33 (2012) 443; (e) B. Delavaux-Nicot, J. Maynadié, D. Lavabre, S. Fery-Forgues, Inorg. Chem. 45 (2006) 5691; (f) T. Lovász, G. Túrós, L. Găină, A. Csámpai, D. Frigyes, B. Fábian, I. A. Silberg, P. Sohar, J. Mol. Struc. 751 (

2005) 100; (g) W.-Y. Liu, Q.-H. Xu, B.-H. Chen, Y.-M. Liang, Y.-X. Ma, W.-M. Liu, J. Organomet. Chem. 637-639 (2001) 782; (h) S.-K. Lee, Y.-S. Noh, K.-I Son, D.-Y. Noh, Inorg. Chem. Commun. 13 (2010) 1343.

[6] (a) E. Erasmurs, Inorg. Chim. Acta 378 (2011) 95; (b) F. O. Ogini, Y. Ortin, A. H. Mahmoudkhani, A. F. Cozzolino, M. J. McGlinchey, I. Vargas-Baca, J. Organomet. Chem. 693 (2008) 1957.

[7] (a) M. F. R. Fouda, M. M. Abd-Elzaher, R. A. Abdelsamaia, A. A. Labib, Appl. Organomet. Chem. 21 (2007) 613; (b) M. Patra, G. Gasser, Chembiochem 13 (2012) 1232; (c) G. Gasser, N. Metzler-Nolte, Curr. Opin. Chem. Biol. 16 (2012) 84; (d) D. R. V. Staveren, N. Metzler-Nolte, Chem. Rev. 104 (2004) 5931.

[8] (a) E. Meggers, G. E. Atilla-Gokcumen, H. Bregman, J. Maksimoska, S. P. Mulcahy, N. Pagano, D. S. Williams, Synlett (2007) 1177; (b) H. Bregman, D. S. Williams, G. E. Atilla, P. J. Carroll, E. Meggers, J. Am. Chem. Soc. 126 (2004) 13594; (c) Y. Liu, B. Spingler, P. Schmutz, R. Alberto, J. Am. Chem. Soc. 130 (2008) 1554; (d) C. Policar, J. B. Waern, M.-A. Plamont, S. Clède, C. Mayet, R. Prazeres, J.-M. Ortega, A. Vessières, A. Dazzi, Angew. Chem. Int. Ed. 50 (2011) 860.

[9] (a) G. Jaouen, A. Vessières, I. S. Butler, Acc. Chem. Res. 26 (1993) 361; (b) C. G. Hartinger, N. Metzler-Nolte, P. J. Dyson, Organometallics 31 (2012) 5677 (c) C. G. Hartinger, P. J. Dyson, Chem. Soc. Rev. 38 (2009) 391; (d) R. H. Fish, G. Jaouen, Organometallics 22 (2003) 2166; (e) M. Navarro, W. Castro, C. Biot, Organometallics 31 (2012) 5715.

[10] (a) O. Payen, S. Top, A. Vessières, E. Brulé, A. Lauzier, M.-A. Plamont, M. J. McGlinchey, H. Müller-Bunz, G. Jaouen, J. Organomet. Chem. 696 (2011) 1049; (b) M. Patra, G. Gasser, N. Metzler-Nolte, Dalton Trans. (2012) 6350; (c) A. R. Pike, L. C. Ryder, B. R. Horrocks, W. Clegg, M. R. J. Elsegood, B. A. Connolly, A. Houlton, Chem. Eur. J. 8 (2002) 2891; (d) M. Patra, G. Gasser, M. Wenzel, K. Merz, J. E. Bandow, N. Metzler-Nolte, Organometallics 29 (2010) 4312; (e) B. Maity, B. V. S. K. Chakravarthi, M. Roy, A. A. Karande, A. R. Chakravarty, Eur. J. Inorg. Chem. (2011) 1379.

[11] (a) H. W. P. N'Dongo, I. Neundorf, K. Merz, U. Schatzschneider, J. Inorg. Biochem. 102 (2008) 2114; (b) D. S. Williams, G. E. Atilla, H. Bregman, A. Arzoumanian, P. S.

Klein, E. Meggers, Angew. Chem. Int. Ed. 44 (2005) 1984; (c) I. Rémy, P. Brossier, I. Lavastre, J. Besançon, C. Moise, J. Pharm. Biomed. Anal. 9 (1991) 965.

[12] (a) S. Top, A. Vessières, C. Cabestaing, I. Laios, G. Leclercq, C. Provot, G. Jaouen, J. Organomet. Chem. 637–639 (2001) 500; (b) A. Nguyen, A. Vessières, E. A. Hillard, S. Top, P. Pigeon, G. Jaouen, Chimia 61 (2007) 716; (c) E. A. Hillard, P. Pigeon, A. Vessieres, C. Amatore, G. Jaouen, Dalton Trans. (2007) 5073; (d) E. A. Hillard, A. Vessières, L. Thouin, G. Jaouen, C. Amatore, Angew. Chem. Int. Ed. 45 (2006) 285.

[13] (a) V. Tirkey, S. Mishra, H. R. Dash, S. Das, B. P. Nayak, S. M. Mobin, S. Chatterjee, J. Organomet. Chem. 732 (2013) 122; (b) S. K. Patel, V. Tirkey, S. Mishra, H. R. Dash, S. Das, M. Shukla, S. Saha, S. M. Mobin, S. Chatterjee, J. Organomet. Chem. 749 (2013) 75.

[14] D. Astruc, Acc. Chem. Res. 30 (1997) 383.

[15] P. A. Etcheverry, D. O'Hare, Chem. Rev. 110 (2010) 4839.

[16] R. Sakamoto, M. Murata, H. Nishihara, Angew. Chem., Int. Ed. 45 (2006) 4793.

[17] (a) Y. Zhu, M. O. Wolf, J. Am. Chem. Soc. 122 (2000) 10121; (b) S. R. Marder, J. W. Perry, B. G. Tiemann, Organometallics 10 (1991) 1896.

[18] (a) J. S. Miller, A. J. Epstein, Angew. Chem. Int. Ed. 33 (1994) 385; (b) B. Delavaux-Nicot, R. Mathieu, D. Montauzon, G. Lavigne, J. P. Majoral, Inorg. Chem. 33 (1994) 434.

[19] J. Kozikowski, R. E. Maginn, M. S. Klove, J. Am. Chem. Soc. 81 (1959) 2995.

[20] U. T. Mueller-Westerhoff, Z. Yang, G. Ingram, J. Organomet. Chem. 463 (1993) 163.

[21] G. M. Sheldrick, A short history of SHELX, Acta Cryst. A 64 (2008) 112.

[22] A. D. Becke, J. Chem. Phys. 98 (1993) 5648.

[23] A. Lee, W. Yang, R. G. Parr, Phys. Rev. B 37 (1988) 785.

[24] A. Ghosh, I. Halvorsen, H. J. Nilsen, E. Steene, T. Wondimagegn, R. Lie, E. Caemelbecke, N. Guo, Z. Ou, K. M. Kadish, Phys. Chem. B 105 (2001) 8120.

[25] Clinical and Laboratory Standards Institute (CLSI, 2006). Methods for Dilution Antimicrobial Susceptibility Tests for Bacteria That Grow Aerobically, Seventh ed. 2006 Approved Standard M7-A7, CLSI, Wayne, PA, USA.

[26] K. Srivastava, S. K. Puri, Exptl. Parasitology 108 (2004) 74.

[27] S. Singh, R. K. Srivastava, M. Srivastava, S. K. Puri, K. Srivastava, Exptl. Parasitol. 127 (2011) 318.

[28] (a) B. H. G. Swennenhuis, R. Poland, W. Y. Fan, D. J. Darensbourg, A. A. Bengali, Inorg. Chem. 49 (2010) 7597; (b) S. E. Lyubimov, V. A. Davankov, N. M. Loim, L. N. Popova, P. V. Petrovskii, P. M. Valetskii, K. N. Gavrilov, J. Organomet. Chem. 691 (2006) 5980.

[29] W. E. Geiger, Coord. Chem. Rev. 257 (2013) 1459.

[30] D. P. Day, T. Dann, D. L. Hughes, V. S. Oganesyan, D. Steverding, G. G. Wildgoose, Organometallics 33 (2014) 4687.

[31] K. Wu, D. R. Laws, A. Nafady, W. E. Geiger, J. Inorg. Organomet. Polym. 24 (2014) 137.

[32] M. Patra, G. Gasser, A. Pinto, K. Merz, I. Ott, J. E. Bandow, N. Metzler-Nolte, Chem. Med. Chem. 4 (2009) 1930.

[33] M. Patra, G. Gasser, M. Wenzel, K. Merz, J. E. Bandow, N. Metzler-Nolte, Organometallics 31 (2012) 5760.

[34] I. Turel, J. Kljun, F. Perdih, E. Morozova, V. Bakulev, N. Kasyanenko, J. A. W. Byl, N. Osheroff, Inorg. Chem. 49 (2010) 10750.

[35] M. Roemer, P. Schmiel, D. Lentz, Organometallics 30 (2011) 2063.

[36] R. Arancibia , C. Biot, G. Delaney, P. Roussel, A. Pascual, B. Pradines, A. H. Klahn, J. Organomet. Chem. 723 (2013) 143.

[37] M. Wenzel,. M. Patra, C. H. R. Senges, I. Ott, J. J. Stepanek, A. Pinto, P. Prochnow, C. Vuong, S. Langklotz, N. Metzler-Nolte, J. E. Bandow, ACS Chem. Biol. 8 (2013) 1442.

Chapter 5

Synthesis of diferrocenyl hydrazone-enone receptor molecule: Biological evaluation, electronic communication and metal binding study

5.1. Introduction

Efficient energy transfer between redox active centers is one of the interesting aspects for organometallic compounds due to their potential in the development of molecular electronic devices.[1] Among a range of redox active species, ferrocenyl system plays a vital role as a remarkable redox signaling unit in various organometallic molecules or scaffold. In recent times, a large number of ferrocene based organometallic molecular entities have been synthesized for their application as chemosensors, energy storage devices, multichannel receptor, biosensor molecules etc.[2-5] Compounds containing multiple redox centers have also been highly focused due to their various application related to electronic communication, sensors and molecular wires.[6] Therefore, design of novel ferrocenyl assemblies with substituent at the cyclopentadienyl ring have attracted considerable interest and led to the development of variety of such derivatives. Molecular system containing more than one ferrocene units shows interesting electron transfer processes when the metal centers are no longer independent of each other and are said to be electronically coupled through suitable bridging chains. The interesting part associated with the design is in the fact that the ferrocene/ferrocenium redox couple can be tuned significantly by the judicious choice of substituents on the rings of the ferrocene moiety and led to the emergence of a large variety of ferrocene based functional compounds using concise synthetic routes. Recently, functionalization of ferrocene has attracted the synthetic community to obtain a range of ferrocene based molecular systems with unique electronic properties and structural variety.[7] Functionalization in the form of mono-substituted and 1,1' symmetrically disubstituted ferrocenyl derivatives are well known and has been extensively studied, while, unsymmetrical 1,1'-disubstituted ferrocenyl derivatives are comparatively less known. The later systems have the ability to show improved multifunctional behavior and redox properties.[8,11]

A disubstituted ferrocene-derived triazoles, 1,1′-Bis[(4-ferrocenyl)-1H-1,2,3-triazol-1-yl]ferrocene and 1,1′-Bis{[4-(phenanthren-9-yl)]-1H-1,3,4-triazol-1-yl}ferrocene, have been prepared from diazidoferrocene using the copper-catalyzed click reaction and have been characterized by spectroscopic analysis (Figure 5.1).[9]

Investigation of the electrochemical behavior of the triferrocenyl triazole compound by cyclic voltammetry with two reversible one electron couple at 544 mV and 953 mV revealed the dependency of ferrocene based oxidation potential on the position of triazole group. Both the triazol based ferrocenyl compounds have been found to act as receptor molecules and showed selective binding interaction with anions as well as cations. A cathodic shift of the receptors by the addition of F^-, AcO^-, $H_2PO_4^-$ and $HP_2O_7^{3-}$ anions and an anodic shift of 1,1′-Bis[(4-ferrocenyl)-1H-1,2,3-triazol-1-yl]ferrocene by the addition of Zn^{2+}, Hg^{2+} and Pb^{+2} with $\Delta E_{1/2}$ = +22mV to +76 mV and that of 1,1′-Bis{[4-(phenanthren-9-yl)]-1H-1,3,4-triazol-1-yl}ferrocene by Hg^{2+} cation have been investigated by cyclic voltammetry.

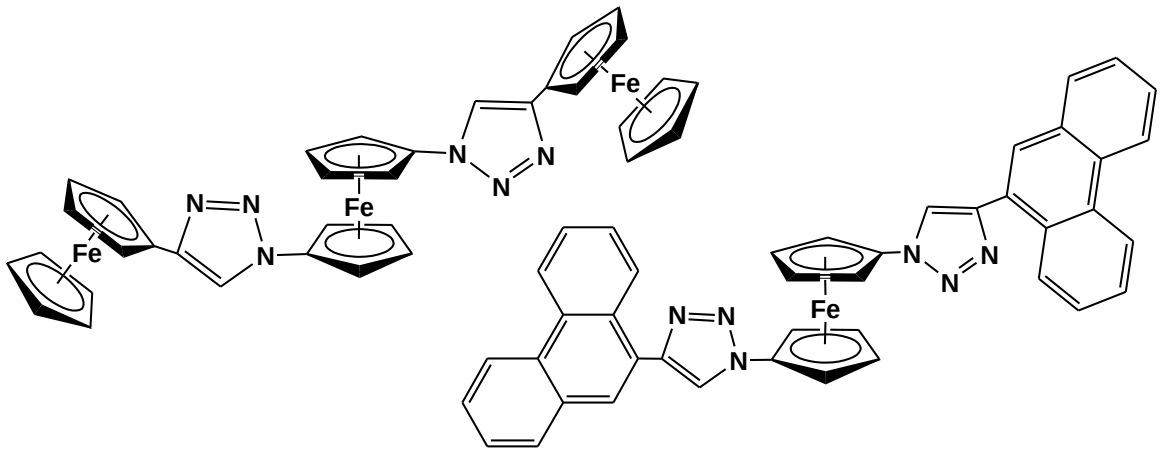

Figure 5.1. Ferrocen-triazole derivatives

Recently, a novel synthetic strategy has been applied for the synthesis of ferrocenyliminophosphorane compound starting from ferrocene through lithiation, click reaction and Staudinger reaction which further undergoes aza-Witting type of coupling reaction with various aldehydes to give the corresponding unsymmetrical diferrocenyl triazole derivative, 1,1'-[Ar-CH=N(η^5-C_5H_4)Fe{(η^5-C_5H_4)(NN=NC=CH)(η^5-C_5H_4)Fe(η^5-C_5H_5)], {Ar = pyrene, quinoline, fluorene} (Figure 5.2).[10] Cyclic voltammetry of the diferrocenyl triazole compound showed two redox couple due to the presence of two ferrocene units positioned in different environment. The lower oxidation potential ($E_{1/2}$ =0.03-0.05V) was for the mono substituted ferrocene and the higher

oxidation potential ($E_{1/2}$ =0.24-0.31V) has been attributed to the di-substituted ferrocenyl fragment. The compound also act as receptor molecule showing distinct shift of the potentials due to the gradual addition of Pb^{+2} and Zn^{+2} metal cations. The metal recognition properties of the ferrocenyl receptors with Ni^{2+}, Cd^{2+}, Zn^{2+} and Pb^{2+} cations have also been confirmed by the blue-shift, red shift or change in intensities of the energy bands in the UV-Visible spectroscopy. DFT calculations revealed that the binding of the receptor with the metal ions take place through imine group of the receptor and the N atom of the quinoline ring with feeble interaction of the triazole unit.

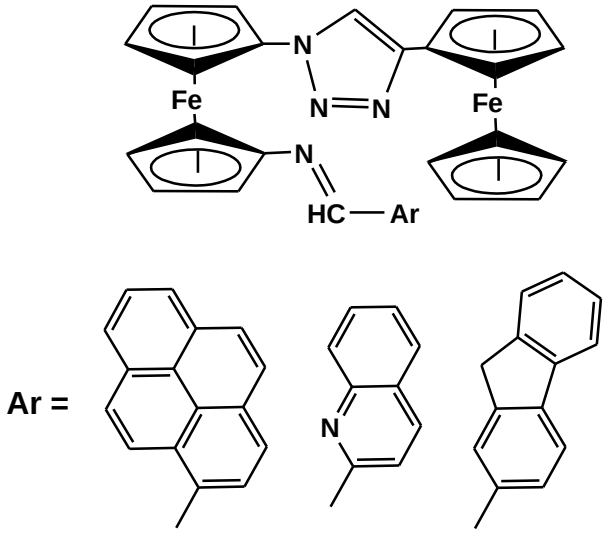

Figure 5.2. Unsymmetrical diferrocenyl triazole

An unsymmetrically substituted ferrocenyl ditopic receptor containing a urea and a benzo crown ether unit has been synthesized by the reaction of ferrocenyl monoaldehyde with N-methyl piperazine, n-BuLi and tri-n-butylborate followed by a Suzuki coupling reaction with 4-bromobenzo-18-crown-6 and subsequent addition of ammonium acetate and 4-nitrophenylisocyanate (Scheme 5.1).[11] The absorption maxima in UV-Visible spectroscopy associated with the free receptor at 304 nm and 332

nm has been shifted to 288 nm and 356 nm along with the appearance of a new absorption peak at 472 nm by the addition of F^- anion. The addition of anoin also shows naked eye colour change of the solution in visible region from colourless to yellow. This chromogenic process was reversed by the addition of K^+ cation with the disappearance of the peak in the visible region at 472 nm and colour change of the solution from yellow to colourless. The ferrocenyl ditopic receptor acts as a chromogenic molecular sensor due to its switching on and off function induced by the addition of anion and cation.

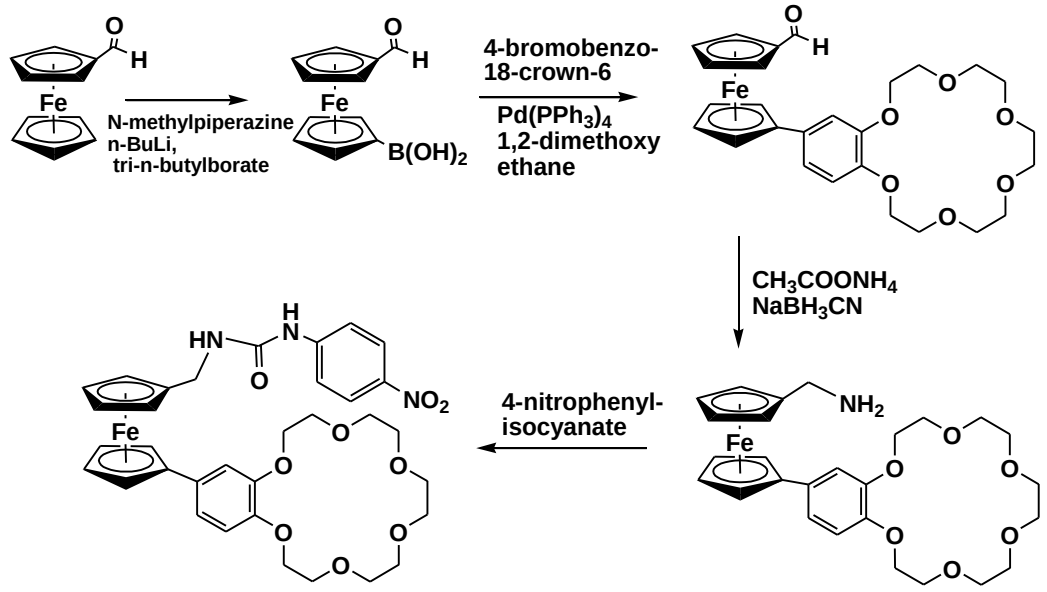

Scheme 5.1

Diferrocenyl molecular systems have been well known to participate in electronic coupling between the ferrocene fragments and play a vital role in the development of intervalence properties in several organometallic compounds. A multistep reaction involving iodo ferrocene, 2,6-dichlorobenzoyl chloride, N-hydroxybenztriazole and amino ferrocene produced a diferrocenyl amide derivative, $[(\eta^5\text{-}C_5H_5)Fe\{(\eta^5\text{-}C_5H_4)NHC(O)\}(\eta^5\text{-}C_5H_5)Fe\{(\eta^5\text{-}C_5H_4)NHC(O)CH_3\}]$. Thionation of the diferrocenyl

amide with Lawesson's reagent gave a diferrocenyl thioamide derivative, [(η^5-C_5H_5)Fe{(η^5-C_5H_4)NHC(S)}(η^5-C_5H_5)Fe{(η^5-C_5H_4)NHC(O)CH_3}] (Scheme 5.2). The structure of the compound, revealed by spectroscopic analysis, shows the presence of unsymmetrically substituted diferrocenyl system, in which the two ferrocenyl moieties are linked together by thioamide bridge. The shifting of absoption band in UV-Visible spectrum of the diferrocenyl thioamide compound to lower energy (λ_{max}= 480 nm) than that of the corresponding diferrocenyl amide (λ_{max}=446 nm) confirms some intervalence charge-transfer character of the compound. In addition, the potential shift in diferrocenyl thioamide towards higher potential region of the first oxidation potential due to Fe (II)/ Fe(III) couple in comparison to the corresponding amides indicates the influence of O to S substitution on the electronic properties of the compound. DFT analysis showed intramolecular hydrogen bonding of diferrocenyl thioamide derivative and both inter and intramolecular hydrogen bonding for the oxidized species.

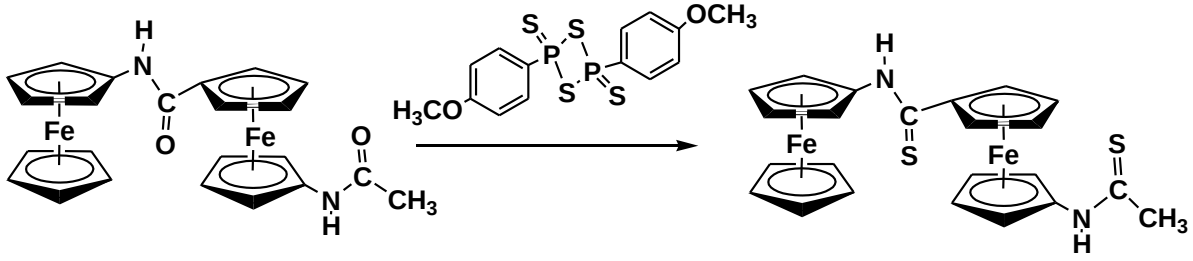

Scheme 5.2

Reaction of 1-bromo-1′-formylferrocene with trimethoxymethane, methylbenzene-sulfonic acid followed by palladium catalysed Negishi cross-coupling with 2,5-dibromothiophene or 2,5-dibromo-3,4-ethylenedioxy thiophene gave the corresponding diformyldiferrocenyl thiophene derivatives [CHO(η^5-C_5H_4)}Fe{(η^5-C_5H_4)(C_4H_2S)(η^5-C_5H_4)}Fe{(η^5-C_5H_4)CHO}] and [CHO(η^5-C_5H_4)}Fe{(η^5-C_5H_4)(3,4-$(OCH_2)_2C_4H_2S$)(η^5-C_5H_4)}Fe{(η^5-C_5H_4)CHO}] (Figure 5.3). One of the diformyldiferrocenyl thiophene has been characterized by single crystal X-ray diffraction study showing parallel orientation of ferrocenyl units with respect to the thiophene core. Electrochemical analysis by cyclic voltammetry showed two reversible one electron

redox couple for both the diformyl diferrocenyl thiophene derivatives. The introduction of electron donating ethylenedioxy unit at the thiophene ring of diformyldiferrocenyl thiophene derivative has been found to increase the electronic coupling between the ferrocenyl groups.

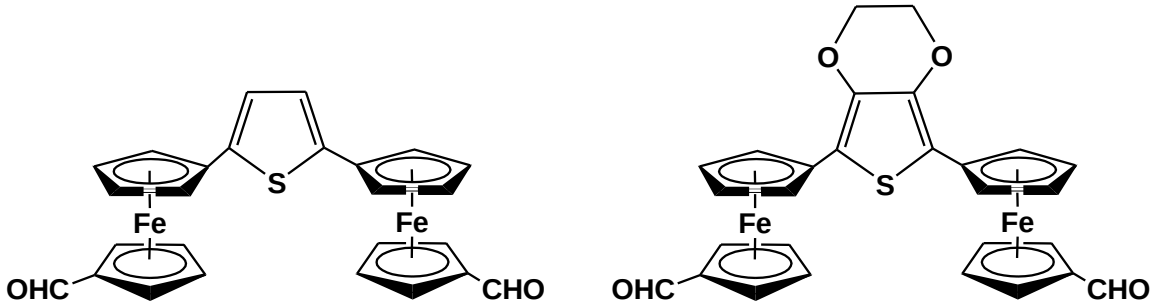

Figure 5.3. Formyl ferrocenyl thiophene derivatives

Recently, functionalization of ferrocene with biologically active groups and their study on different biological properties have led to the immergence of a new field of bio-organometallic chemistry.[14-15] We have been focusing our study on a variety of ferrocene based molecular systems ranging from ferrocenyl hydrazones, hetero-bimetallic ferrocenyl chalcones, ferrocene based cluster compounds, ferrocenyl dithiocarboxylates and multiferrocenyl compounds and reported their synthesis and biological properties.[16] In view of the emerging potential of unsymmetrically functionalized ferrocenyl moieties, we selected to introduce both hydrazone and enone functionality on the same ferrocenyl fragment, anticipating a change in property and unique structural behavior in contrast to either ferrocenyl hydrazone or ferrocenyl chalcone compounds. It has been well understood that hydrazones and chalcones independently constitute a large class of important molecules which show a number of interesting features related to coordination behavior and biological properties and are significant molecules as precursors to several heterocyclic compounds.[17, 18]

In this chapter, we describe the synthesis of a novel diferrocenyl bifunctional molecular system containing hydrazone and enone units using simple and systematic synthetic route. To the best of our knowledge, unsymmetrical difunctionalization of ferrocenyl moiety with hydrazone and enone groups are not known in the literature.

Further to our notice, diferrocenyl systems with two different functional chains are less known and rarely attempted for study. We have been able to synthesize four analogs of the diferrocenyl hydrazone-enone derivatives with different aromatic end groups and describe their unique structural identity and selective metal ion sensing properties. We also report here the antibacterial and BSA binding properties of some of the compounds and carried out cyclic-voltammetric studies to understand electronic communication inside the molecule. DFT calculation was also performed to establish some of the interesting features related to structural stability, metal ion interaction and molecular orbital energies.

5.2. Experimental Sections

5.2.1. General Procedures

All reactions and manipulations were carried out under an inert atmosphere of dry, pre-purified argon using standard Schlenk line techniques. Solvents were purified, dried and distilled under argon atmosphere prior to use. Infrared spectra were recorded on a Perkin Elmer Spectrum Two FTIR spectrometer as CH_2Cl_2 solution and NMR spectra on a 400 MHz Bruker spectrometer in $CDCl_3$ or d_6-DMSO solvent. Elemental analyses were performed on a Vario El Cube analyzer. Mass spectra were obtained on a SQ-300 MS instrument operating in ESI mode. Cyclic voltammetric and differential pulse voltammetric measurements were carried out using a CH Instruments model 600D electrochemistry system. A platinum working electrode, a platinum wire auxiliary electrode and a calomel reference electrode were used in a three–electrode configuration. The supporting electrolyte was 0.1 M $[NBu_4]ClO_4$ and the solute concentration was ~10^{-4} M. The scan rate used was 50 mV s^{-1}. All electrochemical experiments were carried out under a nitrogen atmosphere and are uncorrected for junction potentials. UV-vis spectra were recorded in ethanol solutions at 10^{-5} M concentration. TLC plates (20x20 cm, Silica gel 60 F254) were purchased from Merck. Appropriate salts of Na^+, K^+, Mg^{2+}, Ba^{2+}, Mn^{2+}, Fe^{2+}, Co^{2+}, Cu^{2+}, Zn^{2+}, Cd^{2+}, Ni^{2+}, Hg^{2+} and Pb^{2+} were purchased from Aldrich.

$[Fe(\eta^5\text{-}C_5H_4COCH_3)_2]$, $[(\eta^5\text{-}C_5H_5)Fe(\eta^5\text{-}C_5H_4CHO)]$, $[H_2NN(H)C(O)R]$, (R = $-C_6H_4$-OH, C_6H_4N-p, C_6H_5, C_6H_4N-m) were prepared following reported procedures.[19-21]

5.2.2. Synthesis of $[(\eta^5\text{-}C_5H_5)Fe\{(\eta^5\text{-}C_5H_4)CH{=}CHC(O)(\eta^5\text{-}C_5H_4)\}Fe\{(\eta^5\text{-}C_5H_4)C(CH_3){=}NN(H)C(O)R\}]$ (17 - 20)

In a two neck round bottom flask ethanol solution (10 ml) of compound **5** - **8** (0.1 mmol) was taken and ferrocenyl carboxyaldehyde (21 mg; 0.1 mmol) was added. The reaction mixture was stirred for 15 minutes under inert atmosphere and sodium hydroxide (0.2 mmol) solution was added dropwise and the stirring was continued for 5 hours at room temperature. The reaction mixture was then kept under vacuum for 15 minutes to increase the amount of the product. The reaction was continuously monitored using TLC. After the reaction, the solution was vacuum dried and the mixture was subjected to chromatographic work up using preparative TLC (10% ethanol:n-hexane solvent mixture). Chromatographic elution afforded the unreacted ferrocenyl carboxyaldehyde, a violet colored compound 1,1'-$[(\eta^5\text{-}C_5H_5)Fe(\eta^5\text{-}C_5H_4)CH{=}CHC(O)(\eta^5\text{-}C_5H_4)Fe\{(\eta^5\text{-}C_5H_4)C(CH_3){=}N\text{-}N(H)C(O)\text{-}R\}]$ {R = C_6H_5 (**17**), C_6H_4-OH (**18**), C_6H_4N-p (**19**), C_6H_4N-m (**20**)} and trace amount of the unreacted compound, $[CH_3C(O)(\eta^5\text{-}C_5H_4)Fe\{(\eta^5\text{-}C_5H_4)C(CH_3){=}N\text{-}N(H)C(O)\text{-}R\}]$ in the order of elution. {Yields: **17**, 45 mg (78 %); **18**: 48 mg (80%); **19**: 44 mg (74 %); **20**: 46 mg (78 %)}

17: IR(ν_{CO}, cm^{-1} , CH_2Cl_2): 1671 (s), 1650 (vs), 1602 (m), 1581(s). ^{1}H NMR (δ, d_6-DMSO): 2.25 (s, 3H, CH_3), 4.18 (s, 5H, η^5-C_5H_5), 4.42 (t, 2H, η^5-C_5H_4), 4.45 (t, 2H, η^5-C_5H_4), 4.69 (t, 2H, η^5-C_5H_4), 4.71 (t, 2H, η^5-C_5H_4), 4.79 (t, 2H, η^5-C_5H_4), 4.98 (t, 2H, η^5-C_5H_4), 6.97 (d, J = 15.6 Hz, 1H, CH=CH), 7.53 (d, J = 15.2 Hz, 1H, CH=CH), 7.59-7.93 (m, 5H, C_6H_5), 10.72 (s, 1H, NH). MS (ESI): m/z 585 [M+H].

18: Anal. calcd. (found): C, 64.03 (64.27); H, 4.70 (4.82); N, 4.67 (4.57). IR(ν_{CO}, cm^{-1}, CH_2Cl_2): 3052 (br), 1663 (s), 1647 (vs), 1603 (m), 1585(s). ^1H NMR (δ, $CDCl_3$): 2.2 (s, 3H, CH_3), 4.15 (s, 5H, η^5-C_5H_5), 4.36 (t, 2H, η^5-C_5H_4), 4.45 (t, 2H, η^5-C_5H_4), 4.48 (t, 2H, η^5-C_5H_4), 4.59 (t, 2H, η^5-C_5H_4), 4.86 (t, 2H, η^5-C_5H_4), 4.96 (t, 2H, η^5-C_5H_4), 6.69 (d, J = 15 Hz, 1H, CH═CH), 6.89-7.45 (m, 4H, C_6H_4), 7.65 (d, J = 15 Hz, 1H, CH═CH), 12.03 (s, 1H, OH). MS (ESI): m/z 601 [M+H].

19: Anal. calcd. (found): C, 63.62 (63.79); H, 4.65 (4.57); N, 7.18 (7.26). IR(ν_{CO}, cm^{-1}, CH_2Cl_2): 1666 (s), 1647 (vs), 1588(s, br), 1576(s). ^1H NMR (δ, d_6-DMSO): 2.24 (s, 3H, CH_3), 4.18 (s, 5H, η^5-C_5H_5), 4.42 (t, 2H, η^5-C_5H_4), 4.46 (t, 2H, η^5-C_5H_4), 4.72 (t, 2H, η^5-C_5H_4), 4.73 (t, 2H, η^5-C_5H_4), 4.78 (t, 2H, η^5-C_5H_4), 4.97 (t, 2H, η^5-C_5H_4), 6.95 (d, J = 15 Hz, 1H, CH═CH), 7.53 (d, J = 15 Hz, 1H, CH═CH), 7.80 (m, 2H, C_5H_4N), 8.78 (m, 2H, C_5H_4N), 10.98 (s, 1H, NH). MS (ESI): m/z 586 [M+H].

20: IR(ν_{CO}, cm^{-1}, CH_2Cl_2): 1667 (s), 1650 (vs), 1588(s, br), 1575(s). ^1H NMR (δ, d_6-DMSO): 2.26 (s, 3H, CH_3), 4.18 (s, 5H, η^5-C_5H_5), 4.42 (t, 2H, η^5-C_5H_4), 4.46 (t, 2H, η^5-C_5H_4), 4.69 (t, 2H, η^5-C_5H_4), 4.72 (t, 2H, η^5-C_5H_4), 4.79 (t, 2H, η^5-C_5H_4), 4.98 (t, 2H, η^5-C_5H_4), 6.96 (d, J = 15 Hz, 1H, CH═CH), 7.53 (d, J = 15 Hz, 1H, CH═CH), 7.56 (m, 1H, C_5H_4N), 8.23 (m, 1H, C_5H_4N), 8.78 (m, 1H, C_5H_4N), 9.07 (m, 1H, C_5H_4N), 10.90 (s, 1H, NH). MS (ESI): m/z 585 [M].

5.2.3. Crystal structure determination for 18 and 19

Single crystal X-ray structural studies of **18** and **19** were performed on a CCD Oxford Diffraction XCALIBUR-S diffractometer equipped with an Oxford Instruments low-temperature attachment. Data were collected at 150(2) K using graphite-monochromated Mo Kα radiation (λ_α = 0.71073 Å). The strategy for the data collection was evaluated by using the CrysAlisPro CCD software. The data were collected by the standard phi-omega scan techniques, and were scaled and reduced using CrysAlisPro RED software. The structures were solved by direct methods using SHELXS-97 and

refined by full matrix least-squares with SHELXL-97, refining on F^2 [22]. The positions of all the atoms were obtained by direct methods. All non-hydrogen atoms were refined anisotropically. The remaining hydrogen atoms were placed in geometrically constrained positions and refined with isotropic temperature factors, generally $1.2U_{eq}$ of their parent atoms. The crystallographic details are summarized in Table 5.1. (CCDC Numbers, **18**: 1476350, **19**: 1476349)

Table 5.1. Crystal data and structure refinement parameters for compounds **18** and **19.**

	18	**19**
Empirical formula	C_{32} H_{28} Fe_2 N_2 O_3	C_{31} H_{27} Fe_2 N_3 O_2
Formula weight	600.27	585.26
Crystal system	Orthorhombic	Orthorhombic
Space group	P 21 21 21	P 21 21 21
a, Å	10.7753(7)	10.4527(8)
b, Å	10.8504(8)	22.8217(13)
c, Å	22.4237(15)	10.6484(7)
α deg	90	90
β deg	90	90
γ deg	90	90
V, Å^3	2621.7(3)	2540.2(3)
Z	4	4
Dcalcd, Mg m^{-3}	1.523	1.530
abs coeff, mm^{-1}	1.145	1.177
F(000)	1244	1208
Cryst size, mm	0.33 x 0.26 x 0.21	0.33 x 0.26 x 0.21
θ range, deg	3.23 to 25.00 deg.	3.26 to 25.00
index ranges	$-12 \le h \le 12$, $-12 \le k \le 12$, $-26 \le l \le 26$	$-12 \le h \le 12$, $-23 \le k \le 27$, $-12 \le l \le 10$

reflections collected/ unique	20041 / 4615 [R(int) = 0.1010]	19106 / 4456 [R(int) = 0.1157]
data/ restraints / parameters	4615 / 0 / 358	4456 / 0 / 345
goodness-of-fit on F^2	1.076	0.930
Final R indices [I>2σ(I)]	R1 = 0.0648, wR2 = 0.1493	R1 = 0.0543, wR2 = 0.1127
R indices (all data)	R1 = 0.0879, wR2 = 0.1651	R1 = 0.0861, wR2 = 0.1345
largest diff peak and hole, $eÅ^{-3}$	1.110 -0.409	0.542 -0.467

5.2.4. Antibacterial activity

Compounds **17 - 20** were screened for their antibacterial activity in vitro following the protocol described elsewhere [23]. The antibacterial effect was assayed against both Gram positive bacteria *Bacillus subtilis* and Gram negative bacteria *Escherichia coli* and *Pseudomonas aeruginosa* by the agar well diffusion method [23]. The compounds were dissolved in DMSO at different concentrations ranging from 250 to 7.8125 μg/ml. Mueller Hinton-agar (containing 1% peptone, 0.6% yeast extract, 0.5% beef extract and 0.5% NaCl, at pH 6.9–7.1) plates were prepared and 0.5 – McFarland culture (1.5 X 10^8 cells/ml) of the test organisms were swabbed onto the agar plate. 9mm wells were made in the LB agar petri dishes. 100μl of each of the compound with decreasing concentrations was added to separate wells. DMSO was used as the negative control and *Chloramphenicol* was used as positive control. The plates were incubated at 37°C and observed for zones of inhibition around each well after 24 hours. The results were compared with the activity of *Chloramphenicol* at identical concentrations. The MIC, defined as the lowest concentration of the test compound, which inhibits the visible growth, was determined visually after incubation for 24 h at 37ºC.

5.2.5. BSA binding experiment

BSA protein binding study was performed by tryptophan fluorescence quenching experiments using a BSA stock solution of 0.01M phosphate buffer of pH 7.2. The fluorescence titrations were performed at the fixed BSA concentration (5×10^{-5} M). In the fluorescence quenching experiment, quenching of the tryptophan residues of BSA was done by keeping the concentration of the BSA constant while increasing the compound (quencher) concentration from 0 to 50 μM. The fluorescence spectra were recorded at an excitation wavelength of 290 nm and an emission wavelength of 334 nm after each addition of the compound. The excitation and emission slit widths and scan rates were maintained constant for all of the experiments.

5.2.6. Computational details

Geometry optimization of compounds **18** and **19** and their staggered conformers were carried out by using density functional theory (DFT) at B3LYP level of theory using 6-31G (d,p) (for C, N, H and O) and SDD (for Fe) basis sets.[24,25] In addition to optimization, frequency calculation, Time-Dependent Density functional Theory (TD-DFT) calculations were done at the same level of calculation and using the same basis sets. The absence of imaginary vibrational frequencies in calculated vibrational spectrum ensures the presence of a true minimum in the potential energy surface. The spectroscopic and electronic property of these complexes has been computed by time dependent DFT (TD-DFT) calculation [26] at the same B3LYP level in gaseous phase. The nature and the role of the electronic excitation contributions are rationalized in terms of frontier molecular orbitals (FMO).

5.3. Results and Discussion

Our interest to synthesize multi-ferrocenyl system with diverse functionalization directed us to exploit compounds **5-8** for further reaction at the pendant acetyl group

attached to the ferrocenyl unit. As per strategy, compounds **5-8** was condensed with ferrocenyl carboxyaldehyde at room temperature in presence of sodium hydroxide to obtain a violet colored compound 1,1'-[(η^5-C_5H_5)Fe(η^5-C_5H_4)CH═CHC(O)(η^5-C_5H_4)Fe{(η^5-C_5H_4)C(CH_3)═N-N(H)C(O)-R}] {R = C_6H_5 (**17**), C_6H_4-OH (**18**), C_6H_4N-p (**19**), C_6H_4N-m (**20**)}. Compounds **17-20** was isolated and purified by preparative TLC using n-hexane-ethanol solvent mixture and characterized using IR, NMR and mass spectral analysis. The infrared spectral data for **17** and **18** show bands corresponding to ketonic and C=N units at 1671, 1663, 1650, 1647, 1603 and 1602 cm^{-1} region. ^1H NMR spectra reveals the presence of CH_3 protons at δ 2.2 and unsubstituted ferrocenyl Cp peaks have been observed at δ 4.18 and δ 4.15 region, while peaks at δ 4.36 – δ 4.98 confirm the presence of protons attached to the substituted ferrocenyl Cp rings. Phenyl and olefinic protons have been observed at δ 6.89 - δ 7.93 (multiplet) and δ 6.69 - δ 7.65 (doublets) regions respectively. A broad peak at δ 12.03 shows the presence of OH proton in **18** and a peak at 10.72 in compound **17** has been attributed to NH proton. Mass spectral analysis showed $[M+1]^+$ peak at 585 and 601 region for **19** and **18** respectively.

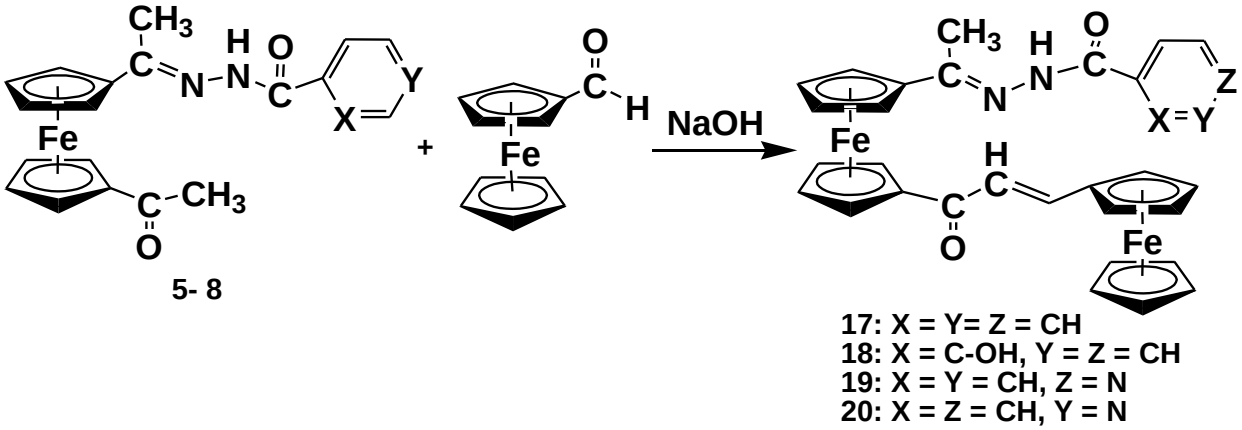

Scheme 5.3

Compounds **19** and **20** also showed IR bands at 1666 (s), 1667 (s), 1647 (vs), 1650 (vs) and 1580 (vs, br) region due to C=O, C=C and C=N functionalities. ^{1}H NMR for each of the compounds show the presence of a singlet (equivalent to 5H) at δ 4.18 due to unsubstituted Cp protons and six triplets at δ 4.42-4.98 due to the presence of substituted Cp protons, while methyl peak has been observed at δ 2.24 and δ 2.26 region. Pyridine ring protons have been observed as multiplet in the region δ 7.56 - δ 9.07 and doublets at δ 6.95 and δ 7.53 reveals the presence of olefinic protons. NH protons have been observed at δ 10.98 and δ 10.90 positions for compounds **19** and **20** respectively. Mass spectrometric data for compounds **19** and **20** reveals the presence of [M+H] and [M] peak respectively.

5.3.1. Molecular structure of 18 and 19

Single crystal X-ray diffraction studies have been carried out for **18** and **19** with good quality single crystals, grown from dichloromethane / n-hexane solvent mixture at -10 ºC using diffusion technique. The molecular structure of **18** shows the presence of two ferrocenyl units linked together via enone type bridge as shown in Figure 5.4. The central ferrocenyl fragment is attached to both hydrazone and enone chain, while the terminal ferrocenyl moiety is mono-substituted and connected to the bridged enone chain. The hydrazone and the enone chains have been oriented in the same direction of the central ferrocene moiety, forming an eclipsed geometry with a dihedral angle of 8.6º. The structure also showed that the two ferrocenyl moieties are oriented opposite to each other revealing a *trans* geometry. Single crystal X-ray diffraction study of **19** also showed similar structural identity with two ferrocenyl moieties attached to hydrazone and enone chains (Figure 5.5). The structure of **19** also revealed eclipsed conformation with a dihedral angle of 8.3º. The C=N bond distance between C(14) and N(1) in compounds **18** and **19** show double bond character (1.281(8) Å (**18**), 1.299(7) Å (**19**)), but the distance is slightly longer in **19** as compared to that in **18** and some of the previously analyzed ferrocenyl hydrazone compounds, [(η^5-C_5H_5)Fe{(η^5-C_5H_4)C(H)=NN(H)C(O)C_6H_4OH}] (1.284(3) Å), [(η^5-C_5H_5)Fe{(η^5-C_5H_4)C(H)=NN(H)C(O)C_6H_5}]

(1.277(4) Å), [(η^5-C_5H_5)Fe{(η^5-C_5H_4)C(H) =NN(H)C(O)C_6H_4N}] (1.291(4) Å).[16, 27] The hydrazone chain in **19** is endcapped with a pyridine ring, while compound **18** shows the presence of a o-hydroxyphenyl group at the end position of the hydrazone linkage.

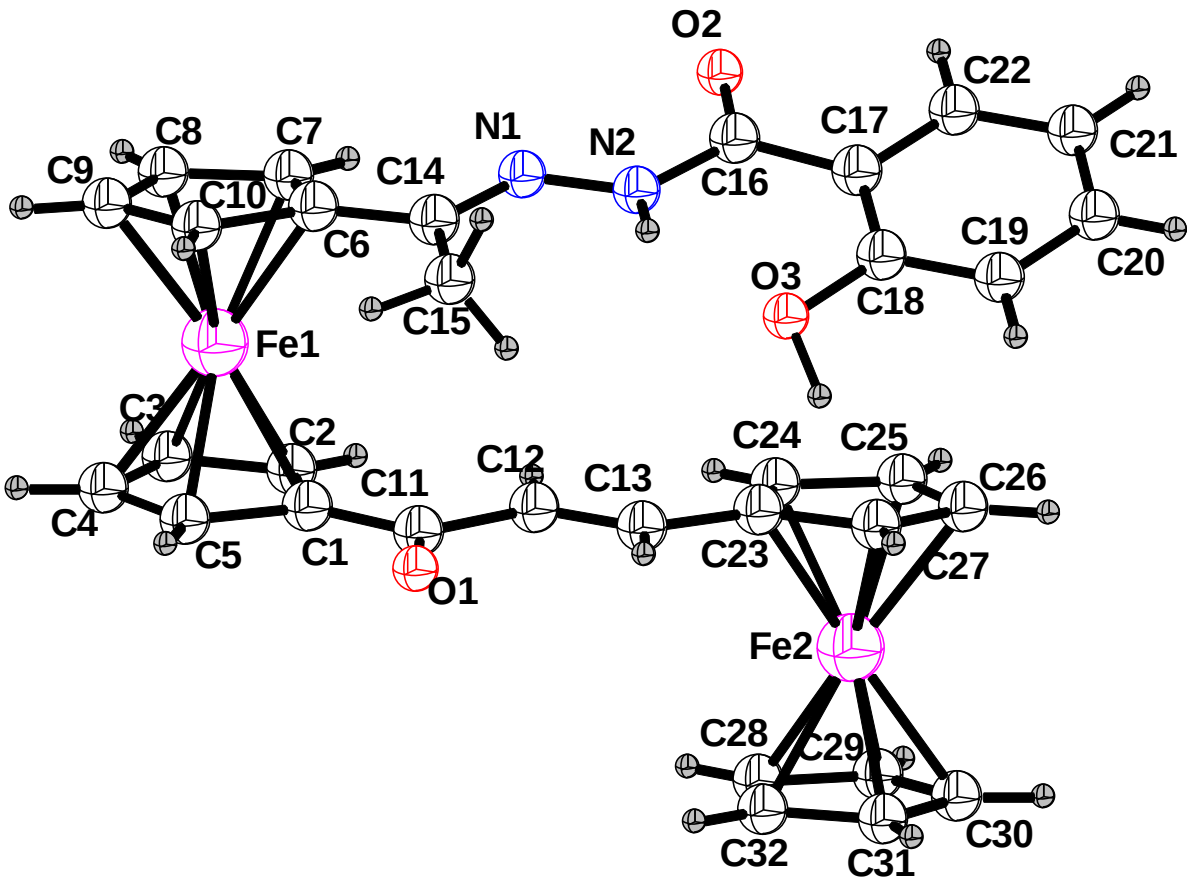

Figure 5.4. ORTEP diagram of **18.** Selected bond lengths (Å) and bond angles (º): C(12)-C(13)= 1.324(9), N(1)-N(2) = 1.378(7), N(1)-C(14) = 1.281(8), O(1)-C(11) = 1.231(8), O(3)-C(18) = 1.362(8), N(1)-N(2)-C(16) = 118.7(5), N(1)-C(14)-C(15) = 123.8(6), C(13)-C(12)-C(11) = 123.5(7), O(3)-C918) –(C17) = 118.2(6).

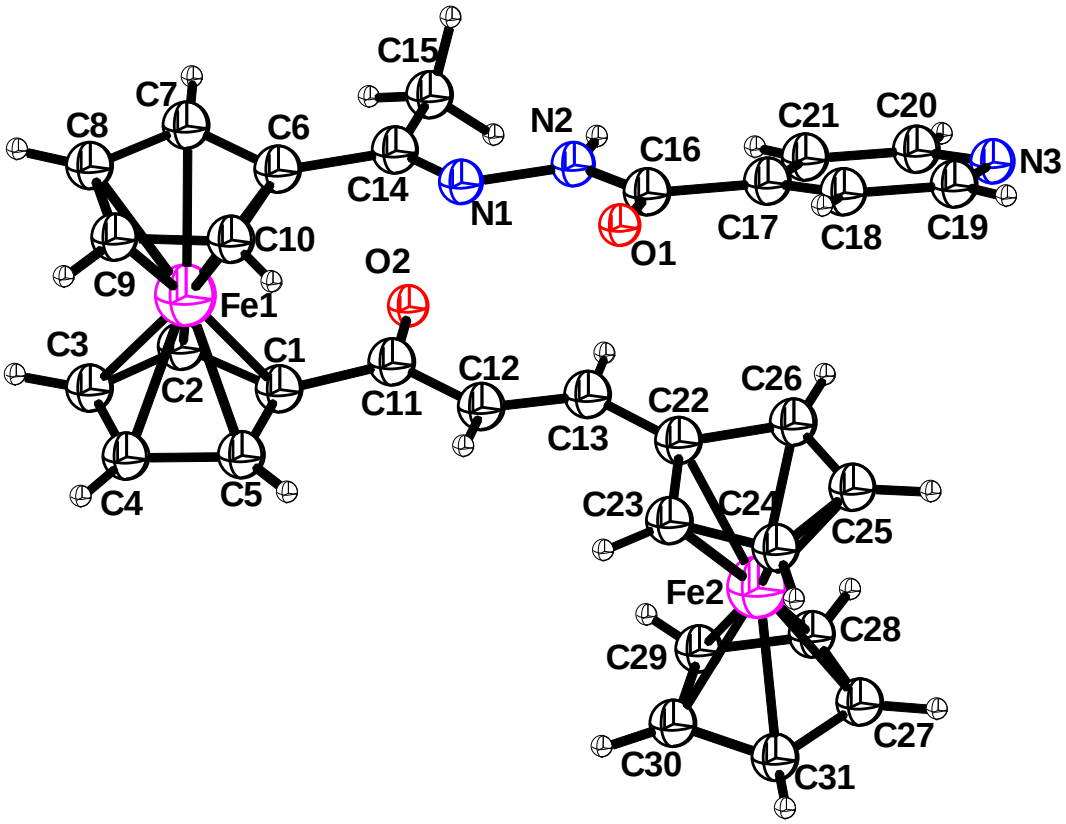

Figure 5.5. ORTEP diagram of **19.** Selected bond lengths (Å) and bond angles (º): C(14)-N(1) = 1.299(7), N(1)-N(2) = 1.395(6), C(16)-O(1) = 1.210(6), C(12)-C(13) = 1.334(7), O(2)-C(11) = 1.224(6), C(14)-N(1)-N(2) = 116.6(5), C(13)-C(12)-C(11) = 122.0(5), C(1)-C(11)-C(12) = 116.2(5), C(6)-C(14)-C(15) = 118.4(5).

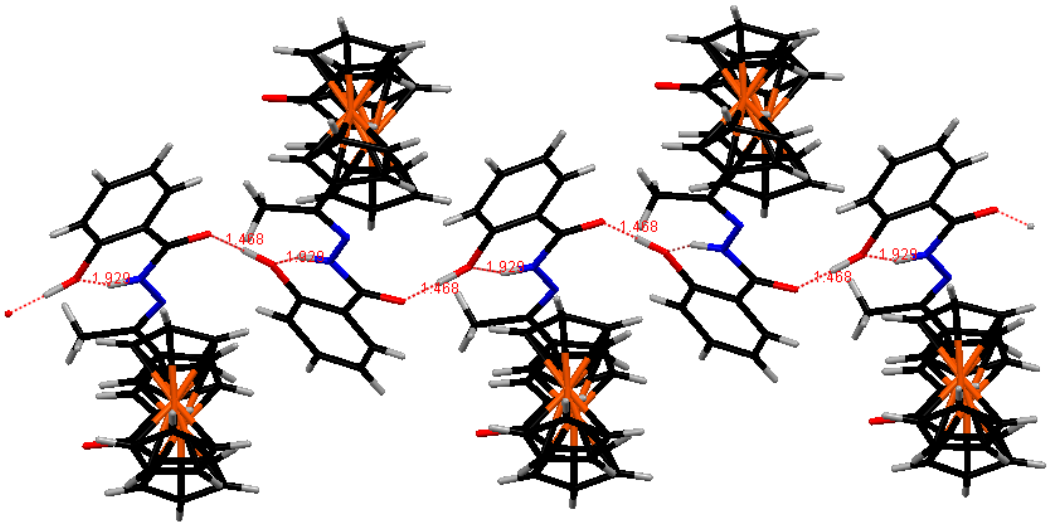

Figure 5.6. Intra- and inter-molecular hydrogen bonding Interaction of **18**

The strctural analysis of **18** also shows the presence of both intra- and inter-molecular hydrogen bonding between N2-H···O3 (1.929 Å) and O3-H···O2 (1.468 Å) respectively which creates a zigzag array of alternate molecular units as shown in Figure 5.6, while compound **19** does not show any hydrogen bonding interaction.

5.3.2. Redox properties of 17-20

Compounds **17**-**20** exhibited two reversible redox processes involving Fe(II) / Fe(III) couple due to the presence of two ferrocenyl moieties. The first redox couple at $E_{1/2}$ in the range 0.42 - 0.44 V is due to the terminal ferrocenyl unit (Fc^T) while the second couple at 0.67 - 0.7 has been due to the disubstituted central ferrocenyl moiety (Fc^C). Presence of both hydrazone and enone chains attached to the central ferrocenyl unit makes the Fe(II) more difficult to oxidize, thereby showing Fe(II)/Fe(III) redox couple at much higher potential range compared to the monosubstituted terminal ferrocenyl fragment. The one-electron nature of these oxidations has been established by comparing its current height with that of the standard ferrocene/ferrocenium couple under the same experimental conditions. The structural features in compounds **17**-**20** with two ferrocenyl species linked together by enone chain has been anticipated to show coupling behavior between the two redox active units. To understand any such electronic communication between the two ferrocenyl units, we carried out cyclic voltammetry and differential pulse voltammetry with the phenyl analog of **17**, (**21**) which contains one central ferrocenyl unit linked via Cp to a benzoyl hydrazone moiety and an enone chain, –C(O)C═CPh attached to the other Cp ring. Surprisingly, compound **21** showed one reversible redox couple at reasonably lower potential (0.66V) as compared to the potential for central ferrocenyl moiety in compounds **5** (0.69V) and **17** (0.71V) as shown in Table 5.2 and Figure 5.8. Analyses of the oxidative potential due to the central ferrocenyl unit in compounds **5**, **17** and **21** revealed that, during the oxidative scan of **17**, the terminal ferrocene (Fc^T) gets oxidized first showing the redox couple at 0.436 V ($E^I_{1/2}$) region (Figure 5.7(II)). The oxidized terminal ferrocene in II can now act as an electron withdrawing center and therefore, relatively more electrons get withdrawn from

the central ferrocene (Fc^C) via the enone chain. This higher electron withdrawing character results in the oxidation of central ferrocene at much higher potential range ($E^{II}_{1/2}$=0.71 V) as compared to that for the phenyl analog ($E_{1/2}$ = 0.66 V). The above potential shift of 50 mV reveals that the two ferrocenes are no more independent to each other and shows considerable amount of electronic communication between the two electroactive groups. Apparently, the formation of species II due to the oxidation of terminal ferrocenyl group results in the formation of a source (Fc^C) and a sink (Fc^T) of electrons and probability of electron flow from Fc^C to Fc^T cannot be ignored Figure 5.7. However, the possibility to regulate the flow of electrons by varying the hydrazone end group and tuning the electron density at the central ferrocenyl moiety is under investigation.

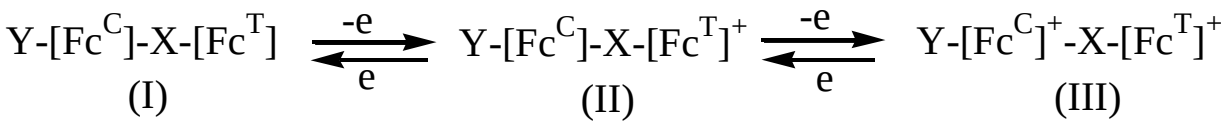

Y= Hydrazone chain; X = Enone chain

Fc^C=ferrocenyl (central); Fc^T=ferrocenyl (terminal)

Figure 5.7

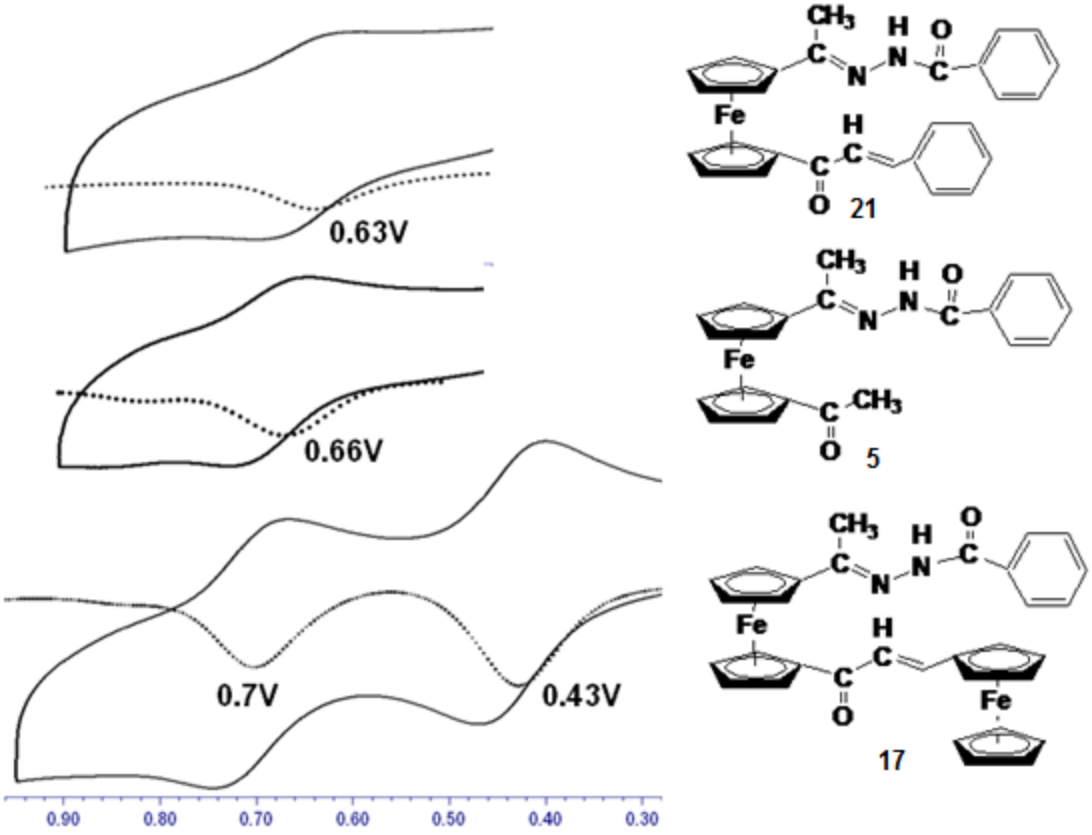

Figure 5.8. Cyclic voltammograms (—) and differential pulse voltammograms (…) of compounds **17**, **5** and **21** in Acetonitrile / 0.1 M TBAP at 298 K. Ferrocene / Ferrocenium was used as standard.

Table 5.2. Cyclic voltammetric data for **5-8** and **17-21**

Compounds	E_{pa}	E_{pc}	dpv (V)	$E_{1/2}$ (V) (ΔE_p (mV))
5	0.717	0.657	0.66	0.69 (60)
6	0.69	0.633	0.634	0.66 (57)
7	0.708	0.643	0.653	0.676 (65)
8	0.70	0.638	0.645	0.67 (62)
17	0.467, 0.742	0.405, 0.68	0.428, 0.7	0.436(62), 0.71(62)

18	0.45, 0.715	0.39, 0.67	0.395, 0.67	0.42(60), 0.69(45)
19	0.47, 0.735	0.413, 0.68	0.423, 0.68	0.442(57), 0.71(55)
20	0.46, 0.72	0.42, 0.686	0.413, 0.68	0.44(40), 0.703(34)
21	0.680	0.633	0.629	0.66 (47)
$Fc(COMe)_2$	0.83	0.77	0.78	0.8(60)
Fc	0.37	0.286	0.315	0.33(84)

*In acetonitrile at a scan rate of 50 mv s^{-1}. $E_{1/2}$ (V) = $(E_{pa}+E_{pc})/2$, where E_{pa} and E_{pc} are the anodic and cathodic peak potentials Vs. Ag/AgCl respectively. ΔE_p (mV) = $E_{pa}-E_{pc}$

5.3.3. Antibacterial activity of 17-20

Antibacterial study was carried out for compounds **17-20** which showed potential inhibition activity against the bacterial strains as shown in Table 5.3. Compound **18** and **19** showed highest antibacterial activity against *E. coli* and *P. aruginosa* bacterial strain respectively, while MIC values for other compounds and against different bacterial strains shows marked inhibition activity, as compared to Chloramphenicol. Recently reported antibacterial study on ferrocene containing compounds showed promising results against different types of bacterial strains,[14-16] whereas inhibition activities of diferrocenyl system with bifunctional chains have been rarely studied. Significant antibacterial activity for the reported organometallic compound could possibly be due to the presence of ferrocenyl and hydrazone-enone moieties that are playing a crucial role to increase the cell permeability and lipophilicity of the compounds. Increased electron delocalization and blocking of metal binding sites of the enzyme of microorganism are some of the factors that may also result in better inhibition activity.

Table 5.3. Minimum inhibitory concentration (MIC) value in μg/ml

Compounds	*B. subtilis*	*E. coli*	*P. aeruginosa*
17	15.6	15.6	15.6
18	N	7.8	15.6
19	N	15.6	7.8
20	62.5	15.6	15.6
Chloramphenicol	4	4	31.25

N – Inhibitory activity not observed

5.3.4. BSA Protein binding studies

Bovine serum albumins (BSA) are the most widely studied proteins due to their ability to transport a variety of endogenous and exogenous moieties such as steroids, drug molecules, metabollites etc. BSA increases the solubility of drugs in plasma and modulates their delivery to cells and is usually selected for protein binding studies.[28] It is sometimes very important to study the interaction of a bioactive compound with proteins, to gain fundamental insights of the binding mechanism and to understand the metabolism and transporting process of a drug compound. Therefore, to understand the protein binding activities of the diferrocenyl compounds **18** and **19,** BSA was used to study the tryptophan emission-quenching experiment.[29] Generally, the fluorescence of BSA is caused by three intrinsic characteristics of the protein, namely tryptophan, tyrosine and phenylalanine. The majority of the intrinsic fluorescence of BSA is provided by the two tryptophan residues, (Trp 134, Trp 213) while the other amino acid residues contribute weakly. The fluorescence from the indole group in tryptophan is extremely sensitive to its surrounding environment and has been extensively used as a

spectroscopic probe for the structural and conformational changes in the protein. Variation in the molecular environment in the vicinity of a fluorophore can be assessed by the changes in fluorescence spectra in the presence of a quencher which provide clues for the understanding of the binding phenomenon.[30] In the present study, the interaction of BSA with compounds **18** and **19** was studied by fluorescence spectroscopy measurement at room temperature. A fixed solution of BSA (1 μM) was titrated with various concentrations of the compound (0−50 μM) and the fluorescence spectra were recorded in the range of 300− 450 nm upon excitation at 290 nm. The effects of the compound on the fluorescence emission spectrum of BSA are shown in Figure 5.9. As can be seen from the figure, the fluorescence emission intensities of BSA at 330 nm show remarkable decreasing trends with increasing concentration of the ferrocenyl compounds **18** and **19**. The data indicates that the interaction of the two compounds with BSA could cause conformational changes in protein structure, leading to changes in the tryptophan environment of BSA. This result suggested a definite interaction of the compound with the BSA protein.

Fluorescence quenching data were analyzed with the Stern−Volmer equation and Scatchard equation using corrected fluorescence data taking into account the effect of dilution. The Stern-Volmer quenching constant (K_{sv}) of the compounds have been calculated using the plot of F_0/F versus [Q], concentration, where F_0 and F are the emission intensity of BSA in the absence and in the presence of the quencher (eqn. 1). The K_{sv} value obtained as a slope from the plot of F_0/F versus [Q] was found to be 1.9 x 10^5 M^{-1} and 1.8 x 10^5 M^{-1} for compound **18** and **19** respectively (Figure 5.9).

$$\mathbf{F_0/F = 1 + K_{sv}\,[Q]} \qquad (1)$$

Proteins may interact with molecules using Van der Waals, electrostatic, hydrophobic and hydrogen bonding interactions. The observed quenching of fluorescence indicates some binding interactions between the compound and suitable sites in the proteins. Binding of small molecules to a set of equivalent sites on a macromolecule can be understood by the Scatchard equation (eqn. 2).[31] The binding constant and the number of binding sites (n) were obtained from the plot of log[(F_0-F)/F]

vs. log [Q] and the values are shown in Table 5.4. The value of n is approximately equal to 1, indicating the presence of one binding site in BSA and follows 1:1 stoichiometric interaction between the compound and BSA protein.[32]

$$\log[(F_0-F)/F] = \log K_b + n \log[Q] \quad (2)$$

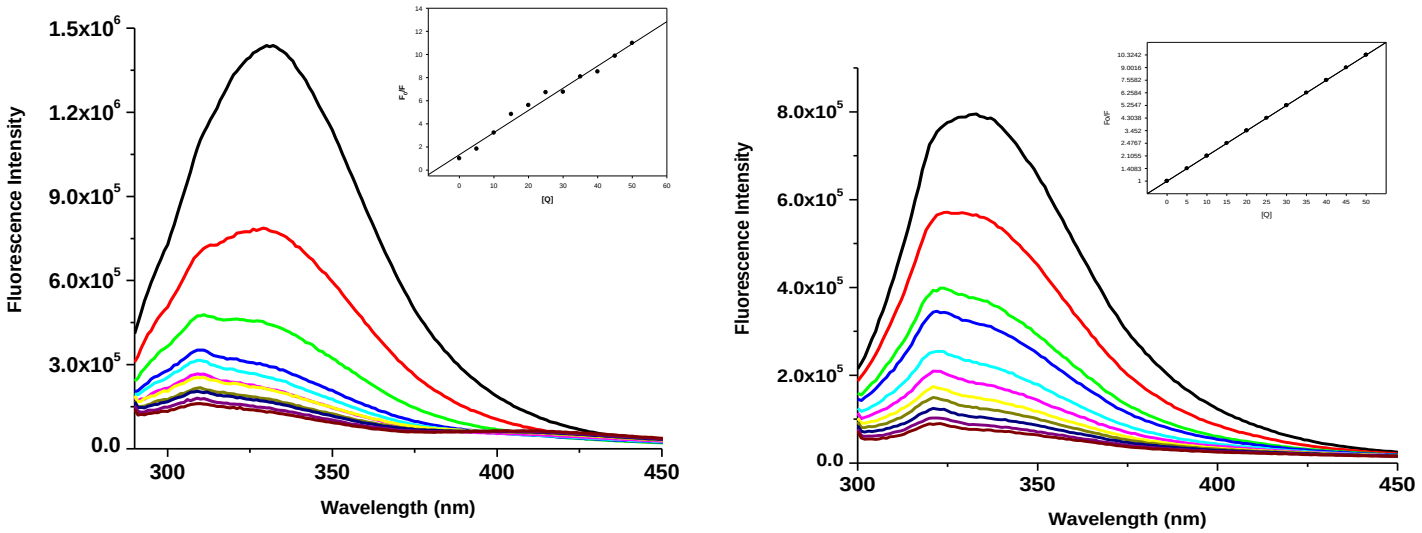

Figure 5.9. Fluorescence spectra of BSA (1μM) in the presence of increasing concentration of (a) **18** and (b) **19**. The inset shows the linear fit of F_0/F vs. [**Q**].

Table 5.4

Compounds	Quenching constant, K_{sv} (M^{-1})	Binding Constant, K_b (M^{-1})	No. of binding sites, n
18	1.9 x 10^5	4.36 x 10^5	1.04
19	1.8 x 10^5	5.53 x 10^6	1.23

5.3.5. Metal ion interaction study by UV–Visible spectroscopy

The unique structural identity with an eclipsed configuration for the diferrocenyl system (**18**, **19**) prompted us to study metal ion interaction properties by UV-Visible spectroscopy. Single crystal structure and DFT calculation showed that the compounds **18** and **19** are energetically favorable with the eclipsed conformation, in which the hydrazone and enone chains are almost parallel to each other. We, therefore, anticipated the possibility of host-guest type of interaction where the guest molecule/ ion may get trapped in-between the two eclipsed chains. The guest ion matching the size and the electronic factors of the cavity may eventually show selective binding with the receptor molecule. To establish the receptor property of these diferrocenyl hydrazone-enone type of compounds, we carried out metal ion interaction study using UV-Visible spectroscopy. To our knowledge metal ion interaction study with unsymmetrically difunctionalized diferrocenyl compounds have been rarely carried out. In most cases metal ion interaction has been studied with receptors having mono substituted ferrocenyl and symmetrically disubstituted ferrocenyl fragments,[33-35] while the unsymmetrically difunctionalized ferrocenyl systems have been comparatively less focused.[8] The UV–Visible binding interaction studies of receptors **18** and **19** in ethanol (10^{-5} M) against cations such as of Na^{+}, K^{+}, Mg^{2+}, Ba^{2+}, Mn^{2+}, Fe^{2+}, Co^{2+}, Ni^{2+} Cu^{2+}, Zn^{2+}, Cd^{2+}, Hg^{2+} and Pb^{2+} as perchlorate salts have been carried out. Gradual addition of Pb^{2+} showed marked shift in the UV–Visible absorbance spectra of both the receptors in ethanol solvent while minor changes have been observed when titration was carried out with copper salt. All other metal ions showed no distinguishable shift in the spectrum during their respective titrations. Addition of upto five equivalents of Pb^{2+} ions to compound **18** result in gradual formation of a new peak at around 236 nm, while the intensity of peak at 212 nm decreases and the peak at 312 nm gradually red shifted to 334 nm. Red shift has also been observed for peak at 508 nm to 526 nm as shown in Figure 5.10(a). Similar, changes in the absorption spectrum have been observed when Pb^{2+} salt was gradually added to compound **19** as shown in Figure 5.10(b). Binding assays using the method of continuous variations (Job's plot) suggest 1:1 (cation/receptor) interaction with Pb^{2+} ion for both the compounds **18** and **19.** Three well-defined isosbestic points at 267, 327 and

469 nm for **18** and 258, 322 and 484 for **19** have been observed revealing a distinct cation –receptor interaction. The addition of increasing amount of Cu^{2+} ions to a solution of **18** and **19** showed a slight increase in a low intensity shoulder peaks at 383 nm and 408 nm. However, no definite isosbestic point was observed in the UV-Visible absorption spectrum in case of Cu^{2+} titration.

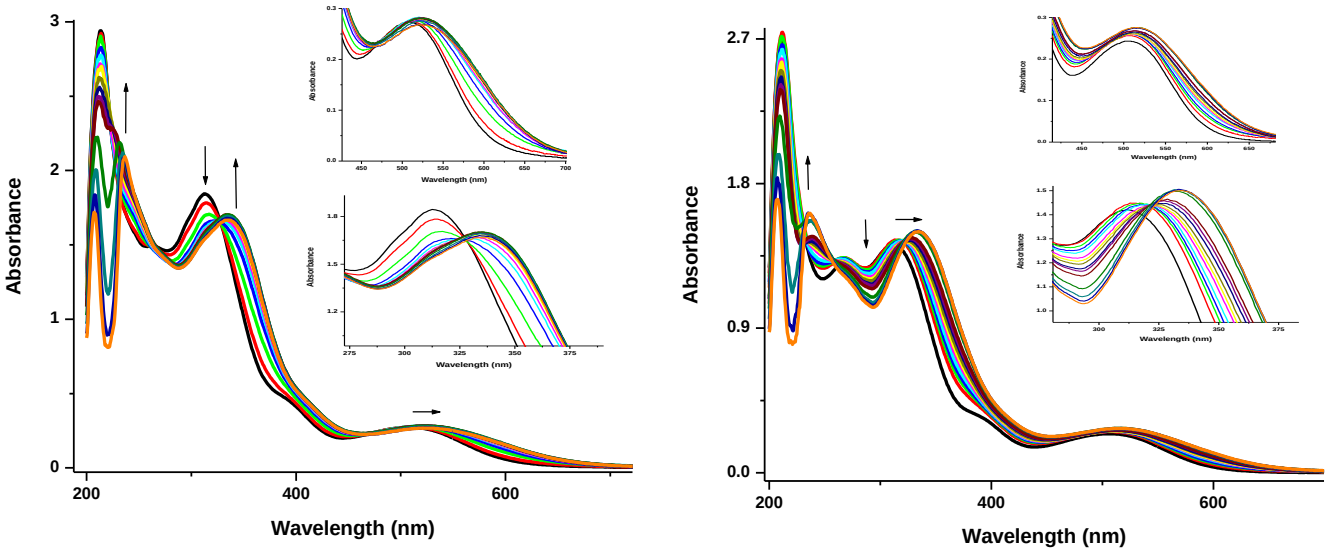

(a) (b)

Figure 5.10. UV-Vis absorbance spectra of (a) **18** (10^{-5} M) and (b) **19** (10^{-5} M) upon gradual addition of Pb^{2+} ion

The shift of around 20 nm in the spectral bands for both the receptor molecules **18** and **19** due to the addition of Pb^{2+} may be due to some metal interaction or metal-ligand ligation. To understand Pb^{2+}-receptor interaction extensively we carried out DFT study with the optimized [**19**-Pb^{2+}] complex. The optimized geometry, as shown in Figure 5.11, presents an idea of the interaction of Pb^{2+} with the ketonic oxygen, imine nitrogen and the Cp of the receptor molecule. The distance between Pb^{2+} and ketonic oxygen of 2.28 Å is within the bonding range while the Pb^{2+}- N (imine nitrogen) and Pb^{2+}- Cp (terminal Fc) are 2.52 Å and 2.84 Å respectively. Selective interaction of the diferrocenyl hydrazone-enone molecules towards lead cation have revealed their potential as receptor molecules and can be further used to expand their ability in various host-guest

recognition processes. We are presently undergoing extensive study on some of the host –guest interaction processes to establish their application as a sensor system.

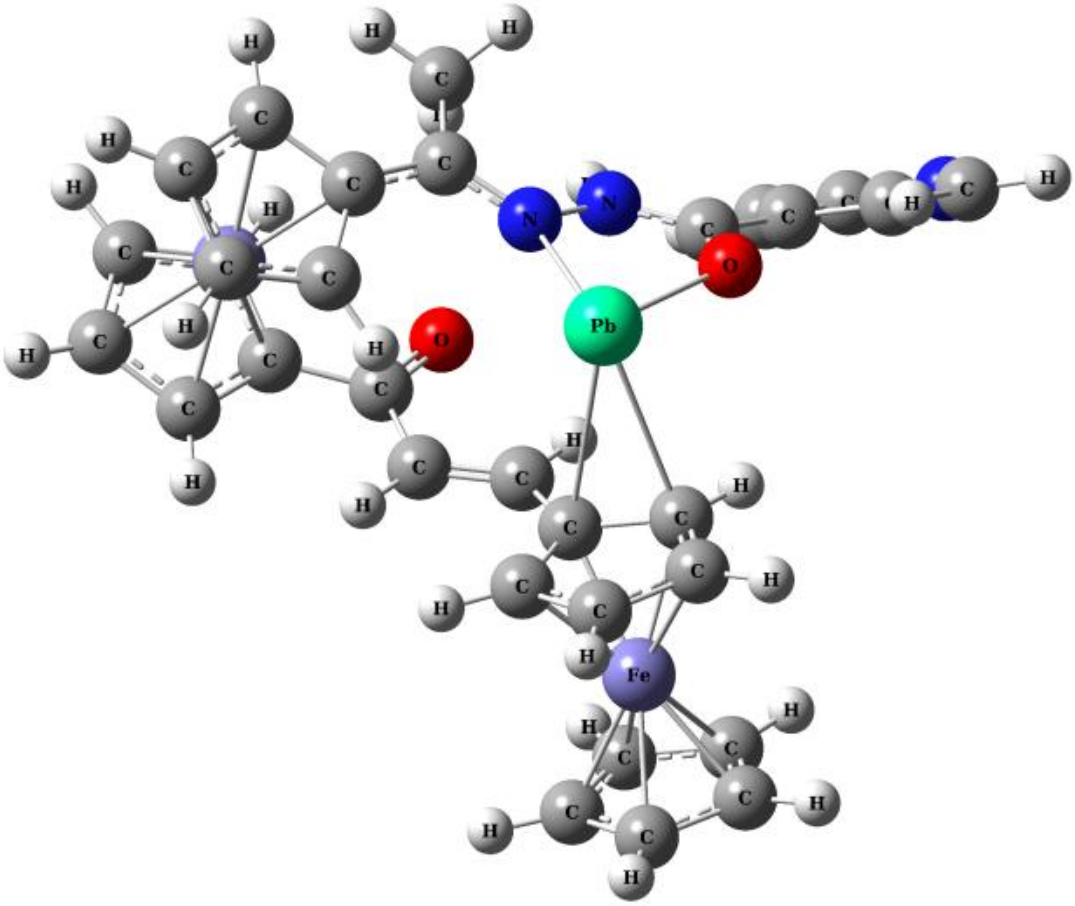

Figure 5.11. Optimized geometry of [1**9**-Pb^{2+}] complex

5.3.6. DFT Studies

DFT calculation was carried out with fully optimized geometry of compounds **18** and **19** for eclipsed and staggered conformation. Initial geometry of **18** and **19** for the eclipsed conformation was taken from single crystal X-ray analysis data. Figure 5.12 depicts the DFT optimized structure of eclipsed and staggered geometry respectively. Time-Dependent Density functional Theory (TD-DFT) calculations was performed to understand the electronic transitions involved and the relative energies of the highest occupied (HOMO), HOMO-1, HOMO-2 and lowest unoccupied molecular orbitals (LUMO). Corresponding absorption bands for the complex in the ground state, oscillator

strengths, energies and the involvement of MO in major transitions occurring at a particular wavelength has been calculated. DFT calculated results showed that the eclipsed conformation of compound **19** is 0.09 eV more stable than that of the staggered conformation, while the eclipsed conformer of **18** is 1.46 eV more stable than the staggered conformation. This reveals that in both the compounds eclipsed conformation is energetically more stable than the staggered conformation. However, in compound **18** the energy difference between the two conformers is so high that the presence of staggered geometry in solution may also be ruled out.

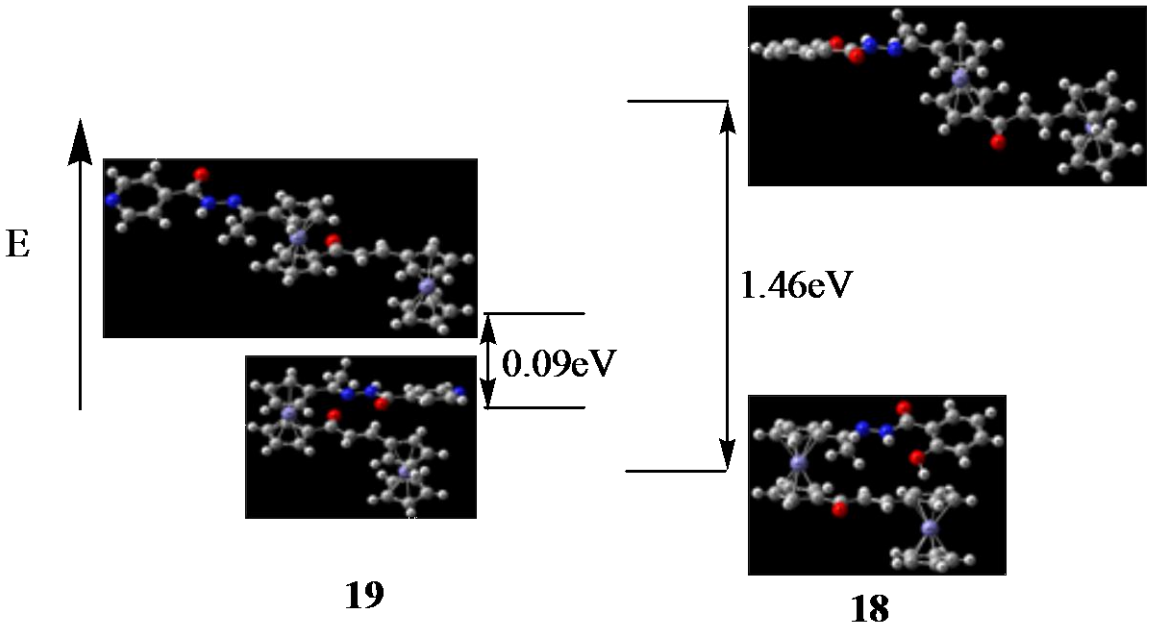

Figure 5.12. Relative energies and the optimized geometry of compound **18** and **19**

Molecular orbital calculation reveals that the HOMO of **19** is metal based and mostly localized on terminal ferrocenyl moiety, while the LUMO is ligand based and has an antibonding character. In comparison, compound **18** has HOMO localized on central ferrocenyl moiety and partly on hydrazone chain and a ligand based antibonding LUMO. HOMO-1 for both the molecules has been localized at the terminal ferrocenyl fragment, while HOMO-2 for compound **19** is central ferrocenyl based and that of **18** is localized on terminal ferrocenyl fragment (Figure 5.13).

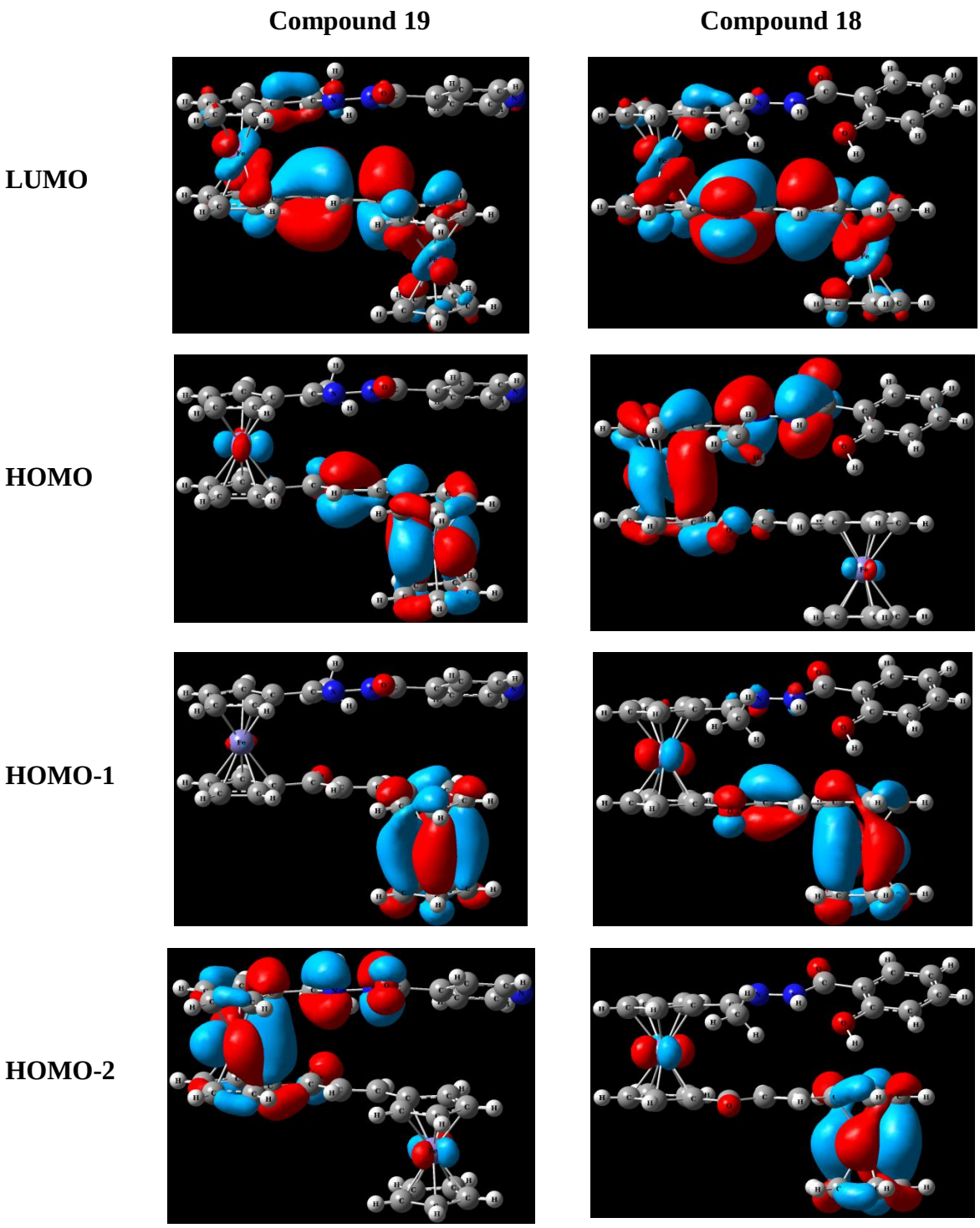

Figure 5.13. Selected Frontier Molecular orbital of **18** and **19.**

In order to understand the reactivity pattern and the relative charge distribution in the molecule, we have computed a popular conceptual density functional theory based reactivity descriptors, dual descriptors, which describe the nucleophilic and electrophilic centers inside the molecule. The electron density mapping reveals that compound **19** has electron deficient center on central ferrocenyl iron, while the terminal ferrocenyl metal has an electron rich center. Compound **18,** on the other hand, shows the opposite behavior in which the terminal ferrocenyl moiety is relatively more electron deficient than the central ferrocenyl and imine group. The different electronic behavior can be partly explained due to the presence of an electron donating end group (O-hydroxyphenyl) in compound **18** and an electron withdrawing pyridyl group in **19**. This also supports the probability of electronic communication between the two ferrocenyl fragments.

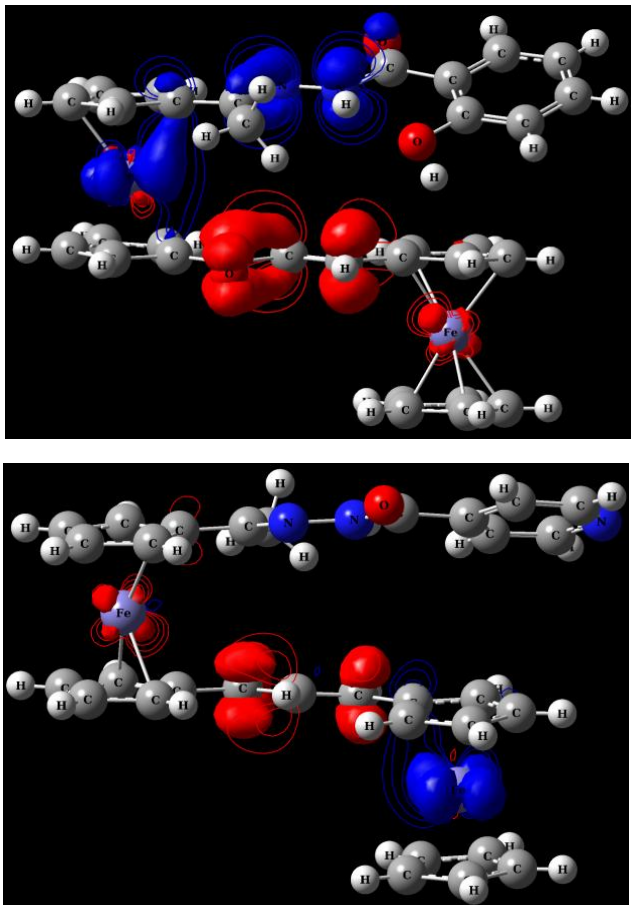

Figure 5.14. Electron density mapping for Compound **18** and **19**

(Red: Electron deficient centers; Blue: Electron rich)

In summary, we have synthesized four analogs of unsymmetrically substituted hydrazone – enone diferrocenyl system capable of selectively interact with Pb^{2+} metal ion and shows potential BSA protein binding property. Structural characterizations of the two diferrocenyl hydrazone-enone compounds, **18** and **19** confirm the presence of more stable eclipsed conformation. Selective interaction towards lead cation has revealed their potential as receptor molecules which can be further extended to study various host-guest recognition processes. We are presently undergoing extensive study to establish their application as sensor molecules in biological system. Some of the compounds also showed excellent antibacterial activity. However, study may be focused to understand the inhibition mechanism and establish the structure –activity relationship on similar compounds with varied heterocyclic fragments. The redox properties for the diferrocenyl compounds with variable end group reveals distinct electronic communication between the two electroactive groups via the enone chain.

5.4. References

[1] (a) D. T. Pierce, W. E. Geiger, J. Am. Chem. Soc. 114 (1992) 6063; (b) W. E. Geiger, Organometallics 29 (2010) 3179; (c) A. M. Tondreau, C. Milsmann, A. D. Patrick, H. M. Hoyt, E. Lobkovsky, K. Wieghardt, P. J. Chirik, J. Am. Chem. Soc. 132 (2010) 15046.

[2] (a) J. Lu, D. Chamberlin, D. A. Rider, M. Liu, I. Manners, Nanotechnology 17 (2006) 5792; (b) T. Ren, Organometallics 24 (2005) 4854.

[3] M. R. Dubois, D. L. Dubois, Acc. Chem. Res. 42 (2009) 1974.

[4] T. R. Cook, D. K. Dogutan, S. Y. Reece, Y. Surendranath, T. S. Teets, D. G. Nocera, Science 110 (2010) 6474.

[5] (a) A. P. De Silva, Nature 445 (2007) 718; (b) S. N. Semenov, S. F. Taghipourian, O. Blacque, T. Fox, K. Venkatesan, H. Berke, J. Am. Chem. Soc. 132 (2010) 7584.

[6] (a) M. I. Bruce, P. Low, J. Adv. Organomet. Chem. 50 (2004) 231; (b) S. Szafert, J. A. Gladysz, Chem. Rev. 2006, 106; (c) T. Ren, Chem. Rev. 108 (2008) 4185; (d) R. Sakamoto, M. Murata, H. Nishihara, Angew Chem. Int. Ed. 45 (2006) 4793; (e) C. Engtrakul, L. R. Sita, Nano Lett. 1 (2001) 541; (f) M. Wagner, Angew. Chem. Int. Ed. 45 (2006) 5916; (g) T. Y. Dong, L. S. Chang, I. M. Tseng, S. J. Huang, Langmuir 20 (2004) 4471; (h) W. Skibar, H. Kopacka, K. Wurst, C. Salzmann, K.-H. Ongania, F. F. Biani, P. Zanello, B. Bildstein, Organometallics 23 (2004) 1024; (i) S. A. Getty, C. Engtrakul, L. Wang, R. Liu, S.-H. Ke, H. U. Baranger, W. Yang, M. S. Fuhrer, L. R. Sita, Condensed Matter (2004) 1.

[7] (a) C. K. W. Jim, A. Qin, F. Mahtab, J. W. Y. Lam, B. Z. Tang, Chem. Asian J. 6 (2011) 2753; (b) X. Ren, C. He, Y. Feng, Y. Chai, W. Yao, W. Chen, S. Zhang, Org. Biomol. Chem. 13 (2015) 5054; (c) E. López, G. Lonzi, L. A. López, Organometallics 33 (2014) 5924.

[8] D. Mandal, P. Deb, B. Mondal, A. Thakur, S. J. Ponniah, S. Ghosh, RSC Adv. 3 (2013) 18614.

[9] T. Romero, R. A. Orenes, A. Tárraga, P. Molina, Organometallics 32 (2013) 5740.

[10] F. Otón, M. C. González, A. Espinosa, A. Tárraga, P. Molina, Organometallics 31 (2012) 2085.

[11] H. Miyaji, S. R. Collinson, I. Prokes, J. H. R. Tucker, Chem. Commun. (2003) 64.

[12] T. Kienz, C. Förster, K. Heinze, Organometallics 33 (2014) 4803.

[13] J. M. Speck, M. Korb, T. Rüffer, A. Hildebrandt, H. Lang, Organometallics 33 (2014) 4813.

[14] (a) M. Patra, G. Gasser, Chembiochem. 13 (2012) 1232; (b) G. Gasser, N. Metzler-Nolte, Curr. Opin. Chem. Biol. 16 (2012) 84. (c) D. R. V. Staveren, N. Metzler-Nolte, Chem. Rev. 104 (2004) 5931; (d) E. Meggers, G. E. A. Gokcumen, H. Bregman, J. Maksimoska, S. P. Mulcahy, N. Pagano, D. S. Williams, Synlett (2007) 1177; (e) C. Policar, J. B. Waern, M.-A. Plamont, S. Clède, C. Mayet, R. Prazeres, J.-M. Ortega, A Vessières, A. Dazzi, Angew. Chem. Int. Ed. 50 (2011) 860; (f) C. G. Hartinger, N. Metzler-Nolte, P. J. Dyson, Organometallics 31 (2012) 5677; (g) C. G. Hartinger, P. J. Dyson, Chem. Soc. Rev. 38 (2009) 391; (h) R. H. Fish, G. Jaouen, Organometallics 22 (2003) 2166.

[15] (a) S. Top, A. Vessières, C. Cabestaing, I. Laios, G. Leclercq, C. Provot, G. Jaouen, J. Organomet. Chem. 637–639 (2001) 500. (b) A. Nguyen, A. Vessières, E. A. Hillard, S. Top, P. Pigeon, G. Jaouen, Chimia 61 (2007) 716. (c) E. A. Hillard, P. Pigeon, A. Vessieres, C. Amatore, G. Jaouen, Dalton Trans. (2007) 5073. (d) E. A. Hillard, A. Vessières, L. Thouin, G. Jaouen, C. Amatore, Angew. Chem. Int. Ed. 45 (2006) 285.

[16] (a) V. Tirkey, S. Mishra, H. R. Dash, S. Das, B. P. Nayak, S. M. Mobin, S. Chatterjee, J Organomet. Chem. 732 (2013) 122; (b) S. K. Patel, V. Tirkey, S. Mishra, H. R. Dash, S. Das, M. Shukla, S. Saha, S. M. Mobin, S. Chatterjee, J. Organomet. Chem. 749 (2013) 75; (c) S. Mishra, V. Tirkey, A. Ghosh, H. R. Dash, S. Das, M. Shukla, S. Saha, S. M. Mobin, S. Chatterjee, J. Mol. Structure. 1086 (2015) 162; (d) V. Tirkey, R. Boddhula, S. Mishra, S. M. Mobin, S. Chatterjee, J. Organomet. Chem. 794 (2015) 88.

[17] (a) G. Nabi, Z. Q. Liu, Med. Chem. Res. 21 (2012) 3015; (b) K. Kumar, S. C. Kremer, L Kremer, Y. Guérardel, C. Biot, V. Kumar, Organometallics 32 (2013) 5713; (c) S. Attar, Z. O. Brien, H. Alhadad, M. L. Golden, A. C. A. Urrea, Bioorg. Med. Chem. 19 (2011) 2055; (d) W. Y. Liu, Y.-S. Xie, B.-X. Zhao, B.-S. Wang, H.-S. Lv, Z.-L. Gong, S. Lian, L.-W. Zheng, J. Photochem. Photobio A: Chem. 214 (2010) 135; (e) S. J. Won, C. T. Liu, L. T. Tsao, J. R. Weng, H. H. Ko, J. P. Wang, C. N. Lin, Eur. J. Med. Chem. 40 (2005) 103; (f) S. Vogel, S. Ohmayer, G. Brunner, Heilmann, J. Bioorg. Med. Chem.

16 (2008) 4286; (g) C.-T. Hsieh, T.-J. Hsieh, M. E. Shazly, D.-W. Chuang, Y.-H. Tsai, C.-T. Yen, S.-F. Wu, Y.-C. Wu, F.-R. Chang, Bioorg. Med. Chem. Lett. 22 (2012) 3912.

[18] (a) M. V. Angelusiu, S. F. Barbuceanu, C. Draghici, G. L. Almajan, Eur. J. Med. Chem. 45 (2010) 2055; (b) P. Barbazán, R. Carballo, U. Abram, G. P. Gabián, E. M. V. López, Polyhedron 25 (2006) 3343; (c) P. Barbazán, R. Carballo, I. Prieto, M. Turnes, E. M. V. López, J. Organomet. Chem. 694 (2009) 3102; (d) Á. Gyömöre, A. Csámpai, J. Organomet. Chem. 696 (2011) 1626.

[19] U. T. Mueller-Westerhoff, Z. Yang, G. Ingram, J. Organomet. Chem. 463 (1993) 163.

[20] M. Vogel, M. Rausch, H. Rosenberg, J. Org. Chem. 22 (1957) 1016.

[21] (a) N. S. Navaneetham, R. Kalyanasundaram, S. Soundararajan, Inorg. Chim. Acta 110 (1985) 169; (b) H. Meyer, J. Mally, Monatshefte fuer Chemie 33 (1912) 393.

[22] G. M. Sheldrick, Acta Cryst. A 64 (2008) 112.

[23] Clinical and Laboratory Standards Institute (CLSI, 2006). Methods for Dilution Antimicrobial Susceptibility Tests for Bacteria That Grow Aerobically, Seventh ed. 2006 Approved Standard M7-A7, CLSI, Wayne, PA, USA.

[24] A. D. Becke, J. Chem. Phys. 98 (1993) 5648.

[25] A. Lee, W. Yang, R. G. Parr, Phys. Rev. B 37 (1988) 785.

[26] A. Ghosh, I. Halvorsen, H. J. Nilsen, E. Steene, T. Wondimagegn, R. Lie, E. Caemelbecke, N. Guo, Z. Ou, K. M. Kadish, Phys. Chem. B 105 (2001) 8120.

[27] P. Barbazán, R. Carballo, U. Abram, G. P. Gabián, E. M. Vázquez-López, Polyhedron 25 (2006) 3343.

[28] (a) Z. G. Yasseen, J. Chem. Pharm. Res. 4 (2012) 3361. (b) D. S. Raja, N. S. P. Bhuvanesh, K. Natarajan, Inorg. Chem. 50 (2011) 12852. (c) T. Banerjee, S. K. Singh, N. Kishore, J. Phys. Chem. B 110 (2006) 24147.

[29] T. T. Xing, S. H. Zhan, Y. T. Li, Z. Y. Wu, C. W. Yan, J. Coord. Chem. 66 (2013) 3149.

[30] (a) S. Bi, D. Song, Y. Tian, X. Zhou, Z. Liu, H. Zhang, Spectrochim. Acta, Part A 61 (2005) 629. (b) J. R. Lakowicz, Principles of Fluorescence Spectroscopy, Springer Science, New York, 3rd edn, 2003, p. 63.

[31] P. Banerjee, S. Ghosh, A. Sarkar, S. C. Bhattacharya, J. Lumin. 131 (2011) 316.

[32] X. L. Han, F. F. Tian, Y. S. Ge, F. L. Jiang, L. Lai, D. W. Li, Q. L. Yu, J. Wang, C. Lin, Y. Liu, J. Photochem. Photobiol. B 109 (2012) 1.

[33] (a) C. Arivazhagan, R. Borthakur, S. Ghosh, Organometallics 34 (2015) 1147; (b) T. Romero, R. A. Orenes, A. Tárraga, P. Molina, Organometallics 32 (2013) 5740.

[34] P. Molina, A. Tárraga, A. Caballero, Eur. J. Inorg. Chem. 2008, 3401.

[35] (a) V. Ganesh, V. S. Sudhir, T. Kundu, S. Chandrasekaran, Chem. Asian J. 6 (2011) 2670; (b) P. Molina, A. Tárraga, M. Alfonso, Eur. J. Org. Chem. (2011) 450.

Summary

Research on metal cyclopentadienyl chemistry has continued to develop at a rapid pace in the last two – three decades giving rise to structurally unique molecules and novel compounds containing sandwich, half sandwich and multidecker sandwich entities. The non ending interest on these organometallic moieties is because of their immense potential to various applications related to organic synthesis, catalysis, bioorganometallic, advance materials, molecular recognition etc. In spite of their increasing attention the synthesis of substituted ferrocene and derivatization of cyclopentadienyl ring in various different metallocenes and half sandwich complexes pose numerous challenges in regard to reaction condition, reagents and methodologies. Therefore, it is essential to optimize the strategies based upon facile synthetic methods and suitability of the precursors for the functionalization of different Cp based organometallic compounds. Chapter 1 introduces various aspects of cyclopentadienyl based metal complexes with significant reactivity and unique structural and electronic properties. Cyclopentadienyl ligand has the ability to stabilize a range of different metal complexes with varying hapticity and results in extensive complex chemistry with flexible electronic, structural and steric behavior. Ferrocene and its derivatives are the most versatile organometallic compounds because of their unique structural integrity, reversible redox properties and exclusive nature of their chemistry which make them an excellent building block in several processes for their use in the field of material science, molecular wires, catalysis, molecular recognition, sensing, electronic communication, bio-conjugates and medicinal chemistry. We have been equally interested to explore the synthesis and reactivity of different sandwich and half sandwich complexes and recognize their potential in biological and sensor applications.

In Chapter 2, we describe the synthesis of four new cymantrenyl hydrazone Schiff base compounds, $[(CO)_3Mn\{(\eta^5\text{-}C_5H_4)C(CH_3)=NN(H)C(O)\text{-}C_6H_4\text{-}OH\}]$ (R = C_6H_5, C_6H_4-OH, C_6H_4N-p, C_6H_4N-m) (**1-4**) by the room temperature reaction of $[Mn(CO)_3\{(\eta^5\text{-}C_5H_4)COCH_3\}]$ with the respective hydrazides and investigate their structural and biological properties. The structural analysis, carried out by X-ray crystallography, showed the presence of three legged piano stool cymantrenyl fragment

functionalized with a hydrazone chain via the cyclopentadienyl ring. Recently, Schiff-base type compounds with organometallic tags are increasingly drawing much interest due to their distinctive properties and features concerning both organometallic and coordination chemistry. Some of them have been found to be potential therapeutics against major diseases and can play a vital role as tracers in immunological analysis based on several analytical methods like FTIR, electrochemical, atomic absorption techniques etc. Antibacterial properties of **1**-**3** have been studied to understand their potential towards inhibition behavior of some bacterial strains.

Chapter 3 describes the synthesis of unsymmetrically 1,1'-disubstituted ferrocenyl compounds containing two different hydrazone units by using simple synthetic methodology involving selective reaction of one of the Cp substituent. Synthetic and biological studies on ferrocenyl mono- and di-hydrazone compounds have been known in the literature, but 1,1'-unsymmetrically substituted ferrocenyl hydrazone compounds have not been explored extensively. Unsymmetrically 1,1'-disubstituted ferrocenyl compounds have been of interest due to their multifunctional properties with unique structural features and tunable electrochemical responses. Our synthesis mainly focuses on the reaction of 1,1'-diacetylferrocene with hydrazide to give [{(η^5-C_5H_4)$COCH_3$}Fe{(η^5-C_5H_4)$C(CH_3)$=NN(H)C(O)R}] (R = C_6H_5, C_6H_4-OH, C_6H_4N-p, C_6H_4N-m) (**5-8**) in which one of the Cp ring of the ferrocenyl moiety is attached to a hydrazone chain while the other Cp ring remains unchanged with an acetyl group. Compounds **5-8** was further used as precursor molecule to prepare 1,1' - unsymmetrically disubstituted ferrocenyl compounds containing two different hydrazone units (**9**). To our knowledge 1,1'-unsymmetrically substituted ferrocenyl mixed hydrazone compounds are novel and the synthetic method described here can be used to prepare a varied range of ferrocenyl hydrazone compounds containing unsymmetrically Cp substituted side chains. We also studied the redox properties for some of the ferrocenyl hydrazones and reported their redox potential.

Recently, a bunch of different ferrocenyl chalcones and their derivatives have been synthesized which show marked electrochemical and biological properties. These systems have been investigated as precursors for a variety of ferrocene containing heterocycles like pyrazoles, pyrimidines etc. In Chapter 4, we explore the synthesis and

properties of different types of ferrocenyl chalcones involving polynuclear bimetallic moieties with multiple redox centers and studied their electrochemical and biological properties. We describe here the synthesis of novel hetero-metallic chalcones containing both ferrocenyl and cymantrenyl fragments (**11-12**) and investigate their reactivity features towards triphenylphosphine and bis(diphenylferrocenylphosphine) (**13-16**). Anti-malarial and anti-bacterial properties were studied for two bimetallic chalcones which showed their moderate inhibition activity. Electrochemical analysis revealed their multi-responsive properties with multiple redox couple during the cyclic voltammetric studies of the bimetallic chalcones. TD-DFT study was also conducted for ferrocenyl-cymantrenyl hetero-metallic chalcone (**11**) to predict the molecular orbitals involved for various electronic transitions and electronic delocalization. Structural characterizations for two new ferrocenyl-cymantrenyl chalcones have been carried out which revealed unique conformational identity of the compounds.

Chapter 5 describes the synthesis of a novel diferrocenyl bifunctional molecular system containing hydrazone and enone units using simple and systematic synthetic route. Recently, functionalization of ferrocene has attracted the synthetic community to obtain a range of ferrocene based molecular systems with unique electronic properties and structural variety. Functionalization in the form of mono-substituted and 1,1'-symmetrically disubstituted ferrocenyl derivatives are well known and has been extensively studied, while, unsymmetrical 1,1'-disubstituted ferrocenyl derivatives are comparatively less known. Anticipating improved multifunctional behavior and redox properties we synthesized four analogs of the diferrocenyl hydrazone-enone derivatives (**17-20**) with different aromatic end groups by systematic reaction process and describe their eclipsed structural identity using single crystal X-ray diffraction study. The antibacterial and BSA binding properties of the diferrocenyl derivatives showed reasonable activity and protein binding interaction, while the cyclic-voltammetric study confirmed the electronic communication behavior between the electroactive ferrocenyl fragments. Compounds **18** and **19** also showed selective interaction towards lead cation and revealed their potential as receptor molecules. DFT calculation has been performed to establish some of the interesting features related to structural stability, metal ion interaction and molecular orbital energies.

Acknowledgments

At the end of the journey to obtain my Ph.D., it is a pleasant task for me to convey my heartfelt gratitude and sincere appreciation to all the people who have helped and encouraged me in many ways to complete my thesis.

At this moment of accomplishment, first of all I express my deepest gratefulness to my supervisor **Professor Saurav Chatterjee** for his eternal guidance, support and constructive criticism. His unflinching advice and enthusiasm will always motivate me to continue my research in future.

I am thankful to the **Director**, National Institute of Technology, Rourkela and the **Head, Department of Chemistry**, for providing me all the necessary infrastructural facilities to accomplish my work

I sincerely show gratitude to my DSC members **Professor R. Dinda**, **Professor G. Hota and Professor A. Sahoo**, for their helpful suggestions and valuable comments during the Ph.D. programme.

I gratefully acknowledge **Dr. S. M. Mobin**, IIT, Indore and **Dr. C. Wölper**, University of Duisburg-Essen, Germany for solving Single crystal X-ray crystallography.

I express my thanks to **Dr. Surajit Das,** NIT, Rourkela for biological studies.

I specially thank **Dr. S. Giri, NIT, Rourkela** and **Dr. S. Saha**, IIT BHU for D.F.T. studies and related discussion.

It is my great pleasure to thank all my past and present colleagues **Sumanta, Vijayalakshmi, Avishek, Smriti, Rajkumar, Suman** for their help and cooperation during my Ph.D.

I would like to thank all the faculty members and office staff of the Department of Chemistry, for the help they have rendered from time to time.

Last but not least, I would like to pay high regards to my **parents**, sisters **Fizy** & **Choosy**, brothers **Babu** & **Babun** and my sweet nephew **Gudul** & niece **Ojol** for their sincere love, blessings and inspiration throughout my research work. I owe everything to them.

February 16, 2017

NIT Rourkela *Sasmita Mishra*

Sasmita Mishra

PERSONAL DETAILS:
Address: Plot-1047, 2nd Floor, Chintamani nivas,
Chandimata colony, Rasulgad, Bhubaneswar-751010
Odisha, India
Mobile: 8895276750 / 9040385833
Email: sasmita.nit@gmail.com
Skype: sas.mishra27

EDUCATION:

2002-2004 Msc in Chemistry, Jyotivihar, Sambalpur University, Odisha
2005 MPhil in Chemistry, Jyotivihar, Sambalpur University, Odisha

WORK EXPERIENCES:

2006-2008 Institute of Minerals and Materials Technology
Position: Project Assistant
Function: extraction, isolation and quantification of major markers in Herbal drugs

2008-2011 Apex Institute of Technology and Management
Position: Faculty
Function: Teaching, counseling of students, supervising and invigilation of BPUT semester and other competitive examinations of Central Govt. conducted at Apex institute

ACHIEVMENTS:

Research stay for a month in University of Duisburg-Essen, Germany during 2016 under Indo-German (DST-DAAD) Joint Research Project.

PUBLICATIONS:

1. Synthesis, characterization and antibacterial studies of ferrocenyl and cymantrenyl hydrazone compounds.
   V. Tirkey, S. Mishra, H. R Dash, S. Das, B. P Nayak, S. M Mobin, S. Chatterjee,
   J. Organomet. Chem. 732 (2013) 122.
2. Synthesis of mono- and bi-metallic dithiocarboxylate-alkyne complexes from sunlight driven insertion reaction and their antibacterial activity.
   S. K Patel, V. Tirkey, S. Mishra, H. R Dash, S. Das, M. Shukla, S. Saha, S. M. Mobin, S. Chatterjee,
   J. Organomet. Chem. 749 (2013) 75.
3. Ferrocenyl–cymantrenyl hetero-bimetallic chalcones: Synthesis, structure and biological properties.

S. Mishra, V. Tirkey, A. Ghosh, H. R Dash, S. Das, M. Shukla, S Saha, S. M. Mobin, S. Chatterjee,
J. Mol. Structure 1085 (2015) 162.

4. Synthesis, structure and antibacterial activity of ferrocenyl diphopshine chelated iron - telluride cluster.
   V. Tirkey, R. Boddhula, S. Mishra, S. M. Mobin, S. Chatterjee,
   J. Organomet. Chem. 794 (2015) 88.
5. Synthesis of diferrocenyl hydrazone-enone receptor molecules: Electronic communication, metal binding and DFT study.
   S. Mishra, S. Dewangan, S. Giri, S. M. Mobin, S. Chatterjee,
   Eur. J. Inorg. Chem., **doi.org/10.1002/ejic.201601072** (accepted)
6. Synthesis, electrochemical and biological properties of a variety of ferrocenyl chalcone compounds having a biological active group
   S. Mishra, S. Dewangan, C. Wolper, S. M. Mobin, S. Chatterjee,
   Manuscript under preparation
7. Synthesis, structure of some cyclopentadienyl based organometallic compounds and their use in metal sensing interactions as fluorescent probe.
   S. Dewangan, S. Mishra, C. Wolper, S. Chatterjee,
   Manuscript under preparation

CONFERENCES:

1. Symposium on Modern Trends in Inorganic Chemistry-XIV (MTIC-XIV),
   School of Chemistry, University of Hyderabad,
   December 10-13, 2011.
2. Pollution prevention day-2011
   Department of Chemistry, NIT, Rourkela,
   December 2, 2011.
3. 14thNational Symposium in Chemistry (NSC) and 6th CRSI-RSC Symposium in Chemistry
   Institute for Interdisciplinary Science and Technology, Thiruvananthapuram,
   February 2-5, 2012.
4. National Conference on Advances in Chemistry and their Biological and Industrial Relevance (ACBIR),
   Department of Chemistry, NIT, Rourkela,
   January 10-11, 2014.
5. Science Academie's Lecture Workshop on "Organic and Inorganic Self Assembly"
   Department of Chemistry, School of Applied Sciences, KIIT University, Bhubaneswar,
   February 21-22, 2015.
6. Symposium on Modern Trends in Inorganic Chemistry-XV (MTIC-XV),
   Indian Institute of Technology, Roorkee,
   December 13-16, 2013.